Soil erosion and sediment yield in the upper Yangtze, China

Xixi Lu

Soil Erosion and Sediment Yield in the Upper Yangtze, China

Xixi Lu

Doctor of Philosophy

University of Durham
Department of Geography

February 1998

Soil Erosion and Sediment Yield in the Upper Yangtze, China

Xixi Lu

Soil erosion and sedimentation are key environmental problems in the Upper Yangtze because of the ongoing Three Gorges Project (TGP), the largest hydro-power project in the world. There is growing concern about the rapid increase of soil erosion over the last few decades and its consequence for potential sedimentation in the reservoir. The study aims to examine controls on the spatial and temporal distributions of sediment transfer within the Upper Yangtze and the hydrological consequences of land use changes, using varied approaches at different catchment scales.

First, soil erosion and sedimentation are examined using the radionuclide Cs-137 as a tracer within a small reservoir catchment in the Three Gorges Area. The results indicates that soil erosion on sloping arable land and the rates of reservoir sedimentation have been severe during the past 40 years, mainly due to cultivation on steep slopes. Changes in reservoir sedimentation rates are mainly attributed to land use changes. The suitability of the Cs-137 techniques for investigating soil erosion and sedimentation in intensely cultivated subtropical environments is also considered. The use of the technique for erosion investigation may have limitations due to the abundance of coarse soil textures, uncertainty about fallout deposition rates and the high incidence of human disturbance, but the technique shows promising perspectives for sedimentation investigation since a few dating horizons might be identified.

Second, sediment and runoff measurement data for around 30 years from over 250 hydrological stations within the Upper Yangtze have been examined within a GIS framework. The dataset has been integrated with catchment characteristics derived from a variety of environmental datasets and manipulated with Arc/Info GIS. The analysis of the sediment load data has permitted identification of the most important locations of sediment sources, the shifting pattern of source areas in relation to land use change and sub-catchments exhibiting trending sediment yields corrected for hydrological variability.

The study demonstrates the importance of scale dependency of sediment yield in both the identification of temporal change and the modelling of relationships between sediment yield and environmental variables, suggesting that the treatment of the scale problem is crucial for temporal-spatial studies of sediment yield.

TABLE OF CONTENTS

1. INTRODUCTION **1**

1.1 THE CONTEXT OF THE STUDY 1

1.2 THE JUSTIFICATION OF THE STUDY 1

1.2.1 The history of TGP 1

1.2.2 Major concerns about TGP 3

1.2.2.1 Resettlement 5

1.2.2.2 Sedimentation 6

1.3 OVERVIEW OF CONVENTIONAL EROSION QUANTIFICATION METHODS AND THEIR PROBLEMS 8

1.3.1 Soil erosion quantification by runoff plot 9

1.3.2 Soil erosion estimation by models 10

1.3.3 Soil erosion investigation by remote sensing 12

1.3.4 Soil erosion assessment using sediment yields obtained from hydrographical measurement . 14

1.3.5 Soil erosion assessment using sediment yields estimated from reservoir deposition 16

1.4 RAPID ASSESSMENT OF SOIL EROSION AND SEDIMENTATION USING CAESIUM-137 TRACER TECHNIQUE 17

1.5 INTEGRATED EXAMINATION OF SEDIMENT YIELDS THROUGHOUT THE UPPER YANGTZE 19

1.6 MONITORING SOIL EROSION AND SEDIMENT YIELDS 21

1.7 THE AIMS AND OBJECTIVES OF THE STUDY 22

1.8 THE ARRANGEMENT AND STRUCTURE OF THE THESIS 23

2. THE CS-137 TECHNIQUE AND SEDIMENT YIELD DATA ANALYSIS: A LITERATURE REVIEW **25**

2.1 INTRODUCTION 25

2.2 Cs-137 APPLICATION IN EROSION INVESTIGATIONS 25

2.2.1 Cs-137 technique and its development 25

2.2.2 The problems 28

2.2.2.1 Uncertainty of uniform fallout and uniform adsorption 30

2.2.2.2 Uncertainty of rapid adsorption by soil 31

2.2.2.3 Uncertainty of uniform distribution through tillage operation 33

2.2.2.4 Uncertainty of preferential adsorption and selective erosion 33

2.2.2.5 Uncertainty of atmospheric fallout 34

2.2.2.6 Uncertainty of erosion quantification 36

2.3 CS-137 TECHNIQUE FOR SEDIMENTATION INVESTIGATION AND SEDIMENT SOURCES FINGERPRINTING 38

2.3.1 Cs-137 technique and its development 38
2.3.2 The problems 39
2.3.2.1 Post-depositional movement 39
2.3.2.2 Equifinality 40
2.3.2.3 Sedimentation rate estimation 41
2.4 TEMPORAL CHANGES OF SUSPENDED SEDIMENT YIELD 42
2.4.1 Methods to detect the change 43
2.4.1.1 Running mean 43
2.4.1.2 Linear regression 43
2.4.1.3 Mann-Kendall correlation 43
2.4.1.4 Non-linear regression 44
2.4.2 Discrimination of the change 44
2.4.2.1 Double mass curve 44
2.4.2.2 Runoff variation removal 45
2.4.3 Difficulties to detect the change 45
2.5 SPATIAL VARIABILITY OF SEDIMENT YIELD 46
2.5.1 Drainage area 48
2.5.2 Hydroclimatic variables 50
2.5.3 Topographic variables 53
2.5.4 Geology, soils and landuse 54
2.6 SUMMARY AND CONCLUSION 58

3. THE STUDY AREA 60

3.1 INTRODUCTION 60
3.2 THE UPPER YANGTZE AND THE THREE GORGES AREA 60
3.2.1 General background of the Upper Yangtze 60
3.2.2 Soil erosion and sediment transport in the Upper Yangtze 66
3.2.3 General background of the Three Gorges area 70
3.2.4 Soil erosion in the Three Gorges area 75
3.3 YIWANSHUI CATCHMENT 80
3.3.1 Climate 81
3.3.1.1 Temperature 81
3.3.1.2 Monthly rainfall 81
3.3.2 Geology and landform 89
3.3.3 Landuse and soils 89
3.3.4 Soil erosion 94
3.4 SUMMARY AND CONCLUSION 99

4. MATERIALS AND METHODS 101

4.1 INTRODUCTION 101

4.2 SAMPLING STRATEGY 101
4.2.1 Soil sampling for reference value 102
4.2.2 Soil sampling from arable lands 102
4.2.3 Topsoil and eroded materials collecting from potential sediment sources and sinks 106
4.2.4 Reservoir cores sampling 106
4.3 LABORATORY ANALYSIS 107
4.3.1 Cs-137 determination 107
4.3.1.1 Measurement of environmental radioactivity 107
4.3.1.2 The determination of ROI 109
4.3.1.3 Calibration 109
4.3.1.4 Measurement errors and counting times 110
4.3.2 Particle size distribution analysis 110
4.3.3 Geochemical analysis 111
4.4 DATA COLLECTION 111
4.4.1 Runoff and suspended sediment loads data 111
4.4.2 The Asian 30arcsecond DEM 115
4.4.3 Global Ecosystems Database (GED) 116
4.4.4 The Asian Population Database 116
4.4.5 The Digital Chart of the World (DCW) 117
4.5 GIS APPLICATION 117
4.5.1 DEM build-up and surface generation 118
4.5.1.1 Surface generation 118
4.5.1.2 DEM build-up for Yiwanshui catchment 120
4.5.2 Watershed delineation in the Upper Yangtze 123
4.5.3 Drainage network extraction in the Upper Yangtze 124
4.5.4 The variables extraction from varied data sources 127
4.5.4.1 Morphometric characteristics of catchment 127
4.5.4.2 Precipitation, population density and NDVI 128
4.6 SUMMARY AND CONCLUSION 128

5. SOIL EROSION ON SLOPING ARABLE LAND IN UPPER YANGTZE: A CASE STUDY IN YIWANSHUI CATCHMENT 129

5.1 INTRODUCTION 129
5.2 ESTIMATE OF Cs-137 ATMOSPHERIC FALLOUT 130
5.2.1 Estimate from soil 130
5.2.2 Estimates of fallout from atmospheric records 136
5.2.2.1 Estimate of fallout for 1954-74 136
5.2.2.2 Estimate of fallout from 1975-94 139
5.2.3 Discrepancy between the two estimates 140

5.3 DIFFERENTIAL Cs-137 ACTIVITY AND GRAVEL CONTENT: POTENTIAL INFLUENCING FACTORS 140
5.3.1 Effects of topography 140
5.3.1.1 Effects of slope position 141
5.3.1.2 Effect of slope angle and length 145
5.3.2 Effects of human activity 148
5.3.2.1 Effect of deliberate soil remove 148
5.3.2.2 Effect of tillage and root-crop harvest 149
5.3.2.3 Effect of terrace forms 151
5.4 ESTIMATES OF NET SOIL LOSS RATES FROM Cs-137 MEASUREMENT 152
5.4.1 Cs-137 enrichment ratio estimate 152
5.4.2 Percentage of Cs-137 loss 154
5.4.3 Quantification of net soil loss rates 154
5.4.3.1 Quantification by mass balance model 155
5.4.3.2 Quantification by simplified mass balance model 157
5.5 THE PATTERNS AND RATES OF NET SOIL LOSS 159
5.5.1 Frequency of net soil loss rates 160
5.5.2 Spatial patterns of net soil loss 162
5.6 SUMMARY AND CONCLUSION 162

6. SEDIMENTATION AND SEDIMENT DELIVERY IN UPPER YANGTZE: A CASE STUDY IN YIWANSHUI CATCHMENT 166

6.1 INTRODUCTION 166
6.2 PROPERTIES OF THE RESERVOIR SEDIMENT 167
6.2.1 Bulk density 167
6.2.2 Particle sizes 168
6.2.3 Cs-137 concentration 168
6.3 IDENTIFICATION OF DATING HORIZONS 171
6.3.1 Identification by Cs-137 profile distribution 171
6.3.2 Identification by particle size and rainfall information 172
6.4 SEDIMENTATION RATE AND TEMPORAL CHANGES 173
6.4.1 Sedimentation rate 174
6.4.2 Temporal changes 174
6.5 SEDIMENT YIELD AND TEMPORAL CHANGES 175
6.5.1 Sediment yield 175
6.5.1.1 Estimate of the sediment deposited in the reservoir 175
6.5.1.2 Estimate of trap efficiency (TE) 177
6.5.1.3 Sediment yield 177
6.5.2 Temporal changes 178
6.5.3 Possible change reasons 180

6.5.3.1 Rainfall changes 180
6.5.3.2 Landuse change 182
6.6 CATCHMENT-WIDE SEDIMENT DELIVERY AND BUDGET 185
6.6.1 Estimate of average soil erosion rate 185
6.6.1.1 Erosion rate for wood & grass land 186
6.6.1.2 Erosion rate for gully and terrace edges 186
6.6.1.3 Average erosion rate for the catchment 186
6.6.2 Sediment yield delivery and budget 187
6.7 SEDIMENT SOURCES DISCRIMINATION 189
6.7.1 A PRELIMINARY EVALUATION 189
6.7.2 Main sediment source identified by Cs-137 technique 190
6.8 SUMMARY AND CONCLUSION 192

7. SEDIMENT YIELD IN THE UPPER YANGTZE: SPATIAL VARIABILITY AND TEMPORAL CHANGES 196

7.1 INTRODUCTION 196
7.2 SPATIAL VARIABILITY 198
7.2.1 Sediment yield - basin area relationships 198
7.2.2 Sediment yield variability 201
7.3 TEMPORAL CHANGES 205
7.3.1 Long-term trends in sediment yields 207
7.3.2 Changes between the three periods 219
7.4 SUMMARY AND CONCLUSION 222

8. SEDIMENT YIELD IN THE UPPER YANGTZE: SPATIAL VARIABILITY MODELLING AND MAPPING 225

8.1 INTRODUCTION 225
8.2 SEDIMENT YIELD VARIABILITY AND CATCHMENT VARIABLES 226
8.3 MODELLING SPATIAL VARIABILITY 232
8.3.1 Interrelationships between catchment variables 232
8.3.2 Relationships between sediment yield and catchment variables 233
8.3.2.1 Basin grouping based on tributary 233
8.3.2.2 Basin grouping based on its size 237
8.3.2.3 Basin grouping based on maximum elevation 238
8.3.3 Discriminating controls on regional sediment yields 238
8.4 SEDIMENT YIELD MAPPING 243
8.4.1 Specific sediment yield calibration 244
8.4.2 Mapping methods 247
8.4.2.1 Polygon Attribution 247
8.4.2.2 Point Interpolation Procedures 249

8.4.2.3 Multiple regression modelling....251
8.5 SUMMARY AND CONCLUSION....254

9. THE POTENTIAL TO MONITOR SEDIMENT YIELD USING REMOTELY SENSED NDVI DATA....258

9.1 INTRODUCTION....258
9.2 NDVI AND THE CATCHMENTS....260
9.2.1 The Normalised Difference Vegetation Index (NDVI)....260
9.2.2 NDVI relations with ecoclimatic variables....261
9.2.3 The catchments....263
9.3 MONTHLY NDVI, RUNOFF AND SEDIMENT TRANSPORT....266
9.3.1 Patterns of monthly NDVI, runoff and sediment transport....266
9.3.2 Correlation between monthly NDVI, runoff and sediment transport....269
9.4 ANNUAL NDVI, RUNOFF AND SEDIMENT TRANSPORT....274
9.5 NDVI SPATIAL VARIATION AND ITS RELATION WITH RUNOFF AND SEDIMENT TRANSPORT....275
9.5.1 NDVI spatial variations....275
9.5.2 Effect of elevation on NDVI....277
9.5.3 Effect of precipitation on NDVI....277
9.5.4 NDVI relations with runoff/sediment transport....279
9.6 SUMMARY AND CONCLUSION....284

10. CONCLUSION AND PROSPECT....286

10.1 A BRIEF OVERVIEW OF THE STUDY....286
10.2 ACHIEVEMENTS FROM THE STUDY AND THEIR IMPLICATIONS....287
10.2.1 Long-term patterns and rates of net soil loss on slopes....287
10.2.2 Sedimentation rate and sediment yield in Yiwanshui catchment....288
10.2.3 Sediment delivery and budget for Yiwanshui catchment....289
10.2.4 Sediment yield in the Upper Yangtze: spatial variability and temporal changes....289
10.2.5 Sediment yield in the Upper Yangtze: variability modelling....290
*10.2.6 The potential to monitor soil erosion and sediment yield using remote sensed NDVI data.*292
10.3 ASSESSMENT OF CS-137 TECHNIQUE APPLICATION IN THE AREA....292
10.3.1 The difficulty to identify Cs-137 reference sites....293
10.3.2 Coarser texture of soils....293
10.3.3 Deliberate soil remove....294
10.3.4 The uncertainty of radionuclide fallout....294
10.3.5 The calibration from Cs-137 to soil erosion....295
10.4 THE LIMITATIONS OF THE STUDY....295
10.4.1 Soil sampling in the small catchment....296

10.4.2 The data access 296
10.5 PROSPECTS AND FURTHER RESEARCH 297
10.5.1 Cs-137 technique application in the area 297
10.5.2 GIS application for large scale catchment modelling 298
10.5.3 NDVI application for monitoring soil erosion and sediment yield 298
10.6 SCALE AND HIERARCHICAL PROBLEMS 299
10.6.1 Temporal scale problems 299
10.6.2 Spatial scale problems 300
10.6.3 Hierarchical problems 304
10.7 CONCLUDING REMARKS 304

APPENDIX 1, GENERAL INFORMATION OF SOIL SAMPLES FROM SLOPES 307

APPENDIX 2, THE SUMMARY OF COLLECTED SOIL SMAPLES FOR SEDIMENT SOURCES IDENTIFICATION 308

APPENDIX 3, CS-137 MEASUREMENTS 311

APPENDIX 4, THE PARTICLE SIZE DISTRIBUTION FOR SELECTED SOIL SAMPLES FROM ARABLE LAND 319

APPENDIX 5, PARTICLE SIZE ANALYSIS FOR RESERVOIR CORE 1 320

APPENDIX 6, AN EXAMPLE SHOWING THE CALCULATION OF EROSION RATES USING THE MASS BALANCE MODEL. THE MODEL WAS PERFORMED IN EXCEL 5.0. 321

APPENDIX 7, THE DRAINAGE NETWORK DIGITISED FROM MAPS 322

APPENDIX 8, ALL THE AMLS USED TO EXTRACT VARIABLES FROM THE VARIED DATABASE 323

APPENDIX 9, THE CATCHMENT VARIABLES FOR THE 62 BASINS IN THE UPPER YANGTZE 328

BIBILOGRAPHY 329

LIST OF FIGURES

Figure 2-1, A diagram showing the routing of Cs-137 on the landscape (after Wise, 1980).....27
Figure 2-2, The chronological development of Cs-137 applications in erosion investigation (after Higgitt, 1995) 29
Figure 2-3, The sediment yield-basin area relationship (after Medkov and Moszherin, 1992).....49
Figure 2-4, Relationships between mean annual sediment yield and mean annual precipitation in drainage basins (after Wilson, 1973).....52
Figure 3-1, The Yangtze River showing upper, middle and lower reaches 61
Figure 3-2, The Upper Yangtze River showing main tributaries 64
Figure 3-3, The Three Gorges area showing county names and the location of Yiwanshui catchment 71
Figure 3-4, Mean monthly temperature and precipitation in Changshou county.....82
Figure 3-5, The mean rainfall per rainday in 6 day periods in Changshou from 1957-87.....84
Figure 3-6, The probability of rain per day in 6 day periods in Changshou from 1957-87.....85
Figure 3-7, The daily rainfall over 25 mm in Changshou from 1957-87.....86
Figure 3-8, Annual rainfall change from 1957-87 in Changshou county 87
Figure 3-9, Frequency of larger than 25 and 50 mm daily rainfall and their correspoding total rainfall 88
Figure 3-10, A schematic section showing geology in Yiwanshui catchment.....90
Figure 3-11, A contour map showing topographic features in Yiwanshui catchment.....91
Figure 3-12, The landuse in Yiwanshui catchment.....92
Figure 4-1, The distribution of soil sampling sites in Yiwanshui catchment.....104
Figure 4-2, 3D model of Yiwanshui catchment.....122
Figure 4-3, The flow chart showing work procedures for watershed delineation and drainage network extraction (after ESRI, 1994) 125
Figure 5-1, The vertical distribution of Cs-137 concentration for reference profiles taken from paddy field.....131
Figure 5-2, Box-and-whisker plot for Cs-137 aerial activities (Bq m^{-2}) for the samples at the reference site. Note the identification of an extreme outlier which is taken out for final mean calculation. 135
Figure 5-3, Annual Cs-137 fallout in Changshou from 1954-74 estimated based on the model proposed by Sarmiento and Gwinn (1986). 138
Figure 5-4, Monthly Cs-137 fallout in Changshou for the four years (1962-65) estimated based on the model proposed by Sarmiento and Gwinn (1986).....138
Figure 5-5, Vertical distribution of Cs-137 of soil profiles from a small sloping terrace 142

Figure 5-6, Slope profiles, sampling locations and Cs-137 inventories for the 11 sampled fields 143
Figure 5-7, Soil particle size (<2mm) distributions showing little variations for different slope positions 146
Figure 5-8, A sketch map showing possible deliberate soil remove by farmer 150
Figure 5-9, Four combinations of different terrace forms found in the catchment 150
Figure 5-10, Frequency distribution of the percentage of Cs-137 loss 156
Figure 5-11, The erosion rates estimated by two methods against Cs-137 loss percentage 158
Figure 5-12, Frequency distribution of erosion rate classes estimated by mass balance model 161
Figure 5-13, Spatial patterns of net soil loss rates in Yiwanshui catchment 163
Figure 6-1, Bulk density, Cs-137 concentration and particle size distribution for the two reservoir cores 169
Figure 6-2, The transects used for bathymetric measurements (a), and water depth of the reservoir (b) 176
Figure 6-3, Sediment load-drainage area relationship in the Upper Yangtze basin Sichuan basin 179
Figure 6-4, Sediment yields changes for the four phases in Yiwanshui catchment 181
Figure 6-5, Rainfall changes for the four phases in Changshou county 181
Figure 6-6, Sediment yield changes assigned based on dating layers and annual rainfall 183
Figure 6-7, Suspended sediment yields changes for Shizhu and Xinshan catchments in the Three Gorges area 183
Figure 6-8, Sediment delivery and budget for the Yiwanshui catchment 188
Figure 6-9, The variability of Cs-137 concentration (Bq m^{-2}) for the potential sediment sources and sediment materials 193
Figure 7-1, Relationships between specific sediment yield and drainage basin area. 199
Figure 7-2, Contribution of upper Yangtze tributaries to sediment load expressed as
(A) Five year running mean of sediment load index compared with Yichang;
(B) standardised proportional contribution (actual yield / predicted yield from sediment yield-basin area regression and;
(C) standardised proportional contribution to annual load, corrected for basin area 203
Figure 7-3, Maps of (A) standardised residual and (B) coefficient of variation of annual sediment yield. 204
Figure 7-4, Distribution of gauging stations with significant sediment yield changes 209
Figure 7-5, Plot of time series correlation coefficients against drainage area 210
Figure 7-6, Sediment yield time series for six selected stations with large drainage area 212
Figure 7-7, Impact of reservoirs on sediment yield time series. Solid lines indicates stations above the reservoir and dashed lines stations downstream of reservoir 213
Figure 7-8, Sediment yield -runoff relationships (a), and time series plot of regression residuals (b) for stations experiencing increasing sediment yield. 217
Figure 7-9, Sediment yield -runoff relationships (a), and time series plot of regression residuals (b) for stations experiencing decreasing sediment yield.. 218

Figure 7-10, Incremental drainage areas undergoing significant change between (a) 1956-67 and 1968-77; (b) 1968-77 and 1978-87 221
Figure 8-1, Topographic map of the Upper Yangtze basin derived from 30arcsecond 228
Figure 8-2, Slope map of the Upper Yangtze basin derived from 30arcsecond 229
Figure 8-3, Precipitation map of the Upper Yangtze basin obtained from GED 230
Figure 8-4, Population density of the Upper Yangtze basin 231
Figure 8-5, Plots of (a) slope (degrees), (b) annual precipitation (mm), (c) population density (number km^{-2}) against elevation (metres) at pixel level 234
Figure 8-6, Specific sediment yield against catchment variables: tributary grouping 235
Figure 8-7, Specific sediment yield against catchment variables: catchment size grouping 239
Figure 8-8, Specific sediment yield against catchment variables: maximum elevation grouping 240
Figure 8-9, Schematic representation of the linked-lumped catchment system 246
Figure 8-10, Sediment yield map generated by polygon attribution 248
Figure 8-11, Sediment yield map generated by point interpolation procedures 250
Figure 8-12, Sediment yield map generated by multiple regression modelling 253
Figure 8-13, Comparison of sediment yield class distributions from alternative mapping procedures 256
Figure 9-1, The catchments examined in the chapter 264
Figure 9-2, The patterns of monthly NDVI and runoff 267
Figure 9-3, The patterns of monthly NDVI and sediment transport 268
Figure 9-4, Monthly runoff against NDVI 270
Figure 9-5, Monthly sediment transport against NDVI 271
Figure 9-6, Monthly sediment transport against runoff 272
Figure 9-7, The averaged NDVI for the 12 catchments 276
Figure 9-8, The relations between elevation and annual NDVI 278
Figure 9-9, The relations between mean precipitation and annual NDVI 280
Figure 9-10, The relations between NDVI and runoff/sediment yields 282
Figure 9-11, The relations between runoff and sediment yields 283

LIST OF TABLES

Table 1-1, A review of TGP history 1
Table 1-2, Basic information on the Three Gorges Project 3
Table 1-3, A brief description of possible benefits and problems of TGP 4
Table 1-4, The standard erosion rates for different erosion classes used in China (after Department of Water and Soil Conservancy, 1988) 12
Table 1-5, The existing soil erosion quantification methods used in China 16
Table 2-1, A summary of Cs-137 variability in the reference sites 32
Table 2-2, Cs-137 fallout (Bq m^{-2}, not decay corrected) from selected Chinese nuclear tests recorded in Japan (after Hirose et al., 1987) 35
Table 2-3, The potential influencing variables examined in global and regional scales 47
Table 2-4, A summary of a few models to predict sediment yield 56
Table 3-1, The size characteristics of different reaches of the Yangtze River (after Huang, 1982) 63
Table 3-2, The principle tributaries in the Upper Yangtze river (adapted from Huang, 1982) 65
Table 3-3, The changes of soil erosion affected areas in some provinces within the Yangtze valley in 1950s and 1980s 67
Table 3-4, The completed water conservancy projects (unit in 10^6 m^3) in the Upper Yangtze (after Gu et al., 1987) 68
Table 3-5, Sedimentation in selected reservoirs in the Upper Yangtze (after CAS, 1988) 69
Table 3-6, Average annual reservoir capacity loss due to sedimentation (from varied literature) 70
Table 3-7, The terrain classification in China (adapted from Zhao, 1994) 72
Table 3-8, Land use in the Three Gorges area (after Chen and Gao, 1988) 73
Table 3-9, The slopes for arable land in the Three Gorges area (after Shi et al., 1987) 74
Table 3-10, Annual soil loss and sediment to the Yangtze river from different landuse in the Three Gorges area (after Shi et al., 1992) 76
Table 3-11, Soil erosion inventory in 1980s in the Three Gorges area (after Yang and Shi, 1994) 77
Table 3-12, The changes of forest land for all the counties in the Three Gorges area from 1950s to 1980s (After Shi et al, 1987) 78
Table 3-13, Sediment yields calculated based on reservoir investigation in the Upper Yangtze (after Yang and Shi, 1994) 79
Table 3-14, Monthly extreme events and their happening years from 1957-1987 in Changsou county 81
Table 3-15, Landuse in Yiwanshui catchment 93
Table 3-16, The areas of soil erosion affected in Changshou County

(after Soil and Water Conservation Office of Sichuan Changshou County, 1988).....97
Table 3-17, The areas (km^2) of soil erosion affected for different geological rocks
(after Soil and Water Conservation Office of Sichuan Changshou County, 1988).....98
Table 3-18, The areas (km^2) of soil erosion affected for different landuse in Changshou
(after Soil and Water Conservation Office of Sichuan Changshou County, 1988).....98
Table 3-19, The areas (km^2) of soil erosion affected for different landforms in Changshou
(after Soil and Water Conservation Office of Sichuan Changshou County, 1988).....99
Table 4-1, The numbers of hydrological stations by main tributaries upstream.....112
Table 4-2, The numbers of gauging stations by measurement years.....113
Table 4-3, The summary information for the 62 catchments in the Upper Yangtze.....114
Table 5-1, Summary statistics and variability of Cs-137 at the reference site.....132
Table 5-2, Additional bulk samples for Cs-137 reference values.....133
Table 5-3, Cs-137 reference values estimated in China.....134
Table 5-4, The mean of Cs-137 for three different slope positions.....144
Table 5-5, The mean percentage of >2mm fraction for different slope positions.....145
Table 5-6, Spearman's correlation matrix between slope degree, length, Cs-137
and >2mm fractions (n=66).....148
Table 6-1, Sedimentation rates of the reservoir calculated based on four phases.....174
Table 6-2, The mean Cs-137 concentration (Bq kg^{-1}) for the materials of potential source
and sinks in the fraction of <2mm.....190
Table 6-3, Cs-137 concentration (Bq kg^{-1}) variability of purple soils for different slope position.....192
Table 7-1, Sediment yields and relative contribution of Upper Yangtze tributaries.....205
Table 7-2, Stations with significant time series trends at significant level $\alpha = 0.05$.....211
Table 7-3, Water conservancy capacities within the Upper Yangtze catchment
(Reservoir capacity data derived from Gu and others, 1987).....214
Table 7-4, Stations exhibiting significant change between successive time periods. 220
Table 8-1, Spearman's correlation matrix of catchment variables (n=62).....232
Table 9-1, The catchments used in this chapter.....265

LIST OF PLATES

Plate 3-1, The up-down slope cultivation and dissected sloping land in Yiwanshui catchment.....95
Plate 3-2, The different landuse forms in Yiwanshui catchment.....96
Plate 4-1, The paddy field in which reference samples were taken, and the tube used for sampling.....103

I confirm that no part of the material offered in this thesis has previously been submitted by me or any other person for a degree in this or any other university. In all case, where it is relevant, material from the work of others has been acknowledged. Quotations and paraphrases are suitably indicated.

Signed: 
.....

Date:
.....

ACKNOWLEDGEMENTS

I am grateful to the Committee of Vice-Chancellors and Principals (CVCP) for the Overseas Research Studentship (ORS) award, and the Department of Geography and the University of Durham for the subsistence provided for the study.

I would like to thank my supervisors, Dr D.L. Higgitt and Dr R.J. Allision, for the guidance and encouragement provided throughout the research project, from whom I have learnt Western-style approaches in dealing with problems. Durham is a new place for both Dave and myself. I arrived in Durham on almost the same day as Dave when he transferred from Lancaster and came back from fieldwork in China. He has been very busy with many things; buying a house, arranging marriage and the subsequent arrival of two babies, but has spared much time to discuss results and co-author a few publications.

The co-operation and assistance when undertaking field work from the staff in the Soil and Water Conservation Office of Changshou County, Sichuan, is gratefully acknowledged. The field work could not have been undertaken without their co-operation. Particular thanks to Dr D.L. Higgitt, Dr J.S. Rowan from Lancaster University, Mr Liang Ying and Mr Xin Tinyan from the Institute of Soil Science (ISS) under Chinese Academy of Sciences (CAS), for the assistance of undertaking field work. This was particularly difficult under nearly 40 degrees of heat during summer in a subtropical environment. Without their help the project could not be completed.

Thanks are also given to the staff in the Department of Durham for their help, especially Dr D.N.M Donoghue, Dr C. Puhr and Dr Y. Zong on GIS/RS, Dr N.J. Cox on Stata, Mr C. Mullaney and Mr M. Scott on computing, and the technicians on laboratory work.

Thanks also to my former supervisors and colleagues, Professors Gong Zitong, Shi Deming, and Shi Xuezheng, in ISS, CAS for invaluable support and comments at the beginning of the project. Last, but not least, thanks to my wife and daughter for accompanying me in Durham.

1. INTRODUCTION

1.1 THE CONTEXT OF THE STUDY

Soil erosion and sedimentation are key environmental problems in the Upper Yangtze basin, where the attention of environmentalists has been drawn to the Three Gorges Project (TGP), the world's largest hydro-power project. These problems include concern about the rapid increase of soil erosion over the last few decades and its consequence for downstream sedimentation. Within this context, the study aims to assemble information on soil erosion and sedimentation, which will be helpful for appropriate sediment management of the Three Gorges reservoir in the near future. The study includes small-scale appraisal of soil erosion and sedimentation using the radionuclide tracer of Cs-137, and large-scale investigation of sediment transport using sediment load data within the Upper Yangtze basin, China.

1.2 THE JUSTIFICATION OF THE STUDY

1.2.1 The history of TGP

Building large scale dams is still a solution to power generation and flood control problems, although it is increasingly being questioned (Edmonds, 1996). A review of TGP history is summarised in Table 1-1. The idea of damming the Three Gorges (*Sanxia*) along the Yangtze River (*Chang Jiang*) was first proposed in the 1920s by Dr Sun Yat-Sen, a founder of the People's Republic (Pan, 1990). Efforts to push the project through China's elaborate decision-making process have been interrupted over the years by war, ideological struggles, the chaos of the Cultural Revolution, and the decade of debate over the project (Ryder and Barber, 1993). On April 3 1992, China's National People's Congress gave formal approval to construct the TGP, following the floods in the low valleys of the Huia and Yangtze rivers in June and July 1991, which took the lives of nearly 3,000 people. The project was started in

1993 and is expected to take 18 years to complete. In November of 1997, the mighty Yangtze was successfully dammed to divert flow to a canal.

Table 1-1, A review of TGP history

1920s	Dr Sun Yat-Sen proposed to build a dam near the Three Gorges.
1932	The Nationalist Party established a committee to investigate the Three Gorges area and proposed a low dam project.
1937	Japanese invaded China.
1944	Dr Savage, an American hydro-engineer , came to China to re-investigate the project.
1949	Communist took over China and the Nationalist Part receded to Taiwan.
1954	Floods in the Yangtze basin.
1956	"Mount Wu's clouds and rains are kept away from the countryside; Calm lakes spring up in the high gorges." Shiu Diuo Ge Tou, Swimming, Mao, Zedong, May 1956.
1958	Great Leap Forward started.
1965	Cultural Revolution started.
1974	Gezhouba dam (between TGP site and Yichang), a preparative project of TGP, started and finally took 19 years to complete the project (only 47 meter with capacity of 2715 megawatts) under the 2 years of performing the modelling experiment for siltation and revising the design.
1976	Mao Zedong died.
1978	China's reform started.
1982	Floods in the Yangtze River basin.
1983	The Yangtze Valley Planning Office, the major proponent of TGP, proposed the 150 meter scheme. The proposal was opposed by the People's Congress and the Political Consultative Committee.
1986	Premier Li Peng, a trained hydro-engineer in favour of TGP, stated that TGP would not be started until all appraisals were completed. Chinese government accepted Canada's offer to finance the feasibility research and established Canadian International Project Managers-Yangtze Joint Venture (CYJV). The feasibility research of TGP within China, the most comprehensive one ever and co-ordinated by State Planning Commission and Chinese Academy of Sciences, also started.
1989	Vice-Premier Yao Yilin announced that a decision to build the dam had been postponed for at least five years.
1991	The floods in the low valleys of the Huia and Yangtze rivers in June and July, which took the lives of nearly 3,000 people. China's National People's Congress gave formal approval to construct the TGP in 1992.
1993	TGP started.
1997	The Yangtze River was dammed to divert flow to a canal.
2011	Expect to complete TGP.

1.2.2 Major concerns about TGP

The Three Gorges Project (TGP) would be the largest single investment (29 billion US$ estimated in 1997) at least in Chinese history, if not in world history. The dam would become the world's largest in terms of many items (Table 1-2). The dam will create a 600 km-long reservoir between Yichang and Chongqing with a reservoir surface area of 1,060 km^2.

Table 1-2, Basic information on the Three Gorges Project

Dam Height	185 m
Dam length	2,150 m
Dam width	1,983 m
Storage capacity	39,300 million m^3
Electric generating capacity	16,750 megawatts
Total cost	29 billion US$ estimated in 1997
Construction duration	18 years
Length of reservoir	500-600 km
Area of reservoir	1060 km^2

Protecting millions of people living along the river banks and flood plains from life-threatening flood is the main rationale for TGP. The Yangtze River and its tributaries are economically vital transport routes, but they have also produced some of China's worst natural flood disasters. Historical records of flood frequencies indicate that major floods occurred once every 18 years in the Tang Dynasty (618-907AD), every 5-6 years in the Song Dynasty (960-1279) and the Yuan Dynasty (1271-1368), every 2 years or less from 1922 to 1949 (Shi et al., 1991). Five times this century, the river floodwaters ravaged the middle and lower valley, killing a total of 300,000 people and leaving millions homeless (Ryder and Barber, 1993). More recently, the Chinese government has been stressing the dam's ability to generate electricity for rapid economic development. When completed in 2011, it will produce hydroelectric power equivalent to the world's two largest existing dams (Itaipu on the Amazon, Brazil and Aswan on the Nile, Egypt) combined. It is claimed that the clean

electricity generated will account for one-eighth of China's total, saving 45 million tonnes of sulphurous coal each year.

However, the fact that close to one-third of the delegates to the congress abstained or voted against this project represented considerable opposition to what is normally an automatic process (Edmonds, 1996). This is quite unusual under the political situation in contemporary China. There has been also strong oppositions from international organisations like World Bank and Probe International, Canada. There are many publications both inside and outside China related to the mega-project. The main books in English include *Damming the Three Gorges* (Ryder and Barber, 1993); *Megaproject* (Luk and Whitney, 1993a); and *Yangtze! Yangtze!* (Dai, 1994). Further detail on the project and its environmental impacts can be found in these books.

Table 1-3, A brief description of possible benefits and problems of TGP

Benefits	Floods control, Clean electricity, Navigation improvement.
Social and cultural problems	Submergence of the Three Gorges' spectacular scenery, 1.2 million population resettlement, Land suitability in upland for those people reallocated, Loss of cultural heritage and archaeological treasures, Dam safety and possible waterbody induced earthquakes.
Environmental and ecological problems	Sedimentation and navigation, Soil erosion by resettlement, Inundation, Waterbody induced landslide, Water pollution, Schistosomiasis (snail-fever), Floods upstream, Bank erosion, Micro-climate change in the reservoir area, Fish migration, particularly endangered Chinese dolphin and Chinese sturgeon, Change of soil quality in the mid-reach and the mouth of the river.

In addition to its high risk of investment and likely low efficiency, the giant TGP may create many potential social and environment problems both upstream and downstream (Table 1-3).The environmental impact assessments had been carried out for a few times, but the latest one organised by State Planning Commission and Chinese Academy of Sciences from the beginning of 1980s is most comprehensive. There were 65 research projects under 11 sections. The outcome of the project is more than 1,000-pages of research proceedings published in 1987: *The Environmental and Ecological Impact of the Three Gorges Project and Countermeasures,* edited by Chinese Academy of Sciences, Leading Group of the Three Gorges Project Ecology and Environment Research Project. Among all the possible problems, resettlement and potential sedimentation of the reservoir are of the most important.

1.2.2.1 Resettlement

It is estimated that more than 1.13 million people will have to be relocated by the time that the water in the reservoir reaches the planned 175 m level. A total of nineteen county-level units including 140 market towns, eleven county seats and the county-level municipalities of Wanxian and Fuling, 657 factory and mining sites, 139 power stations and 956 km of roads will end up under water, and a total of 1,600 enterprises will have to be moved. It is estimated that total spending on resettlement could constitute up to 40% of the total budget (Edmonds, 1996). Along the Yangtze, about 31,600 ha of farmland (paddy field 6,300 ha, arable land 20,000 ha and citrus land 5,300 ha) which is the best land in the area, will be flooded. It is estimated that five times the area of less productive uphill land would be needed to replace the 31,600 ha of prime agricultural land (Shi et al., 1987). This will add enormous pressure on landuse for local area which has been already intensely cultivated. In 1997, Chongqing was separated from Sichuan province and became an independent municipal city under direct control of central government. The new Chongqing with a population of more than 30 million, the largest city in China, also controls Fuling, Wanxian and Qianjiang cities. One of the reasons considered for this is for better management of the project, particularly for people resettlement.

1.2.2.2 Sedimentation

Perhaps the most worrying aspect concerning construction of the dam is sedimentation, because it will affect not only the operating life of the project but also the navigation above the dam. The present knowledge of sedimentation affecting the project is based upon experiments with hydro-sediment models set up in laboratories by engineers (Ling et al., 1990). Dam builders predict that the Three Gorges reservoir storage can be preserved indefinitely, and reservoir sedimentation will not limit the useful life of the project (Qian et al., 1988; Ling et al., 1990). However, the results are based on many assumptions as Professor Leopold, the most eminent US expert in reservoir sedimentology, warned that projections of controlling sedimentation within the reservoir are subject to significant uncertainties (Leopold, 1996). First, dam builders claimed that no obvious increases in the Yangtze's sediment load have been observed and assumed that sediment would deposit in the reservoir at a fixed rate over time (Qian et al., 1988; CYJV, 1988). Second, it is assumed that only 20% of soil eroded from land upstream of the Three Gorges ever reaches the Yangzte River and that sediment which is currently building up behind some dams on upstream tributaries will remain there indefinitely (CYJV, 1988). Third, dam builders have assumed that the bed load (defined as sediment larger than 1 mm) conveyed by the Yangtze is only 0.05% of the total sediment (CYJV, 1988).

Whether or not sediment load to the Upper Yangtze increases is an interesting question both for engineers and geomorpholigists. The answer may be completely different according to the data and the methods they employ. Based upon the measurement in Yichang Gauging Station (controlling the whole Upper Yangtze), many studies found that there was no obvious sediment load increases or decrease during past 40 years (Gu et al., 1987; Gu and Douglas, 1989; CYJV, 1988; Zhuo and Xiang, 1994; Dai and Tan, 1996). However, many Chinese scientists reported that soil erosion is increasing because of population pressure and deforestation upstream of the Three Gorges (Gu et al., 1987; Shi et al., 1987). They argued that the fact of no obvious increases of sediment load to the Yichang was due to a significant amount of

eroded soil was trapped by numerous water conservancy projects built within the Upper Yangtze during the past 40 years. In fact, China's environment is in a state of crisis, as Ryder and Barber (1993, p.6) pointed out: "Three decades of unrestrained industrial development and Mao's "grain-first" policy, which promoted the conversion of all available land and forest into grain fields, had caused untold environmental destruction."

The second assumption of the dam builders discounts a significant amount of eroded soil, which is first transported by floodwater and deposited on flood plains and other low-lying areas, but would be eventually flushed into the Yangtze (Luk and Whitney, 1993b). As to the third assumption, this estimate is contradicted by data from the Yichang station, which indicate that the Yangtze bed load is 1.6% of its total sediment load (CYJV, 1988). In fact, frequent landslides and debris flows in the area contribute huge amounts of coarse materials to the river. Furthermore, the assumption ignored the sediment loads produced by population resettlement. It is estimated that this will be expected to cause an annual 2.5% increase in the river's sediment loads due to activities such as land clearing, cutting down trees for fuel, mining and extraction of building materials (Shi et al., 1987, 1992; Yang et al., 1991; Luk and Whitney, 1993b). Local resettlement at upslope relocation within the Three Gorges are likely to reactivate relict landslides.

It is clear that dam engineers take little consideration of soil erosion and the changing trend of sediment transport upstream. In fact, the technical problem of keeping the Three Gorges reservoir sediment-free became a broader environmental issue related to upstream land use patterns and environmental conditions (Ryder and Barber, 1993). The rate of sedimentation in the reservoir during its lifespan and the proportion of sediment delivered to the river will depend on the patterns and rates of soil erosion and sediment transport upstream. Any difference between the forecast and actual performance has large financial, environmental, and humanistic implications (Leopold, 1996). This was demonstrated by Sanmenxia (Three Gates Gorges) Reservoir in China. The rate of deposition had been grossly underestimated and the sediment deposition was so large that the operation of the reservoir was

completely altered after two years, 1960-62. It is believed that the potential sedimentation of the reservoir will also be a severe problem for TGP due to serious soil erosion within the upper basin:

> "If the Three Gorges Project is completed as planned, it is probable that within a few hundred years the reservoir will almost entirely silt up, creating an unprecedented hazard to the millions of people living downstream, whose culture has survived and prospected for the past 4,000 years with wise management of the Yangtze River."
>
> Ryder and Barber (1993, p.144)

Understanding the patterns and rates of soil erosion and identifying sediment sources are of crucial importance for the management of the potential sedimentation problem associated with the on-going TGP. Meanwhile soil erosion research in the Three Gorges area is of vital importance for sustainable agricultural development especially after the relocation of more than a million people.

1.3 OVERVIEW OF CONVENTIONAL EROSION QUANTIFICATION METHODS AND THEIR PROBLEMS

Understanding, monitoring and ameliorating ecological degradation, whether caused by the natural course of environmental change, the excesses of human exploitation, or some conjunction of the two, implies quantifying the dynamics of change through time (Oldfield et al., 1986; Sutherland, 1989). As far as degradation caused by water erosion is concerned, various methods have been used to collect data such as erosion pin (Haigh, 1977), wash traps (Bollinne, 1978), microrelief meters (Romkens et al., 1988) and runoff plots (Young and Onstad, 1987) on slopes, hydrographic measurement (Walling and Webb, 1996) and reservoir investigation (Neil and Mazari, 1993) from drainage basin studies, and prediction from erosion models (Wischemeier and Smith, 1978) and remote sensing application (Shi et al., 1996). The section focuses on the methods which are frequently used in China. This

includes runoff plot, erosion model, remote sensing, hydrographic measurement and reservoir investigation.

1.3.1 Soil erosion quantification by runoff plots

Many soil erosion investigations have been conducted in the TGP area (Yang et al., 1991; Liu et al., 1991), but has mainly involved the method of runoff plots. The primary advantages of the technique is the access to the detailed event-based information and to allow partial control of factors such as vegetation cover during experiments. The use of runoff plot has two major constraints for erosion studies. First, plot is a bounded small area in which runoff differs from that on the whole slope (Loughran et al., 1989; Walling and Quine, 1990a). Walling and Quine (1990a) pointed out that (1) the measured erosion rate provides a net figure for the entire plot, which may be used to estimate soil losses from a field but provides few data relating to soil redistribution within the field; (2) most erosion plots must be limited in extent to portions of a slope or, at best, slope transect. This may limit the range of potential erosive environments and exaggerate the impact of 'edge effects'. Second, the limited measurement times due to labour and cost intensive (only 2-3 years for most plots in China) cannot cover the variability of climate, particularly rainfall magnitudes and intensities. Erosion data from plots, therefore, have a great limitation in terms of time and space. Furthermore, the most widely used plot is standard runoff plot of 22×5 m^2 originally developed in the USA for large fields with a uniform and gentle slope (Wischmeier and Smith, 1978). However, in general the sloping arable land in the Upper Yangtze is dissected narrow slope terraces on a steep slope. The size of the slope terraces usually is very small with an average width of only a few metres. The details on the steepness and size of the slope arable land will be further introduced in next chapter. If a standard bounded 22 m plot is aligned downslope it will usually transect two or more terraces (depending on slope steepness and therefore terrace width). In doing so the plot will cross several terraces. Obviously it is impractical. Under the circumstance, there are two alternatives. One is to open uniform slopes in which arable land will be exploited and experiment conducted. It is obvious that the results from those plots can not represent actual situation of the dissected terraces. Another is to reduce its dimensions dramatically

so that it can be accommodated on a single terrace. Such small plots may be useful when comparing the relative effect on runoff and erosion of different treatments (crop, fruit, grass and forestry, etc.) but they are clearly unsuitable for predicting runoff or erosion from the dissected terraced unit as a whole (Bruijnzeel and Critchley, 1996). There are two main reasons for this. First, it is difficulty to align these small plots in the direction of the overland flow, since it is quite often that the dissected terraces have two slope directions (main and secondary slope directions, see details in Chapter 5). Second, these small plots exclude runoff and sediment contributed from the dissected terrace wall (riser) which may be a significant source (Bruijnzeel and Critchley, 1996).

1.3.2 Soil erosion estimation by models

On the basis of erosion measurement, it is possible to develop erosion models. Model development can be dated back to 1940s (Zingg, 1940; Smith, 1941; Musgrave, 1947) but historical development was marked by the publication of USLE (Universal Soil Loss Equation) in 1958 (Wischmeier and Smith, 1958). The model was subsequently improved in 1978 (Wischmeier and Smith, 1978) and revised in 1991 (Renard et al., 1991). The basic form of the USLE is as follows:

$$A = R K L S C P \qquad \text{(Equation 1-1)}$$

in which A = soil loss (originally in US tons per acre), R = rainfall energy, K = soil erodibility, L = slope length, S = slope degree C = crop management and P = erosion control. The USLE was originally developed in the USA for large fields with a uniform and gentle slope (Wischmeier and Smith, 1978). There is no specific basis in the model to account for the effect of the terraces in steep landscapes (Hudson, 1995). The factors of LS and P are the least reliable factors when applying USLE in the steep terraced environment (Renard, 1995). The conventional method of calculating soil loss through the USLE for terraced land involves the assumption of LS based on terrace interval and gradient of the terrace bed, in combination with the use of the contour cultivation value for the conservation factor (P) (Bruijnzeel and

Critchley, 1996). However, this method is only suitable for slopes of up to 25% (Wischmeier and Smith, 1978). Furthermore the empirical nature of the USLE misrepresents the interaction of the factors. Though there are many problems, the USLE, with or without modification, is still widely used in China (Yang et al., 1985; Chu, 1988; He, 1989). The application conditions of the USLE were often ignored by most of those applicants as stated by Lu and Shi (1994). The concepts of the model have not been fully understood yet and caused many other problems for those applications. For example, precipitation was taken as rainfall energy, the calculated value of soil erodibilty factor (K) was too big (more than 1), and there is confusion over units for some factors such as rainfall energy (R).

Due to its simplicity, USLE has been hybrid in many models like CREAMS (A field scale model for Chemicals, Runoff and Erosion from Agricultural Management Systems, Knisel, 1980), SLEMSA (Soil Loss Estimator for Southern Africa, Elwell, 1981), GLEAMS (Groundwater Loading Effects of Agricultural Management Systems, Leonard et al., 1987), AGNPS (a nonpoint-source pollution model for evaluating agricultural watersheds, Young et al., 1989) and EPIC (Erosion Productivity Impact Calculator, Williams, 1985; or recently Environmental Policy Integrated Climate, Williams et al., 1996). The basic form of predicting soil erosion for those models is based on original USLE or MUSLE. However, USLE and associated approaches are empirical models which inherit the limitation of extrapolation. Completely empirical models describe only the relationships between model inputs and outputs in the classic 'black box' sense and embody no scientific theories (Favis-Mortlock et al., 1996). The reaction to the deficiencies in empirical erosion models by soil erosion researchers has been to develop process-based models like WEPP (Water Erosion Prediction Project, Nearing et al., 1989), EUROSEM (EUROpean Soil Erosion Model, Morgan et al., 1992), MEDALUS (MEditerranean Desertification And Land Use, Kirkby et al., 1993) and MEDRUSH (Abrahart et al., 1994). However, these newly developed process-based models are in general very complicated and their applications are still in question particularly for policy-makers.

Some model variables can be obtained by remote sensing and GIS. For example, USLE can easily be integrated with the vegetation data obtained by remote sensing and the slope length factor (LS) from Digital Elevation Models (DEM) using GIS. Soil loss can be calculated in grid or pixel level. The model integration with remote sensing and GIS can use the advantages of remote sensing for obtaining vegetation information and GIS for obtaining topographic data but still can not avoid USLE's application problems discussed above. Furthermore, the application of integration was frequently used in non-agricultural land by ignoring the original application conditions of USLE in China (see Lu and Shi, 1994).

Table 1-4, The standard erosion rates for different erosion classes used in China (after Department of Water and Soil Conservancy, 1988)

Erosion classes	Erosion rates (t km^{-2} yr^{-1})
No obvious erosion	<500
Slight erosion	500-2,500
Moderate erosion	2,500-5,000
Severe erosion	5,000-8,000
Very severe erosion	8,000-13,500
Extremely severe erosion	>13,500

1.3.3 Soil erosion investigation by remote sensing

While the erosion plot and model estimation are mainly used for research purposes, large scale soil erosion investigation still relies on remote sensing in China. This work was usually conducted by local soil and water conservation authorities under the direction of central governmental organisation such as Ministry of Water Conservancy. The processes of the work is, first, to identify erosion classes by interpretation (Table 1-4), based on the reflectance of aerial photos or satellite images. Soil reflectance is closely related to vegetation cover and many soil properties such as organic matter (OM), Fe_2O_3, texture, moisture and cation

exchanges, etc. (Xu, 1987; 1991), all of which are also affected by soil erosion for a given soil. Soil reflectance at a certain wavelength increases with the increase of soil erosion classes. In addition, different soil erosion forms, sheet erosion, rill, gully and mass movement, also can be identified from aerial photos or satellite images. This is basic principles for the remote sensing interpretation. However, the reflectance of the land surface is very complicated. The reflectance can be governed by many factors rather than vegetation cover and soil properties. These factors include vegetation type, landform and many other factors. Therefore it was quite often that the standard interpretations, varying from place to place, was drawn by the central government authorities. The remote sensing has many advantages in a large-scale investigation such as less cost and rapid speed, etc. More importantly, erosion history can be retrieved based on past aerial photos or satellite images. However, there are many problems for further consideration. First, the so-called interpretation standards developed by authorities may be very problematic. This is mainly due to the complicated influencing factors on surface reflectance and on soil erosion as well. The newly ploughed paddy field, for example, has a very high reflectance. It is obviously wrong if it is put into the serious erosion class. Second, personal experience plays an important role in interpretation of processes into soil erosion classes, although there is an interpretation standard to follow. The difference between different interpreters may be high; often up to 2-3 erosion classes. Third, and most importantly, remote sensing interpretations can only provide descriptive erosion classes, rather than quantitative erosion intensities. However, these erosion classes are often converted into certain erosion intensities with a range of erosion rates in China (Table 1-4). This conversion causes more problems for the method, since the erosion rates used for this conversion lack sufficient foundation. The reality is that nearly all the inventory data of soil erosion effected areas in China are from this estimation. Therefore, special care must be taken when using this sort of data.

1.3.4 Soil erosion assessment using sediment yields obtained from hydrological measurement

In addition to the three methods introduced above, another common method to evaluate soil erosion is to use sediment load data measured from hydrological gauging stations (hydrography), particularly in China. The earliest hydrological station in the Yangtze river dates from 1865 (Gu and Douglas, 1989) but a network of river gauging and water sampling stations were established after 1950 as part of a major effort to maximise the use of the hydroelectric power potential of the country's major rivers. At the moment, there are about 250 stations with sediment load and many more with water discharge measurement throughout the Upper Yangtze. Sediment load divided by drainage area gives "specific sediment yield" which is usually presented as units of metric tonnes per km^2 per year ($t\ km^{-2}\ yr^{-1}$). The sediment load is the total sediment outflow from a catchment measured at a given cross section of the river. It should include bed load as well as suspended load, but mostly only suspended load is measured due to the difficulty in measuring bed load. Bed load is often assumed to be of minor importance even though in extreme cases it can reach 60% (Lane and Borland, 1951). River station measurements reflect the integrated result of erosional, transportational and depositional processes within the catchment during a certain time, while erosion plot studies only give an indication of the erosional processes on specific types of slope (Jansson, 1988). Sediment yield may be looked upon as *net erosion*, because the material in *gross erosion* measurements (total sheet, gully and channel erosion) may have been deposited many times before it reaches the river, where further deposition may occur on flood plains, in lakes or in broad river sections upstream of the gauging station (Jansson, 1988). At a catchment scale, sediment yield is the best indicator of average soil erosion throughout the catchment. However, there are many problems arising from sediment yield application which need further consideration.

First, the reliability of sediment yield data depends on many factors. The potential sources of error are (1) sampling equipment and techniques of measuring and calculating water discharge; (2) laboratory analysis technique; (3) sampling frequency (Jansson, 1988). If all the methods are standard, the length of record (e.g.

measurement years) is important for assessing the representatives of the data. The length of record may be important for the possible inclusion of high sediment loads generated by large infrequent storms, hurricanes or generated as a consequence of volcanic eruptions or landslides (Meade and Parker, 1985). In general, less than 5 years of measurement is not considered reliable though many studies did not always mention the length of the measurement period (Jansen and Painter, 1974; Probst and Amiotte-Suchet, 1992).

Second, unlike erosion plot measurements, the size of the catchment areas from which specific sediment yield data derive range from very small to very large (over 1 million km^2). Sediment yield-drainage area relationships have been widely examined (Glymph, 1951; Fleming, 1969; Walling, 1983). Traditionally, sediment yield per unit area was plotted against drainage area and it was found that sediment yield decreased with drainage area increase. However, Dedkov and Moszherin (1992) and Slaymaker (1987) also demonstrated that sediment yield might increase with the increase of drainage area. This may happen particularly in mountainous areas (Dedkov and Moszherin, 1992). This area dependent feature makes it very difficult to evaluate soil erosion problem using the data from varied sizes of catchments. This also makes it difficult to map sediment yield (Milliman and Syvitski, 1992), although sediment yield maps have been produced by many researchers at global (Fournier, 1960; Milliman and Meade, 1983; Walling and Webb, 1983; Dedkov and Moszherin, 1984; Jansson, 1988) and regional scales (Gu and Douglas, 1989). More details on sediment yield-drainage basin relationship can be seen in Chapter 2.

Third, previous studies at the global scale used sediment yield data from individual independent catchment but most of the catchments in the Upper Yangtze are nested within each other. The nesting (or hierarchy) problem has not been fully addressed by previous studies. There are no clear established methods on how to calculate and interpolate sediment yield data within nested catchments. There are two alternatives for calculating specific sediment yields in hierarchical sub-catchments. First, it can be calculated by deducing the sediment load at the immediate upstream station from load at the gauging station which is then divided by the incremental catchment area

(Jansson, 1988; Lajczak and Jansson, 1993; Ozturk, 1996). This will give a negative value especially in downstream stretches of a large river, if the river gradient is small and much transported material is deposited in the channel or floodplain. This negative value may indicate there is a real deposition. This is true according to the net erosion concept. However, the deposition may only happen to a small extent such as in lakes, reservoirs, channels and floodplains, therefore the negative value may be misleading for the rest of areas which are mapped using this negative value. The alternative is to express sediment yield as total load divided by total catchment area upstream of the station. This means that the problem of spatial averaging is highlighted in the downstream direction and raises questions such as what is the appropriate mapping unit for those nested sub-catchments?

Table 1-5, The existing soil erosion quantification methods used in China

Method	Time Scale	Spatial Scale	Main problems
Erosion plot	3-5 years	Plot (around 100 m^2)	Time & spatial limitation
Erosion model	Annual average	Field (100-10,000 m^2)	Application condition and extrapolation difficulty
Aerial photograph & Satellite imagery	<40 years	>= County level or Catchment	Interpretation and conversion difficulty
Reservoir investigation	< 40 years	Catchment (<100 km^2)	Lack of trap efficiency and area-dependency
Hydrographic measurement	< 40 years	Catchment (>100 km^2)	Hierarchical and area-dependency
Cs-137 technique	Around 40 years	Point-transect-field-catchment (<100 km^2)	Difficulty for the reference site, uncertainty of input and spatial limitation

1.3.5 Soil erosion assessment using sediment yields estimated from reservoir deposition

Soil erosion can also be quantified using sediment yield data estimated from reservoirs. Numerous reservoirs have been built in China since the 1950s, many of

which have sediment investigation information available. Soil erosion assessment using reservoir sediment investigation is therefore quite common in China. In contrast to hydrographical measurement, reservoir or lake deposition includes bed load, but some fine materials may be lost out of the reservoir's outflow. The ratio of the quantity of sediment deposited in a basin to the total sediment input is trap efficiency. Whitmore et al. (1994) estimated that the trap efficiency for the three lakes in Yunnan province ranges from 76% to 100%. Compared with hydrographical measurement, the size of reservoir catchment investigated for the purpose of erosion assessment is in general smaller. The catchment size is usually larger than 100 km^2 for hydrographic measurement but less than 100 km^2 for the reservoir investigation in the Upper Yangtze (Table 1-4). Another problem for reservoir investigation is that no accurate co-ordinates were given, which means it is difficult to integrate those investigations with broader environmental variables.

The *net erosion* is normally much lower than the *gross erosion*. The ratio of the net erosion to the gross erosion is the sediment delivery ratio. This is an important ratio, because both using downstream estimate of sediment yield (hydrographic and reservoir measurement) to assess soil erosion or using slope erosion to estimate sediment load to the river needs to know the delivery ratio. It is the link between soil erosion within a drainage basin and sediment yield at the basin outlet. This is a very complex ratio and its problem was reviewed by Walling (1983).

1.4 RAPID ASSESSMENT OF SOIL EROSION AND SEDIMENTATION USING THE CAESIUM-137 TRACER TECHNIQUE

These conventional techniques described above provide useful information on the processes of soil erosion and sediment transport, but they are restricted either spatially or temporally. All the quantification methods have been used within the Upper Yangtze, but the long-term patterns and rates of soil erosion and sedimentation are still poorly understood. For example, it is difficult to answer the question, what is the long-term (40 years) erosion rate for those steep arable lands widely distributed in the basin? Erosion plots and models can not answer this question due to their

limitations. In addition, it is often difficult to integrate erosion measurement on slopes with sediment yield data from drainage basins (Sutherland, 1989). This requires an alternative technique beyond the methods reviewed above. Radionuclide tracers provide such tools for erosion measurement and such measurement can be linked with sediment transport if it is integrated with other methods. Any property, or characteristics, which makes it possible to follow the dynamic behaviour of a substance can be considered a tracer (Sutherland, 1989). Various radionuclides (cosmogenic and artificial) have been used in soil erosion and redistribution research (McHenry, 1968), but the one most widely used is Cs-137 (Ritchie, 1975; Campbell et al., 1982; De Jong and Kachanoski, 1988; Sutherland, 1989; Walling and Quine, 1991). More recently, Cs-137 has been coupled with a few other radionuclides such as Be-7 (Burch et al., 1988, Wallbrink and Murray, 1993), excess Pb-210 , Ra-226 and Th-232 (Wallbrink and Murray, 1996; Wallbrink and Murray, 1993).

Cs-137 provides the opportunity to make a quick assessment on the long-term patterns and rates of soil erosion (Ritchie and McHenry 1990). The fallout of caesium-137 (Cs-137), an artificial radionuclide with a half-life of 30.1 years, was introduced into the environment by atmospheric tests of thermonuclear weapons. The technique has been used extensively over the last two decades for tracing soil and sediment redistribution within the landscape and for dating lacustrine and other sediment (Ritchie and McHenry, 1990). This technique has many advantages to investigate soil erosion compared with conventional methods such as runoff plots and remote sensing. Walling and Quine (1990) summarised the following clear advantages:

(1) The erosion rate measured represents the sum of all erosive processes.
(2) The whole field may be studied without disturbance to the slope environment.
(3) The erosion rate measured is an average for the last 25-30 [now over 40] years, and is therefore less influenced by extreme events.
(4) The technique is capable of providing a quantitative measure of both the pattern and the rate of soil erosion, and of the proportion of the eroded soil which is transported beyond the field.

(5) Only a single visit is required to each study site.

Through the comparison of Cs-137 inventories at measured sites with Cs-137 inventories at reference sites (undisturbed sites without erosion and deposition), soil erosion or deposition can be identified. Sites that are experiencing soil erosion will have Cs-137 inventories lower than the reference inventory, whereas sites where deposition is occurring will be characterised by inventories greater than the reference inventory and deeper profile distributions, reflecting the addition of soil-associated Cs-137 to the surface of the pre-existing soil/sediment profile (Walling and Quine, 1990b). The basic unit of measurement is the estimated mass flux at each sampling point. These points can comprise a transect or be allocated throughout a field or catchment. This flexibility may make the Cs-137 technique very useful in the environment such as the Three Gorges area in which varied landuse and soils can be found within a small area and across steep slopes. Cs-137 has also been widely used to date recent sediments from lacustrine, floodplain, wetland and other environments (Foster and Walling, 1994; He and Walling, 1996). This means that the investigation of soil erosion on slopes and sedimentation in reservoirs can be linked, a feature which is unusual in conventional erosion and sedimentation methods. Therefore this study is firstly designed to apply the Cs-137 technique in a small reservoir catchment to examine the patterns and rates of soil erosion and redistribution and reservoir sedimentation. More importantly, the investigation of temporal patterns of sedimentation itself have enabled the effects of intrinsic and extrinsic forcing variables to be examined, thus providing a means of predicting likely future changes in reservoir sedimentation associated with climatic and landuse changes.

1.5 INTEGRATED EXAMINATION OF SEDIMENT YIELDS THROUGHOUT THE UPPER YANGTZE

The Cs-137 technique has mainly been used in relatively small areas (field or small catchment). Although it is possible to conduct Cs-137-based studies at several different locations within a large catchment, it is impossible to conceive a Cs-137-based approach to evaluating a sediment budget for such a large basin as the whole

Upper Yangtze due to its inherent scale handling capability (Table 1-5). Results from the small catchment selected for the Cs-137 study provides information on detailed sediment budgets. To some extent the results from such studies can be regarded as typical of locations with similar environmental characteristics, but clearly cannot cover the whole picture in the Upper Yangtze in terms of climate, geology, landuse and soil variability. The evaluation of overall information on soil erosion and sediment transport in the whole basin requires supplementary methods. In such a large scale, using the network measured sediment yield data throughout the Upper Yangtze presents a suitable way of assessing regional patterns of soil erosion. Therefore, the second part of the study is to examine sediment yield data within the whole Upper Yangtze. As stated earlier, some of the data, particularly data from Yichang Station, have been used for sedimentation analysis in the dam design and its feasibility study (Qian et al., 1988; Gu et al., 1987; Shi et al., 1987). The data, however, have never been used to develop relationships between potential influencing variables and sediment yields, presumably because of the difficulty of obtaining sufficiently detailed information over such a large scale. However, the advent of global environmental datasets offers the potential for integration with sediment yield data (Ludwig and Probst, 1996) with the aid of Geographical Information Systems (GIS).

Human activities such as massive deforestation can result in serious soil erosion and therefore increase sediment load to the river. On the other hand, human activities such as the setting-up of water conservancy projects in headwater catchments can trap a considerable amount of sediment and prevent its transfer to the river either temporarily or permanently. It is estimated that the capacity of total water conservancy projects completed so far in the upstream of the Yangtze River is 16 billion m^3 (Gu et al., 1987) and 0.3 billion m^3 capacity is being lost to sedimentation each year (Chen and Gao, 1988). These two kinds of activities result in some difficulties to the task of attributing sediment yield changes using sediment data from Yichang Station. However, it is likely that the changing trend of sediment yields associated with sediment transport regulation will be detectable in some parts of the basin, through the detailed analysis of the sediment load data.

1.6 MONITORING SOIL EROSION AND SEDIMENT YIELDS

On the basis of basic understanding of soil erosion and sediment yields in the basin, their continuous monitoring appears to be crucial for an effective management of the on-going Three Gorges reservoir in the near future. As described in section 1.2.5, the large scale monitoring of soil erosion and sediment yields mainly relies on hydrographic measurements. The maintenance of the monitoring programs has always been a high cost process. In the current economic situation, there is little possibility to expand, if not shrink, the monitoring network and hence there is an urgent need to find a less expensive approach to monitor or extend large scale soil erosion and sediment yield for ungauged catchments. Empirical or theoretical hydrological modelling seems pragmatic for the purpose but requires detailed information on precipitation and its spatial variability if the catchment is large. In most circumstances the precipitation measurement itself is very limited within a large catchment. Comparatively, as discussed above, remote sensing approaches seem to offer additional capability to other methods. However, the application of remote sensing to soil erosion and sedimentation problems requires a quantitative relationship between soil erosion and the remotely sensed data rather than interpreting soil erosion classes simply based on reflectance as it has been conducted in China (see above for details). The Normalised Difference Vegetation Index (NDVI), derived from the National Oceanic Atmospheric Administration (NOAA), Advanced Very High Resolution Radiometer (AVHRR) satellite data, seems very promising for such monitoring, since they are relatively inexpensive and available on a regular basis (daily or weekly). The remotely sensed NDVI data are related to plant canopy characteristics (see details in Chapter 4), their values are strongly related to leaf area index, percentage vegetation cover and green leaf biomass (Curran, 1980), therefore it has been well examined for vegetation mapping and monitoring (Townshend and Tucker, 1981; Townshend et al., 1987; Townshend and Justice, 1990; Tucker et al., 1983; 1984; 1985; Justice et al., 1985; 1991). Lower values of NDVI represent surfaces with less vegetation or suffering from unfavourable growth.

Since the response of vegetation to climatic conditions, a number of authors have also studied the relationships between NDVI and climatic variables such as precipitation/rainfall, soil moisture and temperature (Malo and Nicholson, 1990; Davenport and Nicholson, 1993; Nicholson and Farrar, 1994; Farrar et al., 1994; Schultz and Halpert, 1993; Schultz and Halpert, 1994). Numerous studies have suggested a simple relationship between NDVI and rainfall, with NDVI generally increasing with rainfall (Nicholson and Farrar, 1994), although the relationship may be more complex (Nicholson and Farrar, 1994; Schultz and Halpert, 1994). More recently NDVI was also used to predict precipitation (Grist et al., 1997). If NDVI has a close relationship with precipitation, it can be argued that NDVI should have an indirect relationship with sediment transport. This highlights the possibility to monitor soil erosion and hence sediment yields using the NDVI data. The study attempts to make a preliminary investigation on the relationship between NDVI and runoff and sediment yields.

1.7 THE AIMS AND OBJECTIVES OF THE STUDY

This study is designed to investigate overall soil erosion and sediment transport within the upper basin of Yangtze, China, at different scales using the two combined methods of the Cs-137 technique and sediment yield data analysis. First, soil erosion and sedimentation will be investigated in detail within a small reservoir catchment using the Cs-137 technique. This small scale study will provide the information not only on long-term patterns and rates of soil erosion on steep arable land, but also sedimentation rates and changes of the reservoir. Soil erosion, sediment delivery and temporal sedimentation changes are fundamental concerns of the first part of the study. Second, suspended sediment data measured at hydrological gauging stations within the whole Upper Yangtze will be examined. Spatial variability, sediment yield changes and the reasons to cause the changes, and sediment yield influencing variables will be examined in this second part. This will provide the basis for the management of the potential sedimentation problems of the Three Gorges reservoir. The third part of the study is to look for the potential to monitor soil erosion and

sediment yield using remotely sensed NDVI data. The detailed aims and objectives of the study are listed below.

1) to examine the potential for using Cs-137 to investigate soil erosion and sedimentation in the particular area dominated with dissected terraces and coarse soil texture;

2) to investigate the long-term patterns and rates of soil erosion on slopes and sedimentation in the reservoir as well as their linkages;

3) to examine spatial variability and temporal changes and the reasons for the change throughout the Upper Yangtze basin;

4) to examine the spatial variability and its relationships with the potential influencing factors such as topographic, hydroclimatic and population density in the Upper Yangtze basin;

5) to investigate the potential to monitor sediment yields in catchment scale using remotely sensed NDVI data.

1.8 THE ARRANGEMENT AND STRUCTURE OF THE THESIS

The thesis is composed of 10 chapters. The second chapter (Literature Review), includes two parts examining previous work on both the Cs-137 technique application and catchment scale sediment yield studies. Chapter 3 (The study area) gives a brief introduction to the selected small catchment within the context of the Upper Yangtze basin. Emphasis is given to providing information on soil erosion and sediment yields and their controlling factors. Chapter 4 (Materals and Methods) outlines the field and laboratory work on soil and sediment samples, the techniques and data sources used for catchment scale sediment yields study. The following five chapters (Chapters 5-9) contain the main results and findings generated from the study. Chapters 5 and 6 are related to Cs-137 technique investigation into soil erosion

on steep arable land and sedimentation in reservoir within a small catchment. Chapters 7 and 8 concentrate on sediment yields studies including spatial variability and temporal changes throughout the Upper Yangtze. Chapter 9 examines the possibility to monitor runoff and sediment yields using remotely sensed NDVI data. The final chapter (Chapter 10) gives a brief summary and conclusion and examines the limitations and prospect of the study.

2. THE Cs-137 TECHNIQUE AND SEDIMENT YIELD DATA ANALYSIS: A LITERATURE REVIEW

2.1 INTRODUCTION

The review consists of two major components: the application of Cs-137 technique in soil erosion and sedimentation investigations, and the analysis of temporal change and spatial variability of sediment yields.

There are a few review papers on the Cs-137 technique (Wise, 1980; Ritchie and McHenry, 1990; Walling and Quine, 1990b), which present information on a range of applications to tracing soil erosion and sediment redistribution, dating lacustrine and other sediment, and fingerprinting sediment sources. More recently, the questions concerning the representativeness of the assumptions of the technique have been challenged (Higgitt, 1995; Quine, 1995). The chapter aims to give a brief review on these questions.

Suspended sediment yield data measured at hydrological stations can be examined in many ways depending upon the study objective. Comprehensive reviews of global sediment yield have been made by Walling and associates at various times (Walling and Webb, 1983; Walling and Webb, 1996; Walling, 1997). As stated previously the fundamental concerns of the study are spatial variability and temporal changes, so the review on the analysis of sediment yield data is mainly focused on these two aspects.

2.2 Cs-137 APPLICATION IN EROSION INVESTIGATIONS

2.2.1 Cs-137 technique and its development

Cs-137, an artificial radionuclide with a half-life of 30.1 years, was introduced into the environment by atmospheric tests of thermonuclear weapons and releases from nuclear reactors. Cs-137 was injected into the stratosphere where it circulated globally and then deposited back on the earth's surface with rainfall as fallout (Longmore et al., 1983; Ritchie and McHenry, 1990). The deposition of Cs-137 is strongly related to the longitude of the earth and local precipitation patterns and rates (Davis, 1963; Longmore, 1983; Basher and Mathews, 1993). Cs-137 with measurable amounts in soils started in 1954, but the major period of global deposition of Cs-137 fallout was in 1963/1964 (Wise, 1980; Longmore, 1983). Properties of Cs-137 make it unique as a tracing technique for studying erosion and sedimentation (Ritchie and McHenry, 1990). Cs-137 is strongly and rapidly adsorbed by soil clay and organic particles and is essentially non-exchangeable, which limits its movement by chemical and biological processes (Schultz et al., 1960; Davis, 1963; Tamura, 1964; Lomenick and Tamura, 1965). Its subsequent redistribution in the environment is associated with physical processes such as erosion and tillage as shown in Figure 2-1 (Wise, 1980). The Cs-137 distribution shows an exponential decrease with soil depth in undisturbed soil profiles and a uniform distribution through the plough layer in ploughed soils (Ritchie et al., 1970; 1972; 1974). The pattern of loss or accumulation of Cs-137 reflects that of the associated erosion or sedimentation and Cs-137 is therefore a very effective tracer of soil movement (Walling and Quine, 1990b). In other words, by comparing the Cs-137 contents of soil cores collected from different locations with a baseline value representing the total fallout to the region, it is possible to assemble information on the patterns and rates of soil loss and accumulation on the basis of a single site visit (Higgitt and Walling, 1993; Higgitt, 1995).

Using fallout radionuclides to study erosion can be dated back to the early 1960s. At this time the environmental mobility of some fallout radionuclides such as Sr-90, S-85 and I-135 were investigated, including mobility induced by soil redistribution, but

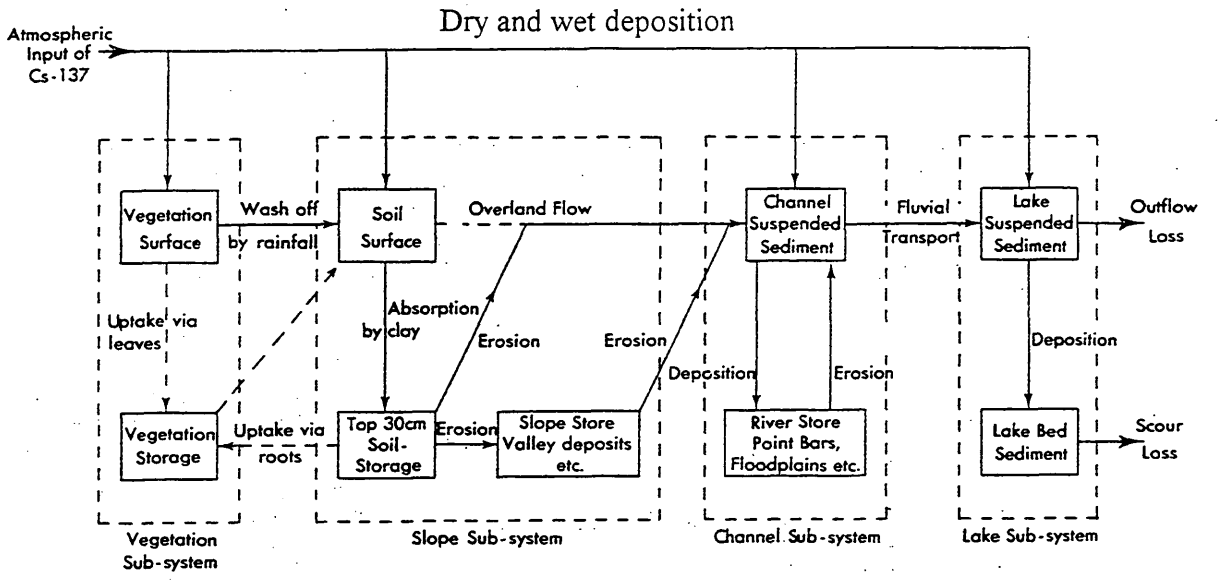

Figure 2-1, A diagram showing the routing of Cs-137 on the landscape (after Wise, 1980)

the potential for using Cs-137 to study erosion did not begin until Rogowski and Tamura (1965) first applied Cs-137 to small grassed test plots in Tennessee and found a logarithmic relationship between measured soil loss and Cs-137 loss (Rogowski and Tamura, 1965). Ritchie et al. (1974) found that fallout Cs-137 loss from different land uses in a watershed had a strong logarithmic relationship with soil loss estimated using the Universal Soil Loss Equation (USLE). Then they combined their results with those of Menzel (1960), Graham (1963), Fiere and Roberts (1963), and Rogowski and Tamura (1970) to show a strong logarithmic relationship between soil loss and radionuclide loss (Ritchie and McHenry, 1990). Since this pioneering work, the technique has experienced a series of overlapping phases (Figure 2-2). The basis for using Cs-137 measurements in erosion investigations is, therefore, now well documented (Wise, 1980) and the value of the technique as a means of obtaining retrospective measurements of long-term patterns and rates of soil loss on the basis of a single site visit is widely accepted (Walling and Quine, 1990), at least in the scientific community. It has been argued that the successful adaptation of the research technique to field situations where information on patterns and rates of erosion is required for management purposes, has yet to be realised (Higgitt, 1995).

2.2.2 The problems

Some uncertainty surrounds the ability of the technique to provide quantitative estimates of rates of erosion (Walling and Quine, 1990b). Many of the simplifying assumptions of the relationship between Cs-137 distribution and soil movement require more detailed investigation:

> "Early applications of the Cs-137 technique tended to take such assumptions for granted, but more recent investigations have attempted to consider the validity, and hence the implications, of these assumptions more fully."
>
> (Higgitt, 1995, p.289).

Except for profound temporal and spatial variation of soil erosion, these uncertainties include the uniformity of fallout (Sutherland, 1991; Owens et al., 1996),

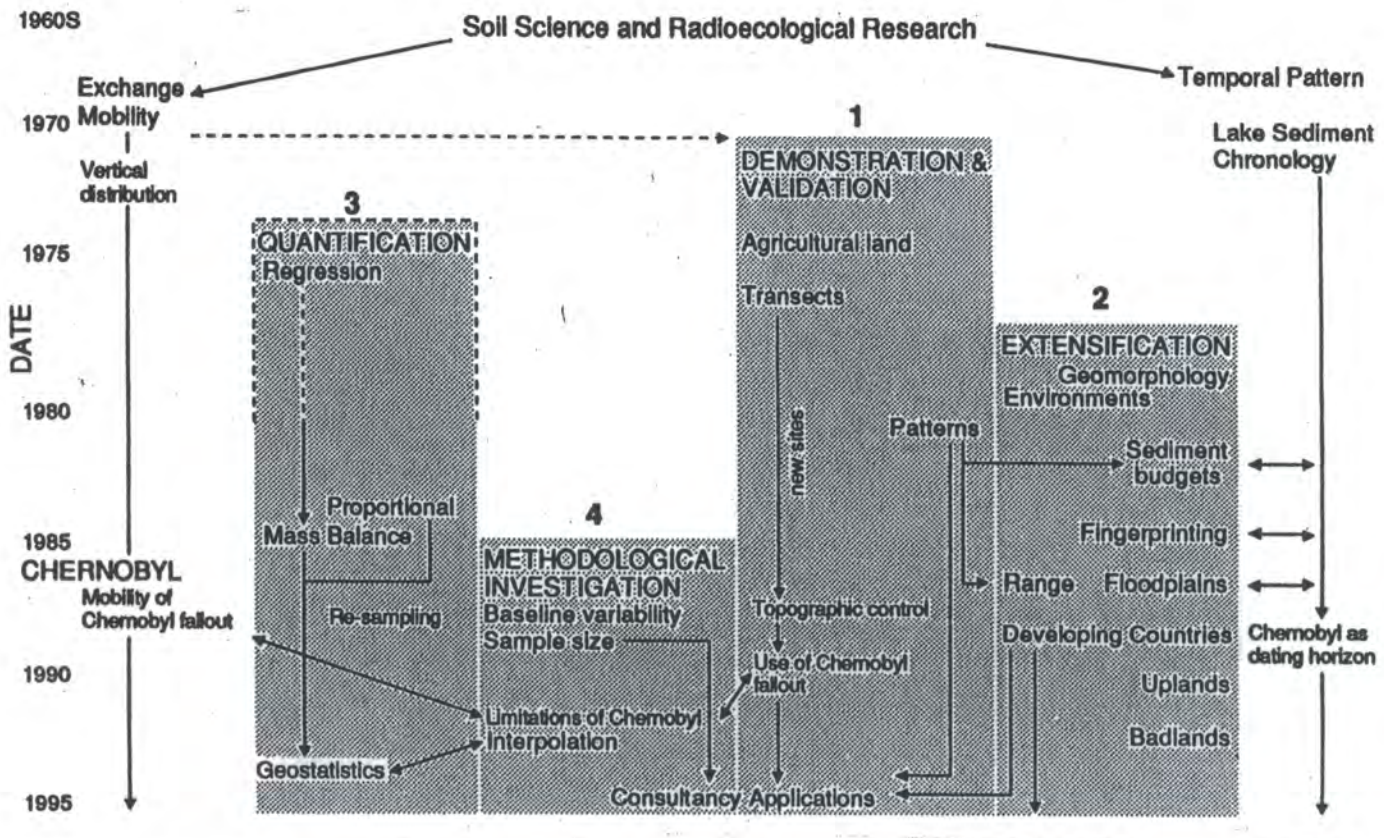

Figure 2-2, The chronological development of Cs-137 applications in erosion investigation (after Higgitt, 1995)

the problem of particle-size sorting (Higgitt, 1995, He and Walling, 1996), Cs-137 loss with runoff prior to adsorption (Dalgleish and Foster, 1996), the methods to calculate soil loss from Cs-137 residuals (Walling and Quine, 1990). For sedimentation dating and fingerprinting, the problems also includes diffusion and focusing (Edgington and Robbins, 1990; He et al., 1996), equifinality due to preferential absorption of Cs-137 in finer soil particles (Higgitt, 1996), and sedimentation rate estimates (Walling and He, 1997).

2.2.2.1 Uncertainty of uniform fallout and uniform adsorption

The baseline Cs-137 deposited in a watershed or a study area is usually estimated by measuring Cs-137 in soil profiles from grass or forest land without obvious erosion and deposition. Many researchers have shown that the spatial distribution of Cs-137 in the reference sites of study area is highly variable. In order to estimate a baseline inventory at a particular level of statistical confidence, a certain number of samples must be required at a given allowable error. Unfortunately, the formulae used to estimate the soil sample numbers proposed by three studies were not same (Sutherland, 1991; Bachhuber et al., 1987; Fredericks et al., 1988). Besides, taking account of the observed spatial variability identified, use of a single figure representing a reference inventory may be misleading (Owens and Walling, 1996). They proposed that a better approach would use a range expressed as the mean value ± SEM (standard error of the mean). The problem with many Cs-137 studies is that they have failed to characterise the statistical variability of Cs-137 within the control locations, and thus their estimates of sediment redistribution are biased (Sutherland, 1991). Table 2-1 summarises the ranges of Cs-137 reference values and their coefficients of variation for some research areas. Coefficients of variation of Cs-137 reference inventories range up to 30% for some places. Factors influencing the variability of Cs-137 in reference sites have not been fully investigated, and there is a distinct need for future work on this topic if Cs-137 is to become a global technique for monitoring sediment redistribution (Menzel et al., 1987; Loughran et al., 1988; Sutherland, 1991).

The variability of Cs-137 within control locations has been statistically examined (Sutherland, 1991; Bachhuber et al., 1987; Fredericks et al., 1988; Owens and Walling, 1996). Higgitt (1995) summarised the possible reasons for the variability as non-uniform deposition of baseline fallout to the area, uneven uptake of Cs-137 at the soil surface, microscale redistribution of topsoil, redistribution of Cs-137 in solution prior to adsorption, and analytical errors associated with the collection, preparation and counting of samples, in addition to the variability attributed to Cs-137 redistribution in association with erosion processes.

2.2.2.2 Uncertainty of rapid adsorption by soil

As mentioned above, redistribution of Cs-137 in solution prior to adsorption by surficial materials may cause Cs-137 variability. The Cs-137 transport with runoff prior to adsorption may also cause problems for sedimentation estimation. Studies following the Chernobyl nuclear accident suggest that on average, about 2% of fallout was transferred directly through 'direct runoff' (Santschi et al., 1988; 1990; Callender and Robbins, 1993) or the 'fast hydrological component' (Smith et al., 1987). The remainder was stored on the watershed and slowly transferred through 'delayed removal' (Santschi et al., 1988; 1990) or the 'slow erosional component' (Smith et al., 1987). It is assumed that this percentage also applies to the direct transfer of Cs-137 where releases are slower than those for Sr-90 used in the analysis of relationship between Sr-90 deposition rates and ensuing concentrations in U.S. rivers (Menzel, 1974; Callender and Robbins, 1993). However, using a rainfall simulator on a small soil box, Dalgleish and Foster (1996) demonstrated that the total amount of Cs-137 lost in solution with overland flow was <0.5% of that applied with simulated rainfall. Although the percentage of the applied Cs-137 is small, it accounted for 21% of the total Cs-137 loss (through runoff, drainage and sediment), which is quite high. Dalgleish and Foster (1996) also demonstrated that the solutional loss of Cs-137 increases with an increase in runoff. Under the subtropical climatic conditions, heavy storms often cause abundant runoff, suggesting that it is likely that higher percentage of Cs-137 could be washed away before being absorbed by soil particles. More importantly, the proportion for reference sites (usually grass

Table 2-1, A summary of Cs-137 variability in the reference sites

Source	Location	Sample numbers	Reference value (Bq/m^2)	Coefficient of variation (%)
Higgitt and Walling, 1993	Bristol, England	11	3099(2478-3890)	13
Loughran et al., 1987	Devon, England	5	4120(3360-4930)	16
		12	3800(2390-5570)	26
Sutherland, 1989	Saskatchewan, Canada	75	2150(2110-2190)	21
Kiss et al., 1988	Saskatchewan, Canada	363	2422(840-4570)	21
Martz and De Jong, 1987	Saskatchewan, Canada	2	2565(2537-2593)	--
Nolin et al., 1993	Quebec, Canada	16	3057(1463-4014)	21
Lance et al., 1986	Oklahoma, US	54	3690(1649-5034)	19
Busacca et al., 1993	Idaho, US	14	(4493-5575)	--
Soileau et al., 1990	Alabama, US	6	4860(4435-5284)	--
Basher and Matthews, 1993	New Zealand	10	568(461-781)	18
		8	710(319-1020)	30
		4	500(432-583)	13
		4	763(636-928)	17
Menzel et al., 1987	Korea	7	3541(2059-4958)	30
Forsyth, 1994	Northern Thailand	7	1199(669-1666)	26
Zhang et al., 1994	Xifeng, China	--	2600	--
Quine et al., 1992	Yangting, China	--	2600	--
McCallan et al., 1980	Australia	6		32*
Brown et al., 1981	Oregon, USA	9		29*
De Jong et al., 1986	Saskatchewan	4		23*
McIntyre et al., 1987	Oklahoma, USA	5		19*
Bunzel and Kracke, 1988	Bavaria, Germany	25		30*
Fredericks et al., 1988	New South Wales, Australia	11		34*
		15		33*

* Cited from Sutherland (1991).

or forest land) may not be same for arable land, indicating the difficulty to incorporate the ratio, which was lost with runoff, into erosion quantification.

2.2.2.3 Uncertainty of uniform distribution through tillage operation

The nature of the depth distribution of Cs-137 is important for erosion quantification. At each tillage event, the radiocaesium deposited at the surface since the preceding tillage event would be mixed through the plough layer (although the degree of homogenisation is uncertain), but in the period between tillage events gradual deposition of Cs-137 would have led to surface accumulation as a result of fallout onto soil particles (Quine, 1995) particularly during the years when majority of Cs-137 fallout took place. Walling and Quine (1990) described the distribution using the formulae:

$$C_d = C_f k e^{-kd} \qquad \text{(Equation 2-1)}$$

$$k = \ln(10)/NL \qquad \text{(Equation 2-2)}$$

Where C_d: Cs-137 activity at depth d (Bq m^{-2} cm^{-1}), C_f: Cs-137 fallout (Bq m^{-2}), d: depth (cm), k: constant and NL: depth above which 90% of fallout is found (cm). This surface accumulation before tillage must be taken into account when quantifying Cs-137 loss into soil loss. In the subtropical areas of the Upper Yangtze, tillage operation is more frequent, two or three times each year, reducing the significance of modelling pre-mixing depth distributions.

2.2.2.4 Uncertainty of preferential adsorption and selective erosion

Detailed examination of the distribution of Cs-137 content within different size fractions has been limited (Higgitt, 1995). Megumi and Mamuro (1977) founded that the concentrations of some uranium series nuclides (U-238, Th-230, Ra-226 and Pb-210) increase with a decrease in particle size (water sieved) in the range of below 0.10 mm, suggesting that the nuclides are mainly enriched in finer particles. Walling and Woodward (1992) confirmed the preferential adsorption of Cs-137 by finer fractions but also demonstrated that Cs-137 was adsorbed by all of the fractions, <8,

8-16, 16-32, 32-63, and >63 μm. This evidence suggests that the preferential transport of fine particles by erosion processes will cause significant bias on the redistribution of Cs-137. However the nuclides-particle size relationship may be very complicated particularly for coarser soils like in the Upper Yangtze (see details in Chapter 3 and 4). The relationship also depends on the sites of erosion and deposition. Higgitt (1995) demonstrated that as the accumulation of Cs-137 at the base of a swale is associated with the deposition of predominantly coarse material, Cs-137 was found to increase with percentage sand content and declined with percentage clay content, while erosional sites appear to lose particles of all sizes, thus maintaining a relatively high clay content but low Cs-137 inventory. The negative Cs-137 and clay content relationship can also be caused by the process in which the fine materials are lost via erosion but supplemented by newly-weathered material with little Cs-137 concentration. Particularly this may happen on purple sandstone in the Upper Yangtze. Another important fact is that in general gravel of >2 mm fraction is not determined for Cs-137 concentration. However, McFarlane et al. (1992) found that the gravel fraction of soil in Western Australia contained up to a third of the total Cs-137 activity. Clearly further research on Cs-137 enrichment, which may be varied at spatial and temporal scales, is required for its incorporation into quantification methods.

2.2.2.5 Uncertainty of atmospheric fallout

Events such as the Chernobyl accident in 1986 have limited impacts on global fallout rates and patterns (Ritchie and McHenry, 1990) but have significant impacts on regional patterns of fallout radioactivity (Higgitt et al., 1992, 1993; De Roo, 1991). The accident resulted in an additional 70 pBq of Cs-137 being released to the atmosphere (Cambray et al., 1989). The fallout was confined to the Northern Hemisphere and was documented mainly in Europe (Hohenemser et al., 1986; Frissel et al., 1987; Rowan et al., 1993). There were also reports in Asia (Aoyama et al., 1986; Cambray et al. 1987). Cambray et al. (1987) estimated that 18% of soil Cs-137 in Hong Kong was from the accident. In Tokyo, Japan, the Chernobyl Cs-137 fallout from 1 to 17 May in 1986 was 0.074 mBq km^{-2}, which was equivalent to 2% of total Cs-137 fallout since 1959 (Aoyama et al., 1986). The deposition must also have

Table 2-2, Cs-137 fallout (Bq m^{-2}, not decay corrected) from selected Chinese nuclear tests recorded in Japan (after Hirose et al., 1987)

Year	6th (6/1967)	8th (12/1968)	10th (9/1969)	11th (10/1970)	15th (6/1973)	16th (6/1974)	21st (11/1976)	26th (10/1980)
1963								
1964								
1965								
1966								
1967	0.2							
1968	47.6							
1969	25.6	29.3	0.4					
1970	8.5	22.6	50.7	0.1				
1971	3.1	7.9	20.1	31.1				
1972	1.2	3.1	7.3	15.9				
1973	0.3	0.8	1.8	4.3	1.4			
1974	0.2	0.4	1.2	2.4	4.9	2.0		
1975	0.1	0.1	0.4	0.7	1.2	14.0		
1976			0.1	0.2	4.3	4.3		
1977				0.1	1.8	1.8	28.1	
1978					1.1	1.0	34.2	
1979					0.4	0.4	14.0	
1980					0.2	0.2	6.1	0.2
1981					0.1	0.1	3.9	26.9
1982							0.8	3.5
1983							0.4	1.7
1984							0.2	0.7
Total	86.9	64.2	82.1	54.9	15.4	23.8	87.6	33.0

happened in China but can not be evaluated due to lack of information in China. The evidence of the deposition was found in some Chinese lakes. This was reported by

Wan et al. (1990) in reservoir sediments in Guizhou of Southwest China which is not far (nearly at same longitude and less than 3 degrees in latitude) from this study site and by Xiang et al (1993) in the lakes of Jiangsu and Anhui of Southeast China. As much of the Chernobyl Cs-137 was transformed by individual rain events, the baseline deposition is highly variable (Higgitt, 1995), this may also be true in China due to a monsoon climate, resulting from highly variable rainfall during its main season of Chernobyl Cs-137 fallout. The high variability of the deposition has restricted the ability of Cs-137 measurements to provide intricate patterns of soil erosion (De Roo, 1991; Higgitt et al., 1992; 1993). Walling and Quine (1991) have suggested that the technique should be used with caution in areas where the Chernobyl-derived Cs-137 input exceeds 25% of the total inventory.

Another uncertainty is the fallout from Chinese nuclear weapons tests. The fallout from Chinese tests can not be fully examined due to lack of information. It is reported that Chinese tests started from 1964 and reached a peak in the late 1970s. Within China there is hardly any record or report on those tests. It is reported that the majority of the fallout, if not all, after 1976 was contributed from Chinese tests. Table 2-2 lists annual Cs-137 deposition originated by a few selected Chinese nuclear tests recorded by the Meteorological Research Institute of Japan (Hirose et al., 1987). The radionuclides fallout from Chinese tests reached the highest in 1977 and 1978. It was estimated that about 12% of total fluvial output of Cs-137 in 1982 in the alpine Rhone watershed of Switzerland would be derived from Chinese explosion in 1981(Dominik et al., 1987). The proportion may be higher in the study area but unfortunately no report has been made within China.

2.2.2.6 Uncertainty of erosion quantification

Another problem for using the technique to investigate erosion and deposition is to establish a calibration relationship which can translate the amount of Cs-137 lost from the soil profile to the rate of erosion and sediment transport. Walling and Quine (1990b), and more recently Quine (1995) have reviewed the calibration techniques and pointed out that estimates of the erosion rate associated with a particular level of

Cs-137 depletion can vary by more than an order of magnitude, according to the calibration relationship used. Two categories, empirical relationships and theoretical models, can be identified (Walling and Quine, 1990b).

Empirical relationships, mainly used by Ritchie and McHenry in USA and by Loughran, Campbell and Elliott in Australia, are developed on the basis of the measurement of Cs-137 depletion in soil profiles and long-term plot-measured or USLE-estimated soil loss. The major limitation of empirical relationships is that it is very difficult to extrapolate them from the area in which they were developed to other areas. It must also be recognised that such relationships will always possess the restriction of being based on net erosion rates for the overall plot and may not be directly applicable to the point measurements of Cs-137 depletion commonly provided by Cs-137 sampling programmes and required in order to investigate detailed patterns of erosion in relation to topography and other variables (Walling and Quine, 1990b).

Theoretical models focus on the relationship between the rate of soil loss and the percentage of the original input lost from the soil profile. Generally, theoretical models were developed on the basis of some important assumptions as discussed above. The main theoretical models can be categorised as proportional and mass balance models (Walling and Quine, 1990b). The proportional model has mainly been used by De Jong and associates, while mass balance models have been advocated by Walling and associates. The mass balance approach calculates the temporal relationship between the change in Cs-137 inventory at a given site and the average annual erosion rate. Interestingly, the concepts of mass balance model were proposed simultaneously by Kachanoski and de Jong (1984) in the soil science community and by McCall and Robbins (1984) in the geochemistry community. In geochemistry the index of Cs-137 loss is termed as residence time (McCall and Robbins, 1984; Smith et al., 1987; Callender and Robbins, 1993) which corresponds to erosion rate. A number of refinements can be incorporated into the mass balance model (Quine, 1995). These include atmospheric fallout deposition (annual or intra-annual variation), radioactive decay, initial soil profile of Cs-137, Cs-137

enrichment, temporal (yearly, monthly or evently) and spatial variation of erosion rates, Cs-137 loss with runoff, tillage and harvest, etc. However, verification of such models will prove difficult, because they are attempting to simulate processes which occurred in the past and which have no direct contemporary analogue (Walling and Quine, 1990b). The development of effective calibration procedures incorporating all possible factors influencing Cs-137 movement and distribution, is needed before the technique for erosion and sediment surveys is to be fully accepted.

2.3 CS-137 TECHNIQUE FOR SEDIMENTATION INVESTIGATION AND SEDIMENT SOURCES FINGERPRINTING

2.3.1 Cs-137 technique and its development

A comparison of the temporal pattern of fallout from atmospheric nuclear testing or release from nuclear facilities to the environment with measurements of Cs-137 in sediment profiles can be used to date different horizons in sediment profiles. By knowing the depths of these different Cs-137 horizons, rates and patterns of sedimentation can be investigated. Similarly, a comparison of source materials with sediment of Cs-137 can be used to identify sediment sources. This is particularly attractive in a comprehensive investigation of soil erosion and sedimentation in a drainage basin.

There are two ways for Cs-137 incorporation in sediment profiles, from the direct deposit of the atmospheric fallout and from runoff and the eroded particles of the upstream watershed (Figure 2-2). In water bodies, Cs-137 deposited on the water surface is adsorbed by suspended materials in the water (Eyman and Kevern, 1975). These suspended materials, which are primarily eroded soil particles and also carry Cs-137, will be deposited as part of the sediment deposition process (Ritchie and McHenry, 1990). The subsequent sediment build-up of these suspended materials will reflect the time distribution pattern of fallout Cs-137.

Two clear dates for sediment horizons (1954 and 1963/4) can be identified in most deposition sites (Ritchie and McHenry, 1990; Higgitt and Walling, 1993). In

addition, 1958 and 1971 sediment horizons can also be identified in some places (Ritchie and McHenry, 1990). The fallout from Chinese tests and the Chernobyl accident may cause problems for erosion measurement but may provide opportunities as dating markers. Thus, with several depositional horizons marked by Cs-137, comparison of sedimentation rates can be made for different time periods (Ritchie and McHenry, 1990; Higgitt and Walling, 1993). The Cs-137 dating technique can be used to determine sediment accumulation rates in a wide variety of depositional environments, including reservoirs, lakes, wetlands, coastal areas and floodplains (Ritchie and McHenry, 1990), to trace recent ecological changes, but the method would be best used in conjunction with other independent techniques (Higgitt and Walling, 1993), because of some limitations for the dating technique such as diffusion, focusing and the problem of equifinality.

2.3.2 The problems

2.3.2.1 Post-depositional movement

Cs-137 markers described above must be preserved well so that they can be used for dating. There are a number of factors such as physical reworking by animals, wave action, diffusion, biological mixing and horizontal focusing, which can affect Cs-137 post-depositional redistribution (Ritchie and McHenry, 1990). Post-depositional movements can spread Cs-137 over a large part of the profile and reduce maximum concentrations of Cs-137. In general, most of those post-depositional movements will not change the position of the major Cs-137 horizon (Ritchie et al., 1973), except for diffusional movement.

Generally, caesium (Cs^{+}) is strongly sorbed by illite in aquatic environments although there is some desorption on time scales of weeks to months (Comans et al., 1991). Cs is absorbed faster in a Ca^{2+} rich environment than in a K^{+} rich environment (Callender and Robbins, 1993). Ritchie and McHenry pointed out that although diffusional movement is usually limited for Cs-137, it does occur and can be a problem in certain environments. Diffusional movement of Cs-137 has a great effect

on the location of the Cs-137 horizon deposited in 1954; thus, care needs to be taken in determining the location of this horizon (Ritchie and McHenry, 1990). Due to the diffusional movement of Cs-137, the 1954 sediment horizon is getting more difficult to identify. In general, a long tail can be found in Cs-137 profiles. It is believed that the tail is due to Cs-137 diffusion. In addition, radioactive decay of Cs-137 continues to reduce the amount of Cs-137 in the environment and thus limits the detection of the 1954 horizon due to the small amount of Cs-137 originally present in the 1954 horizon (Campbell, 1983; Ritchie and McHenry, 1990).

2.3.2.2 Equifinality

The particle size distribution within the sediment profile greatly affects the Cs-137 content because Cs-137 is strongly adsorbed on clay particles. An increase in the amount of sand-size particles in sediment profiles will cause an apparent decrease in the concentration of Cs-137 at that point in the sediment profile that can not be related to any time change in atmospheric fallout rates of Cs-137 (Ritchie and McHenry, 1990). The authors suggested that it is probably better to express Cs-137 concentration in units per unit of clay to account for the differences in Cs-137 distribution due to differences in particle size distribution in the sediment profile.

The selective processes of erosion, and transformation of sediment properties within the fluvial system can also cause problems for sediment source identification. Peart and Walling (1988), therefore, advocated the use of several alternative diagnostic properties, rather than a single Cs-137 indicator, in order to establish the consistency of the results obtained. These include a range of properties such as sediment colour (Grimshaw and Lewin, 1980), clay mineralogy (Wall and Wilding, 1976), sediment chemistry (Peart and Walling, 1986; Collins et al., 1997), and mineral magnetic parameters (Oldfield et al., 1979; Oldfield and Clark, 1990; Foster and Walling, 1994). Multivariate mixing models can be developed to integrate those diagnostic properties for fingerprinting sediment sources (Collins et al., 1997). Besides, it is impossible to identify the sediment deposited before (1954) and during the main period of Cs-137 fallout (1954-1970), because the sediment deposited before 1954 would not be labelled with Cs-137 and the sediment deposited during 1954-1970

would contain radiocaesium associated with direct fallout to the lake surface as well as that originating with the eroded source materials (Foster and Walling, 1994).

2.3.2.3 Sedimentation rate estimation

Similarly as erosion rate estimation, sedimentation rates in lacustrine environments can also be estimated using different methods with varying complexities. First, the dating positions as mentioned above can be used to estimate accumulated sediment depth and hence sedimentation rate (Ritchie et al., 1986). However, it is necessary to take account of the potential for post-depositional redistribution in the sediment profile, since this could influence those peak depths and the maximum depth to which Cs-137 is found. It is also necessary to take account of Cs-137 residence time in the water body. The residence time can be very long, depending on the characteristics of water body such as water depth. Second method therefore is to model sedimentation rate. Callender and Robbins (1993) proposed two models: Constant Sedimentation Rate Model (Model I) and Variable Sedimentation Model. Using Model I sedimentation rate and residence time can be estimated using least squares fit to the data (giving a smooth curve which best fits the shape of Cs-137 profile). The residence time was the lowest in the vicinity of the delta (3.3 years) and nearly twice as high in the open lake (5.7 years) for Lake Oahe in Missouri River (Callender and Robbins, 1993). Similar approaches were used to interpret the Cs-137 profile (Robbins, 1986; Smith et al., 1987; Robbins et al., 1990). Callender and Robbins (1993) and He et al. (1996) also attempted to incorporate multiple-source transfer of the isotope into their models. However, unlike previous studies He et al. (1996) ignored the residence time but incorporated a Cs-137 enrichment ratio for possible sediment sources and diffusion coefficient D (g^2 cm^{-4} yr^{-1}). Nevertheless, sedimentation rate is still assumed to be constant throughout the sedimentation period for their complex model. Like erosion calibration models, the development of effective methods incorporating all possible factors influencing Cs-137 activity at a given depth, is needed. The variable sedimentation rates and temporal changes of possible sediment sources are particularly important for the sediment whose characteristics are mainly controlled by catchment-derived materials.

2.4 TEMPORAL CHANGES OF SUSPENDED SEDIMENT YIELD

While Cs-137 methods can be used to date recent sedimentation changes over past 40 years, available hydrographical data are more commonly used to evaluate a broad hydrological change.

> "Assessment of the significance of anthropogenic activity in changing the sediment loads of the world's rivers affords a useful perspective on global change, but this should be coupled with more wide ranging analysis of the sensitivity of sediment yields to various facets of environmental change, including climate change. Sediment yields represent a key parameter in understanding the global system and assessing its sensitivity to change, but it must also be recognised that sediment transport by rivers has an important social and economic dimension related problems of reservoir siltation and other aspects of water resource development as well as wide-ranging environmental implication, all of which further underscore the importance of its study".
>
> Walling and Webb (1996, p.17)

It is well known that soil erosion rates can increase by an order of magnitude or more under cultivation and other agricultural activity. Walling and Webb (1996) reported that the 99,400 km^2 basin of the Kolyma River in western Siberia had a clear evidence of increasing sediment yields during the period of 1941 to 1964. This upward trend of sediment yield is highly significant at the >99% level. There is no significant change in annual runoff over the period of record and the increased sediment yields can be accounted for by the impact of gold mining activity within the drainage basin. The annual sediment load transported by the River Nile to its delta has decreased from c.100×10^6 t yr^{-1} to almost zero as a result of the closure of the Aswan Dam (Walling and Webb, 1996). Meade and Parker (1985) documented the case of the Missouri River where the construction of five major dams between 1953 and 1963 reduced its load entering the Mississippi to only about 25% of its former value. Since the Mississippi River formerly represented the major supply of sediment to the Mississippi, the sediment load of that river has also declined and the load at its mouth in 1984 was less than one-half of the value before 1953. While there is clear

evidence of the significance of human activity in influencing the sediment loads of some rivers, few systematic evaluations of sediment yield changes within a large basin have been reported. This section gives a brief overview on the methods of discrimination and the difficulties in detecting the change using hydroclimatical data.

2.4.1 Methods to detect the change

There are many statistical procedures for determining the change of time series data such as precipitation, temperature and runoff but more frequently used procedures include moving average (or running mean), linear regression and Mann-Kendall rank correlation.

2.4.1.1 Running mean

Running mean is a conventional procedure used for trend description. The artificial smoothing effect of this procedure suggests climatic evolution which is independent of the non-random components, and the true properties of non-linear components are modified (Sneyers, 1992). The running mean can reduce natural variability for rainfall data which are much more pronounced than temperature. In rainfall change detection, the running mean is used for smoothing data before further analysis (Loureiro and Coutinho, 1995).

2.4.1.2 Linear regression

For each time series linear regression can be used to calculate the slope of the trend by the least squares method for all the pairs of values: time and the corresponding hydrological variable. This is a frequently used method to detect sediment yield change along with runoff data. Student's *t*-test or the correlation coefficient can be used to test the significance.

2.4.1.3 Mann-Kendall correlation

Mann-Kendall test, a rank correlation, is directly analogous to regression. Its application can be stated most generally as a test for whether the variables tend to increase or decrease with time (monotonic change). The Mann-Kendall test does not require assumption of normality but there must be no serial correlation for the resulting p-value to be correct. If a monotonic transformation such as the ladder of

powers is all that is required to produce constant variance, the test statistic will be identical to that for the original units (Helsel and Hirsch, 1992).

Helsel and Hirsch (1992) compared the two methods of linear regression and Mann-Kendall correlation. "If the variable is linear with time and the residuals are truly normal, then fully-parametric regression (linear regression) would be optimal most powerful and lowest error variance for the slope. If the actual situation departs, even to a small extent, from this assumptions then the Mann-Kendall procedures will perform either as well or better."

2.4.1.4 Non-linear regression

Linear regression sometimes is not adequate for revealing a statistically significant trend. In this case, a non-linear regression such as polynomial regression model might reveal the trend. If a trend is detected over the whole length of a time series, it is termed *long lasting*, otherwise it is referred to as *local* (Kottegoda, 1980). Giakoumakis and Baloutsos (1997), for example, used a fourth degree polynomial model to examine rainfall and runoff change. Polynomial regression is particularly powerful for revealing the local changing trend. Similarly as linear regression, the significance can be tested using Student's two-tailed *t*-test.

2.4.2 Discrimination of the change

The existence of an increasing or decreasing trend in a hydrological time series can also be induced by climatic factors. Climatic forcing was more important than land use change in causing increased sediment yields (Walling and Webb, 1996). If a trend is detected, this trend resulting from changes in land use is difficult to detect unless variations in sediment loads that result from runoff variations are removed from the analysis. The discrimination methods include cumulative double mass (sediment yield and runoff) plot and runoff variation removal.

2.4.2.1 Double mass curve

Plots of cumulative runoff against cumulative sediment yield have been used to illustrate graphically the changing relationship between sediment yield and runoff

(Walling and Webb, 1996). Assuming that there is a linear relationship between annual runoff and sediment load, although it is not true in most cases, and the effects of increased runoff will therefore not be reflected by a change in the slope of the double mass plot. The break in the double mass plot suggests the time and impact of land use or catchment characteristic change. Using the method, Walling and Webb (1996) estimated that sediment yield for a catchment of 850 km^2 in the Ukraine has experienced a 1.8 fold increase in the sediment load due to the disturbance by forest clearance.

2.4.2.2 Runoff variation removal

Helsel and Hirsch (1992) proposed that the effects of runoff variations can be removed by computing logarithmic least-squares linear regression equations for sediment load and runoff. The regression residuals (the differences between the observed and predicted values of sediment loads in logarithmic units) are therefore a measure of the variations in sediment loads due to land surface changes. The regression residuals can then be plotted against time to provide a picture of trends. The presence or absence of significant trends can be determined with the Mann-Kendall test.

2.4.3 Difficulties in detecting the change

Sediment yield changes caused by land use change may not been documented through river measurement, due to considerable temporal and spatial discontinuity in the erosion-sediment yield relationship (Walling, 1983). For example, Alford (1992) reported a study of the 14,028 km^2 Chao Phraya river basin draining the highlands of northern Thailand which showed no evidence of a significant increase in sediment yield during the period extending from the late 1950s to the mid 1980s, despite substantial deforestation and extensive expanding agriculture within the basin. This is a similar case as in Yichang station of the Upper Yangtze as introduced in the last chapter. No obvious changes in sediment load may be due to the location of hydrography in the river or more likely due to sediment deposition in the reservoir if there is any, because compared with the increased amount of sediment caused by agriculture activity, the construction of reservoirs can trap considerable amount of

sediment load transported by the river. It is estimated that the capacity of total water conservancy projects completed so far in the upstream of the Yangtze River is 16 billion m^3 (Gu et al., 1987) and 0.3 billion m^3 capacity is being lost to sedimentation each year (Chen and Gao, 1988). Furthermore, the important role of smaller dams and reservoirs in trapping sediment transported from upstream tributaries must also be considered. Walling and Webb (1996) concluded that it seems likely that in some areas of the globe increases in sediment transport caused by land clearance and land use change have been balanced by reductions caused by reservoir development. On the other hand, when improved land use practices were introduced, sediment yield may not decline to the extent that might have been expected, since previous alluvial deposits can be remobilised and transported out of the system (Trimble, 1981).

2.5 SPATIAL VARIABILITY OF SEDIMENT YIELD

Sediment yields and their potential influencing variables have been extensively examined at the global and regional scale. Traditionally these examinations were mainly focused on a few variables such as drainage area and runoff (Table 2-3). The selection of variables has been mainly constrained by availability of information that corresponds to the sediment load data . Moreover, it was quite often that each of the variables examined such as precipitation, temperature and elevation was represented by only one value for each basin. However, the advent of global environmental datasets offers considerable potential for integrating many important environmental variables with sediment yields data through the aid of GIS as Walling and Webb (1996) stated:

> "The marked increase in data availability [sediment yield] that has occurred in recent years now affords a meaningful basis for estimating the annual suspended sediment flux from the land to the oceans and for establishing the key features of the global variation of sediment yield across the land surface of the globe. Scope now exists to undertake more detailed analysis of the

Table 2-3, The potential influencing variables examined in global and regional scales

Authors	Drainage area	Climate & Hydrology				Morphometry & drainage networks						Land surface			Others	
	DA	PP	FN	T	Q	ME	MS	LR	BR	RR	HI	G	S	V	PD	CA
Milliman & Meade, 1983	#				#											
Milliman & Syvitski, 1992	#				#											
Jansen & Painter, 1974	#	#		#	#	#				#		#		#		
Probst & Amiotte-Suchest, 1993	#				#							#				
Neil & Mazari, 1993	#								#					#		
Summerfield & Hulton, 1994	#	#		#	#	#		#	#	#	#					
Ludwig & Probst, 1996	#	#	#	#	#	#	#		#			#	#	#	#	#

Note: DA: drainage area (km^{-2}), PP: precipitation ($mm\ yr^{-1}$), FN: Fournier index, the sum of square of mean monthly precipitation over mean annual precipitation for all 12 months of the year, T: temperature (^{o}C), Q: runoff ($mm\ yr^{-1}$), ME: mean elevation (m), MS: mean slope (degree), LR: local relief (m), BR: basin relief (m), RR: relief ratio ($m\ km^{-1}$), HI: hypsometric integral (%), G: geology (the indices for erodibility of the dominant basin lithology with regard to mechanical and chemical erosion), S: soils (representing soil texture, soil depth and soil organic carbon, see Ludwig and Probst (1996) for details), V: vegetation types or covers, PD: population density (people km^{-2}), CA: the percentage of the cultivated area.

magnitude and spatial variability of sediment yields. Such analysis could be greatly aided by the availability of a range of global environmental data bases and the use of GIS techniques".

Walling and Webb (1996, p.17)

A variety of global datasets with varied resolution have been developed. These include topography, soil, vegetation and population data some of which will be introduced in Chapter 4. These variables can be integrated with global sediment and runoff dadasets using GIS as a tool. More importantly, most of those variables can be averaged through the basin and thus can represent internal variability across the basin. For example, Ludwig and Probst (1996) examined many variables by employing such datasets (Table 2-3). The next section gives a brief review of those frequently examined variables.

2.5.1 Drainage area

Relationships between specific sediment yield and drainage area have been extensively examined through plotting specific sediment yields against drainage area. The sediment delivery characteristics were depicted by the exponent of the relationship. Many researchers reported that sediment yields exponentially decreased with drainage area increases (Glymph, 1951; Fleming, 1969; Walling, 1983). Figure 2-3 shows the sediment yield-basin area relationship. The drainage area itself does not have a direct effect on soil erosion and hence sediment yield. The effect of drainage size can be explained in several ways.

"Small basins generally have steep slopes, steep channels, and other topographic characteristics that favour sediment movement. Also small basins tend to have limited floodplain development, so that most of the material eroded from the basin is flushed out of the system, and little is redeposited within the area. Local factors that favour rapid erosion, such as weak bedrock material, are also more effective in small basins than in large ones."

Wilson (1973, p.343)

However, this is a complex issue as demonstrated by data from western Canada which shows that sediment yields are lowest in the smallest basins (<100 km^2), highest in intermediate sized catchments (1,000-100,000 km^2) and intermediate in the largest basins >100,000 km^2 (Slaymaker, 1987).

Dedkov and Moszherin (1992) summarised the relationship between sediment yield and drainage basin area. Sediment yield could increase or decrease with drainage area, depending on dominant erosion types: channel and slope erosion. The specific sediment yield is positively related to basin area for the basins which are characterised by a predominance of channel erosion, whereas the specific sediment yield has an inverse relationship with basin area for the basins which are characterised by a predominance of slope erosion (sheet and gully).

While sediment yields are compared for disparate river basins using the above method, Waythomas and Williams (1988) and recently De Boer and Crosby (1996) have argued that statistically the comparison of sediment yields vs drainage area can give spurious results, since basin area is common to both axes. Waythomas and Williams (1988) suggested that some surrogate of basin area should be used. They made the case for replacing drainage area with a surrogate in bivariate correlation with sediment yields/loads and found a very strong correlation between distance downstream and sediment load for the Mississippi River. Waythomas and Williams (1988) and de Boer and Crosby (1996) also recommended the use of sediment load rather than specific sediment yields.

2.5.2 Hydroclimatic variables

The frequently examined hydroclimatic variables have been focused on precipitation and runoff (Fournier, 1949; Langbein and Schumm, 1958; Jansen and Painter, 1974; Summerfield and Hulton, 1994; Ludwig and Probst, 1996). Fournier (1949) first established the relationship between sediment yields and precipitation. The relationship showed that two peaks in sediment yield-precipitation curve: one for semi-arid or arid conditions, the other for tropical-wet conditions. The minimum

sediment yields occurred at a precipitation of about 890 mm a year. Using small basins in the central and eastern parts of the United States (in areas of agricultural land use), Langbein and Schumm (1958) also established the relationship between effective precipitation and sediment yields. This relationship shows that sediment yields increase with low precipitation and then decrease in areas of medium precipitation (Figure 2-3). A maximum of sediment yields occurs when effective precipitation is around 300 mm. The sediment yields-precipitation relationship has been termed the Langbein-Schumm Rule" by Fairbridge (1968, p.1126), who considers it a principle of fundamental geomorphic importance (Wilson, 1973). This is because the spatial variation in precipitation changes vegetation type, and the latter in turn changes the land surface erosional resistance, leading to a reduction in erosion intensity. The peak at 300 mm represents the precipitation that promotes ample runoff, yet a plant cover that is not quite sufficient to inhibit effectively erosion processes (Wilson, 1973). The location of the peak in the relationship can shift in response to several factors and need not occur at exactly 300 mm mean precipitation (Wilson, 1973). Douglas (1967) used data from tropical regions to suggest that for very humid areas the Langbein-Schumm curve might be correct rather than the curve published by Fournier. Douglas pointed out many problems associated with a study of sediment yield, especially the importance of non-climatic factors such as land use. He concluded that since virtually no data are available from undisturbed watersheds, it is not practical to extrapolate present rates of erosion into the past (Wilson, 1973). Rango (1970) published a parabolic curve that showed maximum sediment yield at about 710 mm mean annual precipitation. This precipitation value is more than twice as large as that indicated by Langbein-Schumm. Using approximately 1500 drainage basin sediment yield data from throughout the world, Wilson (1969) also published a sediment yield-precipitation relationship (dashed line in Figure 2-4). The relationship showed that there were two sediment yield peaks at 762 mm and 1768 mm and a minimum sediment yield at 1000 mm mean annual precipitation. The literature thus contains curves that predict maximum sediment yield under semi-arid or arid conditions (Fournier, 1949; Langbein and Schumm, 1958), subhumid conditions (Rango, 1970) and tropical conditions (Fournier, 1949; Wilson, 1973).

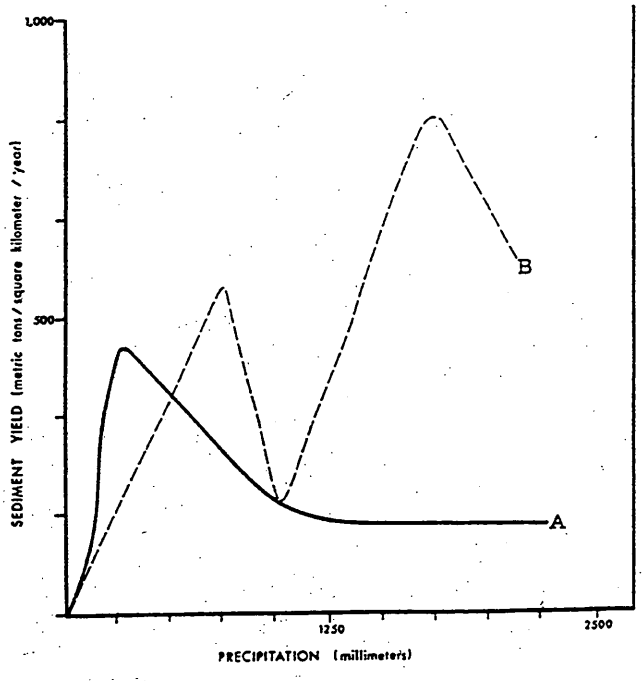

Figure 2-4, Relationships between mean annual sediment yield and mean annual precipitation in drainage basins (after Wilson, 1973)

A. Solid line obtained by Langbein and Shumm (1958) using about 265 basins from the United States.

B. Dashed line obtained by Wilson (1969) using 1500 basins from throughout the world. Data adjusted to basin area of 259 km^2.

Other workers, however, have noted a variety of sediment transport trends relative to precipitation (Ahnert, 1970), leading to the conclusion that,

> "Current evidence concerning the relationship between climate and sediment yield emphasizes that no simple relationship exists"
>
> (Walling and Webb, 1983, p.84).

Recent global scale studies (Summerfield and Hulton, 1994; Ludwig and Probst, 1996) have not demonstrated polynomial relationship between precipitation and sediment yields. However, the Langbein and Schumm (1958) model has won some support in China. Xu (1994) demonstrated that the relation between sediment yield and annual runoff using 700 Chinese river basins (<10,000 km^2) is similar to the Langbein-Schumm's curve, with the maximum sediment yield appeared when runoff was around 40 mm. The contribution of azonal factors such as loess to sediment yield may greatly exceed that of zonal factors but have not changed the macroscopic zonal distribution of sediment yield in the whole of China (Xu, 1994).

2.5.3 Topographic variables

More recently, Pinet and Souriau (1988), Milliman and Syvistski (1992) and Summerfield and Hulton (1994) have emphasised the importance of relief in accounting for global variations in sediment yield (Walling and Webb, 1996) but the frequently examined topographic variables are relief and relief ratio (Table 2-3). This may be due to the fact that maximum and minimum elevations for a catchment can be easily obtained without a detailed contour map, or they can be easily expressed numerically and therefore can be manipulated as a statistical variable (Milliman and Syvitski, 1992). With the aid of GIS, many topographic variables now can be extracted from a DEM so that more topographic variables can be integrated with sediment yield data analysis. For example, mean elevation defined as mean of modal elevation of each grid cell, and mean local relief defined as mean of maximum-minimum elevation within each grid cell, were used by Summerfield and Hulton (1994), whereas mean elevation and slope calculated from DEM were used by Ludwig and Probst (1996). Those studies have demonstrated that sediment yields are

increased with the increase of elevation or relief. Since elevation itself has no effect on sediment yields, Milliman and Syvitski (1992) emphasised that elevation or relief is, in some ways at least, only a surrogate variable for tectonism. The strong correlation between sediment and topographic relief may not indicate that the second is the cause of the first, but rather that both are caused by another factor less susceptible to numerical description-namely, tectonism. It is probably the entire tectonic milieu of fractured and brecciated rocks, oversteepended slopes, seismic and volcanic activity, rather than simple elevation/relief, that promotes the large sediment yields from active orogenic belts (Milliman and Syvitski, 1992).

2.5.4 Geology, soils and land use

The hydroclimatic and topographic variables discussed above are erosive variables and the role of ground erodibility must also be taken into account. Erodibility factors mainly include geology, land use and soils and by comparison with hydroclimatic variables have received less examination. This may be due to the difficulty in obtaining those variables compared with drainage area and some of the erosive variables. In fact, those erodibility factors are arguably much more important than erosive variables in the role of sediment production. Dedkov and Moszherin (1992) reported in the world-wide the sediment yield generated by different rock types as loess, 1800; terrigenic loose rocks, 1300; coarse terrigenic rocks, 550; metamorphic, 420; limestone, 310 and igneous, 100 t km^{-2} yr^{-1}. The importance of different land use or land use change for sediment yield has already been introduced in section 2.5.1. Land use factors can control the location of the peaks in Langbein-Schumm (1958) curve, as well as the magnitude of the peaks (Wilson, 1973). Thus the magnitude of sediment yield values shown in Figure 2-4 for the dashed line is in large part a function of land use practices, not climate (Wilson, 1973). Milliman et al. (1987) concluded that the Yellow River's sediment load was an order of magnitude lower before humans began farming in the Loess Plateau. Saunders and Young (1983) suggested that moderate land use can increase sediment yields by a factor of 2-3, while intensive land use can increase it an order of magnitude. In addition to the difficulty to obtain the information on geology, soils and land use, most of those erodibility factors are difficult to express numerically, therefore dummy variables

have been used. For example, Jansen and Painter (1974) classified geology and soils into the 4 categories based on rock hardness and the cohesion and consolidation of soils: Quaternary, 2; Paleozoic, 3; Mesozoic, 5 and Cainozoic, 6; and vegetation into 3 groups based on the order of decreasing protection, Desert, 1; Steppe, 2; Grass, 3 and Forest, 4, while Probst and Amiotte-Suchet (1992), and Ludwig and Probst (1996) classified rock types based on their mechanical and chemical erosion. Probst and Amiotte-Suchet (1992) gave each lithological formation a coefficient which represents rock erodibility. The coefficient is the ratio between the mechanical denudation rate of a given rock and the denudation rate of granite which is considered to be most resistant to mechanical erosion. Rock erodibility coefficients calculated by Probst and Amiotte-Suchet (1992) are as follows: Granites, 1; Sandstones and limestones, 4; Schist/Micaschists, 10; Shales/Pelites/Marly sandstones/ Marly limestones, 27 and Marls, 50. While the dummy numbers can relatively give an information on those different rocks and land use, such a procedure may seem to be somewhat arbitrary and risk introducing bias. With the rapid development of global ecological databases, it is believed that those important erodibility variables with higher resolution can soon be integrated with sediment yield studies.

It is difficult to imagine any single variable that would explain more than a small amount of the variation in sediment yield observed throughout the world (Wilson, 1973).

> "If one such variable exists, it is probably a function of land use rather than of climate"
>
> (Wilson, 1973, p.339).

This requires multi-component models and equations, which utilise climatic and non-climatic (for example, topography, lithology, tectonic activity, soils and land use) variables. A few attempts have been made to develop such models for the purpose of estimating the sediment flux discharged to the ocean (Table 2-4). It can be seen that the variety of the influencing variables were incorporated into the models. In recent

Table 2-4, A summary of a few models to predict sediment yield

No	Models	Variables	Sites	Authors
1	FTSS=0.02(Q*Slope* Four)	FTSS: sediment yield (t km^{-2} yr^{-1}) Q: drainage intensity (mm yr^{-1}) Slope: average basin slope (degree) Four: Fournier (mm yr^{-1})	Global	Ludwig and Probst, 1996
2	SY=10.9+0.248Cul-0.043Pn+0.045Pi-0.736Dam+3.802Rd+5.678Gu	SY: sediment yield (t km^{-2} yr^{-1}) Cul: % area cultivated Pn: % area native pasture Pi: % area improved pasture Dam: number of dams (km^{-2}) Rd: length of unsealed roads (km km^{-2}) Gu: length of gullies (km km^{-2})	New South Wales	Neil and Mazari, 1993
3	Ln(Tss)=4.79+0.054Ker+0.004R-0.000056A	Tss: sediment yield (t km^{-2} yr^{-1}) Ker: rock erodibility R: mean annual rainfall (mm) A: basin area (km^2)	North Africa	Probst and Amiotte-Suchet, 1992
4	Tss=26.62IL+5.07IP+9.77CT-593.56	Tss: sediment yield (t km^{-2} yr^{-1}) IL: marly rock/total basin area IP: the product of % and frequency of rainfall >20 mm CT: the product of DD and elementary thalweg frequency	North Africa	Demmak, 1984
5	LogS=2.032+0.1LogD +0.314LogA +0.75LogH +1.104+LogP +0.368LogT -2.324LogV +0.768LogG	S: sediment yield (t km^{-2} yr^{-1}) D: runoff (10^3 m^3/km^3) A: basin area (km^2) H: altitude (m) P: precipitation (mm) T: temperature (°C) V: vegetation type G: rock hardness	Global	Jansen and Painter, 1974

global scale studies, using sediment yield data from 33 major world rivers, Summerfield and Hulton (1994) found that the greatest degree of statistical explanation was provided by variables reflecting catchment relief as represented by the basin relief and relief ratio and runoff. These two variables alone account for over 62% of the variance in denudation rates.

> "This is a remarkably high amount of explained variance given the low data quality and the fact that only erosivity variables are included."
>
> Summerfield and Hulton (1994, p.13881)

More recently, using sediment yield data from 58 major world rivers, Ludwig and Probst (1996) found that the three variables, runoff, modified Fournier index (1960) and slope could explain more than 80% of the variance. In terms of the main controlling variables this is quite similar to Summerfield and Hulton's (1994) finding. The estimation of sediment flux to the ocean, Ludwig and Probst's (1996) was 1.48 billion tonnes, whereas Jansen and Painter's (1974) was 2.67 billion tonnes. These two estimations have an almost 100% difference. Therefore, more improvement is required. Recent advances in the development of detailed global environmental and ecological databases coupled with GIS techniques clearly offer considerable potential for such estimation. Meanwhile, more work is clearly required to clarify the relative importance of the variables such relief and climate in influencing the global pattern of sediment yield. Recent increases in data availability will undoubtedly facilitate such work, but there is also a need to develop more meaningful indices to assist in establishing the key relationships involved (Walling and Webb, 1996).

2.6 SUMMARY AND CONCLUSION

The chapter gives a brief review on the key problems for using the Cs-137 technique to investigate soil erosion and sedimentation, and fingerprinting sediment sources. These problems include:

- Uniform fallout and uniform adsorption
- Rapid adsorption by soil
- Uniform distribution through tillage operation
- Uncertainty of atmospheric fallout
- Erosion quantification methods
- Post-depositional movement (diffusion and focusing) in waterbody
- Equifinality of Cs-137 concentration due to preferential adsorption
- Sedimentation rate estimation

A brief review on sediment yields data analysis is followed. For temporal sediment yield change the review has concentrated on the following items.

- Detection methods (Running mean, Linear regression, Mann-Kendall rank correlation and Non-linear model)
- Discrimination of land use induced change (Double mass plot and runoff variation removal)
- Difficulties to the detection due to spatial and temporal discontinuity

For spatial analysis of sediment yield the review is focused on the potential variables influencing sediment variation as list below.

- Drainage area
- Hydroclimatic variables
- Topographic variables
- Geology, land use and soil

The main influencing variables at the global scale are found to be different . Those important variables identified include geomorphic/tectonic (Milliman and Syviski, 1992), relief/runoff (Summerfield and Hulton, 1994), and runoff, Fournier index and slope (Ludwig and Probst, 1996).

3. THE STUDY AREA

3.1 INTRODUCTION

The chapter is designed to give a general introduction to the Upper Yangtze basin, with particular emphasis on information concerning soil erosion and sediment transport. Considering its speciality, the Three Gorges area in this chapter is treated as an independent subsection. The Cs-137 work is conducted within a small catchment, Yiwanshui, located in the Three Gorges area near Chongqing introduced in the second part of the chapter. The main purpose of the chapter is to provide a background to the environmental characteristics of the study area with an emphasis on soil erosion and sediment transport.

3.2 THE UPPER YANGTZE AND THE THREE GORGES AREA

3.2.1 General background of the Upper Yangtze

The Yangtze River, at 6300 km long, is the largest river in China and the third-largest in the world, with a total drainage area of 1.8 million km^2 , which is one fifth of the country's total area. It is known traditionally as a 'golden waterway' linking the East and the West of China. The Yangtze basin is a crucial economic lifeline for the country and home to more than one-third of the 1.2 billion Chinese population. The basin produces 40 percent of the nation's total agriculture and industrial output and 70 percent of the total rice production. There are about 30 large cities along the main channel, the largest of which are Shanghai, Nanjing, Wuhan and Chongqing (Figure 3-1). Originating from the Qinghai-Tibet (*Xizang*) plateau, the river carves its route through the mountains of south-western China and then heads north-east to surge through a spectacular 200-km reach of deep, narrow canyons, known as the Three Gorges. Downstream the river widens and meanders across southern China's

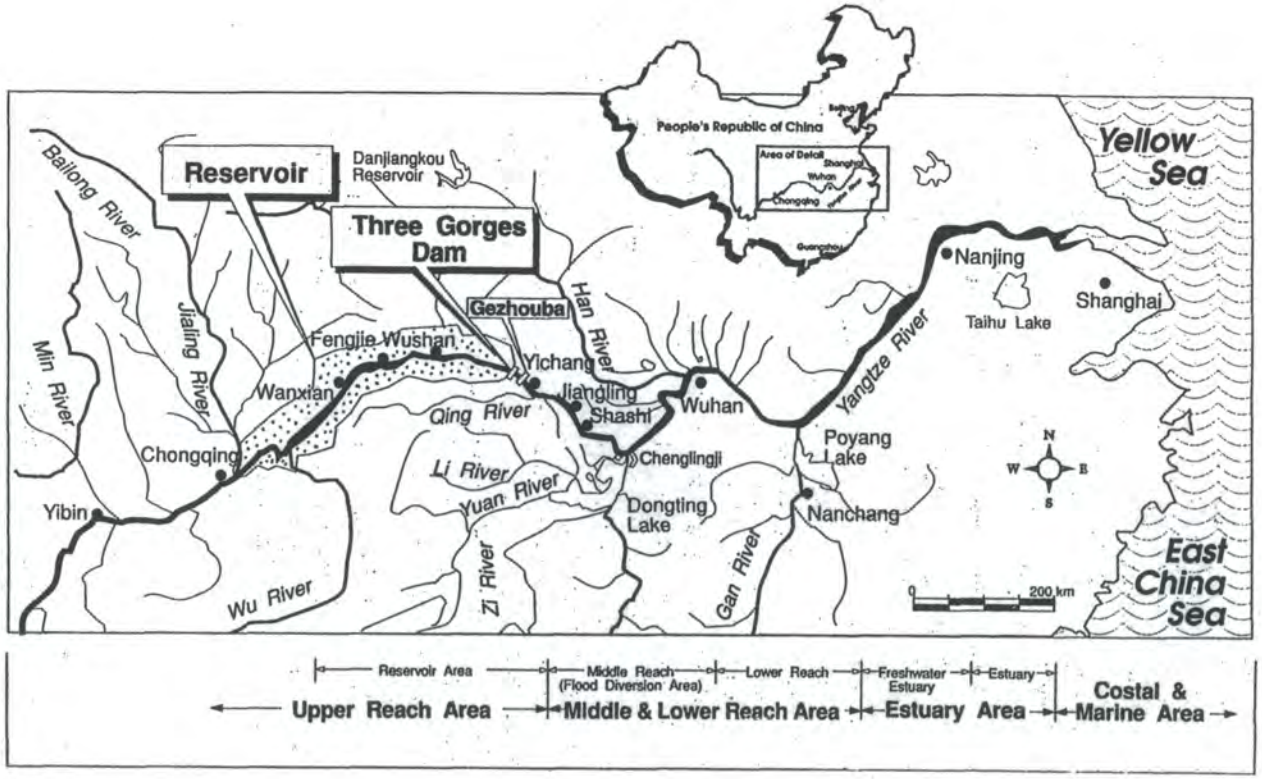

Figure 3-1, The Yangtze River showing upper, middle and lower reaches

vast, fertile plains to the East China Sea at Shanghai (Figure 3-1). Above Yichang in Hubei province is the upper part of the river (the Upper Yangtze). Background information on the different parts of the river is summarised in Table 3-1.

The main channel of the Yangtze is referred to as the Upper Jinsha above Shigu and the Lower Jinsha from Shigu to Yibin (Figure 3-2). The river above Zhimenda flows across the Qinghai-Tibet plateau, and is dominated by ice melt. The plateau was resulted from the collision between the Indian subcontinent and the rest of Eurasia (Ruddiman et al., 1989) and has an elevation of 4000-5000 m. It is referred accordingly as the 'roof of the world' and is the headwaters of several major Asian rivers (Yangtze, Yellow, Mekong, Swalow, Indus, Ganges and Brahmaputra). The environment in this part of the river basin is dominated by lakes, meadow and prairie and is lightly inhabited by Tibetan peoples, with their flocks of sheep and yaks. In the section from Zhimenda to Yibin, the river flows through Hengduang mountain ranges with deep gorges cut of a dramatic elevation difference of over 3000 m and narrow width of less than 100 m. From Yibin the river flows into the Red Basin of Sichuan, China's most populous area, with over 100 million inhabitants - approximately equivalent to the combined populations of England and France. In historic times, the fertile soil in the Red Basin has produced those abundant crops which permit such dense population. In late spring and through summer, the melting of ice and snow in mountainous west combines with heavy monsoon rains to add enormous amounts of water flowing into the Yangtze from all directions:the Yalong, Dadu-Min, Tou, from the north-west and west; the Fu and Qu joining Jialing and then the Yangtze from the north at Chongqing; and the Wu flowing from Guizhou Province in the south. Those principal tributaries are indicated in Figure 3-2, and their drainage areas and water discharge are listed in Table 3-2. The Yalong tributaries also flows through high mountains dominated by meadow and forestry. The Dadu-Min tributary, located in the transition of western mountains and Sichuan basin, accounts for the highest water discharge among all the tributaries (Table 3-2). The well-known and sophisticated irrigation systems, Dujianyan Irrigation Systems, were built in the upper Min river nearly 2,000 years ago (in 256AD), by which

agricultural development in Sichuan basin was further enhanced. The Jialing rise in the southern Loess Plateau and mountainous areas of Gansu and Shanxi Provinces, but mostly flows through the Sichuan basin. The Wu river, rising in the north-west of Guizhou, is the only large tributary to the south of the Upper Yangtze. The tributary mainly flows through Yunnan-Guizhou plateau dominated by karst landforms at an elevation of 1000-2000m. From Table 3-2 it can be seen that the 6 tributaries account to about 77% of the total area of the Upper Yangtze. The rest includes the areas controlled by the Lower Jinsha and the main channel from Yibin to Yichang mostly in the Three Gorges area.

Table 3-1, The size characteristics of different reaches of the Yangtze River (after Huang, 1982)

	Upper reach (Head-Yichang)	Meddle reach (Yichang-Hukou)	Lower reach (Hukou-Shanghai)	Total
Length (km)	4529	927	844	6300
% of the total length	72.0	14.7	13.3	100
Area (10,000 km^2)	100.55	67.74	12.56	180.85
% of the total area	55.6	37.6	6.8	100
Water discharge (billion m^3)	454.3	463.6	61.5	979.4
% of the total discharge	46.4	47.3	6.3	100

The climate in the Upper Yangtze basin is mainly controlled by the Qinghai-Tibet plateau. The characteristics of the plateau result in huge spatial and temporal climatic variations. Most of the basin has a subtropical climate, while the western plateau and mountainous areas fall in a temperate or arid climate. The western plateau and high mountains receive less than 400 mm precipitation whereas the eastern subtropical monsoon areas receive more than 1000 mm. In most areas, 70% of the annual

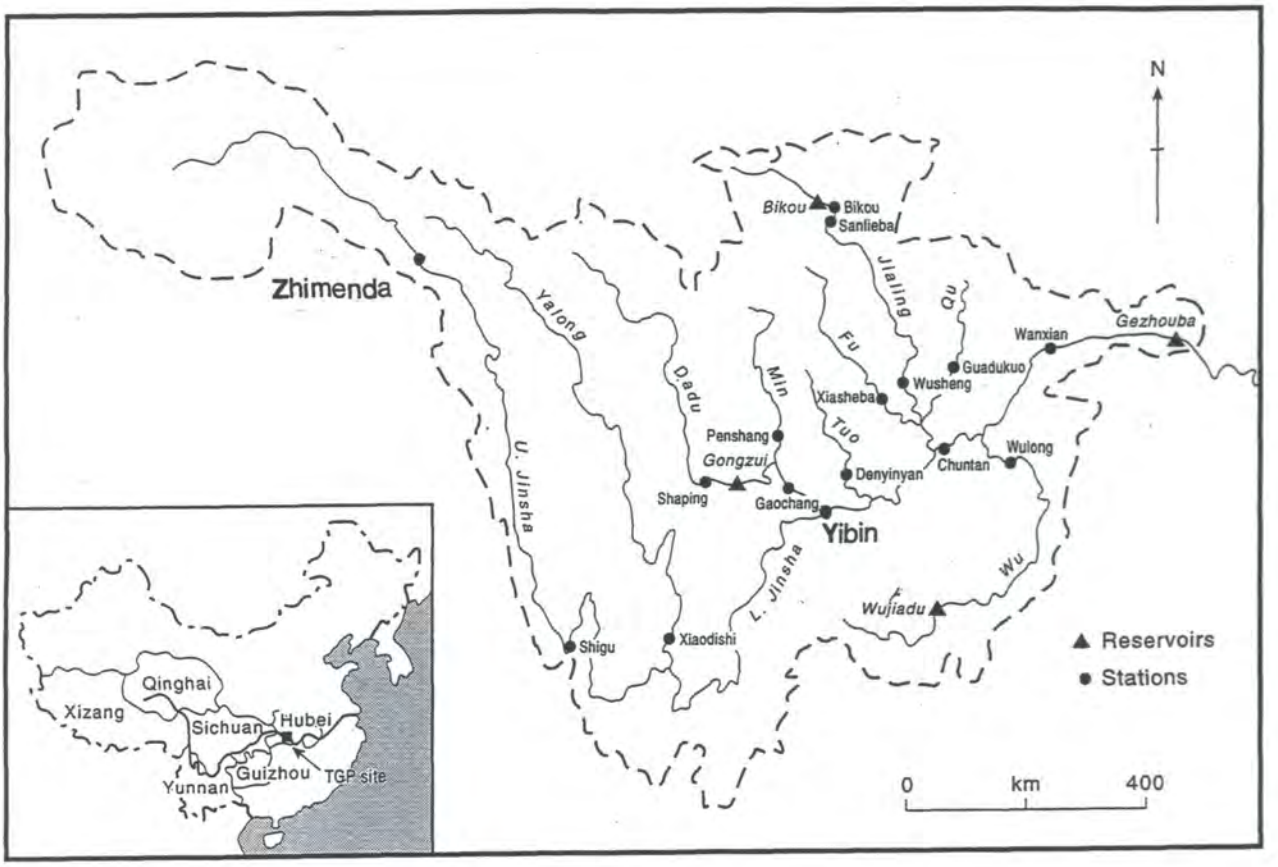

Figure 3-2, The Upper Yangtze River showing main tributaries

precipitation falls in summer (June, July and August) and 50% of the annual water discharge occurs in the period from July to September (Dai and Tan, 1996). At Yichang, average water discharge is 14,300 $m^3 sec^{-1}$ accounting to 80% of the annual total in the months from May to October (Gu and Douglas, 1989). The variations of water discharge for different tributaries is listed in Table 3-2. Due to the varied climates within the basin, in a normal year the flooding of various tributaries and the main Yangtze river do not coincide (Gu and Douglas, 1989). However, in an abnormal year, if storms affect the same tributaries later than usual, the flood peaks of those tributaries and that of the mainstream may combine to form an exceptional flood such as in 1931, 1935 and 1954, during which the changes of water level in the Three Gorges have sometimes reached six metres within 24 hours and 20- 24 m overall.

Table 3-2, The principal tributaries in the Upper Yangtze river (adapted from Huang, 1982)

Tributary	Length (km)	Drainage area (km^2)	Total runoff (billion m^3)
Upper Jinsha	----	232,000	41.6
Yalong	1,500	130,000	56.8
Dadu	735	136,000	86.8
Tuo	623	27,000	15.8
Jialing	1,119	160,000	68.3
Wu	1,018	87,000	52.0
The whole Upper Basin	----	1,005,500	321.3

The section above provides general information in the Upper Yangtze. More details on topography, precipitation and population density will be further introduced in Chapter 8 using the information obtained from varied global environmental databases.

3.2.2 Soil erosion and sediment transport in the Upper Yangtze

The Upper Yangtze used to be dominated by forest land. Due to population pressure, the forest land has been considerably reduced. Before the Qin and Han dynasties (221BC-24AD) both banks of the Yangtze river were densely covered by thick forests, having slight soil loss. Around the year of 256 AD when Dujianyan Irrigation Systems were built, the Upper Yangtze was still dominated by forest land with as much as 80% of the total area (Yu et al., 1991). The population in the basin had surged during the Qing dynasty (1644-1911) due to immigration from the eastern part of China (Shi et al., 1992). It is estimated during the 59 year period from 1753 to 1812AD, the population density in Sichuan increased by 14 times to 40 people per km^2, and to 84 people in 1851 (Yu et al., 1991). The situation continued to worsen after 1949 due to population pressure and in particular to inappropriate polices. Forest land has decreased dramatically due to massive deforestation in the late 1950s and the early 1980s. The forest land, for example, has decreased from 24% in 1950s to 13% in 1990s in Sichuan province. In Sichuan basin it is even less at only 4%, and is less than 1% in 19 counties (Chen and Gao, 1988). The situation is similar for other provinces within the valley of the Yangtze river. The forest land in 1980s, for example, accounts to only 15.1% in Guizhou, 13.5% in Anhui and 8% in Jiangsu (Chen and Gao, 1988). The reduction of forest land resulted in an increase in the land area affected by soil erosion (Table 3-3). It must be stressed that the areas were estimated based on remote sensing and cautions must be exercised when using these sort of data (see Chapter 1 for details).

The widespread erosion-affected areas result in huge soil losses. It is estimated that total loss is 1.8 billion t yr^{-1} in the Upper Yangtze (Shi et al., 1987). Average annual sediment discharge is 523 million t yr^{-1} in Yichang Hydrological Gauging Station (Gu et al., 1987). The sediment load of the Yangtze River measured at the station is the fourth highest in the world, just behind the Yellow River, Brahmaputra and Indus. All the four rivers originate from the Tibet plateau. In very serious areas, average sediment yield can be as high as a thousand or even ten thousand t km^{-2} yr^{-1}. Sediment yield, for example, is 4335 t km^{-2} yr^{-1} for the Qiunjiang catchment of 4,329 km^2 in the Fu tributary and as high as 12,400 t km^{-2} yr^{-1} for a 473 km^2

catchment in southern Gansu province (Chen and Gao, 1988). Both of these catchments are located in the upper Jialing tributary.

Table 3-3, The changes of soil erosion affected areas in some provinces within the Yangtze valley in 1950s and 1980s

	1957		1980s		Increase	
	area	%	area	%	area	%
The whole basin	363,790	20.2	739,376	41.0	375,586	103.2
Sichuan	93,380	16.1	382,000	67.3	283,620	309.1
Guizhou	12,816	11.3	35,300	31.2	22,484	175.4
Hunan	55,880	27.6	56,640	27.9	760	1.4
Jiangxi	11,000	6.6	38,360	23.0	27,360	243.7
Anhui	13,686	21.3	19,263	30.0	5,577	40.7
Jiangsu	1,850	3.8	6,100	12.3	4,250	229.0

The vast area and the variety of physiographic features of the Upper Yangtze results in many different erosion patterns and processes. In general, three sets of erosion processes are encountered in the basin: freeze-thaw processes; mass movement (gravitational erosion in Chinese literature); and water-induced. Understanding the different erosion forms is very important for understanding spatial variations of sediment yield within the basin and is further discussed in a later chapter (Chapter 7). The erosion caused by freeze-thaw processes mainly happens in the Qinghai-Tibet plateau and western mountainous areas. Erosion rates and sediment yields in the areas dominated by these processes are much lower compared with the other two erosion forms. The landforms of the western mountainous areas, located at the geological contact zone between west rising geosynclinal area and east stable plateau, undulate drastically. River valleys are deeply incised and intense tectonic activity has

Table 3-4, The completed water conservancy projects (unit in 10^6 m^3) in the Upper Yangtze (after Gu et al., 1987)

River	Large structure	%	Medium size structures	%	Small structures Type A	%	Small structures Type B	%	Ponds	%	Total	%
Jinsha-Yalong			953.03	27.9	687.26	18.7	105.37	7.1	55.92	1.4	1,801.58	10.8
Dadu-Min	675	16.6	247.70	6.9	341.44	9.3	104.55	6.9	374.73	9.5	1,377.42	10.4
Tuo	185	4.6	542.88	15.4	662.23	18.0	285.69	19.0	873.24	22.1	2,549.04	15.2
Fu	294	7.3	577.39	16.4	405.90	11.0	199.68	13.2	423.12	10.7	1,900.09	11.4
Jialing	1,789	44.1	256.07	7.3	243.52	6.6	192.08	12.7	470.66	11.9	2,951.33	17.6
Qu			462.69	13.1	161.87	4.4	140.89	9.3	783.01	19.3	1,548.46	9.3
Wu			175.75	5.0	366.45	10.0	14.66	1.0	21.14	0.5	578.00	3.5
Main stem	1,112	27.4	312.52	8.9	811.49	22.0	464.05	30.8	953.46	24.1	3,653.52	21.8
Total	4,055	100	3,522.03	100	3,680.16	100	1,506.97	100	3,955	100	16,719	100

Mass movement (debris flows and landslides) frequently occurs in the Lower Jinsha, the Upper Jialing and the Three Gorges area following heavy storms. There are, for example, 3000 debris flow valleys in the Upper Jialing. Water induced erosion, a widespread erosion form within the basin, mainly includes sheet, rill and gully erosion. and is widespread on steep arable land particularly in Sichuan basin. In the Upper Jialing, 70% of arable land is found on slopes of 20-30°, while in the Lower Jinsha sloping arable land accounts for 50-90% of the total arable land, with one third over 25° (Dai and Tan, 1996).

The severe soil erosion can cause serious damage in two respects through the reduction of soil productivity (on-site damage) and by sedimentation (off-site damage). A very serious problem in the basin is reservoir sedimentation. Numerous water conservancy projects with varied structural designs have been constructed in the basin since 1949 and particularly towards the end of the 1950s (Table 3-4). Due to the serious soil erosion, these water conservancy projects have been experienced serious sedimentation problems (Table 3-5). In general, the average reservoir capacity lost to sedimentation is more serious for smaller reservoirs. From this table,

Table 3-5, Sedimentation in selected reservoirs in the Upper Yangtze (after CAS, 1988)

Type of reservoir	Numbers of reservoirs	Reservoir capacity (10^6 m^3)	Reservoir sediment (10^6 m^3)	Capacity lost to sedimentation (%)
Large	23	25,638	1,293	5.04
Medium size	12	257.546	24.181	9.09
Small	182	92.343	19.783	21.42
Ponds	6492	74.240	41.480	55.90
Total	6709	26,062.129	1,378.444	5.29

it is difficult to see annual capacity loss due to sedimentation. Table 3-6 gives annual capacity loss of some reservoirs due to sedimentation. Annual loss can be as high as 10% of the reservoir total capacity, which means that those reservoirs could be totally filled up by around 10 years. Obviously this is much shorter than the designed life span and is one of the main reasons for the opponents of the project to worry about potential problems of sedimentation for the Three Gorges Reservoir.

Table 3-6, Average annual reservoir capacity loss due to sedimentation (from varied literature)

Reservoir	Reservoir capacity ($10,000 m^3$)	Investigation years	Annual capacity loss (%)
Bikou	45,000	6	2.7
Gongzhui	31,000	11	4.4
Xiaojiang	7,142	10	4.2
Baozhigou	100	11	3.6
Bazhaigou	60	20	5.0
Shehong	60	24	1.6
Duangqiao	30	4	10.4
Huojian	20	8	12.5
Hujiawan	0.19	4	7.5

3.2.3 General background of the Three Gorges area

The Three Gorges lie on a west-to-east line between the cities of Wanxian and Yichang. Traditionally the Three Gorges area refers to the larger reach between Yichang and Chongqing which the reservoir water will pond back if the final dam height is 180 m. The Three Gorges area consists of 20 counties in Sichuan and Hubei provinces with an area of 5570 km^2 and a population of 16.36 million (Figure 3-3). The Three Gorges, with scenery of rocky pinnacles and sheer precipices above China's mightiest waterway, is one of the country's most famous tourist sites.

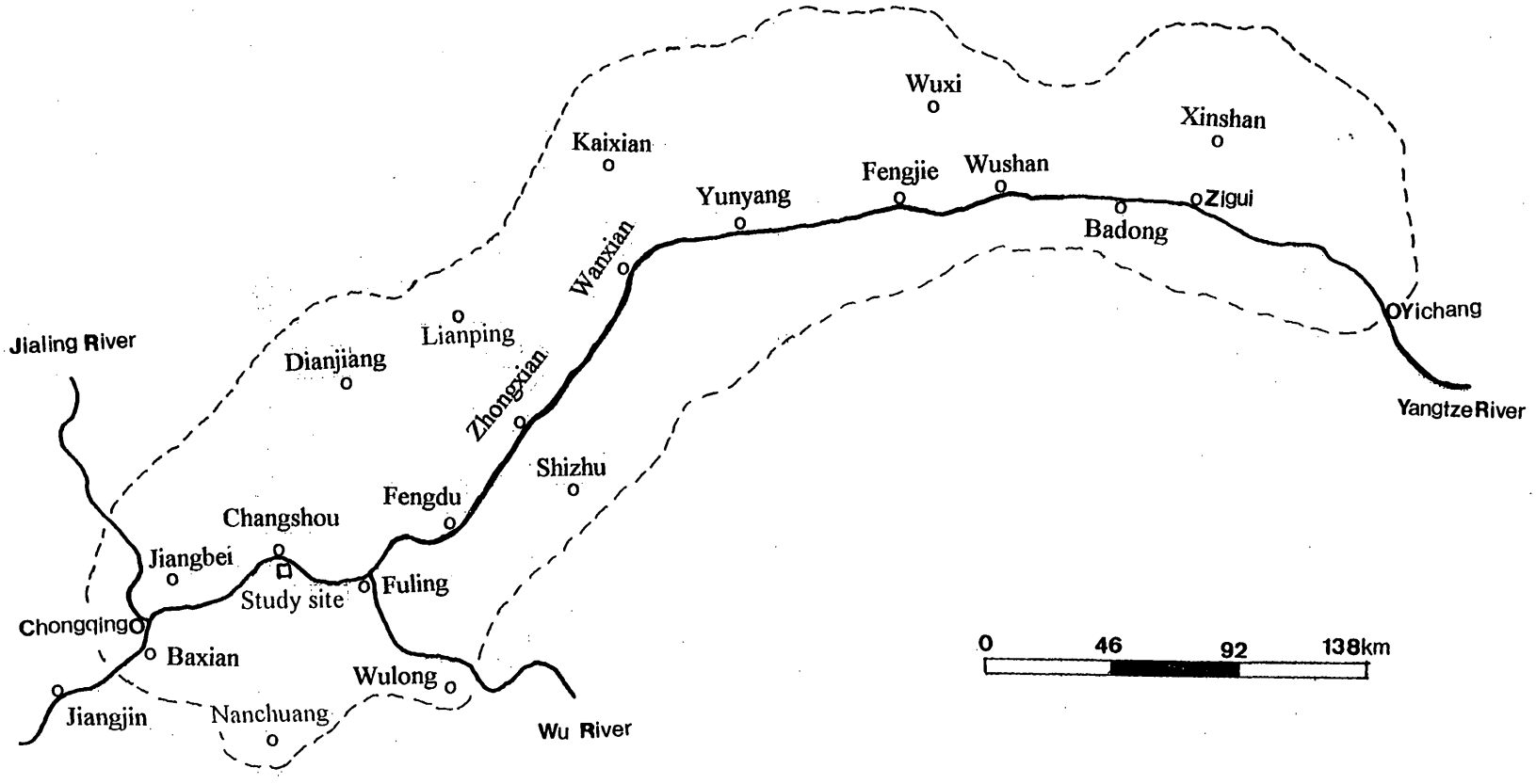

Figure 3-3, The Three Gorges area showing county names and the location of Yiwanshui catchment

classified on the basis of the Chinese terrain classification system (Table 3-7). The classification is mainly based on altitude above sea level. In general, mountain landforms are those areas with an elevation of over 500 m above sea level, whereas hill landforms have an elevation below 500 m with a relative elevations of 100-150 m. The terms mountain and hill are frequently used in the Chinese scientific literature but are only applied occasionally in western literature.

The geological structure in the area is very complicated. Generally, the mountain area is dominated by limestone, and the hilly area by purple sandstone. Land use varies with altitude and contrasting land uses can be found within small areas. Land use, with the highest percentage under arable land (23.8%), is summarised inTable 3-8. Arable land is characterised by steep slopes and thin topsoil, 72% of which is located

Table 3-8, Land use in the Three Gorges area (after Chen and Gao, 1988)

Land use	Area(10^3 ha)	Percentage
Paddy field	903	14.4
Arable land	1486	23.8
Forestry land	940	15.0
Sparse forestry land	440	7.0
Shrub land	400	6.4
Grass land	1077	16.3
Bare land	10	0.2
Water	18	1.6
Residential area	97	0.3
Others	938	15.2
Total	6255	100

on slopes of more than 15 degrees (Table 3-9). The soils of the area essentially reflect the underlying geology. Under the Chinese Soil Classification Systems (NISS-CAS, 1988), four soil types - yellow soils, brown limestone soils, purple soils and paddy soils - can be found in the area (Chen and Gao, 1988). Usually it is difficulty to find an appropriate equivalent name in the American Soil Taxonomy or the FAO-UNESCO System (1977) for those soils and for purple soils in particular. Tentatively, yellow soils are close to Ultisols, while brown limestone and purple

Table 3-9, The slopes for arable land in the Three Gorges area (after Shi et al., 1987)

Slope gradient (degree)	0-7	7-15	15-25	>25
% of the total arable land	4.7	23.8	46.5	25.0

soils would be labelled as Inceptisols in the American Soil Taxonomy. In the FAO-UNESCO System (1977), yellow soils are close to Acrisols, while brown limestone and purple soils resemble Luvisols. A common feature for the latter two soils is that they are both considerably affected by their underlying rocks. Yellow soils and brown limestone soils are predominantly distributed in mountainous areas, while purple soils are mainly found in hilly areas and paddy soils in low valleys. Generally purple soils are reclaimed as arable land because of their high mineral content. Purple soils are also the most erodible soils in the area due to high silt and low organic matter contents. The purple soils are developed from continental Mesozoic red beds which are widely distributed in Central and South China. As most of the serious soil erosion in South China occurs in the soils derived from the red beds, it is salient to consider the formation of the red beds.

"They [Mesozoic red beds] are composed of Jurassic through early Tertiary reddish conglomerate, sandstone and shale, with a total thickness of several thousand meters. They were mostly fluvial-lacustrine deposits in intermontane basins, formed under the post-Yanshan Tectonic Movement, in a hot and dry environment. During the Himalayan Tectonic Movement, the red beds were structurally uplifted and partly tilted; the climate tended to be more humid and, consequently, fluvial erosion more powerful. They were, thus, dissected into different forms of hills and terraces. This reddish, bright hilly basins are dotted conspicuously among the immense expanse of the higher and darker surrounding mountains. The Sichuan Basin, composed chiefly of nearly horizontal Cretaceous reddish sandstone and purple shale, is the largest reddish hilly basin in China. ..."

Zhao (1994)

3.2.4 Soil erosion in the Three Gorges area

Overall evaluation of soil erosion has been undertaken during a recent TGP feasibility study (CAS, 1988). It is estimated that the annual soil erosion in the Three Gorges area amounts to 157 million t and the annual sediment load delivered to the Yangtze is 40 million t (Shi et al., 1992). The percentages of erosion and the delivery ratios they used to estimate sediment load to the Yangtze river for different land uses are presented in Table 3-10. The areas affected by soil erosion exceed 50% for most of the counties (Table 3-11). Severe soil erosion results in high sediment yield and serious off-site damages. The measurement in Xiangxi river near Yichang shows that sediment yield has a significant increased trend since the 1970s, due to the deforestation in Xiangshan county which used to be dominated by forest land. The temporal sediment yield changes will be examined in a later chapter (Chapter 7). Reservoir sedimentation in the whole Upper Yangtze was introduced in a section above (see Table 3-5 and Table 3-6). Here sediment yield estimates based on reservoir investigations are presented in Table 3-13. It can be seen that sediment yields are around 3000 t km^{-2} yr^{-1} for most of the reservoirs investigated.

Table 3-10, Annual soil loss and sediment contribution to the Yangtze river from different land use categaries in the Three Gorges area (after Shi et al., 1992)

Land use	Area (km^2)	% of the total area	Erosion rate ($t\ km^{-2}\ yr^{-1}$)	SDR	Annual sediment to the river (10^3 t)	% of the total sediment
Forest	13000	23.3	750	0.25	2438	6.0
Shrub	11300	20.5	1500	0.30	5085	12.4
Grass	12100	21.7	3000	0.40	1452	35.4
Arable	12600	22.6	7500	0.20	18900	46.2
Paddy	6100	11.0	-----	----	----	----
Water	700	1.3	-----	----	----	----
Total	55800	100		ave. 0.29		100

Frequent mass movement is another feature of serious erosion in the Three Gorges area. Mass movements frequently happen along the Three Gorges and in association with newly built roads causing serious economic damages. Xintan landslide, for example, occurred in Zhigui county on the north bank of the main channel of the Yangtze river on 12 June 1985. This brought about 2 million m^3 of materials into the Yangtze and blocked one third of the river width (Shi et al, 1992). Another example is Jipazi landslide which happened after a heavy storm in July 1982 in Wanxian county. This landslide with a total volume of 13 million m^3 brought 1 million m^3 of materials into the Yangtze river, which resulted in an underwater dam with a height of over 30 m and reduced effective navigation width by 120 m at the landslide site (Shi et al, 1992). Along the two banks of the Three Gorges reservoir region, it is estimated there are total 214 potential landslide sites with the volume varying from less than or equal to 500 thousand m^3 to over 50 million m^3 each. Their total volume amounts to 1.35 billion m^3, a huge potential amount of sediment source for the Three Gorges reservoir (Shi et al., 1992).

Table 3-11, Soil erosion inventory in 1980s in the Three Gorges area (after Yang and Shi, 1994)

County	Total area (km^2)	Erosion affected area (km^2)	% of the total area
Changshou	1443	886.4	60.0
Fuling	2942	---	---
Fengdu	2903	717	24.7
Shizhu	2983	---	---
Zhongxian	2183	1291	59.1
Wanxian	3193	2011	62.9
Kaixian	3970	2863	72.1
Yunyang	3645	3080	84.5
Fengjie	4099	2700	65.9
Wushan	2955	2209	74.8
Wuxi	4025	2942	70.1
Badong	3580	1999	55.8
Zigui	2273	1086	47.8
Xingshan	2327	1423	61.0
Yichang	---	---	---

The serious soil erosion is due to massive deforestation and higher percentage of steep arable land. The changes of forest land for all the counties located in the Three Gorges area are presented in Table 3-12. As noted for the whole Upper Yangtze, forest land has been considerably reduced within the Three Gorges area during the 30 years from the 1950s to 1980s.

A contrasting feature between the Yangtze and the Yellow (*Huanghe*) rivers is the difference in sediment delivery (He, 1989). In most parts of the Yellow river basin, the sediment delivery ratio approaches 1.0, which suggests that virtually all the eroded materials from the hillsides will be transported by the river (Walling, 1983).

Table 3-12, The changes of forest land for all the counties in the Three Gorges area from 1950s to 1980s (After Shi et al, 1987)

County	% of forest land in 1950s	% of forest land in 1980s
Changshou	18.5	7.5
Fuling	---	11.5
Fengdu	23.7	12.6
Shizhu	23.3	11.0
Wulong	---	13.0
Zhongxian	22.2	11.6
Wanxian	20.0	10.2
Kaixian	11.0	5.9
Yunyang	---	8.9
Fengjie	32.2	15.7
Wushan	23.6	11.7
Wuxi	24.0	10.5
Badong	---	38.5
Zigui	---	25.9
Xingshan	---	34.0
Yichang	---	36.0

In the Upper Yangtze, however, the delivery ratio is much lower due to coaser materials (Luk and Whitney, 1993a). This suggests that the bulk of the eroded sediment is deposited on floodplains and other low-lying areas, ready to be flushed by future flood flows. Table 3-10 lists the sediment delivery ratio, around 25%, used by Shi et al (1992). Neverthless, it is noted that the ratios were used for different land use categaries, therefore, they are not comparable with the ratio obtained for a catchment.

Table 3-13, Sediment yields calculated based on reservoir investigation in the Upper Yangtze (after Yang and Shi, 1994)

Reservoir	Drainage area (km^2)	Years	Sediment yield ($t\ km^{-2}\ yr^{-1}$)
Xinlun	22.9	15	3574
Qiunli	6.0	27	3025
Dachi	9.4	15	1877
Changnian	2.3	16	2283
Pashiyan	10.4	6	2356
Shuangkan	1.6	15	3925
Tunle	0.8	25	4741
Shian	2.3	23	1913
Dalong	6.3	25	4784
Mahuangou	0.4	9	3660
Gule	0.3	23	4547
Panlou	0.1	24	2819
Changyan	2.3	16	2283

The potential soil erosion caused by the resettlement of the displaced population in the area should be also taken into account. More than 1 million people will move from the reservoir flooded area to upslope locations requiring 80-133 thousand ha of farmland to be reclaimed to replace the flooded fertile land (Shi et al., 1992). Assuming an average erosion rate of 5,000 $t\ km^{-2}\ yr^{-1}$, this may increase soil loss by 4-7 million t (Shi et al., 1992). In addition, the destruction of vegetation due to road construction, house building and domestic fuel demand will add about 100 thousand ha of new land exposed to soil erosion, and consequently ca. 5 million t of soil loss per year. As a result, an additional 10-12 million t of soil loss and 5-6 million t sediment load to the river (assuming a delivery ratio of 0.5) may occur in this area each year. In fact, if soil erosion caused by earth-rock excavation for road construction and house building is taken into consideration, the above figures will be

far higher (Shi et al., 1992). In total the sediment load delivered to the river from the Three Gorges area alone may be 46 million t each year. It is clear that the implementation of soil conservation is important to prevent soil loss and hence to reduce the sediment load to the river.

3.3 YIWANSHUI CATCHMENT

According to the aims and objectives of the study, a small representative reservoir catchment was selected to examine the patterns and rates of soil erosion and sedimentation as well as their linkages using Cs-137 tracing technique. The Yiwanshui catchment is located in Changshou county near Chongqing city (Figure 3-3). Situated in the east of the Sichuan basin and between 106°49'22'' to 107°27'30''E and 29°43'00'' to 30°12'30''N, Changshou county is divided into two parts by the Yangtze river (Figure 3-3). The geomorphology and geology of Changshou County is typical of the Three Gorges area described above. Most of the county has an elevation above sea level of 300-400 m with the highest point at 880 m and the lowest at 150 m. The geology is dominated by purple sandstone with a little limestone and Quaternary deposits along river terraces. Soils, determined by the structures of the geology, are dominated by purple soils and paddy soil. The county has a total area of 1444 km^2 with a total agricultural land of 478 km^2. Population increased very rapidly during the past 40 years from 510 thousand before 1949 to 855 thousand in 1986, 85% of which are agricultural population. The average agricultural land is only 0.06 ha per person.

The Yiwanshui catchment lies about 5 km south of the main river channel. The construction of the reservoir began in 1957 and was finished in 1958. The reservoir impounds a small stream which is a tributary on the right bank of the Yangtze. It has a total storage of 150 000 m^3 and is mainly used for irrigation but now also for fish feeding. The dam is 18 m high and constructed with earth-fill. The catchment with an area of 0.7 km^2 provides a very good opportunity to examine the potential for using Cs-137 measurements to identify the patterns and rates of soil erosion and

sedimentation. The catchment is very typical of the Sichuan basin in terms of its landforms, land use and soils.

3.3.1 Climate

With the general climatic information introduced for the Three Gorges area above, here more details will be given for the catchment. The temperature and rainfall data are obtained from the county meteorological station in county town with the measurement of 31 years from 1957 to 1987. The small catchment is located less than 5 km away to the south of the station.

3.3.1.1 Temperature

Annual mean temperature is 17.6 °C. The hottest month is August with mean temperature of 28.4 °C, and the coldest is January with temperature of 6.7 °C (Figure 3-4). Monthly temperature extremes and the year of their occurrence are summarised in Table 3-14. The highest mean monthly temperature for the 31 years is 40.5 °C in August 1959 and the lowest is -2.3 °C in December 1975.

Table 3-14, Monthly extreme temperatures and their occurrence years from 1957-1987 in Changsou county

	Jan.	Feb.	Mar.	Apr.	May	Jun.	Jul.	Aug.	Sep.	Oct.	Nov.	Dec.
The highest	17.6	22.5	31.9	35.6	35.6	38.8	39.3	40.5	39.2	32.8	26.8	18.7
Year	1969	1978	1973	1964	1966	1961	1961	1959	1975	1973	1979	1968
The lowest	-1.9	-1.7	2.9	2.5	11.3	14.9	18.0	17.1	13.6	7.3	2.9	-2.3
Year	1977	1964	1975	1969	1962	1970	1972	1962	1972	1959	1978	1975

3.3.1.2 Monthly rainfall

The wettest month is June with mean rainfall of 166.0 mm, and the driest month is January with only 16.1 mm (Figure 3-4). Under monsoon climate regime, seasonal change in rainfall and temperature is very strong. Figure 3-4 indicates high

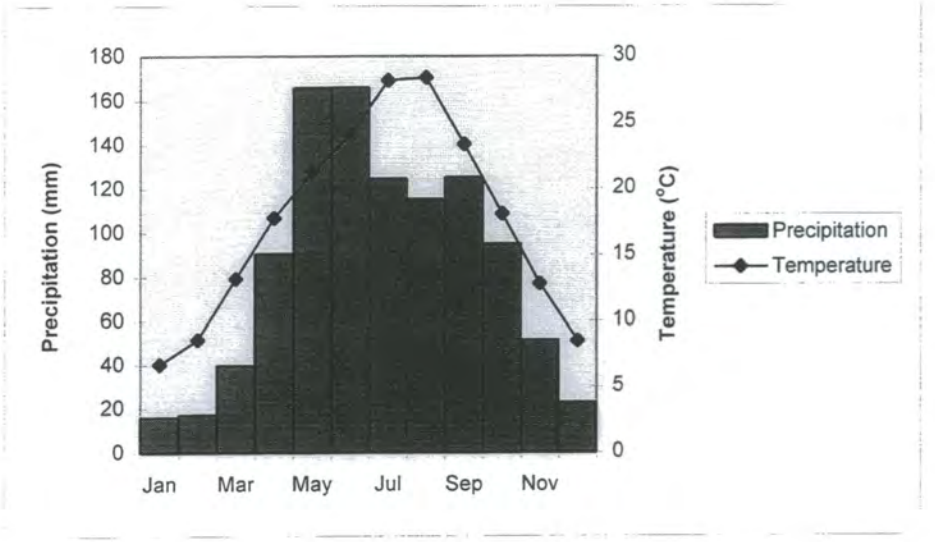

Figure 3-4, Monthly mean precipitation and temperature in Changshou from 1957-87

rainfall corresponds with high temperatures, which is favourable to crop growth. However, the highest rainfall generally occurs in May and June, whereas the highest temperatures occur in July and August. These characteristics can easily cause flooding in May and June, and drought in July and August. In addition, the rainfall in May and the three summer months (June, July and August) is often in the form of storms which can cause serious soil erosion. The daily rainfall for the 31 years from 1957 to 1987 is presented in Figure 3-5 in which the fitted line represents mean rainfall per rainday in 6 day periods. It can be seen that mean rainfall per rainday is higher in summer. This contrasts with the probability of rain per day presented in Figure 3-6 in which the fitted line represents the probability of rain per day in 6-day periods. Figure 3-5 and Figure 3-6 demonstrate that the probability of storms in summer particular in July and August is much higher than in any other month. The historic daily rainfall over 25 mm for the 31 years is presented in Figure 3-7. Again, this shows that storms mainly happened in summer. This figure also shows that the daily rainfall can be very high, many times higher than 50 mm and occasionally higher than 100 mm. These heavy storms can produce huge runoff and serious soil erosion on slope, and flooding and sedimentation in lower areas.

Annual mean rainfall is 1030.8 mm for the 31 years from 1957-87. Intra-annual changes of rainfall indicates that there was usually a dry year following each wet year, except from the late 1960s to late 1970s, during which time rainfall was higher except in 1975 and 1976 (Figure 3-8). The rainfall was the lowest in 1976 throughout the period. The yearly rainfall fluctuation in the 1980s was more severe than in the 1960s. This severe fluctionation could result in frequent drought and flooding, which is consistent with many reports. Whether this relates to global long-term climatic change or local ecological changes are not clear yet. For the events of >25 mm daily rainfall the frequency and particular corresponding rainfalls increased from the 1950s to 1980s. The frequency of events of >50 mm and their corresponding rainfall totals were more or less stable before the 1980s but record a notable increase during the 1980s (Figure 3-9). There were 4 instances of extreme daily rainfall of >100 mm recorded during the examined 30 years, comprising 181.2 mm in August of 1974,

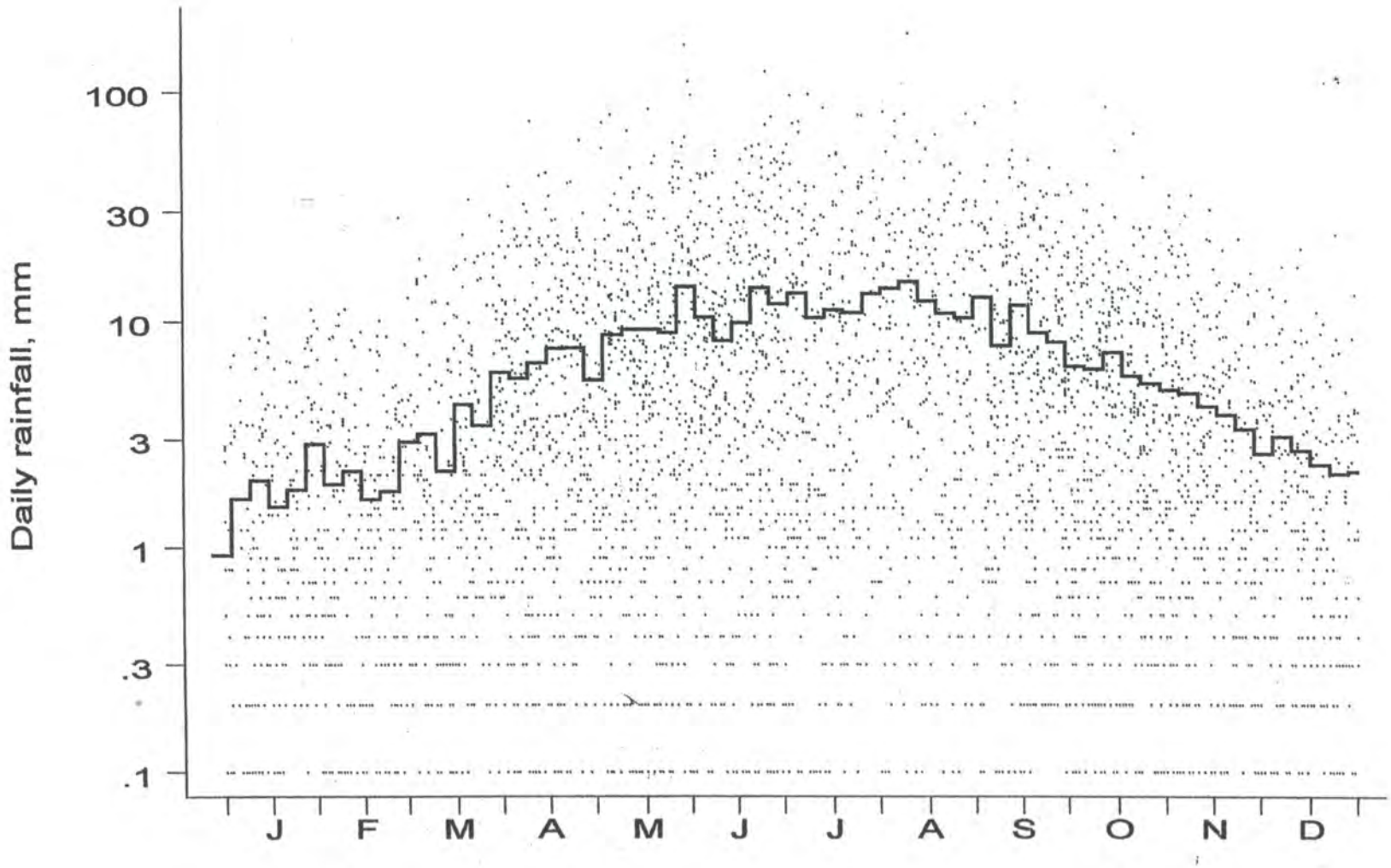

Figure 3-5, Mean rainfall per rainday in 6 day periods in Changshou from 1957-87

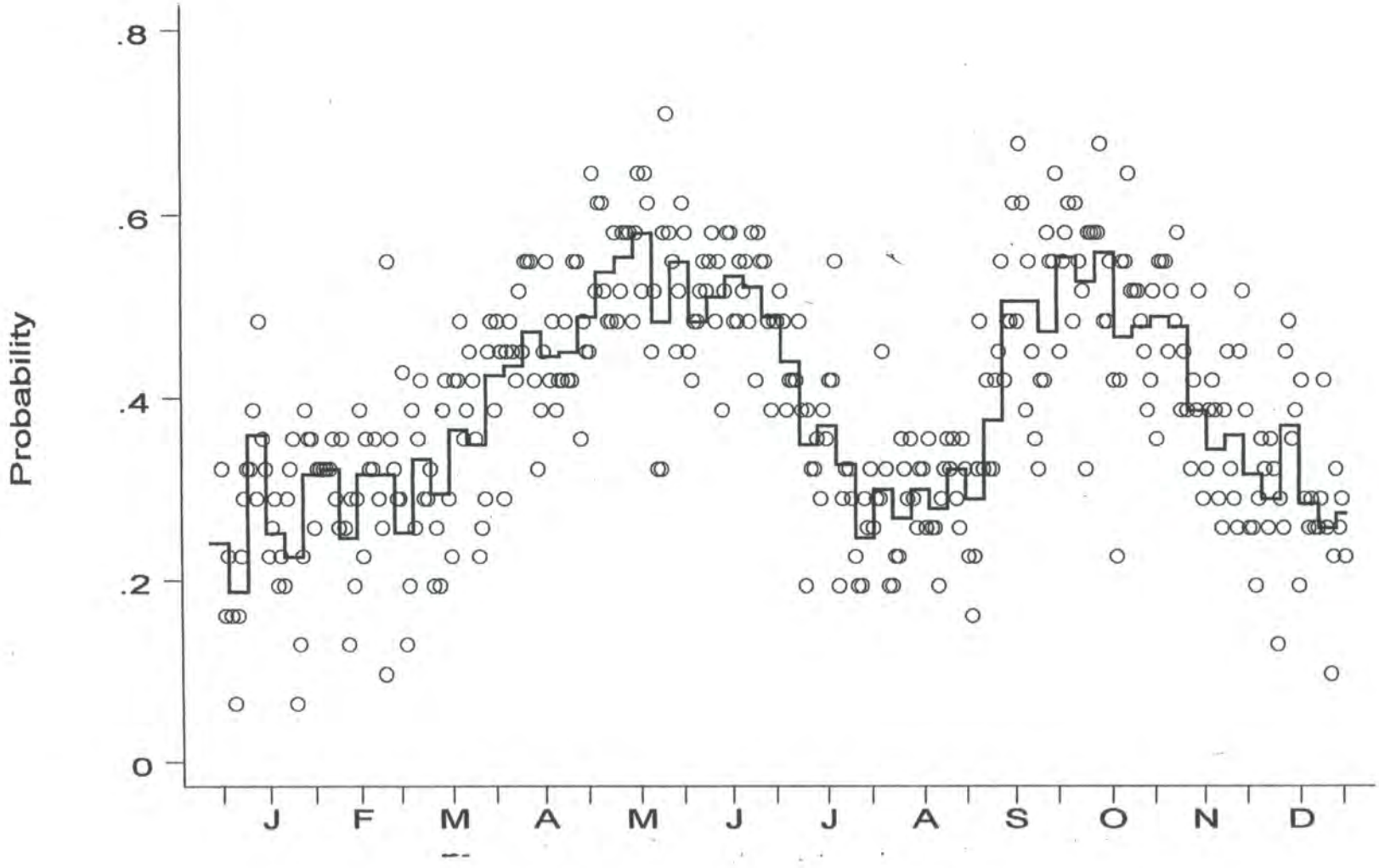

Figure 3-6, The probability of rain per day in 6 day periods in Changshou from 1957-87

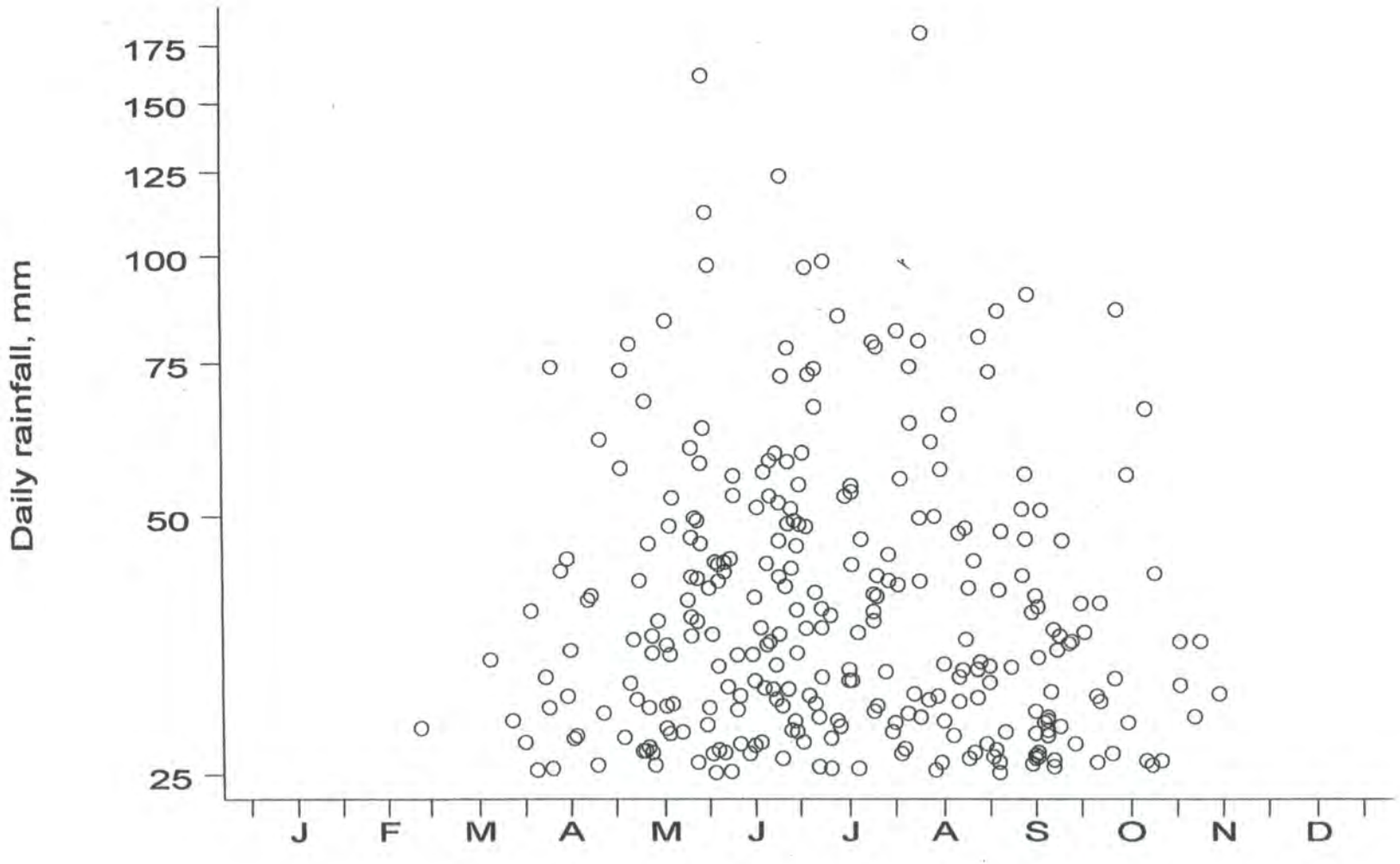

Figure 3-7, The daily rainfall over 25 mm in Changshou from 1957-87

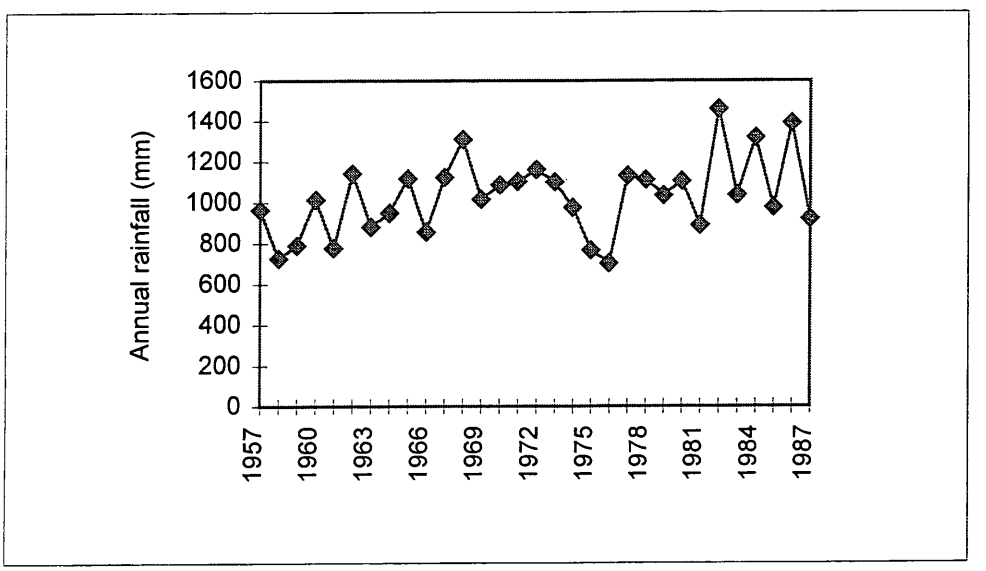

Figure 3-8, Annual rainfall from 1957-87 in Changshou county

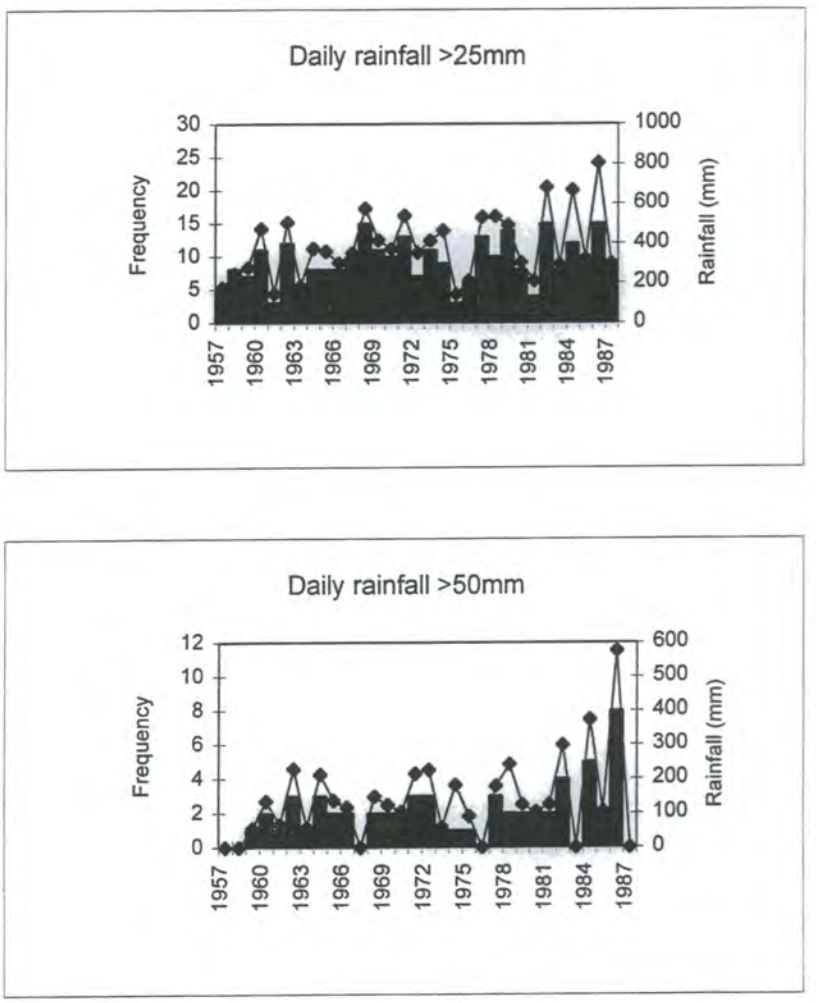

Figure 3-9, Frequency and rainfall of larger than 25 and 50 mm daily rainfall

161.6 mm in May of 1978, 123.9 mm in June of 1984, and 112.2 mm in May of 1986.

3.3.2 Geology and landform

There is no detailed geology map available for the catchment. Based on field investigation the catchment is dominated by purple sandstone, except on the tops of small hills where sandstone is in general located (Figure 3-10). In general, the small percentage of yellow sandstone is occupied by woodland, whereas the purple sandstone is occupied by arable land (see details below for land use information). The landform of the small catchment can be seen from a topographic map with a scale of 1:10,000 and 5 m interval of each contour line (Figure 3-11). The highest and lowest elevations are 385 and 245 m, respectively. According to Chinese terrain classification, this is a typical hilly landform. The catchment consists of a long stream flowing from northeast toward to southwest and a shorter tributary stream with roughly parallel flow direction (Figure 3-11). There is a gentle elevation change along the two streams but steep valley side slopes abut the floodplain. A DEM will be built based on the contour map in next chapter. With the DEM many topographic features can be derived.

3.3.3 Land use and soils

The land use map of the catchment is shown in Figure 3-12. Three types of land use, wood & shrub land, arable land and paddy field, can be identified within the catchment. Wood and grassland is mainly distributed on the top of hills or on the very steep slopes, whereas paddy fields are mainly in the valley and lowland. Arable land is distributed on the slopes of higher ground. The areas for the three types of land use obtained from the land use map are presented in Table 3-15. In addition to the three main types of land use, gullies, terrace walls and ditches also account for a small percentage of the total area but can not be identified from the 1:10,000 map. Based on land use structure investigated in Sichuan basin (Soil & Water Conservation Office of Sichuan Province, 1983), the percentage in general accounts for around 10% of the land surface. It can be seen that the catchment is dominated

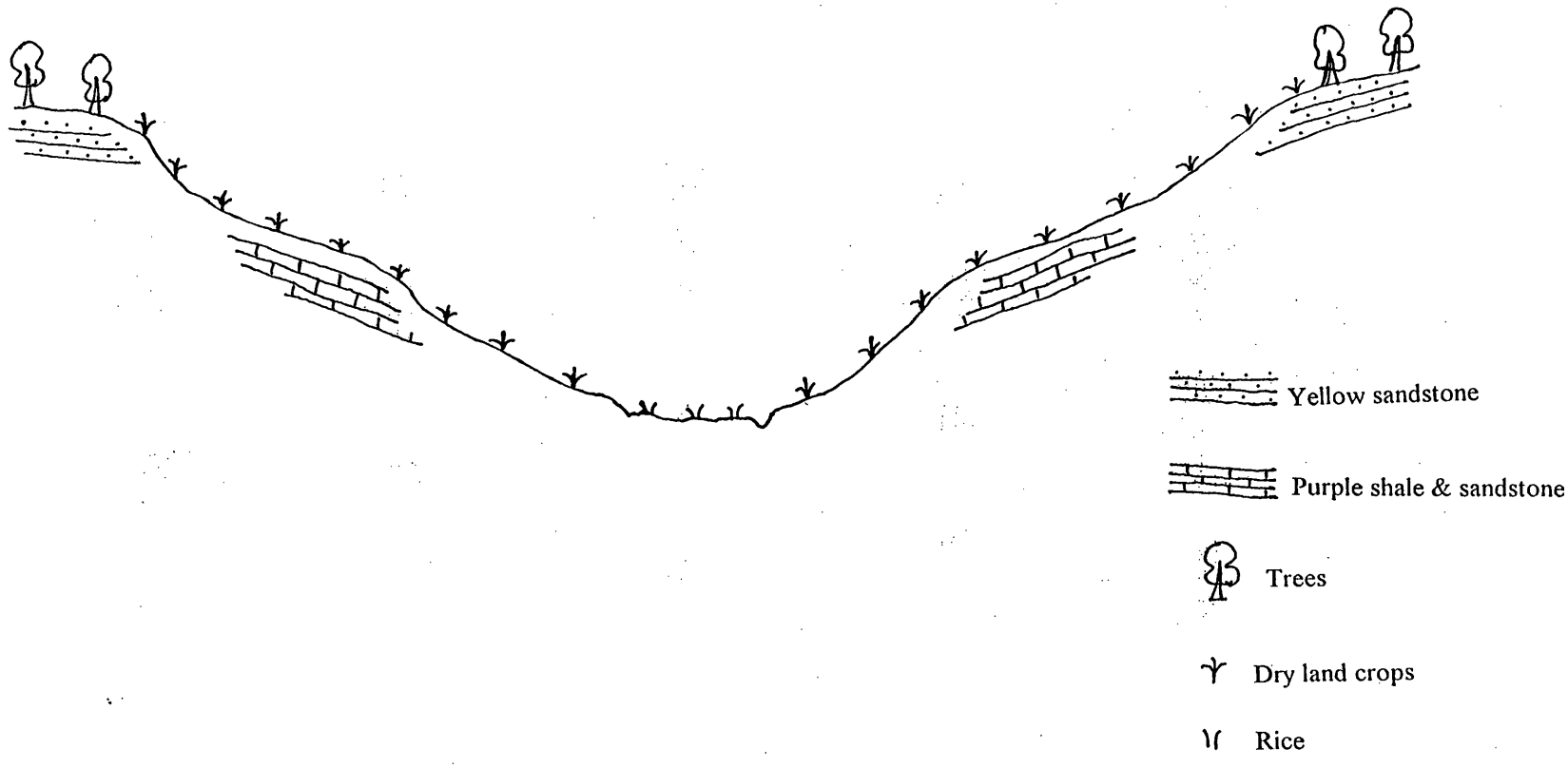

Figure 3-10, A schematic section showing geology in Yiwanshui catchment

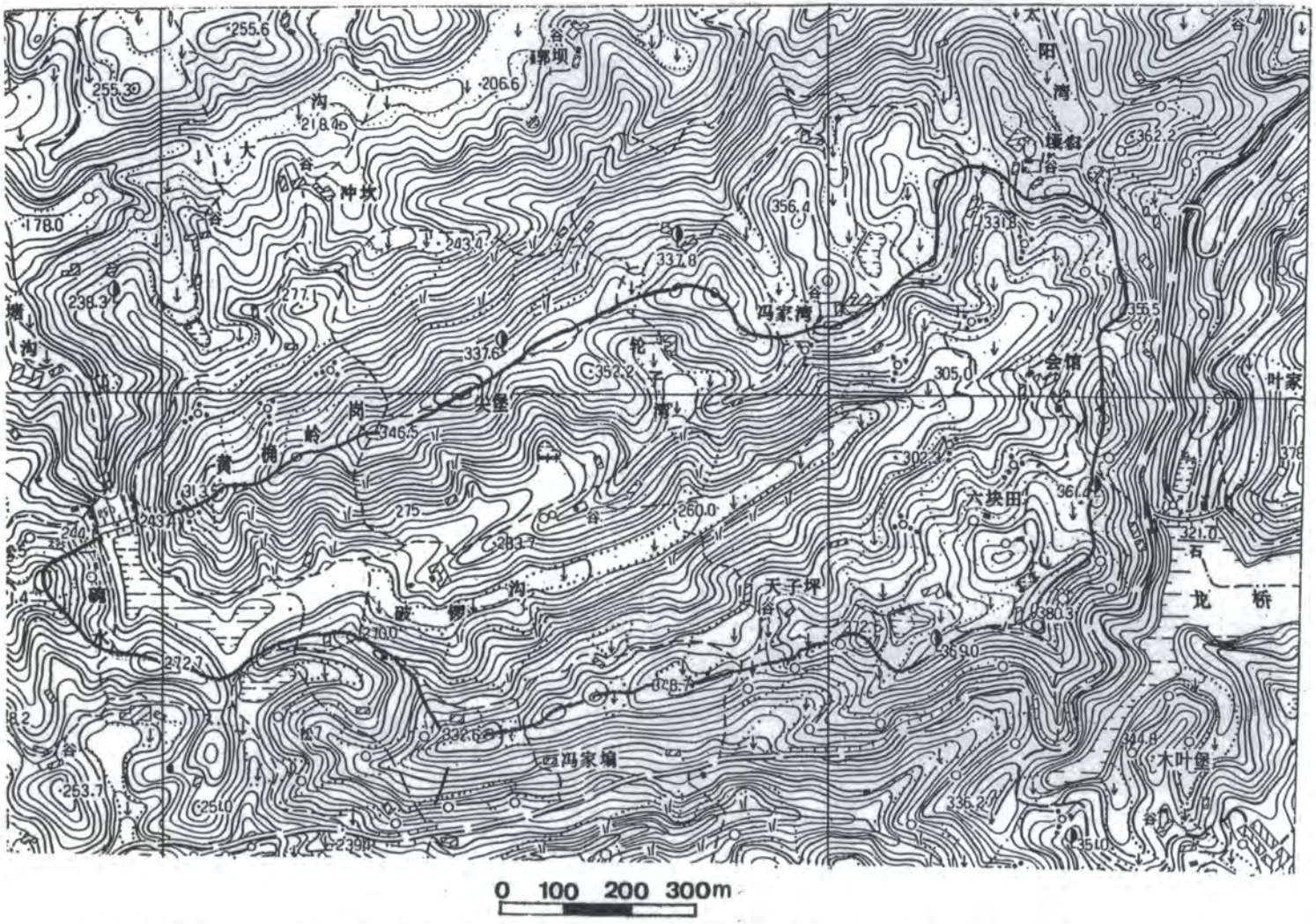

Figure 3-11, A contour map showing topographic features in Yiwanshui catchment

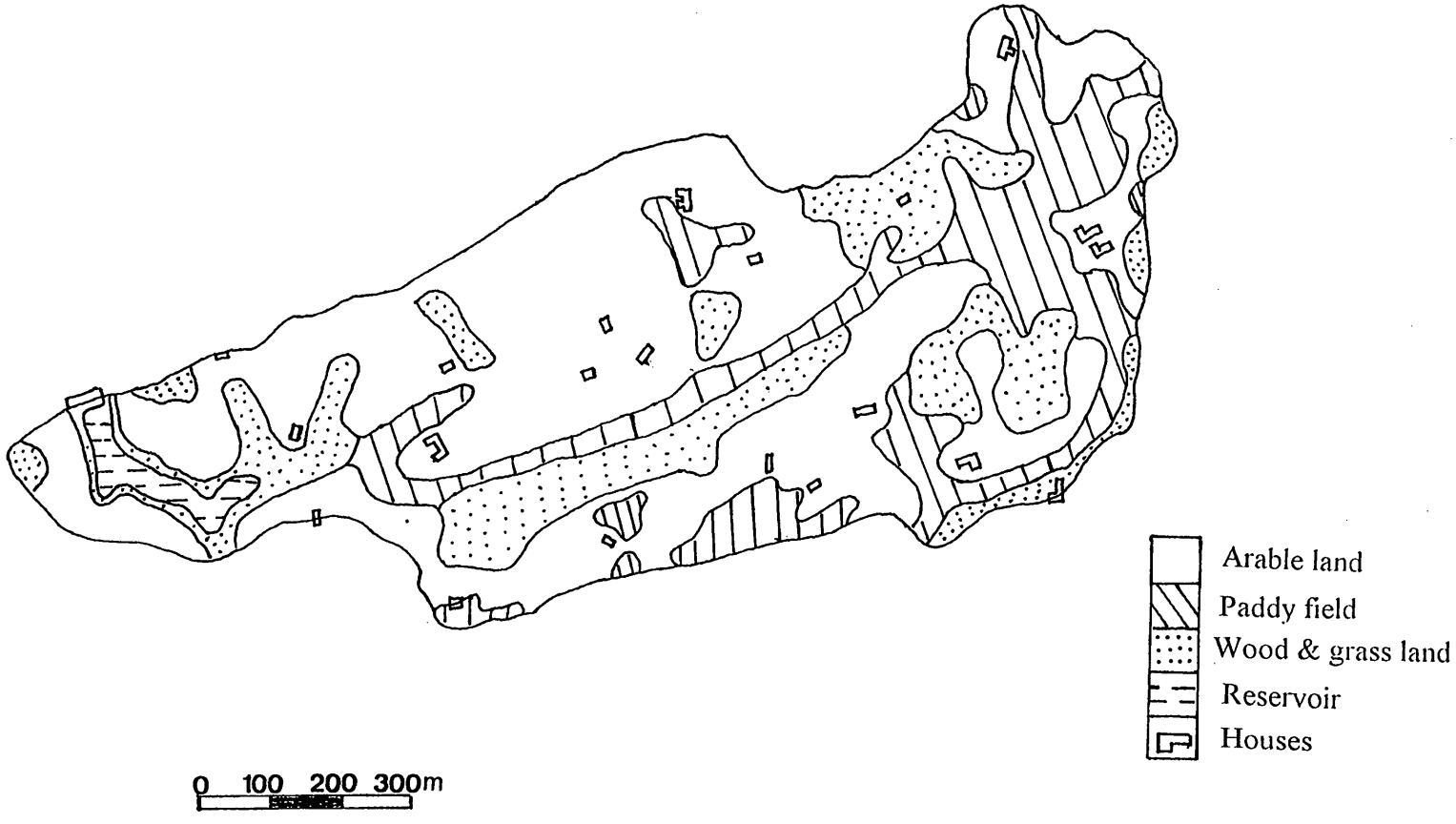

Figure 3-12, The landuse in Yiwanshui catchment

by arable land, accounting for 57% of the total area. Paddy fields accounts for 20% of the total area, and wood & shrub land 10%. It must be stressed that wood & shrub land here is mixed with grass and bare land which are not further classified as independent land use categories.

Table 3-15, Land use in Yiwanshui catchment

Land use	Area (km^2)	Percentage
Arable land	0.40	57
Paddy field	0.14	20
Wood & grass land	0.07	10
Gully, ditch and bare land	0.07	10
Reservoir	0.02	3
Total	0.70	100

The soils of the catchment essentially reflect the geomorphology and underlying geology. Sloping arable land is dominated by purple lithomorphic soils which are derived from Triassic purple sandstone. Purple sandstone can be easily weathered under the subtropical monsoon climatic conditions. This results in a soil with high mineral content which is very suitable for cultivation. The easily weathered property also makes the purple soil very coarse with high gravel content. The high content of gravel in the soils may also be enhanced by preferential removal of fines by soil erosion processes.

The subtropical climate provides the potential for two or two and a half crops per year with harvests in May, July and October. During winter and spring, the main crops are rape on the valley floors and footslopes, and wheat on the sloping terraces. During summer and autumn, the main crops are rice on the valley and the irrigated footslopes, and maize and sweet potatoes on the sloping cultivated land. The rotation

of each year is rape-rice or rice-rice for paddy fields, and wheat-maize-sweet potato or wheat-maize-beans for the sloping land.

Traditional cultivation practices benefit soil conservation. Slope length and angle are frequently controlled by subdividing the natural terraces into several fields. Small channels have often been constructed above the upslope edge of fields to divert runoff from the adjacent steep cultivated or uncultivated slopes. Ditches have been constructed at the lower margins of fields for diverting runoff. Some practices such as up-down slope cultivation, however, are not beneficial for soil protection (see Plate 3-1). Based on local experiments, it is estimated that contour cultivation (parallel to the contour) can hold 10-50 mm more rainfall than up-down cultivation and hence reduce soil loss by 50% (Soil and Water Conservation Office of Sichuan Changshou County, 1988). For farmers it is easier and safer to practise up-down slope cultivation on steep slopes. On the other hand, local farmers think that up-down slope cultivation is helpful to drain excess moisture particularly in wet seasons of spring and autumn.

The period following the May harvest is characterised by high intensity rainfall as discussed above. Sloping land is very susceptible to water erosion during summer. Sheet and rill erosion are very severe on the sloping land because of steep slopes and high erodibility of soils. In addition, channels and small gullies between sloping fields also contribute a considerable amount of sediment because of steep edges and the existing weathered materials.

3.3.4 Soil erosion

Due to the steep slopes, the purple soil is easily susceptible to soil erosion under the monsoon climatic condition. Erosion mainly happens on arable land in the catchment based on field investigation as shown in Plate 3-2. There has been no specific soil erosion investigation undertaken within the catchment by the local authority. However, a soil erosion inventory investigation within the whole county was made in 1986 using remote sensing techniques. For a general understanding of the problem,

Plate 3-1, The up-down slope cultivation and dissected sloping land in Yiwanshui catchment.

Plate 3-2, The different landuse forms in Yiwanshui catchment.

the information obtained by this investigation is provided here. The information is from Soil and Water Conservation Office of Sichuan Changshou County (1988). As introduced in Chapter 1 the remote sensing investigation was undertaken by local authorities. The principle of the interpretation is ground reflectance. While the reliability of the method is still quite arguable, the data presented here can only give a general view on the background of soil erosion in the county. It was estimated that the area subjected to erosion was 866 km^2, accounting for 60% of the total area, with an average soil erosion rate of 5500 t km^{-2} yr^{-1}. The areas with detailed erosion rates are summarised in Table 3-16. Based on this table, soil erosion-affected areas were dominated by the serious erosion class with a rate of 6500 t km^{-2} yr^{-1}. However, it must be reiterated that the determination of erosion rates using remote sensing is still problematic.

Table 3-16, The areas of soil erosion affected in Changshou County (after Soil and Water Conservation Office of Sichuan Changshou County, 1988)

Erosion Classes	Area (km^2)	% of the total area	Erosion rate (t km^2 yr^{-1})
Slight	63.58	4.40	1500
Medium	237.72	16.46	3750
Severe	523.10	36.23	6500
Very Severe	42.02	2.91	10000
Extremely Severe	0.02	0.00	20000
Total	886.40	60.0	

The report also listed the erosion-affected areas for different geology, land use and landforms. As with data derived from the soil erosion inventory, special care must be taken when quoting those results, which are provided here for general information (Table 3-17). It can be seen that affected areas are mainly distributed on rocks of Jurassic and Triassic age, which is consistent with the situation in the whole Three Gorges area as described above. In terms of land use, it can be seen that soil erosion

mainly happens on sloping arable land (Table 3-18), but the erosion rates are still arguable. In terms of terrain, soil erosion mainly happens on so-called hills (altitude <500 m), accounting for more than 70% within the three landforms, mountain, hill and plain (Table 3-19).

Table 3-17, The areas (km^2) of soil erosion affected for different geological rocks (after Soil and Water Conservation Office of Sichuan Changshou County, 1988)

Rock Types	Slight	Medium	Severe	Very Severe	Extremely Severe	Total	%
Quaternary	0.30	0.12	2.22	0.00	0.00	2.63	1.0
Jurassic	83.90	36.53	85.50	24.72	0.02	230.66	87.4
Triassic	13.64	0.05	14.53	0.00	0.00	28.47	10.7
Permian	1.51	0.58	0.13	0.18	0.00	2.40	0.9
Total	99.34	37.28	102.38	24.90	0.02	263.91	100.0

Table 3-18, The areas (km^2) of soil erosion affected for different land use in Changshou (after Soil and Water Conservation Office of Sichuan Changshou County, 1988)

Land use	Slight	Medium	Severe	Very Severe	Extremely Severe	Total	%
Arable land	73.89	1.02	101.07	24.77	0.00	200.75	76.1
Forest	20.33	35.46	0.75	0.00	0.00	56.54	21.4
Shrub & grass	3.00	0.24	0.09	0.00	0.00	3.33	1.3
Bare rock	2.12	0.55	0.47	0.14	0.02	3.29	1.2
Total	99.34	37.28	102.38	24.90	0.02	263.91	100

Table 3-19, The areas (km^2) of soil erosion affected for different landforms in Changshou (after Soil and Water Conservation Office of Sichuan Changshou County, 1988)

Landforms	Slight	Medium	Severe	Very Severe	Extremely Severe	Total	%
Plain	10.56	0.28	0.51	0.00	0.00	11.35	4.3
Hills (altitude <500 m)	66.35	31.11	82.73	16.39	0.02	196.60	74.5
Low Mountain (altitude 500-1000 m)	22.43	5.89	19.14	8.51	0.00	55.97	21.2
Total	99.34	37.28	102.38	24.90	0.02	263.91	100

3.4 SUMMARY AND CONCLUSION

The chapter introduces general information on the Upper Yangtze with emphasis on the factors relevant to soil erosion and sediment yields. Under monsoon climatic conditions and steep terrain, soil erosion rates and hence sediment yields are very high. Serious soil erosion makes the Yangtze river one of the four most heavily silted rivers in the world. The Upper Yangtze used to be the second largest forest reserve in China but forest land has been decreased dramatically in the 1950s and 1980s due to massive deforestation and agricultural expansion under rapid population pressure and irrational policies. For example, the forest land has decreased from 24% in the 1950s to 13% in the 1990s in Sichuan province. The situation regarding soil erosion has deteriorated. It is estimated that total soil loss is 1.8 billion t per year in the Upper Yangtze. Average annual sediment discharge is 523 million t in Yichang, Hubei Province. Serious soil erosion in the basin causes severe sedimentation problems for many reservoirs in the basin and the prospect of sedimentation in the Three Gorges Reservoir is a fundamental problem for the TGP. The rate of sedimentation for the reservoir during its operating lifespan depends, in part, on land use and soil erosion patterns upstream. Therefore a detailed assessment on soil erosion and sediment yields is required for a proper management of the on-going project.

The second part of the chapter introduced a small catchment, Yiwanshui, located in Changshou County in the Three Gorges area near Chongqing. The section is mainly focused on climate (temperature and rainfall), geology and landform, land use and soil, and previous soil erosion estimates for Changshou County. Further information on Yiwanshui is incorporated into the discussion of sampling methods and results in the subsequent three chapters.

4. MATERIALS AND METHODS

4.1 INTRODUCTION

The chapter is designed to give a general introduction on materials and methods used in the study. This includes field, laboratory and GIS work involved, which together with the previous chapter provides the necessary background information for the investigation. Some additional specific detail about methods used is also incorporated into later chapters where appropriate.

4.2 SAMPLING STRATEGY

The sampling design of the small catchment study has three components. First, soil samples were taken from sloping arable fields, which are assumed to be the main sediment sources, for determining the rates and patterns of soil erosion using Cs-137. Second, sediment cores were taken within the reservoir for examining the rates of sedimentation and reconstructing sediment yields. Together, it is hoped that Cs-137 contents of soil cores and reservoir sediment can be used to derive a sediment budget. Third, topsoil and eroded materials from all possible sediment sources and sinks were collected. These samples together with the sediment deposited in the reservoir will be analysed for various physical and chemical properties (particle size distribution, Cs-137 and geochemistry) which may be used to fingerprint the sources and sinks of eroded materials and possibly to establish temporal changes in sediment sources.

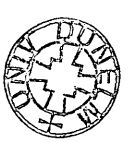

4.2.1 Soil sampling for reference value

The soil samples for Cs-137 reference value were taken in August 1994. Ideally, the samples for the reference value should be collected from flat grassed land or forest land without any evidence of erosion or deposition (Sutherland, 1992). It is difficult to find such a site or any other place which has not been disturbed by human activity within the catchment, or indeed throughout the agricultural regions of China. After thorough exploration of the catchment, one piece of flat farm field (about 500 m^2) , located between the tops of two hills on the catchment watershed was identified as a reference site (Figure 4-1). The field is used as rice paddy in the wet season and for wheat during the winter (Plate 4-1). From the literature review chapter, it can be noted that the reference site selected is atypical compared to previous studies but considered to be a site where limited transfer of sediment takes place either downslope or from above. Eight core samples were taken using hydrological tubes which were driven down to the depth of 40 cm using a hammer. Three of them were taken using a 9 cm diameter hydraulic tube. The three soil cores were then sectioned in 10 cm increments. The other five cores were taken using a 4 cm diameter tube and sectioned in 20 cm increments in order to minimise the cost of transport and determination. The location of the reference site and the distribution of samples can be seen in Figure 4-1.

4.2.2 Soil sampling from arable lands

First, for investigating background information on the behaviour of fallout Cs-137 within soil profiles and at different slope positions for sloping arable land, a small piece of sloping land was selected for detailed sampling (Figure 4-1). The field dimensions were 10×8 m with a gradient of 28° up-down slope and 5° parallel slope. There is a terrace wall with small ditches above the field. The samples were collected using a 4 cm diameter hydrological tube which was vertically driven into the ground by a hammer to a depth of 40 cm. Soil samples at 5 cm vertical increments were taken from three slope positions at the upper, middle and bottom of the field

Plate 4-1, The paddy field in which reference samples were taken, and the tube used for sampling.

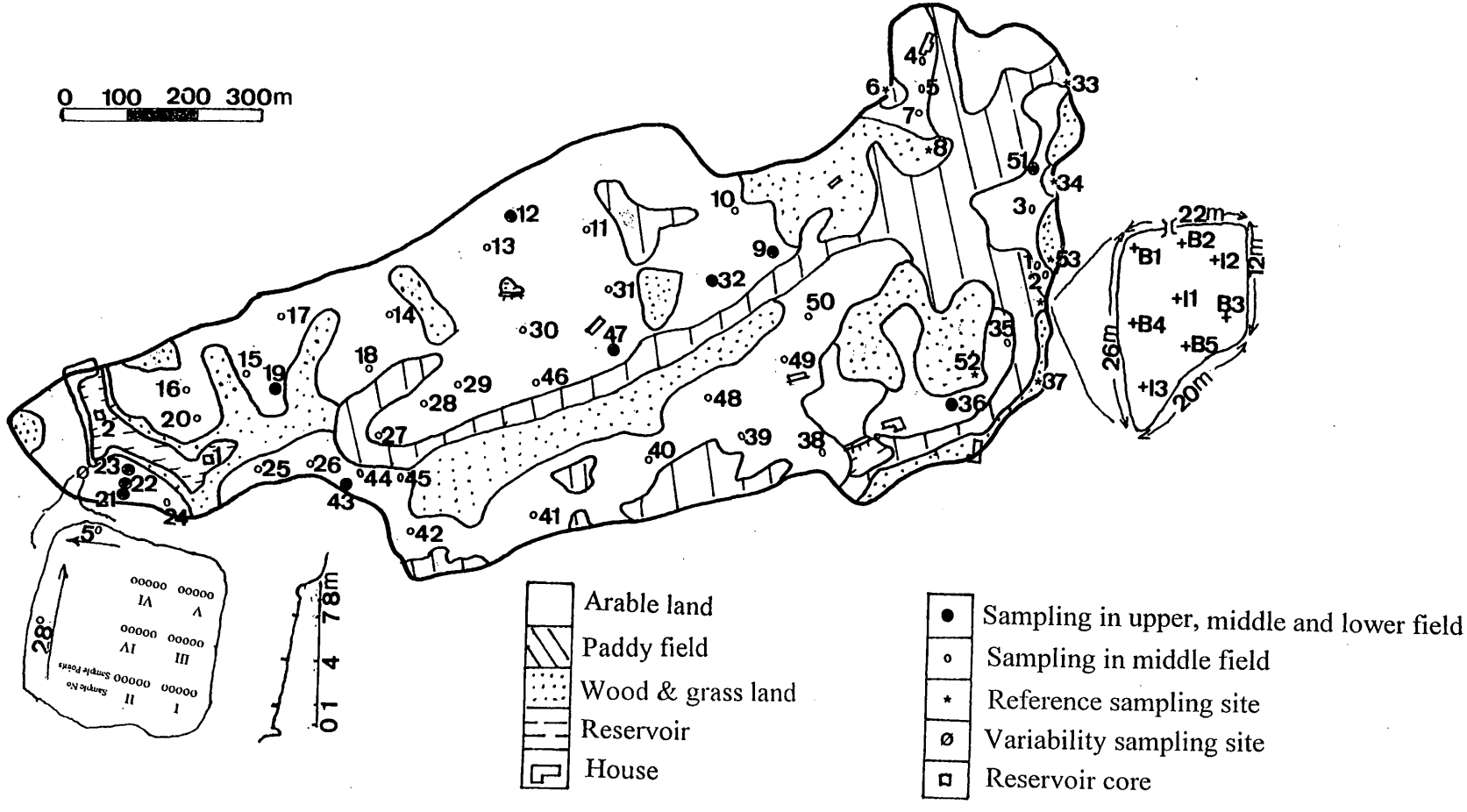

Figure 4-1, The distribution of soil sampling sites in Yiwanshui catchment

(Figure 4-1). In order to minimise the cost for sample transport, the samples from 5 cores, about 0.5 m apart each, were mixed. Through the detailed sampling it is found that, in general, topsoil depth is around only 15 cm below which there is partly weathered parent materials or bed rock.

Subsequently, a detailed sampling from slopes was followed throughout the catchment. Originally a grid system was designed for this sampling, but it was found that the grid system was difficult to follow due to the steep landform and discontinuous sloping land. The sloping land, therefore, was sampled systematically within a distance of approximately 100-200 m. The sampling on sloping land was undertaken in April 1994. 33 bulk core samples were taken from the middle part of sloping fields. In addition, 11 pieces of sloping fields were sampled from the upper, middle and lower parts of the fields. The sampling depth is 20 cm, which is down to the weathered or half-weathered materials, due to very thin soils. The distribution of soil sampling sites is presented in Figure 4-1.

The steepness and field length of sloping land were measured and recorded for each sampling site (see Appendix 1). The sloping fields are characterised by steep slopes and small size. The slopes range from 16° to 36° with an average of 23°. The field length, with an average of 8 m, ranges from only 3 to 18 m at the longest. The characteristics of steep slope and small field make this study very unique compared with previous studies using the Cs-137 technique. Sometimes trees and shrubs, used for stabilising terrace edges or cash crops, can be found on some edges of arable land. Channels dug by farmers, or small gullies cut by overland flow, can be found in the upper parts of fields, which dissect arable land and reduce the area available for cultivation. The discontinuous distribution of arable land on slopes results in difficulties in measuring or estimating the rates of soil erosion using runoff plots or the Universal Soil Loss Equation (USLE) which has been developed and used on uniform slopes. The Cs-137 technique may be very suitable for investigating erosion rates in such conditions, providing the assumptions of the technique are justified.

The easily-weathered property of purple sandstone resulted in the soils with very high gravel contents (Appendix 3). The gravel contents (>2 mm fraction) are dramatically variable, ranging from 0 up to 63.3% of total soils with an average of 15.4%. The higher contents of gravel in the soils may also be caused by soil erosion or through the deliberate removal of soil by farmers. Under these circumstances, there will be some difficulties for the study to use Cs-137 to investigate the patterns and rates of soil erosion and deposition, since it assumed that Cs-137 is absorbed by finer materials and subsequently its transport is associated with soil transport. Therefore, any attempt to convert Cs-137 loss to soil loss should consider this fact.

4.2.3 Topsoil and eroded materials collected from potential sediment sources and sinks

The collection of a small amount of topsoil (0-5 cm) and eroded material samples was undertaken throughout the whole catchment. Topsoil samples were collected up and down slope at points representative of the various land use types, soils and slope positions. Eroded material samples were collected from channels, gullies, ditches, paths, roads, terrace edges, and fans, respectively. Approximately 80 samples were taken for the purpose of fingerprinting sediment sources. The detailed descriptions on those samples are summarised in Appendix 2.

4.2.4 Reservoir cores sampling

Two reservoir cores were sampled using a Russian-type corer (see Figure 4-1 for coring locations). A 50 cm corer that was connected to steel nodes was pushed manually into the sediment from two small boats fixed together. The sediment depth from 1958 could be identified because of the difference in colour and density between the 1958 pre-impoundment paddy soil surface and the reservoir-deposited sediments. The sediment cores were cut into 5 cm sections beginning at the sediment surface and each section was put into plastic bags. The depth of the sediment is 140 cm for core 1 and 105 cm for core 2, respectively. Water depth was measured using a bamboo probe at 58 sites, and each site was spaced about 4 m apart along 8 transects. The transects were about 30 m apart (see Figure 6-2 in Chapter 6).

Soil and sediment samples were transported to Nanjing. The samples were air-dried, disaggregated, ground and sieved through a mesh of 2 mm. The fractions of >2 and <2 mm for samples from sloping fields were weighed, and 500 g soils were subsampled from the fraction of <2 mm. All of these subsamples together with reservoir sediment and collections for fingerprinting sediment sources were packed and transported to England for laboratory analysis.

4.3 LABORATORY ANALYSIS

4.3.1 Cs-137 determination

All the samples transported from China were subjected to analysis for Cs-137 content in the laboratories of the Department of Geography, University of Durham. An EG&G Ortec LO-AX detector was installed in the Department in 1996. The methodology of gamma spectrometry is introduced in most papers concerning the application of radionuclide tracers (e.g. De Jong et al., 1982; Murray et al., 1987) and the technical aspects of the technique are not dealt with in great detail. However, it is considered appropriate to provide a brief description of the equipment and to focus on two aspects of the analysis: the ranges for the region of interest (ROI) and measurement errors.

4.3.1.1 Measurement of environmental radioactivity

The emission of electromagnetic energy from the nucleus of atoms as gamma rays is a form of electromagnetic radiation. Sources of radiation are both natural (such as cosmic rays, cosmogenic and primordial sources) and artificial. The most important artificial source of radiation in the environment arises from military and domestic nuclear industries. The occurrence of Cs-137 is associated with such sources.

Nuclear weapons technology is based around the fission reaction which generates daughter nuclei. Depending on the nature of the fissile fuel used, a range of different nuclides can be produced by fission reaction and many of these have radioactive

daughter products. Most fission products have excess energy in the nucleus which is lost through the emission of gamma rays. In the case of Cs-137, beta decay produces the excited daughter isomer of barium (Ba-137m) which has a half-life of 2.55 minutes, which in turn emits a gamma ray. Caesium-137 has a half life of 30.1 years which, in combination with its environmental mobility characteristics, makes it ideal for medium-term tracing experiments.

The SI unit of radioactivity is the Becquerel (Bq) which is defined as one nuclear disintegration per second. This unit replaced the Curie (Ci) although some articles continue to quote activities in picocuries (pCi). The process of gamma spectrometry therefore depends on counting the number of nuclear disintegrations which emit gamma rays over time. The recognition of the origin of specific gamma rays is made possible by the distinctive energy levels possessed by different gamma rays. The electromagnetic energy possessed by gamma rays is measured by the electron volt (eV). In the case of Cs-137, the gamma ray emitted by the daughter isomer Ba-137m has an energy of 661.6 keV. The principle of Cs-137 determination is therefore to establish the number of gamma emissions at this energy level over time.

Caesium-137 measurements were made using a hyperpure germanium (HPGe) detector. The model used is the EG&G Ortec LO-AX 51370 co-axial low energy photon detector. The detector is connected to a multiple channel analyser (MCA). The interaction of gamma ray photons with the detector leads to a voltage pulse with an amplitude proportional to the photon energy. Thus the MCA produces a spectrum of various gamma photopeaks at different energy levels. The detector used in Durham has been set up to measure gamma ray energies between 10 and 800 keV. This range includes energy levels associated with the decay chain of Pb-210, but in the present study only Cs-137 has been examined. The energy output from each sample analysis is observed using MAESTRO for Windows MCA Emulator software, also supplied by EG&G Ortec. The software allows the spectrum for each sample to be stored on disk. Several operations can be performed on the spectrum, including peak search, ROI insertion and report generation.

4.3.1.2 *The determination of ROI*

The peaks corresponding to different radionuclides can be identified by the MAESTRO software. Individual peaks can be selected by the operator for further investigation by defining a Region of Interest (ROI). The net area of Cs-137 counts and the errors associated with the net counts are increased as the range of the ROI increases. After some experimentation, the ROI was fixed from 659.34 to 663.99 keV for soil sample measurements used in the study. Depending on the particular soil samples, the centroid of the measured peak ranged from 661 to 663 keV. No discernible shift in the position of the Cs-137 photopeak was observed during the measurement period (of approximately 12 months).

4.3.1.3 *Calibration*

The detector has been calibrated using standard sediment samples provided by the International Atomic Energy Authority. The supplied standard was repacked into cylindrical pots, providing two samples of 25 g and one of 50 g. These standards have been run on numerous occasions. By comparing the reported radionuclide levels for the IAEA material with the counts, efficiencies have been calculated for 25 g and 50 g cylindrical pots. A third counting geometry is used in the laboratory consisting of a 500 ml Marinelli beaker. The Marinelli beaker is re-entrant and surrounds the active detector, whereas the cylindrical pots are placed on the top of the detector. By measuring samples in a Marinelli Beaker and then splitting them into 25 or 50 g subsamples it is possible to derive efficiencies for the Marinelli beaker. Efficiency calculations based on the IAEA sample have been supported by cross-calibration for a small number of samples with gamma spectrometry laboratories at the Department of Geography, University of Exeter, and NES, Coventry University.

The calibration procedure using environmental samples supplied by IAEA has been used in preference to making standards from artificial carrier solutions. In part this has been due to the length of time required to obtain permission to use unsealed sources.

4.3.1.4 *Measurement errors and counting times*

After the Range of Interest has been fixed, the measurement error in gamma spectrometry results primarily from counting error. Detection of radioactive emissions is a statistical time dependent process, such short count periods which yield only low numbers of counts, are very prone to error with poor repeatability (Durance, 1986). Cs-137 measurement errors are determined using the following equation adapted from the manual provided by EG&G Ortec:

$$\text{Error} = 1.96*A^{1/2}/A*100 \qquad \text{(Equation 4-1)}$$

where A is the net area (gross area minus the background area) of Cs-137 activity; and 1.96 is the 95% confidence level. For achieving less than 10% measurement error, Equation 4.1 requires a net area of 400 counts. The counting times required are therefore dependent on activity and the size of the sample. Smaller samples (25-50 g) typically require count times of 16-24 hours. Larger samples in Marinelli beakers (c. 500 g) yielded sufficient counts to be analysed in 8-12 hours.

The results of Cs-137 concentrations are presented in Appendix 3, in which Table 1 refers to reference samples, Table 2 presents the samples used for estimating variability, Table 3 is for soil samples from arable land, Table 4 for reservoir sediments and Table 5 for topsoil and deposited materials.

4.3.2 Particle size distribution analysis

Selected soil samples from arable land were analysed for particle size distribution (Agricultural Bureau of USA System) using pipette methods in China before they were transported to Britain. The original results are presented in Appendix 4. For USA systems, 2-0.1, 0.1-0.002, <0.002 mm are classified as sand, fine sand silt and clay. Below <2 mm soil particle sizes are dominated by fine sand and silt (0.25-0.002 mm), which are very susceptible to water erosion. Coarse sand contents (2-0.25 mm) account for very low (less than 10) percentages of total soil. Sediment

samples from reservoir core 1 were measured for the absolute particle size distributions using a Coulter Counter, following pre-treatments with hydrogen peroxide and sodium hexametaphosphate. This was undertaken in UK and the results are presented in Appendix 5.

4.3.3 Geochemical analysis

It was planned that detailed geochemical analysis would be undertaken for the sediment samples from the reservoir and the collected topsoil and deposited samples throughout the watershed in order to supplement interpretations based on the Cs-137 technique. Regrettably, insufficient time has prevented full analysis of sample taking place.

4.4 DATA COLLECTION

The large scale sediment yield study in the latter three chapters (Chapter 7 to 9) involves the compilation of many datasets including runoff discharge and sediment loads and the potential influencing variables. The runoff and sediment discharge data are from the Chinese Hydrological Year Book (CHYB), whereas the potential influencing variables are from varied sources including several environmental databases derived via the Internet. The following sections will give a brief introduction on those variables and the original sources from which the data are obtained.

4.4.1 Runoff and suspended sediment load data

The runoff and sediment load data are from the network measurement throughout the Upper Yangtze. The record of the measurement series date back to the 1930s for a few stations but the majority originate in the 1950s. The original records for each station are co-ordinates (latitude and longitude), catchment area, mean monthly and annual discharge, maximum daily discharge and its date of occurrence. The annual sediment loads were recorded in units of 10^6 or 10^4 t varying on the station basin area

or measurement year and it is apparent that the compilation of records into yearbooks has led to some mistakes of units. Recalculation of annual load from monthly load data has enabled several transcription errors to be corrected. The recorded catchment areas and locations of many stations are inconsistent within the measurement series and might reflect correction of previous area measurement or a slight change of station location. Error is also introduced through the use of daily or weekly measurements rather than continuous monitoring which may underestimate sediment discharges in peak flows. Similarly, the reported load is suspended sediment and ignores any bed load contribution. The data used for this study are from 255 hydrological gauging stations with up to 30 years measurement ranging from 1956 to 1987 and are maintained within a series of spreadsheets. At the time of data acquisition, 1987 was the latest year for which runoff and sediment yield data are available.

On the basis of its main tributaries, the upper catchment of Yangtze River can be divided into 5 parts, Jingsha-Yalong, Dadu-Min, Jialing, Wu river and main river (Figure 3-2). The numbers of stations by catchment area for these tributaries are summarised in Table 4-1. The catchment area for most stations ranges from 100 to

Table 4-1, The numbers of hydrological stations by main tributaries upstream

Catchment area (km^2)	Jinsha-Yalong	Dadu-Min	Jialing	Wu	Main River	Total
<100	1	0	0	0	0	1
100-1,000	29	7	13	5	6	60
1,000-10,000	29	22	42	15	12	120
10,000-100,000	11	19	14	6	1	51
100,000-1,000,000	14	2	1	0	5	22
>1,000,000	0	0	0	0	1	1
Total	84	50	70	26	25	255

1,000,000 km^2. Within the period of available data (1956-87), measurements were not continuous with some stations withdrawing their measurement and other new stations set up. The numbers of stations by measurement years are summarised in Table 4-2. Many stations have a relative short measurement period. Generally, the stations on main tributaries and channels have a longer series. The stations with a history of less than 5 years are mainly located around lower Jinsha tributary.

Table 4-2, The numbers of gauging stations by measurement years

Measurement years	Numbers	Percentage
1-4	68	26.6
5-9	30	11.8
10-14	22	8.6
15-19	29	11.4
20-24	50	19.6
25-32	56	22.0
Total	255	100

Many analytical procedures could be undertaken based on the dataset but the fundamental concerns of the study are spatial variability and temporal changes of sediment yields and the reasons for the variability and changes. Longer term measurement series which can be used to develop the relationships between sediment yields and potential controlling variables are very important, particularly in an area such as the Upper Yangtze which experiences large climatic and hence sediment loads variations from year to year. A sub-dataset on runoff and sediment is extracted from the dataset. This sub-dataset consists of the catchments with longer measurement. There are 56 stations with at least 25 years of measurement (Table 4-2). These 56 stations together with a further 6 stations from the Wu tributaries (which

Table 4-3, The summary information for the 62 catchments in the Upper Yangtze

No	Tributaries	Stations	DA (km^2)	Years	Mean ($t\ km^{-2}\ yr^{-1}$)	SD	Min.	Max.
1	Jinsha-Yalong	zimenda	137704	28	68	38	9	139
6		shigu	232651	28	91	42	30	182
16		huatan(qiaojia)	450696	30	366	133	221	707
23		ninnan	3074	25	1191	764	330	3193
25		qianxinqiao	2549	27	65	40	22	177
29		meigu	1607	25	1152	653	473	3103
30		pingshang	485099	31	505	177	260	1034
31		hengjiang	14781	25	919	367	429	1629
32		zhutuo	694725	26	459	102	296	668
36		dianwei	120	29	262	245	20	931
42		qinkoutang	2109	29	798	364	272	1629
64		lounin	108083	28	175	79	77	333
67		xiaodeshi	118294	27	249	114	107	544
69		anninqiao	937	27	657	372	238	2159
70		sunshuiguan	1596	26	1770	1523	350	7237
71		manshuiwan	3817	32	975	659	263	3042
73		wantan	11100	26	973	587	389	2707
81	Dadu-Min	zengjianguan	4486	27	124	72	38	295
83		shaba	7231	31	344	211	94	1034
84		jiangsheba	14279	26	307	198	75	915
85		zagunao	2404	26	284	170	63	810
86		shuangping	4629	30	387	216	145	1145
91		yanliuping	363	26	812	794	23	3695
92		xinxinchang	396	26	1257	1242	139	5315
94		pengshan	30661	30	337	157	131	721
97		qinshuixi	3330	28	487	230	86	1346
98		gaochang	135378	32	363	160	167	897
105		dajin	40484	27	107	53	31	266
116		shaping	75016	21	420	146	189	732
125	Tuo	shanhuangmiao	6590	28	853	440	204	1954
128		denyenyan	14484	31	617	365	73	1571
129		lijiawan	23283	29	537	351	94	1532
133	Jialing	yunninzeng	2071	25	458	420	46	1513
140		liuanyang	19206	30	1706	1327	273	6638
149		wudu	14288	25	1194	860	223	4660
153		bikou	26086	27	632	453	79	1609
154		sanleiba	29247	29	563	359	110	1381
156		tinzhikou	61089	28	1027	644	196	2681
160		qinquanxian	5011	25	598	562	96	2821
164		wusheng	79714	31	928	562	123	2542
165		beipei	156142	31	955	469	189	2284
168		bixi	2124	28	661	475	55	1605
171		qilitou	6382	27	586	393	72	1389
178		dunlin	6462	29	1216	726	273	3394
179		minyuantan	736	27	1108	447	423	2024
180		guodukou	31626	30	630	344	102	1517
182		jinbian	2740	27	395	263	31	1022
183		luoduxi	38071	31	760	442	94	1757
189		fujiangqiao	11903	25	992	921	139	4056
190		guanyinchang	1933	26	228	172	14	726
195		shehong	23574	29	705	527	43	2584
197		xiaoheba	29420	30	650	566	59	3121
200	Wu	yachihe	16541	21	886	409	193	1727
201		wujiangdu	26496	23	498	305	9	1131
206		shinan	50791	21	345	186	17	746
207		wulong	83035	27	390	148	134	730
208		gongtan	58346	21	366	149	70	719
220		duntou	6917	26	94	49	17	176
236	Main channel	chuntang	866559	30	518	127	333	823
242		shizhu	898	25	719	1013	157	5377
243		wanxian	974881	20	503	122	346	819
250		yichang	1005501	31	524	98	361	725

is deficient in long-term stations) have been extracted from the larger dataset. The 62 catchments comprises 17 in Jinsha-Yalong, 12 in Dadu-Min, 23 in Jialing (including Tuo), 6 in Wu and 4 in the Main channel region. Details of the stations are provided in Table 4-3. Chapter 7 will introduce the detailed methods on how to examine spatial variability and temporal changes mainly using those 62 catchments. The spatial variability modelling will be introduced in Chapter 8. The sediment transport data used in Chapter 9 are also from this sub-dataset.

4.4.2 The Asian 30arcsecond DEM

The most common digital data of the shape of the landsurface is cell-based Digital Elevation Models (DEM). The DEM can be used to quantify the characteristics of the land surface. A DEM is a raster representation of a continuous surface, usually referring to the surface of the Earth. The accuracy of these data is determined primarily by the resolution (distance between sample points). The Asian 30 arcsecond DEM is the highest resolution DEM (or elevation data) in the public domain found so far for this part of China. The DEM was compiled from several data sources. The primary source was a generalisation of the Level 1 Digital Terrain Elevation Data (DTED). DTED is a 1 degree by 1 degree dataset produced by the US Defence Mapping Agency (DMA) that contains digital parts of the world. It was originally designed to provide basic quantitative data for military training, planning and operating systems that require terrain elevation, slope and related information. The DTED data cover over 95% of the landmass of Asia. The elevation data for the areas of Asia which are not covered by the DTED data were developed using the 1:1,000,000 scale Digital Chart of the World (DCW). The DTED has been derived from a number of cartographic and photographic sources, and by using various techniques. The spacing of elevation for the DTED is according to the latitude. It is 3 by 3 arcseconds for 0-50 N-S, with the accuracy of 130 meters of absolute horizontal at 90% circular error and of +/- 30 meters of absolute vertical at 90% linear error. The original 3 arcsecond DTED data for Asia were resampled to 30 arcsecond and produced Asia 30 arcsecond DEM (approximately 1 km).

4.4.3 Global Ecosystems Database (GED)

Global Ecosystems Database (GED) version 1 is an integrated and global database related to global environmental and ecological change study (NOAA-EPA Global Ecosystems Project, 1992). In the database, there are many useful data including temperature, precipitation, vegetation, land use, cultivation intensity and soils. Unfortunately, most of those ecological datasets are with resolutions 1 by 1 degree, which are not high enough for this regional study. At the end, monthly and annual average precipitation data are taken from this database. The resolution for this data are 0.5 by 0.5 degree (Legates and Willmost, 1992).

The Normalised Difference Vegetation Index (NDVI), derived from the National Oceanic Atmospheric Administration (NOAA), Advanced Very High Resolution Radiometer (AVHRR) satellite data, are also taken from the GED CD-ROM. The NDVI data are from the Monthly Experimental Calibrated GVI with the resolution of 10×10 minutes developed from weekly visible and near-infrared AVHRR channel data from 1985-1990 (NOAA-EPA Global Ecosystems Database Project). The more details on the NDVI data (e.g. its definition and measurement) will be introduced in Chapter 9.

4.4.4 The Asian Population Database

The database was downloaded from the Asian Population Database (APD) from the Internet in compressed ASCII format, and converted into grid using Arc/Info. The resolution for the original grid is 2.5 by 2.5 minutes, which is only lower than the Asian 30 arcsecond DEM among the data sources used in the study. The development of the APD was supported by the United Nations Environment Programme/Global Resource Information Database (UNEP/GRID) and the Consultative Group for International Agricultural Research (CGIAR) in the context of the UNEP/CGIAR Initiative on the Use of GIS in Agricultural Research. Additional support and facilities were provided by the National Centre for Geographic Information and Analysis (NCGIA). The current database builds upon earlier work at NCGIA. The Asian population database is part of ongoing effort to

improve global, spatially referenced demographic data holdings. Such databases are useful for a variety of applications including strategic level agricultural research and applications in the analysis of the human dimensions of global change. This project has pooled available data sets, many of which had been assembled for the global demography project. For China, the data were the census products undertaken in 1992. The information provided here is from the Asian Population Database Documentation.

4.4.5 The Digital Chart of the World (DCW)

The DCW was digitised from 1:1,000,000 scale maps, except over Antarctica where the scale is reduced to 1: 2,000,000, by Environmental System Research Institute (ESRI) under contract from the US Defence Mapping Agency (DMA) from their Operational Navigation Chart (ONC) series (ESRI, 1993). This is the largest scale unclassified map series that provides consistent, continuous global coverage of essential basemap features. It is composed of 17 thematic vector layers which include political boundaries, coastlines, cities, transportation networks, hydrography, landcover, hypsography and place names. There are some blank areas (no data) for elevation contours for the Upper Yangtze. The drainage network is contained in drainage layer.

4.5 GIS APPLICATION

The study involves many aspects of GIS application for data capture and manipulation and map generation. The GIS application introduced in the section is mainly focused on the analysis of land surface and surface hydrology, including surface generation, DEM build-up for the small catchment used for Cs-137 study, watershed delineation, stream network analysis, and extraction of the potential influencing variables from the varied databases introduced above.

4.5.1 DEM build-up and surface generation

It may be possible that there is an existing DEM available for large scale study such as the 30 arcsecond DEM introduced above, but it is more commonly the case that a DEM must be constructed from contour lines or / and height points for a small scale study. This process involves the use of a GIS package. In Arc/Info Version 7 (ESRI, 1994), the TIN (Triangulated Irregular Network) and GRID provide the functionality. The functionality are also very useful for surface generation of any continuous variable such as Cs-137 inventory and sediment yield (see Chapter 8 for details), therefore, a brief introduction is made below for surface generation.

4.5.1.1 Surface generation

In the frame of TIN in Arc/Info, CREATETIN command uses a linear relationship between the sampling points to establish a surface based on a triangulated irregular network. Tin is a set of adjacent, non overlaying triangles computed from irregular spaced points (ESRI, 1994). Using CREATETIN, the regions with constant value or without data can be specified. With the tin created using contour lines and height points it is easier to convert into a lattice (equivalent to a grid). The tin model stores the topological relationship between triangles and their adjacent neighbours. This data structure allows for the efficient generation of surface models for the analysis and display of terrain and other types of surface (ESRI, 1994).

GRID provides five powerful surface generators, inverse distance weighted interpolation (IDW), trend surface interpolation (TREND), kriging (KRIGING), spline (SPLINE), and topogrid (TOPOGRID). The first four methods are general purpose interpolation methods, whereas TOPOGRID is particularly designed for creating hydrologically correct DEM.

IDW, the most commonly used method (Eklundh and Martensson, 1995), determines cell values using a linearly weighted combination of a set of sample points. The weight is a function of inverse distance. IDW allows control of the significance of known points upon the interpolated values, based upon their distance from the output point (ESRI, 1994). There is a power option when using IDW. A larger power will

result in less influence from surrounding points, i.e., nearby data will have the most influence, and the surface will have more detail (be less smooth) (ESRI, 1994). The characteristics of the interpolated surface can also be controlled by limiting the input points through defining the number of sample points to be used or a radius within which all points to be used in the calculation of the interpolated points (ESRI, 1994). Because the IDW is a weighted distance average, the average cannot be greater than the highest or less than the lowest input. Therefore, it can cannot create ridges or valleys if these extremes have not already been sampled (ESRI, 1994).

KRIGING is an advanced geostatistical procedure that generates an estimated surface from a scattered set of points. In Arc/Info Version 7, KRIGING offers two types of surface estimates: ordinary kriging and universal kriging. Ordinary kriging is represented by the SPHERICAL, CIRCULAR, EXPONENTIAL, GAUSSIAN, and LINEAR methods, Universal kriging is represented by the UNIVERSAL 1 and UNIVERSAL 2 methods. Each kriging methods uses a mathematical function to model the spatial variation within the input sample points. The spatial variation is quantified by the semi-variogram, a graphical plot of semi-variance against the distance between the pairs of sample points. The sample semi-variogram is calculated from the sample data and modelled by fitting a theoretical function to the sample semi-variogram. An optional output of kriging is a variance grid which shows the difference between predicted and actual variance at each cell. This can be used to determine the reliability of interpolated points.

SPLINE performs a two-dimensional minimum curvature spline interpolation on a point set resulting in a smooth surface that passes exactly through the input points (ESRI, 1994). The methods of SPLINE to be performed are REGULARISED and TENSION. The REGULARISED option usually produces more smooth surfaces than those created with the TENSION option. SPLINE interpolation ensures a smooth (continuous and differentiable) surface together with continuous first-derivative surface. Rapid changes in slope (the first derivative) may occur in the vicinity of the data points; hence this model is not suitable for estimating second derivative (curvature).

The TREND interpolator uses a polynomial regression to fit a least-squares surface to the input points. The order of the polynomial used to fit the surface can be controlled. A first order surface interpolation simply performs a least-squares fit of a plane to the set of input points. As the order of the polynomial is increased, the surface being fitted becomes progressively more complex. Trend surface interpolation creates a smooth surface. The surface generated will seldom pass through the original data points since it performs a best fit for the entire surface.

TOPOGRID, recently integrated in Arc/Info from Version 7, is optimised for creating hydrologically correct DEM models from comparatively small, but well selected elevation and stream coverage (ESRI, 1994). It is based upon the ANUDEM program developed by Hutchinson (1988, 1989). The most obvious feature is that TOPOGRID incorporates the drainage and sink enforcement processes, so that it can create hydrologically correct DEM, e.g. a point coverage representing known topographic depression and a line coverage representing streams can be integrated as input coverage. Water is the primary erosive force determining the general shape of most landscapes. For this reason, most landscapes have many hill tops and few sinks, resulting in a connected drainage pattern. TOPOGRID uses this knowledge about surfaces and imposes constraints on the interpolation process that result in connected drainage structure and correct representation of ridges and streams (ESRI, 1994). The purpose of the drainage enforcement process is to remove all sink points in the output DEM that have not been identified as sinks in the input sink coverage. The program assumes that all unidentified sinks are errors and should be cleared. The TOPOGRID command requires that stream network data have all arcs pointing down slope, and that there be no polygons (lakes) or braided streams in the network (ESRI, 1994).

4.5.1.2 DEM build-up for Yiwanshui catchment

A DEM was created for the small catchment of Yiwanshui using a contour map of 1:10,000 with 5 m interval of each contour line as a base map. The catchment boundary was drawn manually from the contour map. The contour lines, catchment

boundary and shoreline of the reservoir were digitised as three coverage, respectively. The DEM was built using TIN (ESRI, 1994). Flat triangles are created whenever a triangle is created from three nodes with the same height value, such as when the three nearest sample points are located on the same contour arc (ESRI, 1994), and those flat areas were generated along ridges, streams and depressions because of sparse contour lines along them. Some intermediate points (label points), therefore, were added using keyboard along ridges, streams and depressions between the input contours. The final DEM was generated using contour lines and those additional points. A 3-dimensional (3D) model with a surface resolution of 2.5 m was exaggerated 1.5 times in a vertical direction (Figure 4-2). The 3D model can give a good visualisation of the surface of the catchment. This features can be clearly visualised from a 3-dimensional model of the catchment. The 3D model is viewed at a site on the south bank of the reservoir towards the north-east.

With the DEM available, many topographic features such as slope, aspect and convatures can be derived for any point within the catchment. The mean elevation averaged from 10×10 m grid is 305 m with a standard deviation of 36 m. Gentle slopes are mainly located along ridges and streams, and steep slopes located at the sides of streams. However, these gentle areas along the streams and ridges include many flat areas generated due to inherited GIS problems as discussed above. The mean slope is 21.0° with minimum, maximum and standard deviation of 0.0°, 42.8° and 9.6°.

Curvature including profile and planform curvature are secondary derivates which can also be derived from the DEM. A positive curvature indicates that the surface is upwardly convex at that cell. A negative curvature indicates that the surface is upwardly concave at that cell. The profile curvature shows the rate of change of slope from each cell. This is the curvature of the surface in the direction of slope. It affects the acceleration and deceleration of flow, and therefore influences erosion and deposition (ESRI, 1994). The planform curvature shows the curvature of the surface perpendicular to the slope direction and influences convergence and divergence of flow (ESRI, 1994).

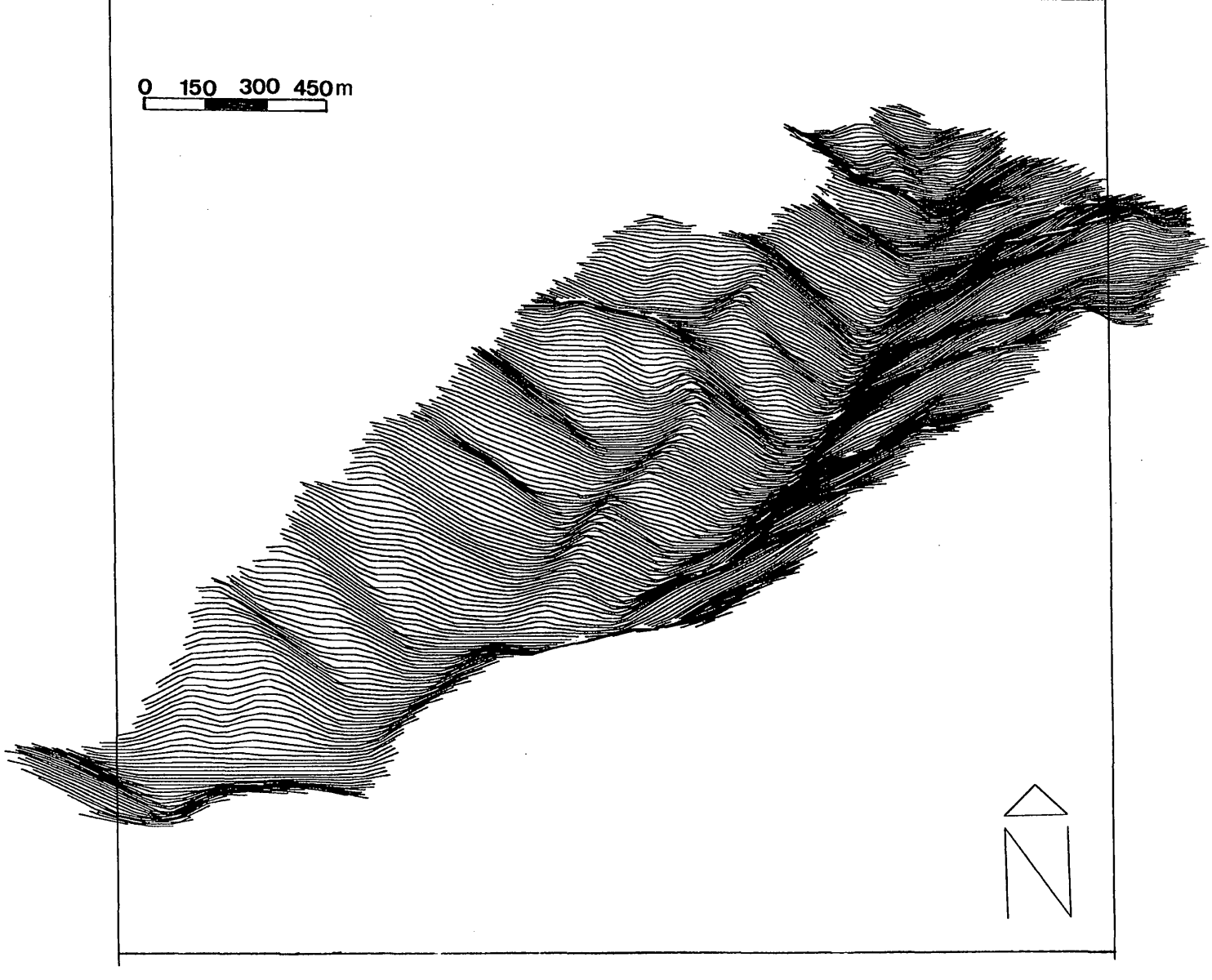

Figure 4-2, 3D model of Yiwanshui catchment

All the variables extracted from the DEM can be integrated with the Cs-137 study. Unfortunately, it is found that the resolution of the DEM developed based upon the topographic map, was not high enough to indicate actual topographic features. This is mainly due to the dissected terraces constructed by farmers. Due to long-term human activities, there are few natural slopes within the catchment, perhaps throughout the Three Gorges area particularly in arable slopes. Cs-137 and soil erosion can be considerably affected by micro topographic features. Therefore, subsequent analysis between Cs-137 and topographic features cannot be based upon the DEM.

4.5.2 Watershed delineation in the Upper Yangtze

As the basic unit for specific sediment yields is the individual catchment, identification of boundaries for each catchment is an essential stage for extracting the potential influencing variables using GIS. Given the co-ordinates of the gauging station a high resolution DEM can be employed to derive catchment boundaries and hence most catchment morphometric variables. The Asian 30 arcsecond DEM has the highest resolution elevation data available in the public domain for this part of China. With the DEM available, some catchment boundaries can be delineated using Arc/Info GIS (ESRI, 1994). Flow across a surface will always be in the steepest downslope direction. Once the direction of flow out of each cell is known, it is possible to determine which and how many cells flow into any given cell. This information can be used to define watershed boundaries and stream networks (ESRI, 1994). The detailed procedures for watershed delineation can be found in the section of surface hydrologic analysis in on-line help (ESRI, 1994). The flow chart showing the process of extracting watershed boundaries and stream networks from the 30 arcsecond DEM is presented in Figure 4-3 . Errors in DEM are usually classified as either sinks or peaks. A peak is an area surrounded by cells of lower value. These are more commonly natural features, and less detrimental to the calculation of flow direction. Likewise, a sink is an area surrounded by higher elevation values, and is also referred to as a depression or pit. This is an area of internal drainage (ESRI, 1994). Some of these may be natural, particularly in glacial or karst areas, but many sinks are imperfections in the DEM. Those spurious sinks within a DEM must be

filled to obtain a depressionless DEM before further processing. The quality the flow accumulation grid generated from the depressionless DEM was quite good in the mountainous west of the basin, but not as good in the Three Gorges area and relatively flat areas which are mainly located in Sichuan basin. This means that watershed delineation would not work adequately in those areas. Subsequently, the 42 catchments which have relatively longer sediment load measurement series in the sediment dataset obtained from CHYB were delineated. The catchments located in those relatively flat areas therefore were digitised from 1:1,500,000 map. There are also some difficulties to identify the catchment boundaries, since there are no contour lines on the maps, except for some shadings showing elevation features which can be traced for the identification. There is no doubt that this process will introduce some errors both on the areas and locations of the catchments digitised using the map of smaller scale. Furthermore, the errors also might come from the original records in the CHYB as stated above. The catchment boundaries obtained through the delineation and digitising are compared with that recorded in CHYB. The discrepancies between the delineated/digitised and the recorded areas were generally small a difference of <5% for 40 of the 62 basins (64.5%), 5-10% for 19 basins (30.6%), and three had difference between 10 and 15% (4.7%). The higher variations occurred for smaller catchments and in Yunnan-Guizhou plateau where the relief is relatively low. The agreement between the delineated/digitised catchment areas and the recorded catchment areas is very good, considering the lower resolution of the DEM and small scale topographic map and many problems on the locations and basin areas for the records in CHYB. In addition, the co-ordinates for hydrographical stations were recorded as latitude and longitude with an accuracy of two decimal minutes for the basin in CHYB. Therefore, the accuracy can be further improved through interactively selecting the outlet points for catchment delineation. Overall, the results from delineation and digitising are sufficient enough for the catchment based studies.

4.5.3 Drainage network extraction in the Upper Yangtze

Many variables have been examined for developing the relationship between sediment yield and its potential influencing variables in regional and global sediment yields studies but little attention has been made on drainage density as listed in

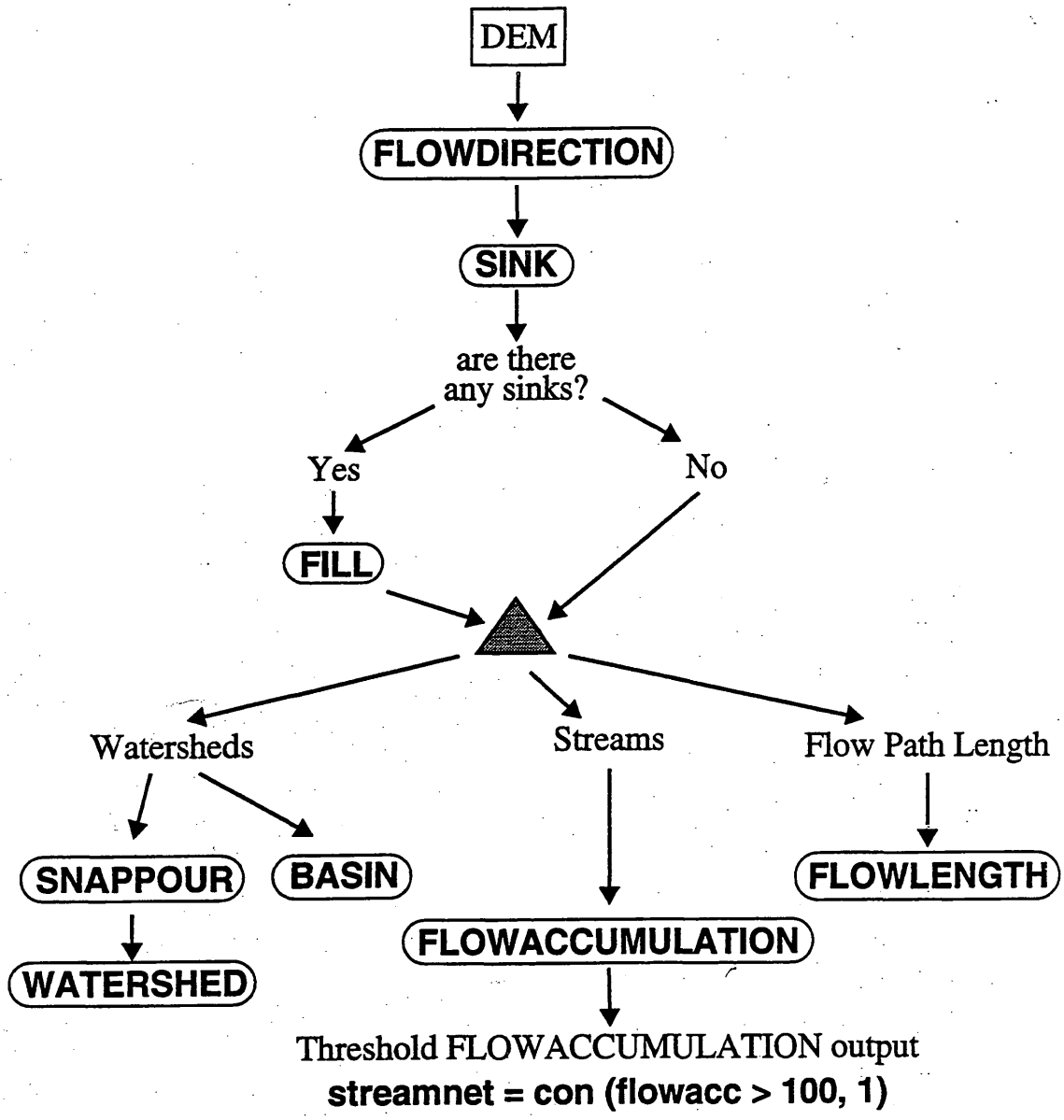

Outline of steps to derive surface characteristics from a DEM

Figure 4-3, The flow chart showing work procedures for watershed delineation and drainage network extraction (after ESRI, 1994).

Table 2-2. This is mainly because of the difficulties in obtaining the total stream length for large scale areas using traditional methods, as drainage density is calculated as mean length of total stream channels per unit area. The study tried three ways to obtain the drainage network as part of a large dataset development for integration with sediment load datasets in the Upper Yangtze. First, the networks were digitised from 4 map sheets, three of which have a scale of 1:1,600,000 and another has a scale of 1:2,500,000 (see Appendix 6). After digitising the maps, it is found that there is drainage information in the drainage layer of the DCW. The scale is larger than that for the four digitised maps, therefore an attempt was made to extract drainage information from DCW. The drainage density obtained from DCW is very low ranging from 0.03-0.2 km km^{-2} (see Appendix 8), indicating there are no detailed streams in DCW. Therefore the study also attempts to extract the drainage information from 30 arcsecond DEM. It can be obtained through selecting different thresholds of flow accumulation (Figure 4-3). As stated above, the poor quality of the flow accumulation grid in relatively flat areas also means that the drainage networks would not work. In the end, those areas were separated from the whole DEM and processed individually for drainage network extraction. This separation greatly improved the quality of the networks, which implied that although watershed delineation did not work, the drainage network might still be possible to extract from the DEM. The networks obtained through selecting different thresholds were somewhat similar as digitised from the paper maps of different scales. The higher threshold might represent the drainage networks on smaller scale maps with sparser streams, whereas the lower threshold on larger scale maps with more detailed streams. Based on the 42 catchments extracted, drainage density ranges from 0.1-0.2 and 0.3-0.4 km km^{-2} for the threshold of >20 and >5, respectively, which indicated much detailed stream data can be extracted from the DEM compared with the drainage density of 0.03- 0.2 km km^{-2} obtained from DCW. The drainage density extracted from DEM is resolution dependent variable. This drainage density extracted from the DEM can represent certain landscape features at certain scales but is still much low compared with the report of 5-500 km km^{-2} reported by Summerfield (1991). Therefore the drainage density extracted has not been used for further sediment yield analysis.

4.5.4 The variables extraction from varied data sources

With the catchment boundaries delineated from Asian 30 arcsecond DEM and digitised from paper maps, the following variables can be extracted from different datasets for each catchment. The extraction can be efficiently processed using AML (Arc Macro Language) files in Arc/Info. All the files used in the process are listed in Appendix 7. The variables extracted for those 62 catchments are listed in Appendix 8. Most of the extracted variables will be examined along with sediment yield data in the latter three chapters from Chapter 7 to Chapter 9, while some of the variables will not be used in the study but are listed in Appendix 8 as part of database development.

4.5.4.1 Morphometric characteristics of catchment

Many morphometric variables can be extracted from the 30 arcsecond DEM but the study is focused on the relief properties such as mean elevation (ME), basin relief (BR), relief ratio (RR), local relief (LR) and mean slope (MS). Some of those variables have not been examined in Chapter 8 but are also described here.

ME is defined as the mean of elevation of each cell, whereas BR is the difference between maximum and minimum cell values. Mean, maximum and minimum cell values for each catchment can be obtained from a statistical file after clipping the DEM using the available catchment boundary. RR is obtained by dividing basin relief by basin length (BL), a straight-line distance from catchment outlet (gauging station) to the most distant point on catchment boundary. Using Arc/Info distance functionality, BL can be obtained using the co-ordinates of gauging station and delineated / digitised boundary. LR is the mean of the local relief over cells of a given size across an entire catchment (Summerfield, 1991). In this case a reduced resolution DEM (60 by 60 seconds) was generated to produce a local relief grid from 4 neighbouring cells of the original 30 arcsecond DEM. Similarly, a slope grid can be generated using slope commands in GRID from which MS, defined as mean of slope of each cell, is extracted for each catchment. The slope is calculated based on maximum elevation changes within 9 neighbouring cells (ESRI, 1994).

4.5.4.2 *Precipitation, population density and NDVI*

Precipitation and NDVI are extracted from GED and population density from the Asia Population Database. Average annual precipitation (PP) is the mean of each cell over an entire catchment. A modified Fournier index (FN) is calculated as the sum of the square of mean monthly precipitation over mean annual precipitation for all 12 months of the year (Fournier, 1960). Mean monthly NDVI is the mean of each cell over an entire catchment. Average annual NDVI is the mean of mean monthly NDVI for all the months of the year. Population density (PD) is the mean of each cell over an entire catchment.

4.6 SUMMARY AND CONCLUSION

The chapter focused on field, laboratory and GIS work. Some preliminary results such as arable field characteristics and soils in the small catchment and the drainage basins within the Upper Yangtze is also introduced. The large scale sediment yield modelling needs many environmental and ecological data. The extraction of those data involves GIS application in many aspects. Considerable time was spent on data searching and GIS practice during the three-year PhD programme, but the data are still quite limited in the study particularly on land use and soils. However, it is quite likely that some data sources can be obtained from the Internet without any charge such as Asian 30 arcsecond DEM and population density data. With global and regional database development, it is quite likely that many environmental and ecological variables can be integrated with runoff and sediment yield data. For example, the global 1 km resolution vegetation map developed by the USGS from NDVI will be completely finished soon. In some case, data are available but are not accessible. For example, Chinese land use map of 1:1,000,000 in digital format is available at Grifffith University, Australia, but it was not possible to obtain it due to the data regulation.

5. SOIL EROSION ON SLOPING ARABLE LAND IN UPPER YANGTZE: A CASE STUDY IN YIWANSHUI CATCHMENT

5.1 INTRODUCTION

Sloping arable land is a major land use form in the Three Gorges area and one of the main sediment sources in the Upper Yangtze. In Chapter 3 it was stated that arable land accounted for 23% of the total area in the Three Gorge area and produced 46% of the total sediment to the Yangtze river, according to the estimates of Shi et al. (1992) (Table 3-10). Furthermore, the resettlement of people from within the Three Gorges Reservoir area will produce a tendency to locate new arable land on much steeper slopes than the prime agricultural land which would be flooded by the reservoir. Therefore, it is important to understand the patterns and rates of soil erosion on this sloping land. However, the information is rarely available in the area due to the difficulty in quantifying soil erosion for these steep slopes using conventional methods as described in Chapter 1. This chapter is mainly designed to investigate soil erosion using the Cs-137 technique on sloping arable land within Yiwanshui catchment, located in Changshou near Chongqing city (Figure 3-3). The main purposes of the chapter are:

1) to examine the potential for using Cs-137 to investigate soil erosion on steep arable land in the particular area with a subtropical environment;

2) to investigate soil erosion using Cs-137within terrace fields frequently maintained and disturbed by farmers;

3) to evaluate the main available quantification models from Cs-137 investigation to erosion rates for the particular soil with high gravel content;

4) to quantify the long-term patterns and rates of soil erosion on those sloping terraces using Cs-137.

The application of Cs-137 to the development of a catchment sediment budget is considered further in Chapter 6.

5.2 ESTIMATE OF Cs-137 ATMOSPHERIC FALLOUT

The application of Cs-137 based erosion estimates requires comparison of soil core inventories with an estimate of baseline fallout. Estimation of baseline fallout can be problematic in China, due to landscape disturbance by human activity. Though Cs-137 reference values used for erosion investigation have been reported for a few places in China (Zhang et al., 1990; 1994; Quine et al., 1992), uncertainties still exist for those values due to no independent ways of testing the validity of those estimates. The study aims to estimate total Cs-137 fallout by two different methods as discussed below.

5.2.1 Estimate from soil

Traditionally a Cs-137 reference value is estimated from reference sites, which are defined as those without obvious erosion and deposition (Ritchie and McHenry, 1990). In most applications of Cs-137 as a soil erosion tracer, reference sites have been located under light woodland or permanent pasture on flat interfluves. Accuracy of the estimate is affected by sampling strategy and sample size. It is, however, difficult to find such a site which has not been disturbed by human activity within the catchment, or indeed within Chinese arable environments. After thorough exploration of the catchment, one small paddy field was identified as a reference site (see Chapter 4 for detail). In order to investigate basic information on the behaviour of fallout Cs-137 within the paddy soil the vertical distribution of Cs-137 was plotted in Figure 5-1. First three samples with 10 cm increments indicates that peak Cs-137 is located at 10-20 cm and no Cs-137 was found below 30 cm except for sample 1. This suggests that Cs-137 has limited migration below the plough layer. This may

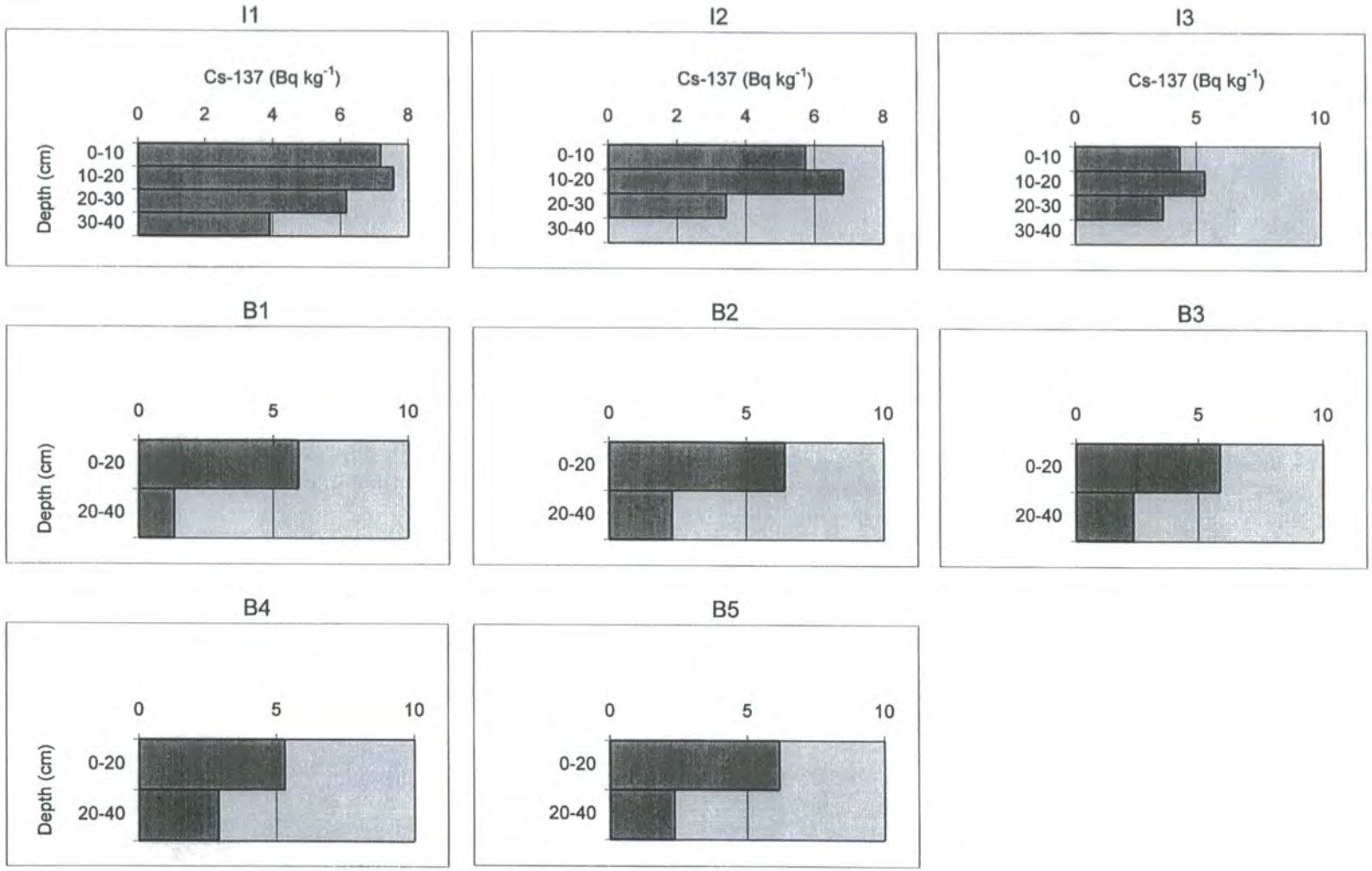

Figure 5-1, The vertical distribution of Cs-137 concentration for reference profiles taken from paddy field

be due to the formation of a hard plough pan particularly in paddy fields. The plough layer is not deep because of local tillage methods, mainly by buffalo or manually which results in a relatively shallow plough layer. In general, the depth distribution of Cs-137 was similar to dry arable land in China documented by others (Zhang et al., 1990; Quine et al., 1992) but more uniform within the upper 20 cm. Cs-137 activity and variability for the 8 samples are presented in Table 5-1. The variability of Cs-137 with coefficient variation (CV) of 13.6% in the paddy field is very small compared with previous reports (Table 3-1). The low variability may be attributed to the unusual conditions of paddy fields, long-term saturation by water in which the incoming Cs-137 fallout associated with precipitation which may contribute to even distribution and adsorption by fine soil particles. The soil moisture regime is the main difference between dryland and paddy fields, but the soil cores indicate that the unevenness of fallout in this location is relatively subdued.

Table 5-1, Summary statistics and variability of Cs-137 (Bq m^{-2}) at the reference site

	n	Ranges	Mean	STD	CV (%)
All samples	8	1807-2862	2250	306	13.6
The samples except an outlier	7	1807-2373	2163	201	9.3

Soil sampling size required to achieve an acceptable uncertainty in the determination of the mean activity of Cs-137 is one of major concerns for the sampling strategy, not least because of the implications it has for the logistics of using the Cs-137 technique for rapid appraisal of erosion status (Higgitt, 1995). The methods to estimate sampling numbers have been proposed by a number of researchers (Bachhuber et al., 1987; Fredericks et al., 1988; Sutherland, 1991). Obviously these methods are slightly different and calculations are based on the formula proposed by Sutherland (1991):

$N = (t*CV/AE)^2$ (Equation 5-1)

Where N is the required number of samples, t is the t value at 95% confidence (1.96), CV is the coefficient of variation (decimal fraction), and AE is the allowable error (10%) (decimal fraction). Based on the equation, the sample numbers required from the input site to estimate baseline fallout within the allowable error is seven. This suggests that sample numbers are sufficient to estimate a reliable mean of Cs-137 value for the small field.

This low variability of Cs-137 may be also due to the small area in which soil samples were taken. However, the result from another seven bulk reference samples (see Figure 4-1 for locations) confirms this low level of variability (Table 5-2). Among the seven samples, three were taken from the paddy fields with similar conditions as the above paddy field and four samples from woodland assumed no obvious erosion and deposition when samples were taken. It can be seen that one sample (No 52) from woodland has exceptionally high Cs-137 activity. The reason for higher Cs-137 is not clear but the ages of the trees (around 20 years old which means that the trees were planted after the peak fallout in 1960s) suggest that it is not

Table 5-2, Additional bulk samples for Cs-137 reference values

No	Land use	Cs-137 activity (Bq m^{-2})
6	Paddy	2155
33	Paddy	1824
34	Paddy	2158
8	Woodland	2127
37	Woodland	2200
52	Woodland	5092
53	Woodland	2662

reliable to develop a reference based on the samples from those afforested areas. However, the remaining six samples fall in the range determined in the first paddy field. This confirms that spatial variability for the paddy fields located in watershed boundary is small and subsequently the mean value constructed from that small paddy field is used as a Cs-137 reference value for this study.

For investigating the internal consistency and the occurrence of outliers, a box plot is drawn for the eight samples taken from the small paddy field (Figure 5-2). The figure shows that there is an outlier, although the variability is small. The outlier of the sample is located in the middle of the paddy field. Based on statistical principles, the outlier should be taken out from final mean calculation (Owens and Walling, 1996). Based on the other seven samples the estimated mean reference value is 2163 Bq m^{-2}. Table 5-3 lists Cs-137 reference values and rainfall reported from the studies undertaken in China. The value estimated from this study is very close to those reports. For example, it is quite close to the value of 2600 Bq m^{-2} used by Quine et al. (1992) in their study at Yanting near Chengdu. Yanting, located to the north of

Table 5-3, Cs-137 reference values estimated in China

Authors	Cs-137 (Bq m^{-2})	Numbers of samples	Annual rainfall (mm)	Location
Zhang et al. (1990)	2150-2529	3	506-622	Lishi and Louchuan in Loess Plateau
Quine et al. (1992)	2600	unknown	900-1100	Yanting, Sichuan
Wang et al. (1991)	1731	1	1285	Kangxian, Sichuan
Zhang et al. (1992)	1465-1633	2	680-1200	Norther Guizhou
Pu (1997)	4023	2	1612	Saxian, Fujian

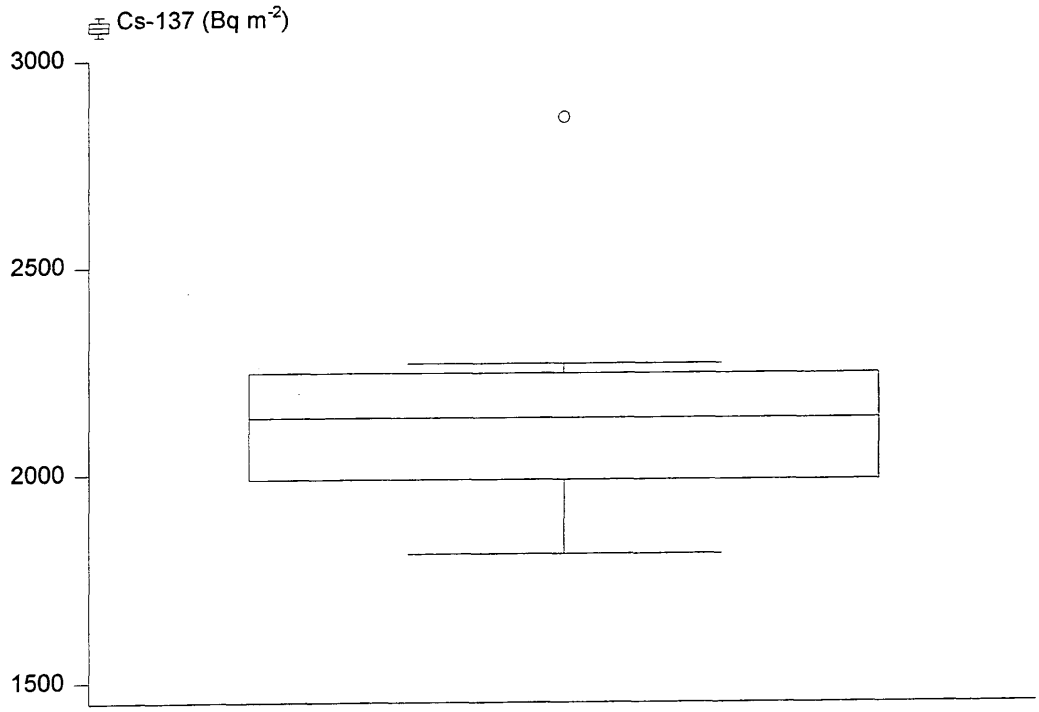

Figure 5-2, Box-and-whisker plot for Cs-137 aerial activities (Bq m^{-2}) for the samples at the reference site. Note the identification of an extreme outlier which is taken out for final mean calculation.

Changshou, has a mean annual rainfall of 900 and 1100 mm, which is close to the annual rainfall of 1030 mm in Changshou. Cs-137 fallout was mainly determined by latitude and precipitation. The estimated reference is also close to the values reported by Zhang et al. (1992) and Wang et al. (1991) but much lower than the value in Fujian reported by Pu (1997).

5.2.2 Estimates of fallout from atmospheric records

No systematic records on atmospheric fallout of Cs-137, to my knowledge, has been reported in China. The estimates from atmospheric records here are based on the model introduced below and the fallout information recorded in Japan.

5.2.2.1 Estimate of fallout for 1954-74

A reliable quantification of erosion from Cs-137 measurement requires not only a total inventory but also yearly or monthly fallout (Quine, 1995). Besides, using Cs-137 profiles obtained from reservoir cores to estimate sedimentation rates (detail will be introduced in next chapter) it also relies on its preservation compared with atmospheric fallout. Therefore an estimate of the monthly deposition of radionuclides for this area is required. Globally, as stated earlier, Cs-137 deposition is a function of latitude and mean annual rainfall. Under a given latitudinal zone, atmospheric fallout is a linear function of rainfall (Davis, 1963; Mathews, 1989). The relationships between Cs-137 fallout and precipitation have been studied in many places (Lance et al., 1982; Loughran et al., 1988; Kiss et al., 1988; Basher and Matthews, 1993). The developed relationships can not be used outside of the latitudinal zone in which the relationships were developed. A semi-empirical formula developed by Sarmiento and Gwinn (1986) for deposition of Sr-90 is employed for this estimate. Sr-90 concentration (in femtocuries per cubic meter, $fCi.m^{-3}$) in surface air is given by,

$$C(t, \phi) = R(\phi)\, Cref(t)[1+g(m, \phi)] \qquad \text{(Equation 5-2)}$$

Where m is the month, ϕ is latitude, and t is time in months running from 1 to 252 for January 1954 to December 1974. Values of the function Cref(t) were tabulated by Sarmiento and Gwinn (1986). $R(\phi)$ and $g(m, \phi)$ can be calculated for the latitude of

Changshou (29.83°N) based on the related tables provided by Sarmiento and Gwinn (1986). The Sr-90 deposition rate (F_A) was then calculated as

$$F_A=C(t, \phi)[Vd(\phi)+Vw(\phi,t)]/100 \qquad \text{(Equation 5-3)}$$

where Vd and Vw are the dry and wet deposition rates (cm sec^{-1}) and Vw is expressed in terms of the monthly precipitation P (cm) as

$$Vw= aPb \qquad \text{(Equation 5-4)}$$

Using tables provided by Sarmiento and Gwinn (1986), the dry deposition rate Vd, and constant a and b for wet deposition can be obtained. Values of monthly precipitation (P) were obtained from a local county meteorological station based on daily rainfall records. The rainfall measurements in Changshou county started in 1957 (see details in Chapter 3), monthly rainfall for the three years (1954-56) uses average monthly rainfall from 1957-87. The Sr-90 fallout (F_A) is calculated for months between January 1954 and December 1974. The rates of deposition of Cs-137 was calculated as 1.65 times the rate for Sr-90 using Equation (5-2). This ratio is characteristic of production rates of isotopes and is essentially independent of location (Callender and Robbins, 1993). However, the ratio may be slightly varied throughout the year (Sarmiento and Gwinn, 1986; Hirose et al., 1987).

The calculated monthly values from 1954 to 1974 are integrated into an annual flux of Cs-137 which is presented in Figure 5-3. It exhibits the well-known feature that deposition rates were highest during the periods of most intense atmospheric nuclear testing between 1958-1959 and 1963-1964. The marked inter-annual variation of Cs-137 must be integrated with soil erosion quantification. Fallout deposition also exhibited marked intra-annual variation (Figure 5-3). The monthly variation was influenced by the timing of nuclear tests and its precipitation. For the 4 years (1962-65) exhibited in Figure 5-4, peak fallout was in the late spring and small peaks also occurred in the later autumn. This suggests that erosion and fallout could have

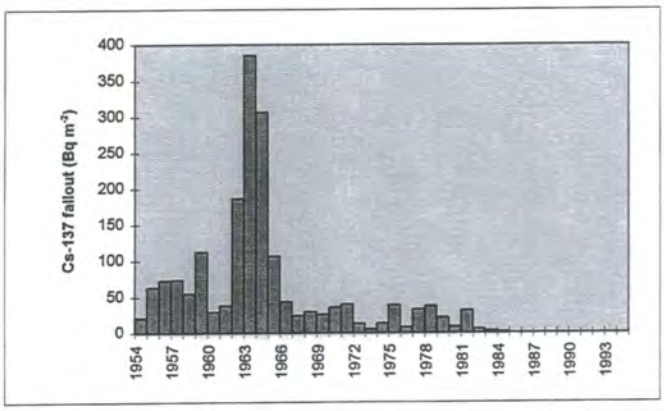

Figure 5-3, Annual Cs-137 fallout from 1954-74 estimated based on Sameriento and Gwinn (1986) model, and 1975-84 based on the records in Japan (Hirose et al., 1987)

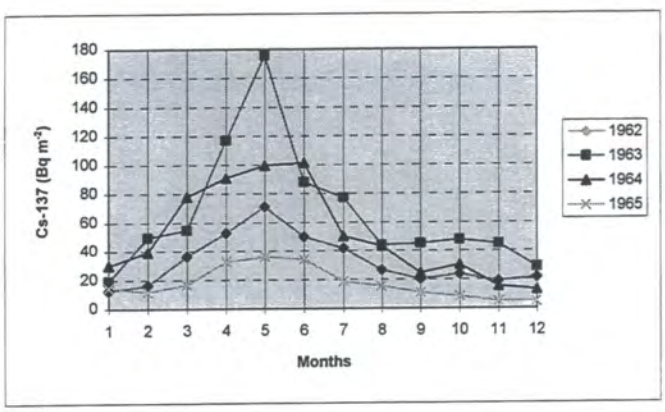

Figure 5-4, Monthly Cs-137 fallout for the four years (1962-65) estimated based on Sameriento and Gwinn (1986) model

occurred synchronously, indicating that it is likely that part of the fallout Cs-137 would be washed away before being mixed up by tillage operation. Therefore, the quantification of erosion will be more realistic if the monthly variation can be integrated in the quantification models.

The model for calculating Sr-90 (and Cs-137) deposition provides a useful tool for estimating monthly deposition in the area without any record. Uncertainties in calculated total deposition at mid-latitudes (45°-50°N) were estimated at roughly 10%, while comparisons with measured values were considerably better at less than 1%. Greatest uncertainty was associated with estimates of deposition during seasonal lows (±50%) (Callender and Robbins, 1993). The model was developed mainly using the data from Europe and North America (see Sarmiento and Gwinn, 1986), its accuracy in lower latitudes as the study area has not been examined. The total flux of annual Cs-137 from 1954-74 is 1683 Bq m^{-2} (decay corrected to 1994). Comparing this value with 2163 Bq m^{-2} estimated from reference samples indicates that the model estimate of Cs-137 deposition from 1954-74 is 78% of the total fallout estimated by reference samples. The model estimate does not cover the period from 1975-94. Although the atmospheric fallout world-wide was small fraction after 1970s but the total accumulated fallout during the 20 years can not be ignored due to frequent bomb tests in the late 1970s in China and the Chernobyl accident in 1986.

5.2.2.2 Estimate of fallout from 1975-94

Based on the fallout recorded by the Institute (Hirose et al., 1987), which is the nearest place to the study area, Cs-137 fallout from 1975 to 1984 is also depicted in Figure 5-3. The fallout in this period was mainly from Chinese nuclear tests as described in Chapter 2. Total fallout is around 200 Bq m^{-2} with an annual average of 20 Bq m^{-2} (both decay corrected to 1994). It must be admitted that the estimate is very crude and must be treated with great care, due to the large distance between Tokyo and the study area. The fallout for the latest 10 years from 1985-94 can not be estimated due to lack of data. The fallout during this period was mainly from the Chernobyl accident in 1986, which has been described in Chapter 2.

5.2.3 Discrepancy between the two estimates

If the fallout of 1683 Bq m^{-2} estimated by the model of Sarmiento and Gwinn (1986) from 1954 to 1974, and 200 Bq m^{-2} tentatively calculated for the period of 1975 to 1984 based on the data from Japan, are added together, it gives a total Cs-137 fallout of 1883 Bq m^{-2}. This is 87% of 2163 Bq m^{-2} estimated from reference soil samples. This demonstrates that it may be possible to develop a reliable reference value of Cs-137 using detailed monthly precipitation data in China where the landscape is heavily disturbed by human activity. However, further study is needed in different environments. The errors may come from many sources such as sampling, model application and the estimate for the latest 20 years, which have been discussed above. More importantly, the estimates from atmospheric records did not include the fallout generated from the Chernobyl accident. As described in Chapter 2, the Chernobyl fallout has been documented in South China. In the study area the Chernobyl fallout was also documented from reservoir sediments. The details will be introduced in the next chapter.

5.3 DIFFERENTIAL Cs-137 ACTIVITY AND GRAVEL CONTENT: POTENTIAL INFLUENCING FACTORS

Cs-137 activity can be affected by many factors. For sloping arable land, assuming the same cultivation practice, Cs-137 is mainly controlled by landform and the direct impact of human activity. Cs-137 sorption characteristics and vertical profile distribution may also be affected by soil types, but is not discussed here due to the fact that the catchment is dominated by purple soils.

5.3.1 Effects of topography

Many topographic factors such as slope angle, curvature and runoff concentration area may affect Cs-137 activity (Marts and De Jong, 1987). Initially, it was intended that those topographic features would be extracted from DEM. However it was found that the DEM developed based on the contour map of 1:10,000 can not fully represent the man-made terraced features (dissected but still with steep slope). The

study examines the effects of slope position, slope angle and length which were recorded when soil samples were taken.

5.3.1.1 Effects of slope position

For investigating background information on the behaviour of fallout Cs-137 for sloping arable land within soil profiles and at different slope positions, a small sloping arable land was sampled in detail (see location and sampling method in Chapter 4). The depth distribution of Cs-137 for the six samples was plotted in Figure 5-5. A few characteristics can be summarised from this preliminary investigation. First, Cs-137 is predominantly distributed in the upper 20 cm for most profiles, particularly those from upper and middle slope positions. This indicates that the 20 cm depth designed for sampling on sloping terraces throughout the study catchment is reasonable (see sampling strategy in Chapter 4). Second, Cs-137 is very variable even within such a small piece of land, Cs-137 increases in two slope directions (up-down and parallel). It is likely that this variability was caused by water-induced soil erosion. This investigation indicates that soil redistribution has taken place within the small arable fields. If the total Cs-137 for the samples at same slope position is averaged, the mean Cs-137 is 316, 332 and 685 Bq m^{-2} for the slope of upper, middle and bottom positions, respectively. The results indicate that the Cs-137 concentrations for the upper and middle slope are very close but significantly different from the bottom position. The middle slope position might be a suitable sampling location for representing the relative erosion status of the whole field.

Having considered the Cs-137 variability for different slope positions within the same field, spatial variability can be further examined using the bulk samples taken from the slope positions of the upper, middle and bottom in the 11 fields throughout the catchment. The Cs-137 concentration for the three different positions are plotted in Figure 5-6. It can be seen that the characteristics found above in the small field are not always consistent in the 11 fields such that Cs-137 activity is not always higher at bottom slope position. No clear pattern can be determined based on this plot. In order to further examine the difference of Cs-137 between the three different slope

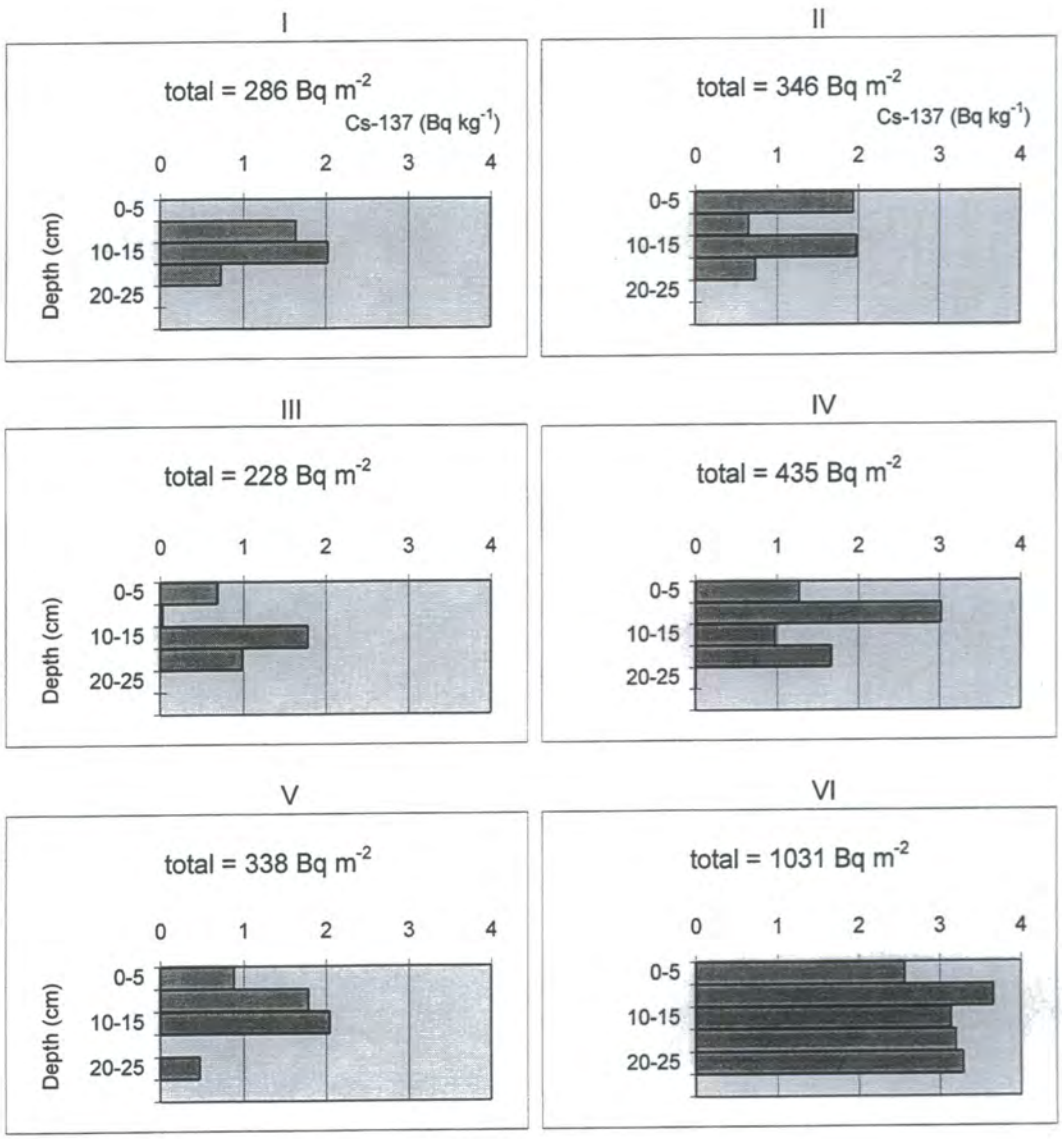

Figure 5-5, The vertical distribution of Cs-137 for the soil samples from a small terrace

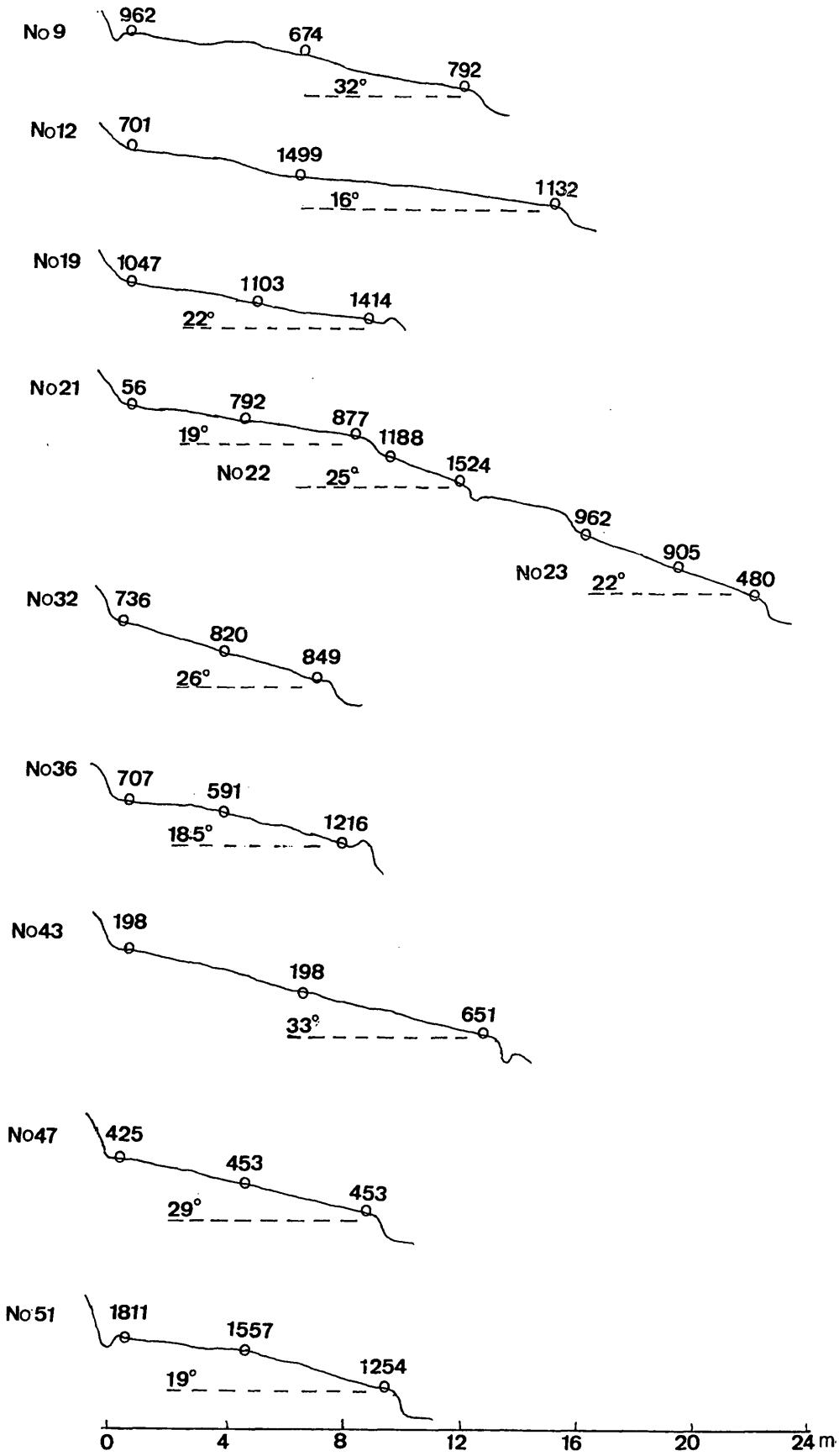

Figure 5-6, Slope profiles, sampling locations and Cs-137 (Bq m^{-2}) inventories for the 11 sampled fields

positions, activity statistics are summarised in Table 5-4, from which it can be seen that the mean Cs-137 is lowest at upper slope positions and highest at bottom slope positions. However, variability in Cs-137 activity as indicated by standard deviations of Cs-137 at these slope positions indicate the largest variability at upper slope positions and the lowest variability at bottom slope positions. Although the difference is very little but consistent with the result found in the small sloping terrace.

Having examined Cs-137 variation, it is necessary to examine the soil particle size distribution for different slope positions, since it can also indicate the sequence of soil erosion. More importantly, soil particles play an important role not only in soil erosion through the formation of soil structure (Wischemier and Smith, 1978) but in chemical adsorption such as Cs-137. In general, the soils from the upper parts of the fields show higher gravel contents than those from the lower parts of the fields. The mean percentage of >2mm fractions for the three different slope positions were summarised in Table 5-5. In contrast to Cs-137, >2mm fractions are higher at the upper position but lower at the bottom position. The variation of particle sizes with slope positions are consistent with that of Cs-137. As discussed above, this variation may be caused by soil erosion. While >2 mm fractions are variable for different slope positions, the fractions of <2 mm soil particle sizes have little variation (Figure 5-7). The particle size distributions also indicate that the soils in the catchment are dominated by fine sand and silt (0.25-0.002 mm) particularly 0.05-0.01 mm based on the classification by the United States Agriculture Department

Table 5-4, The mean of Cs-137 for three different slope positions

Slope position	Sample numbers	Mean (Bq m^{-2})	Std. Dev.	Min.	Max.
Upper	11	802	484	59	1803
Middle	10	860	426	212	1542
Bottom	11	971	364	461	1535

Table 5-5, The mean percentage of >2mm fraction for different slope positions

Slope position	Sample numbers	Mean	Std. Dev.	Min.	Max.
Upper	9	21.5	20.9	0.0	63.3
Middle	9	13.2	16.0	3.4	53.1
Bottom	9	10.3	10.6	0.0	27.7

(USDA) which are very susceptible to water erosion. Coarse sand contents (2-0.25 mm) account for very low (less than 10) percentages of total soil.

The results from Cs-137 activity and gravel content indicate that Cs-137 activity and gravel content for different slope positions within the same terrace are different. In general soil samples from middle slope positions are most representative for a single terrace. Again, this suggests that soil sampling strategy from middle slope is reasonable. If the particle size variability is caused by soil erosion, the differential indicates net erosion varies with slope position.

5.3.1.2 Effect of slope angle and length

Based on the 47 fields in which soil samples were taken, the average slope angle is nearly 25 degree ranging from around 15 up to 36 degrees. This degree of steepness of the arable land is quite common in the Three Gorges area as discussed in Chapter 3. Another topographic characteristic for those terraced fields is short slope length, with an average of 8 m, ranging from 2.5 to 18 m. Therefore, the terraced fields are characterised by small size and steep slopes. Those two features (slope angle and length) will be examined for their relationships with Cs-137 and soil particle sizes in this section. The analysis of Cs-137 for different slope angle and length will help to interpret soil erosion on those steep slopes.

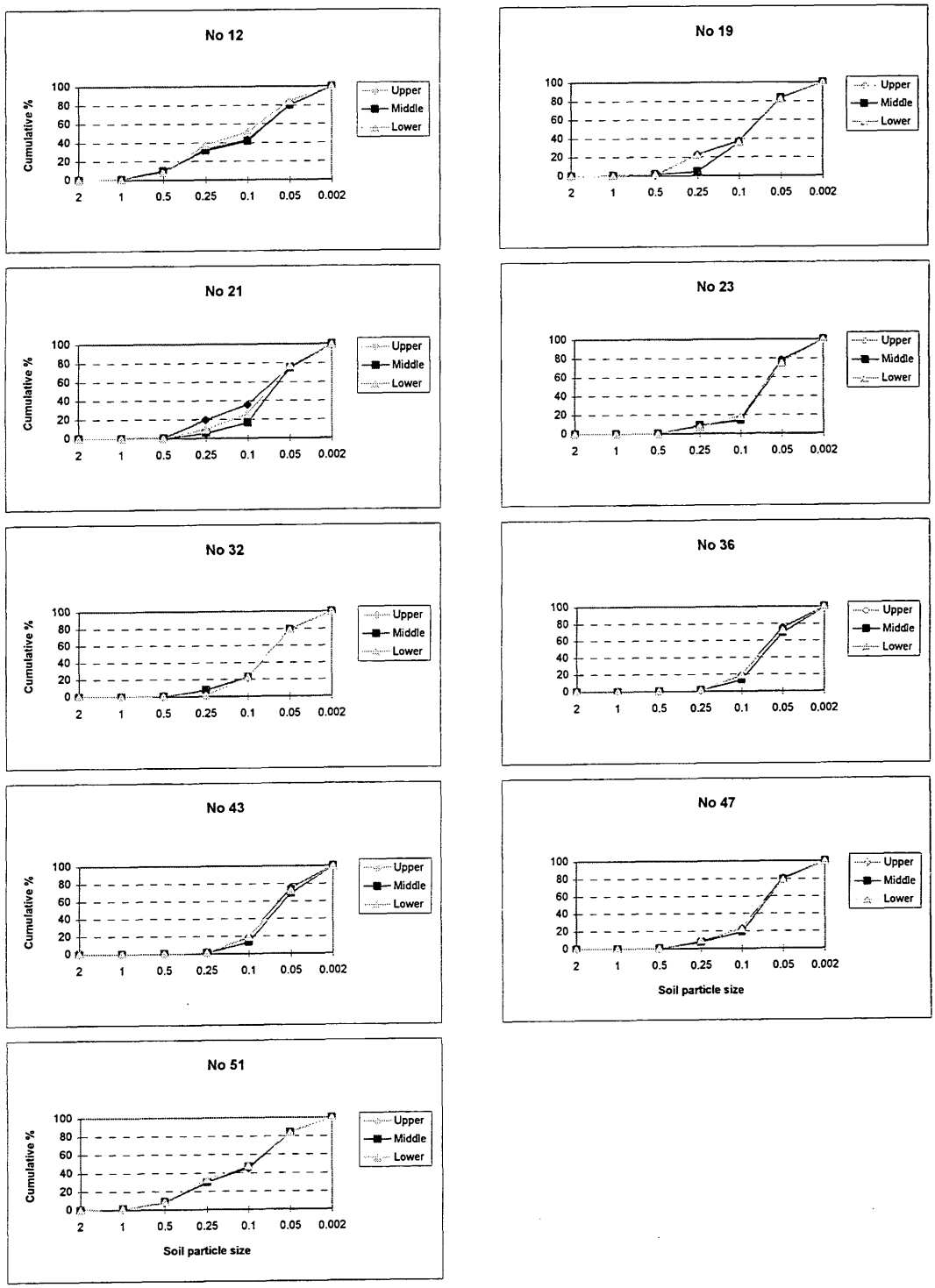

Figure 5-7, Soil Particle size (<2mm) distributions showing little variations for different slope positions

Under the same rainfall, land use and similar soils, it is assumed that soil erosion is controlled by topographic factors. The detailed relationships between Cs-137 and topographical factors were examined by Martz and de Jong (1987). The study examines the relationships between Cs-137 and two topographical factors: slope angles and length, which were measured in the field. The correlation between Cs-137 activity in total soil (including >2mm fraction) and slope angle and length are summarised in Table 5-6. Cs-137 is significantly correlated with slope angle but not with slope length. Dealing with slope length is a major difference between the Cs-137 technique and USLE (Wischemier and Smith, 1978). In USLE it is assumed that soil erosion increases with slope length increasing but most of Cs-137 studies indicate Cs-137 decreased or had no relation with slope length increasing (Kiss et al., 1986; Higgitt et al., 1992). Kiss et al. (1986) suggested the decreased erosion on longer slopes was due to their slope gradients. There is no relation between slope angle and slope length for this study (Table 5-6), indicating the control of human construction on the dissected terrace topography. Higgitt et al. (1992) reported that the lack of a relationship between topography and Cs-137 reflected a combination of the influence of other factors and the inherent variability of Cs-137 fallout. The scatter in the relationship between Cs-137 and slope angle and length may be caused by many factors but it is believed that effect of human activities such as deliberate soil removal and control of terrace forms is one of the main reasons. It is also believed that slope curvature plays an important role but can not be examined without more detailed survey records.

Pearson's correlation between the fractions of >2 mm particle sizes and slope angle, slope length and Cs-137 activity are also listed in Table 5-6. In contrast to Cs-137 activity, the percentage of >2mm fractions increases with increasing slope gradient, indicating the effect of slope angle on soil erosion. Similar to Cs-137, >2 mm fractions have no close relations with slope length.

As stated in previous chapters, the steepness of the slopes for the sloping terraces are far beyond the upper limits defined in USLE (Wischemier and Smith, 1978). More importantly, the relationships between Cs-137 and >2 mm fractions with slope

Table 5-6, Spearman's correlation matrix between slope angle, length, Cs-137 and >2mm fractions (n=66)

	Slope angle (°)	Slope length (m)	Cs-137 (Bq m^{-2})	% of >2 mm
Slope angle (°)	1.00			
Slope length (m)	0.07	1.00		
Cs-137 (Bq m^{-2})	-0.34**	-0.02	1.00	
% of >2 mm	0.46**	-0.03	-0.62**	1.00

** Significant at 99% level (critical value=0.31)

angle and length clearly indicate that soil erosion does not increase with slope length for such short yet steep sloping terrace. Therefore, any attempt to examine the effect of the combined topographic index (LS) on soil erosion using USLE topographic factor is not reasonable, suggesting USLE is not applicable for those sloping arable lands with characteristics of steep slope and short length.

5.3.2 Effects of human activity

Having examined the effects of topography on Cs-137 activity and gravel content, this section will discuss possible effects of human activity on the redistribution of Cs-137 activity and gravel contents. The human activity includes farmer's deliberate soil removal, terrace development and tillage operation.

5.3.2.1 Effect of deliberate soil removal

Deliberate soil redistribution is a frequent activity in the region, in order to maintain the productivity of land. This includes adding the newly-weathered materials from the edges of terraces or channels and the sediment deposited in ditches to upper or bottom positions of terraces (Figure 5-8). In general, the newly-weathered materials from the terrace wall are very coarse while the sediments deposited in ditches are very fine. There is no doubt that this kind of soil removal will result in Cs-137 redistribution vertically within the soil profile and spatially within the field. Farmers may also remove soils from upper slope locations towards the lower edge of the

slope, in order to reduce slope angle (Figure 5-8). The dimensions and magnitude of this deliberate soil removal can not be assessed in the absence of further detailed information, though it might be regarded as a relatively small component of the Cs-137 flux. While Cs-137 can provide background information on soil erosion within such small fields, which is impossible using traditional methods such as runoff plots, the farmers' deliberate soil removal result causes further uncertainty for the examination of soil erosion and sediment redistribution in this particular environment as discussed by Quine et al. (1992). Without further information, the Cs-137 technique can not distinguish those soil removals by soil erosion or farmer. The human interference on the terraces is the main difference between this study and many previous studies elsewhere.

5.3.2.2 Effect of tillage and root-crop harvest

While tillage process can mix up Cs-137 vertically within the plough layer, it can also lead to a horizontal displacement of soil. There is increasing evidence that this displacement may be as important, or in some cases more important than water erosion processes in determining long-term patterns of soil redistribution on agricultural land (Quine, 1995). Tillage redistribution at each position on a cultivated field is the result of an influx of soil from upslope and an outflux downslope, with the magnitude of the fluxes defined by the slope angle (Lindstrom et al., 1992; Govers et al., 1993, 1994). The soil redistribution due to tillage process is termed as tillage erosion (Quine, 1995). The tillage erosion may be significant in western countries due to the frequency and depth of tillage operations. It may also be significant on gentle sloping land in China. It was, for example, estimated that tillage erosion can be as high as 2380-6720 t km^{-2} yr^{-1} for purple soil with 5.2-7.4° of gentle slope but average erosion rate is only 1210 t km^{-2} yr^{-1} for same terraces in Yangtin near Chengdu (Zhang et al., 1993). However, the tillage erosion, if there is any, may not be so obvious for steep sloping land compared with severe water-induced erosion. In the study area tillage operations are carried out mainly using buffalo and in some cases manually. Disruption of the profile is less than mechanised tillage

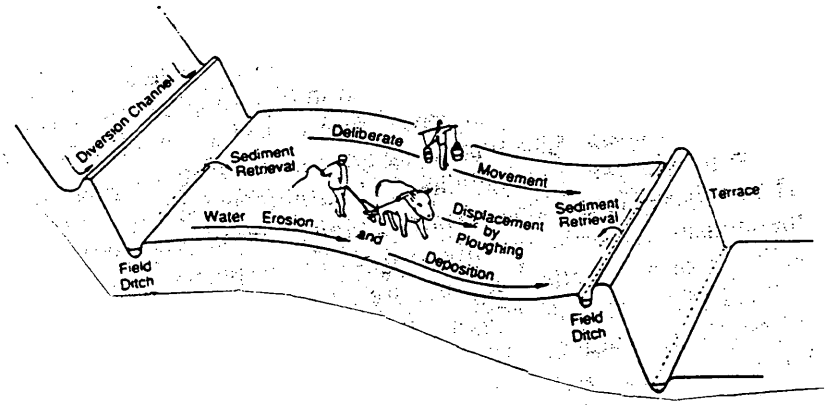

Figure 5-8, A sketch map showing possible deliberate soil remove by farmer (after Quine et al., 1992).

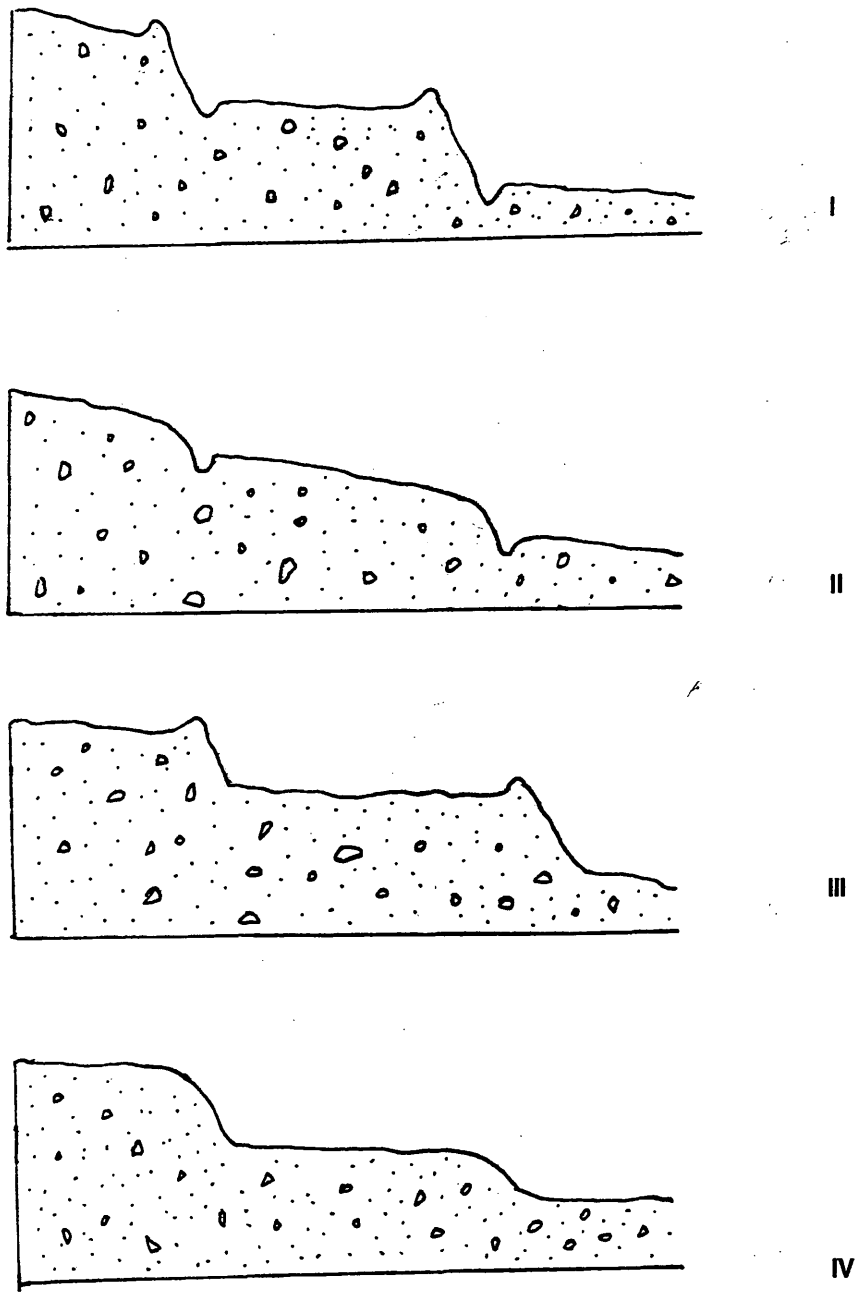

Figure 5-9, Four combinations of different terrace forms found in the catchment

although activity may be more frequent due to at least 2 crops in a year. An insignificant effect of tillage erosion is supported by Cs-137 profile distributions of soil samples taken from that the small land as discussed in section 5.3.1.1. Cs-137 has been found only above 25 cm, slightly deeper than assumed tillage horizon of 20 cm. Assuming no Cs-137 leaching, this may be due to deposition and not necessarily due to tillage effect. The harvest of root-crops like sweet potato and peanut frequently cropped in local area may also cause a certain amount of soil redistribution on such steep slopes but it is difficult to evaluate without further information. Therefore erosion quantification at later stage will not consider soil redistribution caused by tillage and root-crop harvest.

5.3.2.3 Effect of terrace forms

The form of the dissected terrace may be varied for each individual terrace, depending on its development stage. Four combinations of terrace forms can be found within the catchment (Figure 5-9). Among the 4 forms, the first may be the best and the fourth may be the worst in terms of preventing soil erosion and trapping mobilised soil material. It is apparent that soil Cs-137 activity and gravel content will be impacted by those different forms through the combination of water-induced erosion and deliberate soil removal by farmers. The terrace form for an individual terrace may be changed, depending on development stage and the individual farmer. Terrace morphology can also be changed by heavy storms which often result in terrace collapsing. Therefore the impact of those different forms on differential Cs-137 activity can not be evaluated without systematic sampling. The ditch can divert runoff from upper terraces and hence prevent soil erosion, while the terrace wall (which is slightly elevated above the terrace surface) will trap sediment. This can explain higher Cs-137 activity in top positions of field 9 & 51 and in bottom positions of fields 19 and 36 (Figure 5-6). Meanwhile the sediment deposited in the ditch may also be spread into the terrace by the farmer. This may explain higher Cs-137 activity in field 22 and the bottom of field 43. Nevertheless, Cs-137 activity on those heavily disturbed terraces is very complicated. The complexity is demonstrated in a longer transect from field 21 to 23. The transect includes 4 terraces among which

three terraces were sampled. The change of Cs-137 activity from the top terrace to bottom is completely different for field 21 and field 23.

The deliberate soil removal/retrieval can not be evaluated without further information. In the study it is assumed that residual Cs-137 is the net outcome of both natural erosion and direct human activity in the study area. The soil loss estimated based on the residual Cs-137 indicates net soil loss, including deliberate soil removal and possible displacement through tillage and root-harvest.

5.4 ESTIMATES OF NET SOIL LOSS RATES FROM Cs-137 MEASUREMENT

5.4.1 Cs-137 enrichment ratio estimate

Given the coarse particle size properties of the soils in the catchment, preferential transport of fine material is likely to occur. In general those fine materials eroded are enriched with Cs-137, since Cs-137 is mainly absorbed by fine materials (as discussed in Chapter 2). The study attempts to estimate Cs-137 concentration using reservoir sediment. The input of Cs-137 into the reservoir consists of the atmospheric-derived input and the catchment-derived contribution. In recently accumulated sediment the Cs-137 content can only be derived from catchment sources due to negligible atmospheric fallout concentrations. Cs-137 concentration in recent sediment can be estimated using Cs-137 profile of the two reservoir cores in Figure 6-1 in the next chapter, where the detail of Cs-137 dating will be further discussed. Based on the dating, the top 35 cm of the reservoir sediment can be identified as the sediment deposited after the late 1970s. Mean Cs-137 concentration tentatively averaged from the two cores is 7.5 Bq kg^{-1}. It must be noted that it is a crude method to estimate sediment Cs-137 concentration, since many possible factors should be taken into the estimates. These include the finer materials lost through the reservoir, the representativeness of the two cores, dating reliability (see details in next chapter), Cs-137 measurement reliability, coarser sediment deposited within the catchment prior to arrival at the reservoir, etc.

Estimation of topsoil Cs-137 concentration for a small runoff plot is relatively easy but can be problematic for a catchment. This is due not only to the representatives of topsoil samples but also the percentage of erosion contribution from possible sediment sources and the varied sediment delivery for those source materials. Topsoil sampling was undertaken throughout the catchment as described in the previous chapter. Cs-137 concentration in <2 mm fractions for those samples is summarised in Table 6-2 in the next chapter. Based on the tentative estimate of sediment contribution discussed in the next chapter, the contribution is 62%, 7% and 31% for arable land, wood & grass land and gully & terrace edges, respectively. Mean Cs-137 concentration for those eroded materials can be estimated as:

$$C_w = P_a * C_a + P_{w\&g} * C_{w\&g} + P_{g\&t} * C_{g\&t} \qquad \text{(Equation 5-5)}$$

Where C_w is a weighted Cs-137 concentration for the watershed. P_a, $P_{w\&g}$ and $P_{g\&t}$ is the percentage of erosion contribution for arable land, wood&grass and gully&terrace edges, respectively, and C_a, $C_{w\&g}$ and $C_{g\&t}$ is topsoil Cs-137 concentration for arable land, wood&grass and gully&terrace edges, respectively. The calculated Cs-137 concentration is 5.0 Bq kg^{-1}.

This gives the Cs-137 enrichment ratio 1.50. Begg (1982) found that Cs-137 concentration in eroded soils were 5 to 15% higher than concentrations in the source material. The enrichment ratio estimated here is higher than the report but is close to the enrichment ratios of total phosphorus and potassium (1.7 and 1.5, respectively) investigated in red soils of badlands in Jiangxi (Lu and Shi, 1994). This may be due to similar coarse source materials. However, it must be noted that controls on the enrichment ratio are complex and it is likely that the enrichment ratio is varied with inter- and intra-annual rainfall. Heavy storms, for example, may result in a lower ratio due to the incidence of erosion of subsoil materials of lower Cs-137 concentration (by gully or bank erosion). Historically the ratio may also have varied due to a possible shift in the main sediment source but can not be estimated without

detailed information. The estimated enrichment ratio used here therefore remains tentative.

The ratio may be overestimated due to Chinese bomb tests and Chernobyl fallout deposition occurring after the 1970s. Nevertheless, it indicates Cs-137 enrichment in sediment compared with original soils due to very coarse soil texture. Although the estimated ratio here is at a catchment scale rather than for an individual land use, the ratio will be integrated into erosion quantification for arable land as described later.

5.4.2 Percentage of Cs-137 loss

The percentage of Cs-137 loss is calculated by the formula:

$(Cr-Cs)/Cr*100\%$ (Equation 5-6)

Cr: Cs-137 reference obtained from reference samples (Bq m^{-2}),
Cs: Cs-137 inventory at each sampling site (Bq m^{-2}).

The distribution of the percentage Cs-137 loss is depicted in Figure 5-10. It can be seen that majority of samples have more than 50% of Cs-137 loss due to soil erosion. The mean of the percentage of loss is 62% with a minimum of 22% and a maximum of 98%. The critical problem is how to convert the Cs-137 depletion into soil erosion estimates.

5.4.3 Quantification of net soil loss rates

As discussed in the literature review, there are a handful of models developed for soil erosion quantification using the residual Cs-137 activities. The conditions of model use and their advantages and disadvantages were also discussed in Chapter 2. Walling and Quine (1990) examined the differences of erosion rates for most of those models and found that estimates of erosion rate associated with a particular level of Cs-137 depletion can be highly varied even among theoretical models. Fredericks

and Perrens (1988) compared the rates of soil loss estimated using three different methods in Australia and found that the estimates were highly variable, ranging from 1.2 to over 100 t ha^{-1} yr^{-1}, depending on the assumptions and methods used. This suggests that use of quantification models is very critical for erosion rate estimates.

Mass balance models, developed by two research communities in geomorphology and geochemistry, have been gradually accepted as the appropriate quantification tool using Cs-137 residuals, since a number of refinements can be incorporated into a mass balance model (Quine, 1995). The study therefore employs a mass balance model to estimate erosion rates.

5.4.3.1 Quantification by mass balance model

The mass balance model was first proposed by Kachanoski and De Jong (1984). The rate of change of total Cs-137 in the plough layer for an eroding soil can be given:

$$d_{At}/d_t = D_t - (E_tK_2/M + K_1)A_t \qquad \text{(Equation 5-7)}$$

t: time (yr),
A_t: total Cs-137 in plough layer (Bq m^{-2}),
D_t: average atmospheric deposition rate of Cs-137 (Bq m^{-2} yr^{-1}),
E_t: average erosion rate (kg m^{-2} yr^{-1}),
K_1: radioactive decay constant for Cs-137 (0.023 yr^{-1}),
K_2: enrichment ratio,
M: mass of soil in plough layer (kg m^{-2}).

The model assumes that tillage during the year would mix Cs-137 throughout the plough layer and the concentration of Cs-137 (C) in the plough layer can be given by:

$$C_t = A_t/M \qquad \text{(Equation 5-8)}$$

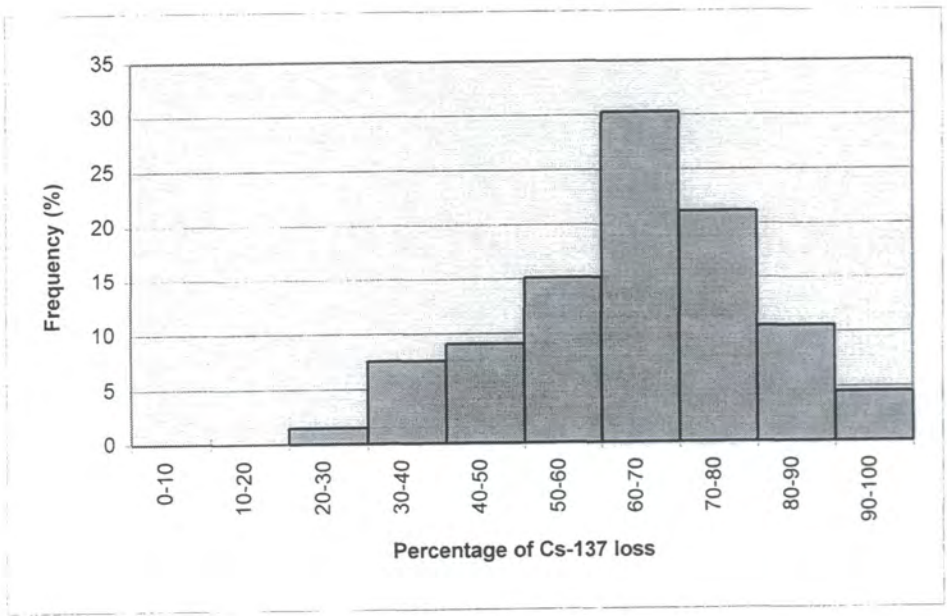

Figure 5-10, Frequency distribution of the percentage of Cs-137 loss

The model requires detailed records of atmospheric deposition. The estimates of yearly Cs-137 fallout from atmospheric records can be integrated with the model. The model estimates that net soil losses varied from 508 to 12527 t km^{-2} yr^{-1} and a mean rate of 4387 t km^{-2} yr^{-1} for all samples from sloping land.

5.4.3.2 Quantification by simplified mass balance model

Considering the uncertainties of annual atmospheric fallout of Cs-137 after 1974 in the area, a simplified model proposed by Zhang et al. (1990) is also used to estimate erosion rates. The model assumed that all Cs-137 fallout happened in 1963. The mean soil loss can be estimated as:

$$\Delta H = K_2^{-1} * H * [1-(X/Yr)^{1/(N-1963)}] \qquad \text{(Equation 5-9)}$$

ΔH: depth of annual soil loss (cm),
K_2: enrichment ratio,
H: depth of plough layer (cm),
X: measured Cs-137 amount in profile (Bq m^{-2}),
Yr: base level input measured in reference sites (Bq m^{-2}),
N: year of sampling.

The depth of the plough layer, H, can be assumed as 20 cm as used in the proportional model. The model estimates that net soil losses varied from 317 to 20920 t km^{-2} yr^{-1} and a mean rate of 6272 t km^{-2} yr^{-1} for all samples from sloping land.

It can be seen that the simplified method gives higher estimates. The erosion rates estimated by the two methods are plotted against the percentage of Cs-137 loss for soil samples taken from sloping land (Figure 5-11). It can be seen that the difference of erosion rates are more apparent when the percentage of Cs-137 loss is higher. It is believed that the higher estimates of erosion rates for the simplified mass balance model is due to the simplification that all atmospheric Cs-137 fallout happened in

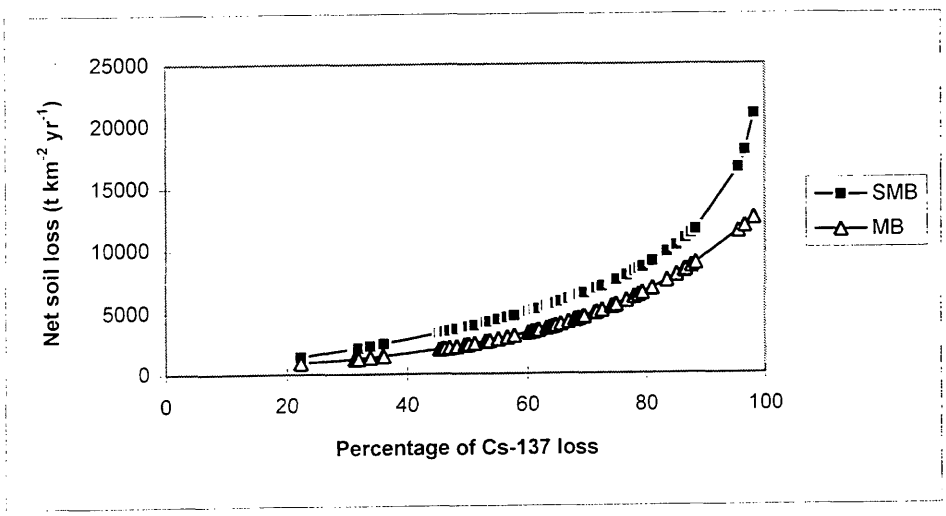

Figure 5-11, Net soil loss estimated by two methods against Cs-137 loss percentage
SMB: Simplified Mass Balance Model (Zhang et al., 1990)
MB: Mass Balance Model (Kachanoski and De Jong, 1984)

1963 and the model's sensitivity to plough layer depth (H). This demonstrates that larger errors might be introduced by simplifying the variable of atmospheric Cs-137 fallout. Many factors can be integrated with the mass balance model. The model used here assumes a long-term average erosion rate. Different seasonal or yearly erosion rates can also be integrated with the model based on the information of yearly rainfall (Kachanoski and De Jong, 1984; Fredericks and Perrens, 1988). In fact, the model can be used in monthly or even on a daily and event basis, if the corresponding fallout and rainfall are available. The model also assumes that Cs-137 concentration within the tillage horizon is uniform. On the basis of this assumption, the model may overestimate erosion rates, since Cs-137 fallout may concentrate on the soil surface before being mixed within a tillage horizon. The model can also integrate the concentration based on profile distribution of Cs-137 (Quine, 1995). The temporal concentration was greatly varied during the peak fallout in the 1960s (Quine, 1995), depending on local tillage practices. In the study area, the tillage practices are more frequent than in western countries, because of the system of two crops in a year. Quine (1995) summarised that the most common limitations occur as a result of failure to account for the following factors:

1) The concentration of Cs-137 at the soil surface during the period of atmospheric fallout
2) The seasonal variation in erosion and fallout
3) The variation in depth and extent of erosion
4) The redistribution of soil tillage
5) The potential for both erosion and aggradation to take place at one location.

The model will be more realistic if all of those factors are incorporated. Obviously this requires further study. However, if all those factors are considered, the complexity of quantification may outweigh the technique's advantages.

5.5 THE PATTERNS AND RATES OF NET SOIL LOSS

The erosion rates estimated by mass balance model (Kachanoski and De Jong, 1984) will be used to evaluate the patterns and rates of soil erosion in the catchment.

5.5.1 Frequency of net soil loss rates

The net soil loss rates are grouped into six classes (t km^{-2} yr^{-1}) based on the Chinese classification (see details in Chapter 1):

No Obvious:	<500
Slightly:	500-2,500
Moderate:	2,500-5,000
Severe:	5,000-8,000
Very Severe:	8,000-13,000
Extremely severe:	>13,000

Figure 5-12 shows the frequency distribution of net soil loss for all sampling points. One marked feature is that 100% of the sites were subjected to net soil loss and no site to net soil gain. Forty percent was suffering moderate loss, about 25% each slightly and severe loss, and 10% was suffering very severe loss. The average net soil loss rate is around 4400 t km^{-2} yr^{-1}. By international standards, the field area has high erosion rates. The explanations can be made from many aspects such as rainfall, soils, cultivation practice, and steep slopes in particular. This information, particularly on soils and slopes, has already been introduced in previous sections or chapters and will not be discussed here. The high erosion rates caused serious land degradation and reservoir sedimentation. Erosion-induced land degradation in those steep arable lands made soil depth very thin and the soil very coarse. This is a very general problem in the Sichuan basin and, in particular, in the Three Gorges area. For instance, arable land was lost at the rate of about 0.9% per year due to soil erosion in Zhongxian county (near Changshou county). The bare rocks caused by soil erosion accounted for 7.7% of the total area in a village of the county. Reservoir sedimentation caused by serious erosion will be discussed in the next chapter.

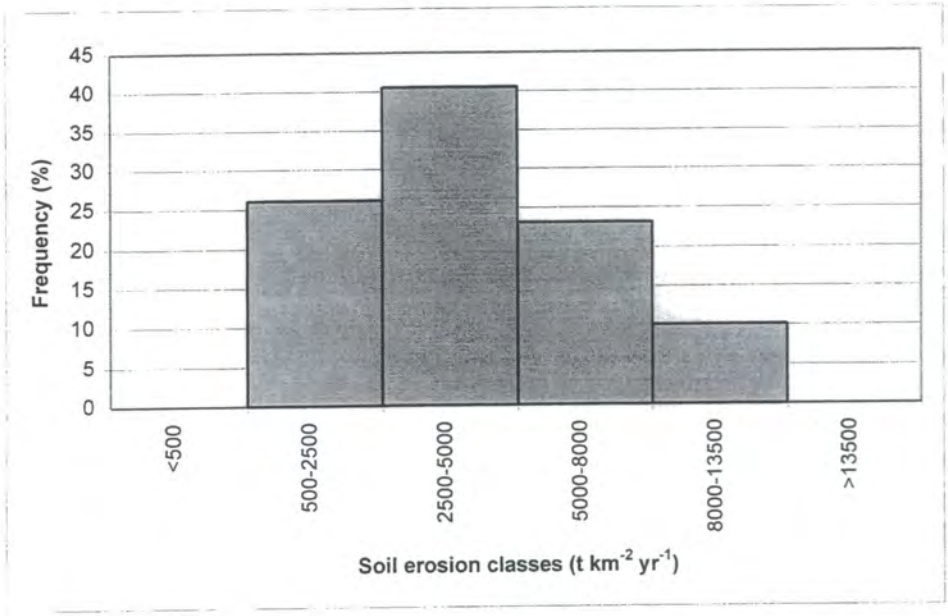

Figure 5-12, Frequency distribution of net soil loss classes estimated by mass balance model

5.5.2 Spatial patterns of net soil loss

Net soil loss rates estimated by the mass balance model (Kachanoski and De Jong, 1984) are assigned to each sampling site in Figure 5-13. Due to the varied situation (topography and human activity) in terms of possible effects on Cs-137 for those dissected terraces and sparse sampling points, any surface interpolation of the net soil loss will be meaningless. It seems that no obvious spatial patterns of net soil loss can be determined. This is because the net soil loss was mainly dependent on the morphology of each individual terrace, assuming the same crops and management practices. Net soil loss is also affected by the management of those terraces in terms of deliberate soil removal and terrace form. During the 40 years investigated by the Cs-137 technique, the forms of those terraces as discussed above may be not consistent, therefore it is difficult to make a general assessment about their effect on soil loss.

5.6 SUMMARY AND CONCLUSION

The reference value of Cs-137 fallout was successfully estimated within a small piece of paddy field located on the watershed of the catchment. If one outlier is excluded, the reference ranging from 1807 to 2373 with a relatively low coefficient variation (CV, 9.3%) is 2163 Bq m^{-2}. It is believed that the low variation is due to uniform redistribution of Cs-137 in the paddy field. However there are some uncertainties around fallout distribution in paddy fields. This includes Cs-137 loss and addition by the irrigation and drainage water. Monthly Cs-137 atmospheric fallout from 1954-1974 was also estimated based on the model proposed by Sarmiento and Gwinn (1986). The integrated fluxes of Cs-137 from 1954-1974 is around 1683 Bq m^{-2}. The possible fallout, 200 Bq m^{-2}, from 1975-1984 was also tentatively estimated based on the records in Japan. This gives an estimated fallout of 1883 Bq m^{-2} for the two periods, 1954-1974 and 1975-1984. The estimated value accounts for 87% of the reference value estimated from the paddy field. This demonstrates that monthly Cs-137 estimates based on the model is possible. This is very useful in the heavily disturbed Chinese environment. The monthly Cs-137.

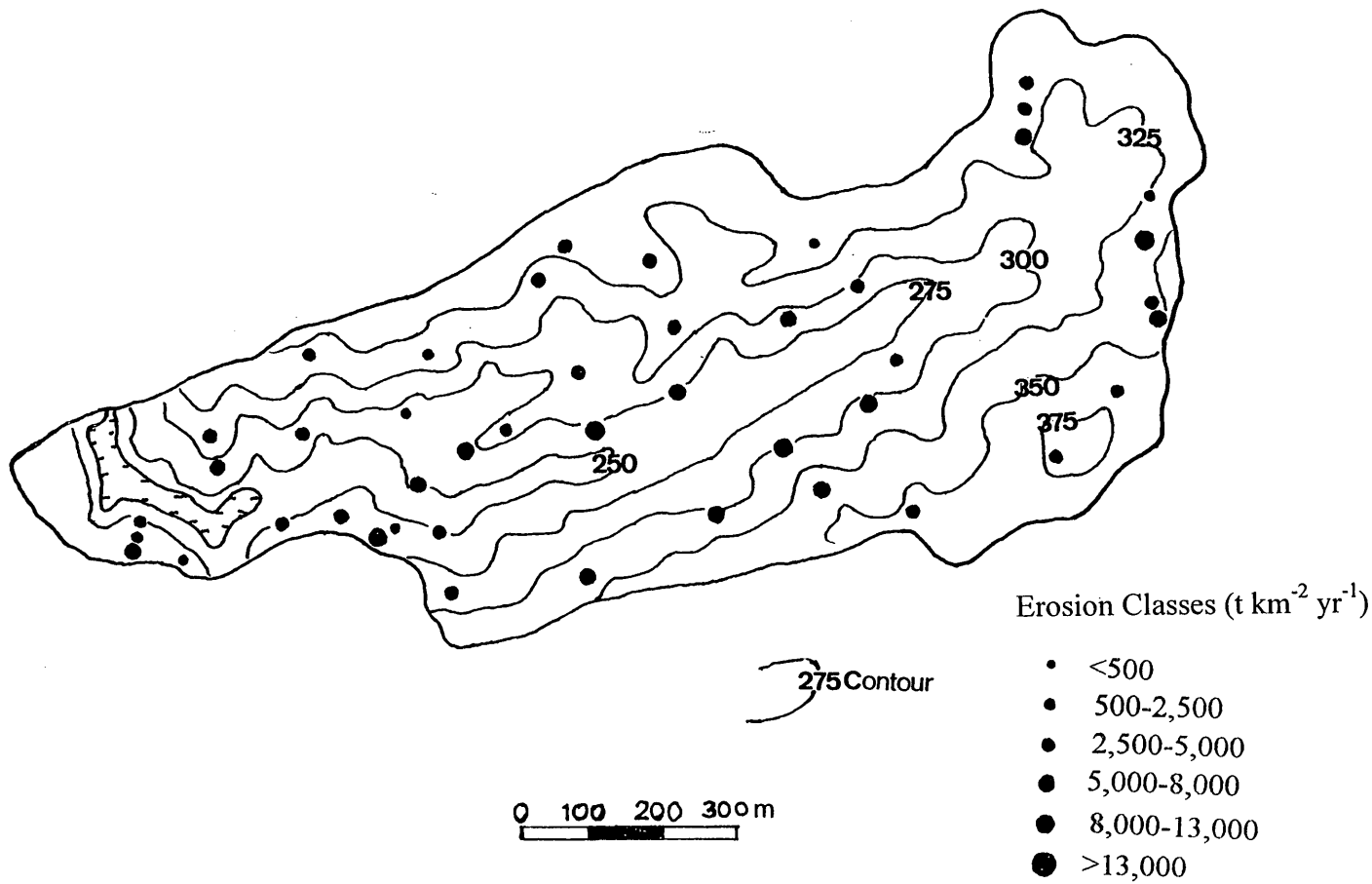

Figure 5-13, Spatial patterns of net soil loss rates in Yiwanshui catchment

fallout is also very useful for erosion quantification and reservoir sedimentation estimation. Cs-137 inventory was clearly varied with slope positions in a small piece of arable land. This was confirmed by the averaged results further investigated in the 11 fields.

The relationships between the remaining Cs-137 activities, slope angle and slope length were also examined. As a result, it is found that Cs-137 decreases with slope angle increasing. The Cs-137 variations with slope position and angle were confirmed by the variation of soil particle size changes. Cs-137 activity increases with the percentage of <2mm fraction. These results suggest that Cs-137 can be used to quantify soil erosion and sediment redistribution in the area. The differential Cs-137 activity is also influenced by direct human activity such deliberate soil removal, tillage operations and terrace development stage. Deliberate soil removal including adding newly-weathered materials from terrace walls and the sediment deposited in the ditches is quite frequent but its overall contribution to soil flux is thought to be relatively minor, although it cannot be evaluated without further information. Erosion rates estimated based on Cs-137 remaining represent net soil loss.

Considering the problem of particle size sorting and preferential transport of Cs-137 in a catchment dominated by relatively coarse materials, a mean Cs-137 enrichment ratio (1.5) was estimated using reservoir sediment. The ratio was integrated into an erosion quantification model. Mass balance models were employed to convert residual Cs-137 activity into net soil loss. It is found that the simplified mass balance model (Zhang et al., 1990) may overestimate net soil loss, particularly when Cs-137 loss is high, compared with the model proposed by Kachanoski and De Jong (1984). The mean net soil loss estimated by the latter is 4400 t km^{-2} yr^{-1}. This is consistent with many reports and very high in an international context. High rates of soil loss are due to many reasons mainly steep slopes, erodible soils and cultivation practice. The high erosion rates cause serious soil degradation and reservoir sedimentation. Local implications of sedimentation will be discussed in the next chapter, while the broader downstream impacts of high erosion rates are evaluated in Chapters 7-9.

The prevalence of coarse soil materials and the incidence of deliberate soil removal during agricultural practices raised the question of whether the Cs-137 technique is suitable in such an environment. In addition, there are many uncertainties in the fallout from Chinese nuclear weapons testing and the fallout from the Chernobyl accident is also identified in the reservoir (see next chapter for details). All those facts add uncertainty to the procedure for investigating soil erosion using the Cs-137 technique. However, compared with other available methods discussed in Chapter 1, the Cs-137 technique is a useful method, due to its flexible sampling strategy in this heavily disturbed environment. Erosion quantification seems still problematic. The study considers yearly variation of fallout but assumes a long-term erosion rate. In fact, monthly variation of fallout and yearly and monthly soil erosion rates, and Cs-137 surface concentration, can also be integrated with mass balance models. Clearly further experimentation, beyond the scope of the present study, is required on erosion quantification.

6. SEDIMENTATION AND SEDIMENT DELIVERY IN UPPER YANGTZE: A CASE STUDY IN YIWANSHUI CATCHMENT

6.1 INTRODUCTION

In addition to examining the patterns and rates of soil erosion on sloping arable land, the reservoir, built in 1958, within the catchment provides an opportunity to examine sediment delivery and sedimentation as part of a comprehensive application of the Cs-137 technique to investigate soil erosion and sediment problems. The existence of serious sedimentation problems in reservoirs within the Three Gorges Area due to severe soil erosion has been introduced in Chapter 3. The intended lifespans for many reservoirs cannot be fully realised because of the sedimentation problem. Traditionally, reservoir sedimentation is investigated by bathymetric survey in which the total sediment volume deposited in the reservoir is estimated. The bathymetric approach, unless attempted at a series of time intervals, gives an averaged sediment yield for the whole catchment which cannot be fully linked with temporal changes of land use and rainfall. In contrast, the combination of traditional bathymetric measurement and the Cs-137 techniques with the possibility of identifying a few recent dating horizons can overcome this limitation. More importantly, by using the Cs-137 technique, the reservoir investigation can be integrated with slope investigations discussed in the previous chapter. This includes a catchment-based budget development and sediment source identification. The chapter is designed to investigate sedimentation, sediment delivery and the main sediment sources using the Cs-137 technique in Yiwanshui catchment, Changshou County (Figure 4-1). The main objectives of the chapter are:

1) to investigate possible dating horizons for the reservoir sediment using Cs-137 integrated with other properties in the typical environment;

2) to examine reservoir sedimentation rates and sediment yield and their changes using the identified dating horizons;

3) to estimate the sediment delivery ratio and develop a catchment-based sediment budget based on the information obtained from slopes and the reservoir;

4) to examine the potential to identify sediment sources among the main three land use types using Cs-137 technique.

6.2 PROPERTIES OF THE RESERVOIR SEDIMENT

Two cores were taken from the reservoir (location and sampling method see Chapter 4). The sediment from the two cores were determined for basic properties including bulk density, particle size and Cs-137.

6.2.1 Bulk density

The variations of bulk density for the two cores are depicted in Figure 6–1. The bulk density profiles in core 1 show high density values at the base of profiles. The bulk density together with abrupt colour change suggests that core 1 penetrated the original soil. The profile of bulk density in core 1 shows a gradual increase from top (sediment-water interface) to a depth of 105 cm and then a decrease to the base of the core. This may be due to the sediment materials with different properties. The changes in core 2 are not as clear as core 1 but show a similar variation. The mean bulk density for core 1 averaged throughout the profile (from top to 135 cm) is 0.82 g cm^{-3} with a maximum of 1.25 g cm^{-3} at the depth of 95-100 cm, for core 2 is 0.60 g cm^{-3} with a maximum of 0.80 g cm^{-3} at the depth of 50-55 cm. This is very high compared with previous studies (Walling and He, 1992; Foster and Walling, 1994; He et al., 1995), suggesting that the deposited materials have lower organic matter which were washed down through serious soil erosion as discussed in the last

chapter. The bulk density for core 1 is higher than that for core 2 particularly in the lower profile, although the latter is located near the dam with deeper overlaying water. This suggests that the water body plays a less important role in compacting sediment compared with the sediment itself.

6.2.2 Particle sizes

The composition of particle sizes for core 1 has been analysed. The percentages of sand (>2 mm), silt (2-0.002 mm) and clay (<0.002 mm) are depicted in Figure 6–1. It can be seen that the particle sizes vary considerably throughout the profile. The existence of >2 mm fraction occurs around 40 cm and 100 cm depth. It is noted that around 100 cm the fraction accounts for more than 30% of the total. It is possible that those layers with a high percentage of >2mm resulted from extreme rainfall events. Those coarse textured materials also posed a certain effect on bulk densities. The depth with the highest bulk density, for example, corresponds to the depth with the highest percentage of >2mm fraction at the depth of 105 cm (Figure 6–1). Coarse materials of >2mm were found in core 1 but not in core 2. It is not surprising, since core 2 is closer to the dam. The difference of the textures for different layers and the two cores will pose effect on Cs-137 downcore variation as discussed below, due to Cs-137 enrichment in finer materials.

6.2.3 Cs-137 concentration

The profile variation of Cs-137 concentration for these two cores are presented in Figure 6–1. The input of Cs-137 into a lake or reservoir consists of the atmospheric-derived input and the catchment-derived contribution, and subsequently its profile is also controlled by a number of processes such as the upward and/or downward diffusion of radionuclides in water, bioturbation of sediments and mixing of sediments by physical reworking (Stanners and Aston, 1984; He et al., 1996). Considering the serious soil erosion within the catchment, and hence very fast sedimentation rates in the reservoir, it can be assumed that post-depositional redistribution in the sediment of the reservoir is negligible and hence atmospheric

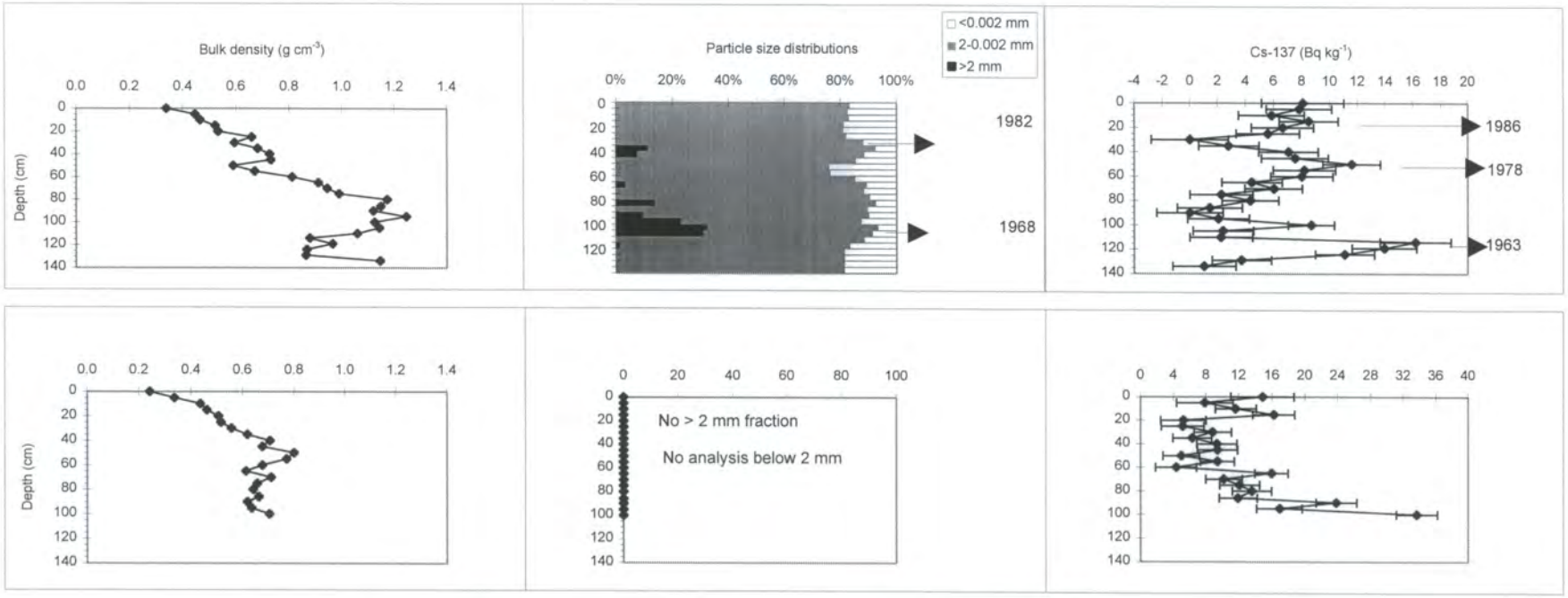

Figure 6-1, Bulk density, particle size distributions and Cs-137 concentration of the sediment for two reservoir cores

and catchment derived input of Cs-137 dominates in the processes of forming the Cs-137 profile. Cs-137 concentrations in both cores fluctuate throughout the profiles. The fluctuations were generally much greater than analytical uncertainties. In general, core 1 has a lower Cs-137 concentrations than core 2 due to the difference of particle sizes. For core 1 the highest Cs-137 concentration is found at a depth of 115-120 cm and a few small peaks can be identified, for examples, at the depths of 15-20, 50-55 and 100-105 cm. No detectable Cs-137 is found at two depths of 30-35 cm and 90-95 cm, suggesting that the Cs-137 profile is governed by variation in catchment-derived sediment source, particularly in the deeper core which is assumed to be sediment deposited at an early stage when Cs-137 fallout was still significant. Similar characteristics can be also drawn from core 2, except that peak Cs-137 is found in the base of the core. It is likely that the core did not penetrate the pre-reservoir valley sediments at this location.

The total amount of Cs-137 in each core may be compared with the amount of atmospheric input estimated for the reference value as discussed in the last chapter. The total Cs-137 activity is 7926 and 9325 Bq m^{-2} for the two cores as compared with the estimated reference value, 2163 Bq m^{-2}, representing about 3.7 and 4.3 times as much Cs-137 than can be accounted for by direct atmospheric deposition. This is comparable to that in other reservoirs or lakes reported by Ritchie et al. (1973) in Northern Mississippi and by He et al. (1996) in southern England. The explanation of the enhanced deposition are due to either the focusing of Cs-137 into the two core sites of the reservoir or that the major Cs-137 input came from drainage basin. Without detailed extensive coring of the reservoir, it is impossible to rule out sediment focusing, unequivocally, but it is believed that the drainage basin represents the most important source of Cs-137 in the cores. The delivery of catchment Cs-137 can be accomplished through 'direct runoff' (Santschi et al., 1988; 1990; Callender and Robbins, 1993) or the 'fast hydrological component' (Smith et al., 1987). It is estimated that 2% was transferred through this way in U.S. rivers (Menzel, 1974; Callender and Robbins, 1993). Under subtropical climatic conditions with frequent heavy storms in the study area, it is likely that a higher percentage of Cs-137 could

be washed away before being adsorbed by soil particles. The rest of the Cs-137 was stored in the watershed and transferred with soil movement.

6.3 IDENTIFICATION OF DATING HORIZONS

6.3.1 Identification by Cs-137 profile distribution

Comparing the yearly atmospheric Cs-137 fallout (Figure 5-3) reconstructed using the Sarmieto and Gwinn (1986) model in the previous chapter with the Cs-137 profile distribution of the two reservoir cores (Figure 6–1), it can be seen that core 1 is more likely to be complete and has better preservation than core 2. Therefore subsequent dating and sedimentation analysis will be based on core 1. The broad maximum at the lower part of the core is most likely associated with peak fallout of Cs-137 in the mid-1960s from atmospheric nuclear weapons testing. However, there is far more activity in the most recently deposited sediments than can be explained by the direct atmospheric fallout of Cs-137. This is associated with the transport of sediment-bound Cs-137 from the catchment and the possible additional fallout from Chinese nuclear weapons testing and the Chernobyl nuclear accident in 1986 (see Chapters 2 and 4 for details on Chinese test and Chernobyl accidents). The lack of information in the public domain about the ambient concentrations of atmospheric Cs-137 fallout across China resulting from these sources prevents precise calibration of residual Cs-137 activity into soil erosion, but does provide additional opportunities for sediment dating. If diffusion and Cs-137 residence time in the water column are ignored in a reservoir with high sedimentation rates, an absolute chronology for the sediment sequence can be identified based on core 1.

- The bottom of the reservoir can be dated to 1958 when the reservoir began to store water.

- The first peak at a depth of 115-120 cm can be identified as the period of maximum atmospheric fallout in 1963.

- The second Cs-137 peak at the depth of 50-55 cm from the profile is likely to correspond with the peak fallout in 1977 and 1978 generated by Chinese nuclear test (see details on Chinese test in Chapter 2).

- The small peak at the depth of 15-20 cm is likely to represent Chernobyl fallout in 1986. Although the peak at the depth of 15-20 cm is not marked, the possibility of being formed by finer materials can be excluded, due to nearly identical particle size distribution above 25 cm (Figure 6–1). The Chernobyl fallout is consistent with reports by Wan et al. (1990) and Xiang et al. (1993), as described in Chapter 2. If the assumption that there Chernobyl derived radiocaesium existed in the atmosphere across this part of China is correct, the likelihood of deposition is compounded by the high rainfall recorded at the time. The year was one of the wettest on record (1393.4 mm), only second to 1460.9 mm in 1982 (Figure 3-8). Furthermore, one of the four highest daily rainfall totals in the meteorological record, with daily rainfall of 112.2 mm, happened in May of 1986, soon after the Chernobyl accident. Unfortunately, there appears little chance of corroborating the presence of Chernobyl fallout independently.

6.3.2 Identification by particle size and rainfall information

In addition to the Cs-137 profile distribution, other properties can be also used to identify dating horizons. Foster and Walling (1994), for example, identified a dating horizon using the abrupt change of bulk density due to reservoir drawdown during the 1976 drought in Devon, UK. In this study, the obvious changes of soil particle sizes in the profile of core 1 might be used to identify additional dating horizons. As stated above there are two obvious changes at 35-40 and 100-105 cm in core 1. Those coarse materials most likely correspond to extreme rainfall events. The confirmation requires an analysis of historical rainfall data (see detail in Chapter 3). The rainfall data being examined include total annual rainfall (Figure 3-8), the annual frequency of daily rainfall larger than 25 and 50 mm and the corresponding total rainfall of those events (Figure 3-9). Comparing the annual rainfall with the profile of particle sizes, it may be concluded that the first broad peak in the upper part of the

profile (35-45 cm) was caused by high rainfalls in 1982. The annual rainfall in 1982 is the highest rainfall over the 30 years, and accumulative rainfall and the frequency for the daily rainfall above 25 mm in this year were also very high (Figure 3-9). Furthermore it was followed by high rainfall in 1984 with an extreme daily event of 123.9 mm. These 2-year's rainfall must have generated serious soil erosion and hence washed down a considerable amount of sediment into the reservoir, which were dominated by the coarse subsoil and materials from gullies and terrace walls. Since there was little atmospheric fallout during this period, it resulted in no detectable Cs-137 at the depth 30-35 cm. Similarly, it is believed that the peak in lower part of the core from 85-110 cm was due to a phase of continuous high rainfall in the late 1960s (Figure 3-8), and it is suggested that the peak at the depth of 100-105 cm corresponds to 1968, the highest annual rainfall in the 1960s. If the correlation between rainfall totals and particle size anomalies is accepted the two years 1982 and 1968 can also be used as dating for this particular reservoir.

The three dating horizons, 1963, 1978 and 1986 identified from Cs-137 profile and two horizons, 1968 and 1982 from particle size distribution in core 1 (Figure 6–1) can be used to reconstruct the temporal pattern of sediment yield by subdividing the total period into a few phases. Considering time scales, this study divides the whole period into four phases, Phase 1 (1958-67), Phase 2 (1968-77), Phase 3 (1978-85) and Phase 4 (1986-94). The division gives each phase around 10 years. The former three phases are very close to the division used to examine temporal changes of suspended sediment data within the whole Upper Yangtze basin (see Chapter 7 and 8 for detail). This provides an opportunity to compare the sediment yield change determined from the small catchment with the changes throughout the Upper Yangtze basin.

6.4 SEDIMENTATION RATE AND TEMPORAL CHANGES

6.4.1 Sedimentation rate

The average linear sedimentation rate throughout the period from 1958 (when the reservoir was built) to 1994 is 3.65 cm yr^{-1} at the point of core 1. This is very high compared with the sedimentation rates in UK (Higgitt and Walling, 1993; Foster and Walling, 1994; He et al., 1996). The higher sedimentation rates are reflections of the serious soil erosion on slopes within the catchment as discussed in last chapter. However, the sediment rates is much lower than the 10 cm yr^{-1} of average sedimentation rate estimated by local government (Soil and Water Conservation Office of Sichuan Changshou County, 1988). This may reflect a relatively high percentage of woodland (10%) in the catchment compared with the average value in the county (7.5%). More importantly, the lower sedimentation rate may indicate smaller catchment-reservoir ratio as described later.

6.4.2 Temporal changes

The four phases identified from core 1 are used to reconstruct the temporal pattern of sedimentation rates of the reservoir. The results are summarised in Table 6-2. The differences in sedimentation rates for this four phases, Phase 1 (1958-67), Phase 2 (1968-77), Phase 3 (1978-85) and Phase 4 (1986-94), are distinctive. The average sedimentation rate was the highest (5.0 cm yr^{-1}) for Phase 2 of 1968-77 and the lowest (only 2.2 cm yr^{-1}) for the recent phase, e.g. Phase 4 from 1986-94.

Table 6-1, Sedimentation rates of the reservoir calculated based on four phases

	Years	Accumulated depth (cm)	Averaged sediment rate (cm yr^{-1})
Phase 1 (1958-67)	10	30	3.0
Phase 2 (1968-77)	10	50	5.0
Phase 3 (1978-85)	8	35	4.4
Phase 3 (1986-94)	9	20	2.2

6.5 SEDIMENT YIELD AND TEMPORAL CHANGES

The sedimentation rates expressed by depth per year (cm yr^{-1}) or so-called linear sedimentation rates (Edgington et al., 1991) can directly indicate the rates of reservoir sedimentation but care is needed in comparing linear sedimentation rates between reservoirs. Bias is introduced into rate comparisons through a number of factors, including reservoir trap efficiency and catchment-reservoir surface area ratio, in particular. The latter varies enormously. For example, the catchment-reservoir ratio is 35 for this Yiwanshui reservoir but 1700 for the Three Gorges Reservoir. Sedimentation rates are also not comparable even for same reservoir due to transect shape of the reservoir and bulk density of the deposited materials. In other words, the rapid sedimentation rates in Phase 1 or 2 for this reservoir may also be caused by the shape of the transect of the reservoir. The direct comparison for the degree of erosion between catchments or different period requires specific sediment yield (t km^{-2} yr^{-1}).

6.5.1 Sediment yield

The calculation of sediment yield requires information on reservoir trap efficiency and the total sediment deposited in the reservoir.

6.5.1.1 Estimate of the sediment deposited in the reservoir

The reservoir with initially designed 18 metre high dam has a total storage of 150 thousand m^3. Bathymetric measurement of water depth was made along eight transects when sediment samples were undertaken (Figure 6–2). The measurement points are around 4m apart along each transect. The depths from water surface to the dam top were also measured along the reservoir boundary. The actual water depth at the measurement time plus the depth from water surface to the dam top and the co-ordinates of those points are converted into digital format, and Arc/Info TIN function was used for volume estimates. The estimated non-sediment-occupied volume is 55,000 m^3. This gives 95,000 m^3 of total volume of the sediment deposited in the reservoir since 1958. Thus the total sediment deposited is 80,000 t, assuming the average bulk density is 0.82 g cm^{-3} based on core 1.

a

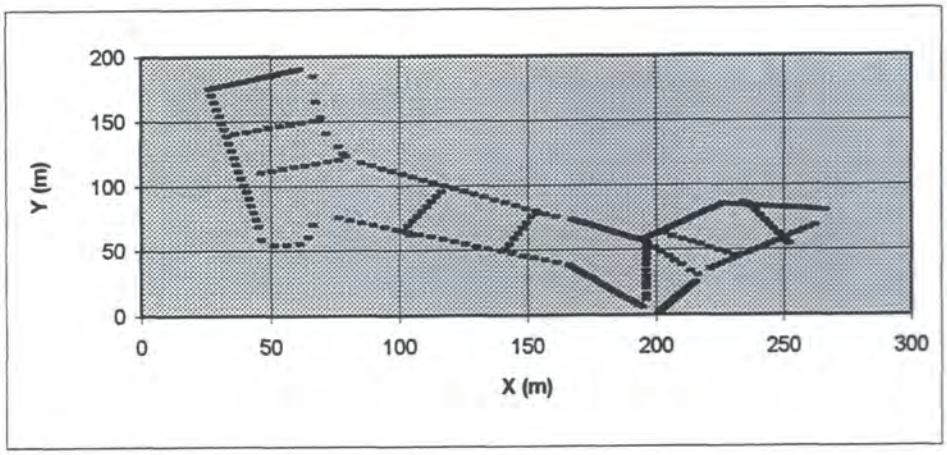

b

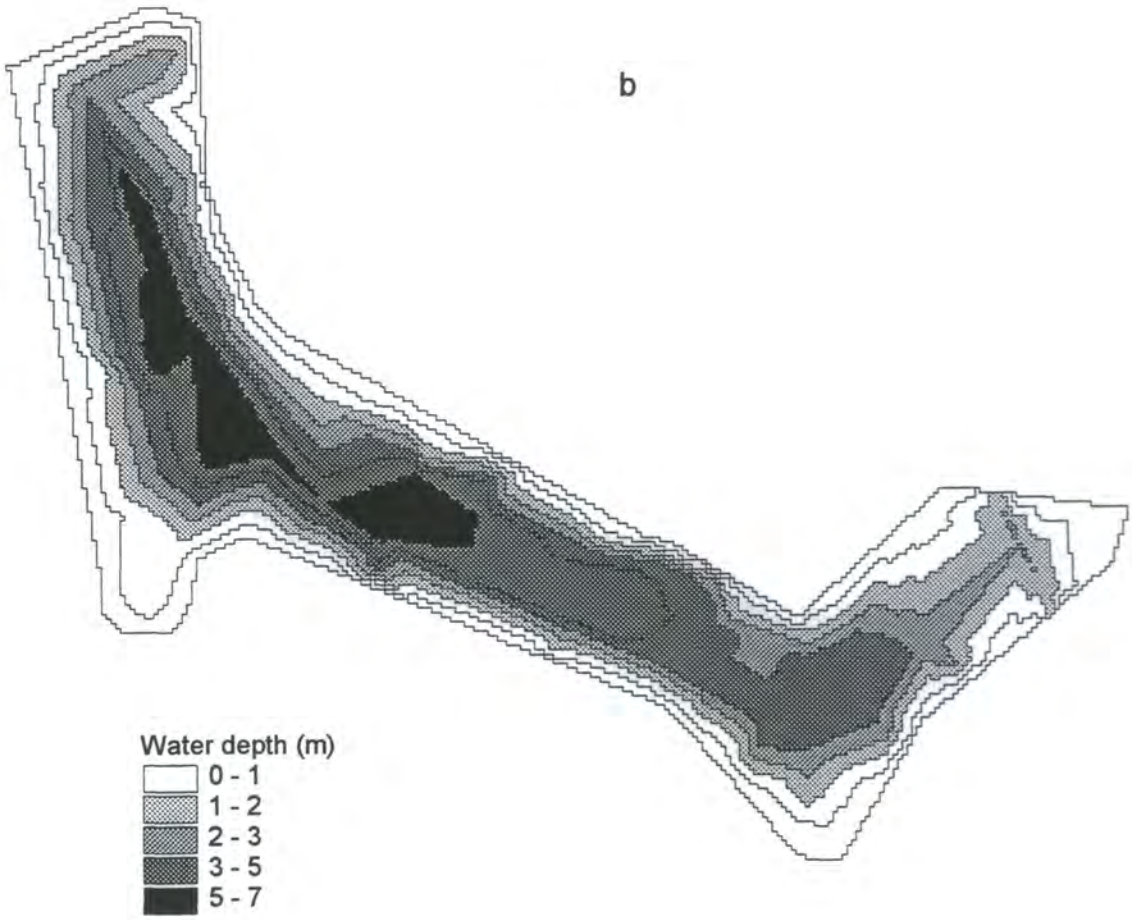

Figure 6-2, The transects used for bathmetric measurement (a), and water depth of the reservoir (b)

6.5.1.2 Estimate of trap efficiency (TE)

Trap efficiency is the ratio of the quantity of sediment deposited in a reservoir to the total sediment input, and it is typically expressed as a percentage. Trap efficiency is required to estimate sediment yield for the catchment, because the above estimate of the sediment deposited in the reservoir does not account for material lost through the outflow. The estimate can be made using Brune curve (Brune, 1953), requiring both input and output flows which are not available for the reservoir. Alternatively, trapping efficiencies can be calculated as a function of residence time (Ward, 1980; Vorosmarty et al., 1997):

$$TE = 1 - (0.05 / t^{0.5}) \qquad \text{(Equation 6-1)}$$

Where t: water residence time in a reservoir (years). Wan et al. (1990) estimated that water residence time (t) was 0.26 year for a reservoir in Guizhou, which is near to the study area. Water residence time varies with reservoir properties such as size and water depth, etc. If the value is used, this gives a TE of 90%. This is higher compared with English lakes and reservoirs (Owens et al., 1997) but quite close to Er Hai (89%), Qilu Hu (100%) and Xingyun Hu (100%) reported by Whitmore et al. (1994) for the lakes in Yunnan. In part, this higher trap efficiency reflects a coarser texture of purple soils as discussed previously.

It must be stressed that the TE estimated is an average value for over 30 years. In fact, TE varies with the change of reservoir storage. TE gets smaller when the reservoir is filled with sediment. Thus any sediment yield estimate and sediment yield changes in particular must take this change into account.

6.5.1.3 Sediment yield

The sediment deposited in the reservoir (80,000 t) plus that lost to the outflow (10%) gives the total sediment of 88,900 t transported for 36 years (from 1958 to 1994). This gives a sediment yield of 3490 t km^{-2} yr^{-1} for the catchment. The high sediment

yield reflects serious soil erosion and high sediment delivery (sediment delivery will be discussed latter). The result of this study fits the scenario of sediment yield in the Upper Yangtze basin quite well as shown in Figure 6–3. The figure shows sediment load and drainage area relationships using the data from 38 reservoirs with sizes of smaller than 100 km^2 and 187 hydrographic stations. The 38 reservoir data are from bathymetric investigations in Sichuan basin (Soil and Water Conservation Office of Sichuan Province, 1983; Soil and Water Conservation Office of Sichuan Nanchong County, 1988; Soil and Water Conservation Office of Sichuan Pengxi County, 1988). All the 38 reservoirs had a deposition history of at least 15 years ranging from 1955 to 1982. A common property for those catchments is predominant purple soils with relatively lower elevation as Yiwanshui catchment (see Chapter 3 for details). The 187 hydrographic data are from the sediment load dataset described in Chapter 4 and have more than 5 years measurement series. Figure 6-3 shows that the overall relationship between sediment load and drainage area is very significant. The result demonstrates it is possible through examining a typical smaller catchment to understand larger catchments with similar environmental settings. However, the scatter for the hydrographic data indicates that sediment yield scale issue is much more complicated for larger catchments due to the combination of contrasting environmental factors. Attempts to determine the controls on sediment loads within the Upper Yangtze and a more detailed examination of sediment yield-drainage basin area relationships will be discussed further in Chapters 7 and 8.

6.5.2 Temporal changes

Based on bathymetric measurement, bulk density and the dating horizons identified using Cs-137 and particle size distributions, sediment yield for the four phases, can be estimated (Figure 6–4). Sediment yields for the four phases, Phase 1 (1958-67), Phase 2 (1968-77), Phase 3 (1978-85) and Phase 4 (1986-94), display considerable difference, varying from 6170 t km^{-2} yr^{-1} in the period of 1968-77 to 1180 t km^{-2} yr^{-1} in recent period of 1986-94. It should be noted that the certainty with which each of the dating horizons is identified can introduce a large amount of error to the

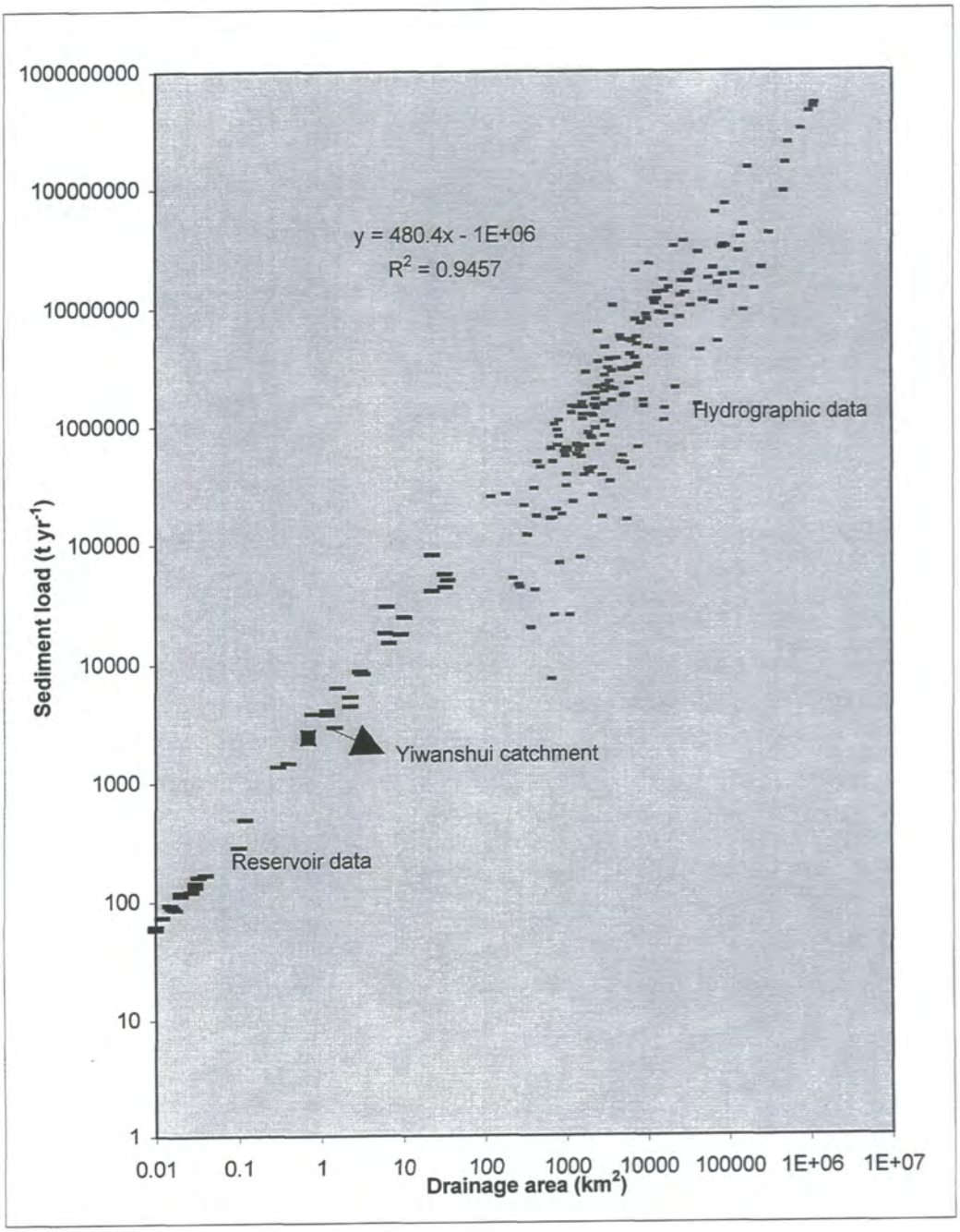

Figure 6-3, Sediment load-drainage area relationships in the Upper Yangtze showing that Yiwanshui fits quite well within the broad scale The data are from 38 reservoirs and 187 hydrographic stations

sedimentation estimates, but possible reasons for sediment yield variability are discussed below.

6.5.3 Possible reasons for changes in sediment yield over time

The explanation for the variation of sediment yield with time is complicated, which could be caused by rainfall and/or land use changes throughout the lifespan of the reservoir.

6.5.3.1 Rainfall changes

Time series changes of annual rainfall and of daily rainfall totals of >25 mm and >50 mm, have already been introduced in Chapter 3. The rainfall information of some individual years such as 1986, 1982 and 1968 has also been used to aid and identify dating horizons. The rainfall data are divided and examined as the four phases applied to the sediment core. The latest phase can not be evaluated due to lack of rainfall data. Annual total rainfall for the first three phases is plotted in Figure 6–5. It can be seen that the increase of sediment yield from Phase 1 to 2 corresponds with annual rainfall increase but the decrease of sediment yield from Phase 2 to 3 does not correspond with annual rainfall change. As the majority of sediment was transported by heavier storms, it is appropriate to investigate the incidence of storms in the rainfall record.

Average annual frequencies of >25 and 50 mm of daily rainfall and the corresponding mean rainfall of those events are also presented in Figure 6–5. It can be seen that the lower sediment yield during Phase 3 is not associated with the number of extreme events and their corresponding rainfalls. This means that sediment yield is not fully consistent with those storms in terms of their frequencies and corresponding rainfall. Figure 3-9 indicates three events of daily rainfall >100 mm happened during Phase 3 and 4. This again demonstrates that lower sediment yields for Phase 3 was not fully due to rainfall reduction. The above discussion from two aspects, total annual rainfall and the events of heavier storms suggest that the decreasing sediment yield from Phase 2 to Phase 3 are not completely due to the changes of rainfall. In other words, the higher sediment yield for Phase 2 might be due to land use changes.

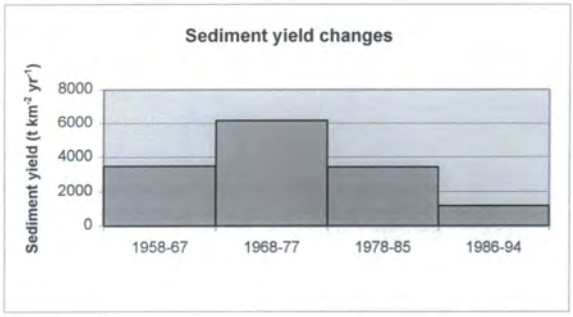

Figure 6-4, Sediment yield changes for the four phases in Yiwanshui catchment

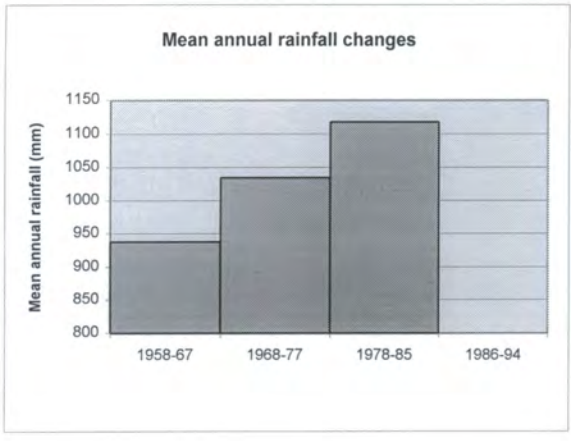

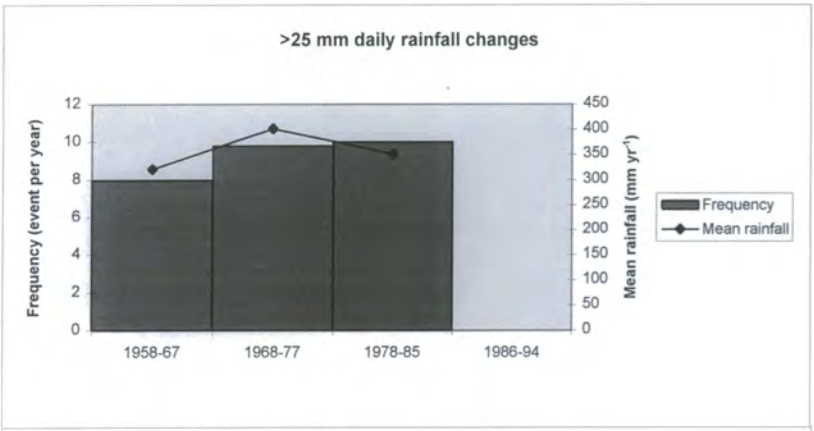

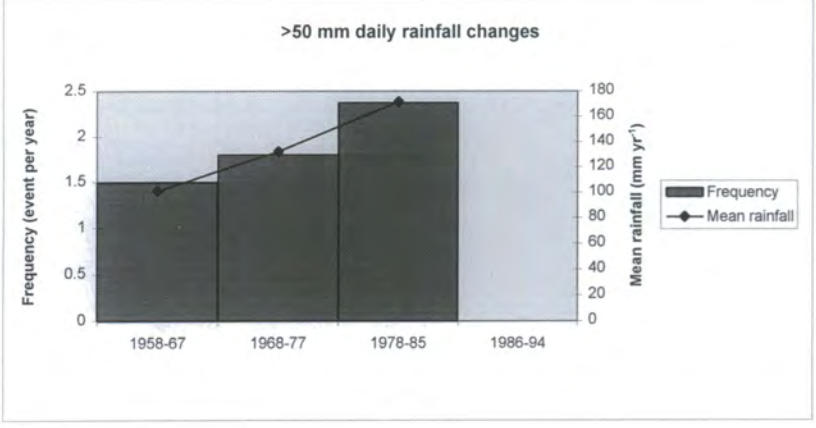

Figure 6-5, Rainfall changes for the four phases in Changshou county

6.5.3.2 Land use change

There is little information available on historical land use changes in the catchment. However, it is believed that the highest sediment yield for Phase 2 was caused by the reduction of forest land by massive deforestation. The significant change of forest land in the Three Gorges areas between the 1950s to 1980s was summarised in Table 3-10. It can be seen that forest land decreased from 18.5% in the 1950s to 7.5% in the 1980s in Changshou County. This massive deforestation inevitably caused serious soil erosion and hence high sedimentation. For this small catchment, little woodland has been left after the massive deforestation, and arable and paddy fields dominated the scene. In other words there is limited scope for further deforestation which might explain why recent sedimentation rates appear to have been lower than during the deforestation phase. Furthermore, the remaining woodland and grassland are mainly distributed on the crests of hills or valley sides with steep slopes. This suggests that the land uses in the catchment after massive deforestation are relatively stable and are dominated by agricultural land. In addition, Phase 4 from 1986-94 is almost 10 years after rural reform in China started from 1978. At this stage, some farmers began to leave rural areas for better incomes. This means that the pressure on land has eased and hence soil erosion reduced as reported by Higgitt and Rowan (1995) in Fujian, Southeast China. The details on this campaign and the affect of this incident on land use changes and hence sediment yield in a broad area will be described in Chapter 7 and 8 using sediment load data measured at hydrographic stations within the whole Upper Yangtze.

The sediment yields calculated, based on the 4 phases give a clear temporal trend but cannot fully indicate dynamic changes within each phase. With 4 divisions identified, e.g. 1958-67, 1968-77, 1978-85 and 1986-94, a possible sediment depth can be assigned to each year, if it is assumed that yearly sediment yield within each division was proportional to its rainfall. This assignment can give a sediment yield for each year. The changes of the assigned annual sediment yield with time is presented in Figure 6–6. The results clearly show dynamic changes over the 30 years from 1958 to 1985.

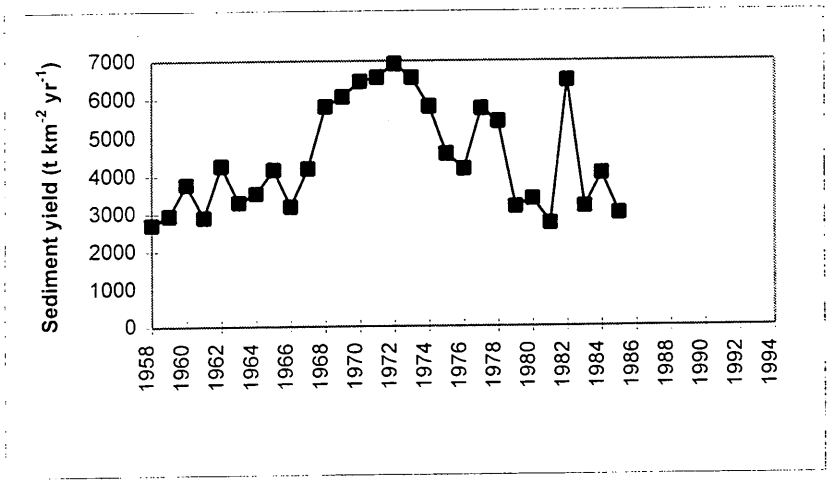

Figure 6-6, Sediment yield changes assigned based on dating layers and annual rainfall in Yiwanshui catchment

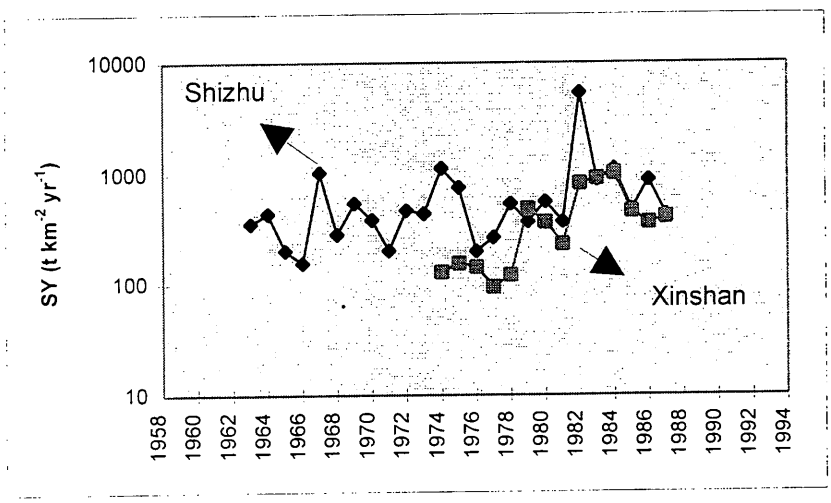

Figure 6-7, Sediment yield changes in Shizhu and Xinshan catchments in the Three Gorges area

The yearly sediment yield changes determined by the assignment provide an opportunity to make a comparison with other catchments. Figure 6–7 depicts suspended sediment yield changes for two catchments located in Shizhu and Xinshan county in the Three Gorges area (Figure 3-3). The trends for the two catchments are quite similar to Yiwanshui catchment. However, the latter two catchments show a clear increase trend since the 1970s, which contrasts with Yiwanshui catchment. As discussed above the small Yiwanshui catchment left few trees which can be cut down after massive deforestation in the 1950s and 1960s. Sediment yield already reached much higher levels. Comparatively, the larger catchments (drainage size is 898 and 1900 km^2 for Shizhu and Xinshan catchments) still consist of a large percentage of forest land. For those catchments sediment yields are still relatively low compared with catchments dominated by arable land such as Yiwanshui catchment. Therefore there is a potential that sediment yield will increase if deforestation happens. For example, Shennunjia forest area (a place well-known for the discovery of "wild man") is located in the Xinshan catchment. It is reported that massive deforestation began from the 1970s (Shi et al., 1992). This is consistent with an increase in sediment yield since the 1970s for the catchment (Figure 6–7). However, care must be taken for the sediment yield changes determined by dating methods. The larger errors can be introduced by Cs-137 dating and subsequent linear assignment. As discussed before, Cs-137 dating in 1978 and 1986 needs further attention. The errors on those two dating years can lead to considerable differences in sediment yield. The errors associated with dating methods may also come from the estimates of trap efficiency and reservoir transect shape. An averaged trap efficiency used throughout the period, for example, may also lead to a smaller sediment yield estimate for the most recent period, since the trap efficiency may be lower after a certain amount of storage was filled by sediment. Considering the problems associated with dating methods, it is clear that sediment yield changes determined by suspended sediment load measurement are more reliable compared with dating methods.

Identifying the controls on changing trends in sediment yield is a complicated issue. The details of the changes throughout the Upper Yangtze will be examined in Chapter 7, where a diversity in sediment yield time series is demonstrated. Most of the catchments examined have stable sediment yield but some catchments do show significant increases or decreases since the 1950s. It is also demonstrated that the sediment yield changes are due to human activity such as deforestation and damming rather than hydrological variation.

6.6 CATCHMENT-WIDE SEDIMENT DELIVERY AND BUDGETS

The sediment delivery ratio (SDR) is a linkage between the soils eroded from slopes and the sediment transported at the outlet of a river (see detail in Chapter 1). Compared with conventional methods, the application of the Cs-137 techniques makes it possible to estimate the sediment delivery ratio within fields (Owens et al., 1997). The ratio gives a clear indication of in-field erosion and deposition. However, the ratio has been more frequently used at the catchment scale, indicating the quantity of sediment which is transferred from eroding sources through the channel network to a basin outlet (Ferro and Minacapilli, 1995). SDR can be calculated as:

$$SDR=ER/SY \qquad \text{(Equation 6-2)}$$

Where ER is average erosion rate (t km^{-2} yr^{-1}) and SY is sediment yield (t km^{-2} yr^{-1}) for a catchment. The estimate of the sediment deposited in the Yiwanshui reservoir provides an opportunity to estimate the sediment delivery ratio, if it is possible to estimate average soil erosion rate for the whole catchment.

6.6.1 Estimate of average soil erosion rate

Erosion estimate for sloping arable land in Chapter 5 together with other available information such as land use (Table 3-14) provides an opportunity to estimate

average soil erosion rates for the catchment. The accuracy will be dependent on the estimates of erosion rates for each type of land use and its area.

6.6.1.1 Erosion rate for wood & grass land

Soil samples have not been taken from wood & grass land and hence erosion rates can not be estimated using Cs-137. As described in Chapter 3, these lands are not fully covered by the vegetation and hence are susceptible to some soil erosion. Erosion rates can be hugely different depending on the type and cover of trees and grass based on the studies (Shi et al., 1987) (see details in Table 3-13). In the study area, erosion rate for those lands is tentatively estimated to be 3000 t km^{-2} yr^{-1}.

6.6.1.2 Erosion rate for gully and terrace edges

These typical landforms account for only a small percentage of land use (Table 3-14), but total sediment produced can not be ignored due to higher erosion rates. Erosion rates for those typical landforms are more difficult to quantify. There is little data on erosion rates for terrace edges in particular. Li (1993) examined erosion rates for two years for gullies and bare soils in Sichuan basin. A natural gully with an area of 1053 m^2 was measured for runoff and sediment, while erosion pins were used on bare soil. They found that the proportion of erosion for arable land, gully and bare soil is 1:3:3.5 under the same rainfall conditions. The proportion may be higher under storms. Based on the ratio and erosion rate for arable land determined using Cs-137 in last chapter, it tentatively gives long-term erosion rates of 12,000 t km^{-2} yr^{-1} for gully and 14,000 t km^{-2} yr^{-1} for bare land in the catchment. The erosion rates are consistent with that for "white hill" and "red desert", which have extremely high erosion rates in south China (Lu and Shi, 1992). For the study, the mean value of 13,000 t km^{-2} yr^{-1} is employed for erosion rate of gully, bare land and terrace edges.

6.6.1.3 Average erosion rate for the catchment

With erosion rate and the area available for each type of land use, an average erosion rate (ER) for whole catchment can be calculated:

ER=(ERa*DAa+ERw&g*DAw&g+ERg&t*DAg&t)/DA (Equation 6-3)

Where ERa, ERw&g and ERg&t is erosion rate for arable land, wood & grass land and gully & terrace edges, respectively. DAa, DAw&g, DAg&t and DA is drainage area for arable land, wood & grass land, gully & terrace edges and total drainage area. The calculated ER for the catchment is 4170 t km^{-2} yr^{-1}, which is close to 4400 t km^{-2} yr^{-1} for arable land estimated in Chapter 5.

6.6.2 Sediment yield delivery and budget

With an average erosion rate (ER) of 4170 t km^{-2} yr^{-1} and a sediment yield (SY) of 3490 t km^{-2} yr^{-1} available, based on Equation 6-2 it can be calculated that SDR is 0.84 for the catchment. The SDR is not comparable among the catchments with varied sizes, because in general SDR decreases with increasing basin size, indexed by area or stream length (ASCE, 1975):

$SDR=k(DA)^n$ (Equation 6-4)

where k and n are numerical constants and DA is drainage area (km^2). The exponent n varies between -0.01 and -0.25, indicating transport capability. Compared with the ratios listed in Table 3-13 which was used by Shi et al. (1992), the estimated ratio is quite high. It must be noted, however, the ratios used by Shi et al. (1992) were for individual land uses rather than at the catchment scale. Assuming a similar surface erosion situation for the catchments of varied sizes, sediment load and drainage area relationship indicates sediment delivery (Walling, 1983). The estimated SDR for the catchment is reasonable, since close sediment load and drainage basin relationships as indicated in Figure 6–3. The higher SDR reflects steep landforms, the small size of the catchment and limited opportunities for storage.

SDR indicates that only 16% of the sediment is deposited within the catchment before arriving at the reservoir. The sediment eroded from the three different sources can be temporarily deposited in roads and ditches but it is believed that majority of the sediment is deposited in paddy field before arriving the reservoir. Assuming all of those sediment deposits in paddy field, a tentative sediment budget can be developed (Figure 6–8). This also gives an average aggradation rate of 3300 t km^{-2} yr^{-1} for

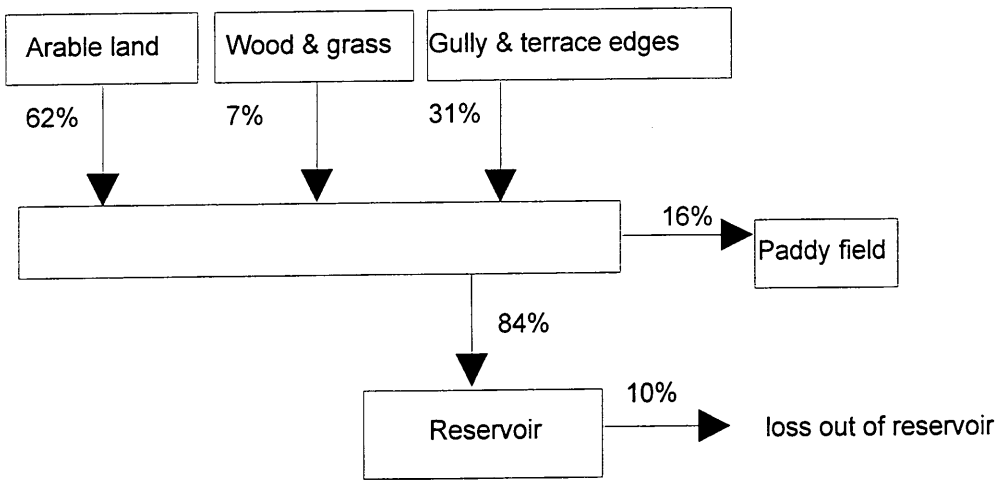

Figure 6-8, Sediment delivery and budget in Yiwanshui catchment

paddy fields based on the assumption. With the erosion rates for the potential sediment sources available, it is estimated the proportion of the soil is eroded from sloping arable land, wood & grass land and gully & terrace wall is 62%, 7% and 31%, respectively (Figure 6–8). This means that majority of the soils eroded from arable land and one-third from gully & terrace walls.

6.7 SEDIMENT SOURCE DISCRIMINATION

Having examined the patterns and rates of soil erosion on slopes and sedimentation in the reservoir, now it is necessary to look at the information on the *type* of source involved. In particular sediment source discrimination attempts to determine whether the sediment has originated primarily from erosion of cultivated land, woodland, or from erosion of channel and terrace wall, irrespective of the precise spatial location of the source. This information can offer a direct method for guiding the long-term soil and water conservation work (Olley et al., 1993). The dilemma of identifying the mechanism of the sediment production in the Loess Plateau (gully or slope), for example, mislead soil conservation work for a long time.

6.7.1 A PRELIMINARY EVALUATION

Assuming similar delivery ratios for different erosion mechanisms within the catchment, the proportion of different sediments deposited in the reservoir reflects the relative percentage of sediment production in the catchment (Figure 6–8). This means that the majority of the sediment (nearly two-thirds) was from sloping arable land. It is also noted nearly one-third of the sediment was from gully & terrace walls. The proportion can be higher under heavy storms, which resulted in no detectable Cs-137 in the profile of core 1 (Figure 6–1). This can provide a preliminary evaluation on sediment source. As a matter of fact, the textures of the soils eroded from different types of land use are varied. It may be much coarser for the soils eroded from gully & terrace wall but much finer for the soils eroded from wood & grass land. More importantly, sediment delivery also depends on the distance from sediment sources to a channel network. Therefore SDR for the soils eroded from the

three types of land use may not be same. These suggest that supplementary information is needed to identify main sediment source. The study examines the potential of using Cs-137 techniques to identify main sediment sources in the particular environment of the Three Gorges area, where soils are relative coarse.

6.7.2 Main sediment source identified by Cs-137 technique

By comparing Cs-137 activity of sediment with that of sediment source materials, it is possible to identify the main sediment source (see Chapter 2). The possible sediment deposition included in the permanent sinks like reservoirs and paddy fields, and temporary sinks like gullies, roads and ditches. The average caesium-137 content of the upper portion of the core 1 (0-35 cm) should directly reflect that of the sediment sources involved because current atmospheric fallout inputs are insignificant (Foster and Walling, 1994). The mean Cs-137 activity for paddy fields is determined from top 5 cm paddy soils. The deposited materials on roads, ditches and channels are collected for Cs-137 measurement. Cs-137 concentrations for those potential sediment sources and sinks are listed in Table 6-2. It can be seen that paddy

Table 6-2, The mean Cs-137 concentration (Bq kg^{-1}) for the materials of potential source and sinks in the fraction of <2mm

Materials	Obs.	Mean	Std. Dev.	Min	Max
Sediment from:					
Reservoir (0-35 cm)	14	7.5	3.6	0.0	10.4
Paddy field	13	6.7	2.3	2.7	9.3
Road, channel and ditch	7	2.4	1.8	0.0	5.5
Materials from:					
arable land	27	6.1	2.5	1.6	11.3
Wood & grass land	7	26.7	14.1	11.0	46.1
Terrace edges	4	4.9	3.3	0.0	7.0
Channel bank	2	4.2	1.8	2.9	5.5

soils have similar Cs-137 activity as reservoir deposition but temporary sediment materials deposited in paths, roads, channels and ditches, etc. have low Cs-137 concentrations. This is due to the coarse texture of the materials which were temporarily deposited, which are different from that deposited in the reservoir and can not be used for the purpose of fingerprinting. The topsoils for paddy fields have a lower variability as shown in Figure 6-9. This low variability is consistent with that for soil samples taken for reference values in that small paddy field as discussed in Chapter 5. Cs-137 concentrations are very high for the topsoil taken from woodland, which may be caused by the combined effects of slight soil erosion and the fact that most Cs-137 is retained in topsoil for woodland. The overall information on soil erosion for wood & grass land can not be evaluated in the absence of detailed soil sampling on it. However, certain degrees of soil erosion happened in wood & grass land as discussed above, so it is believed that the high Cs-137 concentrations are mainly caused by surficial retention. The materials taken from channels and terrace edges have the lowest Cs-137 concentration compared with former two potential sediment sources. If taking into consideration the >2mm fraction content in the total soils, Cs-137 concentrations are further reduced for channel banks and terrace edges.

By comparison between Cs-137 concentrations in sediment sources and sinks, it is found that arable sloping land has a close Cs-137 activity with paddy field soils and reservoir sediment, suggesting that main sediment source comes from arable land. The result is consistent with the above discussion which suggests that the majority of eroded soils in the catchment is from sloping arable land. Having identified arable land as the main sediment source, an attempt was made to further distinguish main sediment source within different arable lands such as at different hill positions. The topsoil samples used above were re-grouped and their mean Cs-137 concentrations are summarised in Table 6-3. It can be seen that Cs-137 concentrations among those re-grouped materials are not very varied and the limited information can not provide further information on sediment source.

Table 6-3, Cs-137 concentration (Bq kg^{-1}) variability of purple soils for different slope position

Slope position	Sample numbers	Mean	Std. Dev.	Min.	Max.
Upper	8	6.5	2.3	3.4	10.4
Middle	5	5.3	1.4	4.2	7.4
Bottom	5	5.5	3.0	1.6	9.5

The Cs-137 fingerprinting technique must be used with caution, noting the inherent problems described in Section 3 of Chapter 3. The averaged Cs-137 concentrations within the upper 35 cm of the reservoir core could also be due to the combined results of the materials eroded from channel bank and terrace edges, both of which have lower Cs-137, and woodland with high Cs-137 concentrations. This can be demonstrated by Figure 6–9, showing Cs-137 variation within the sample taken from same type of sediment source and sink. It can been that there is much overlapping for the Cs-137 activity among each group, suggesting that it is possible that the averaged Cs-137 activity of sink materials can result from the combined materials from varied source materials. Therefore further study is needed for this identification. Collins et al. (1997) proposed a composite method to determine main sediment sources. The method integrated many properties into a composite model, which overcomes the uncertainty in using a single index such as Cs-137. A similar approach can also be undertaken in the Yiwanshui, if further laboratory work on the large number of soil samples can be undertaken. For the purposes of the present study there is insufficient time and resources to undertake additional composite fingerprinting work, but the prospect of refining the sediment budget model is acknowledged.

6.8 SUMMARY AND CONCLUSION

Estimated average sedimentation rates of the reservoir and sediment yield for the catchment are 3.65 cm yr^{-1} and 3490 t km^{-2} yr^{-1} for the 36 years from 1958 to 1994.

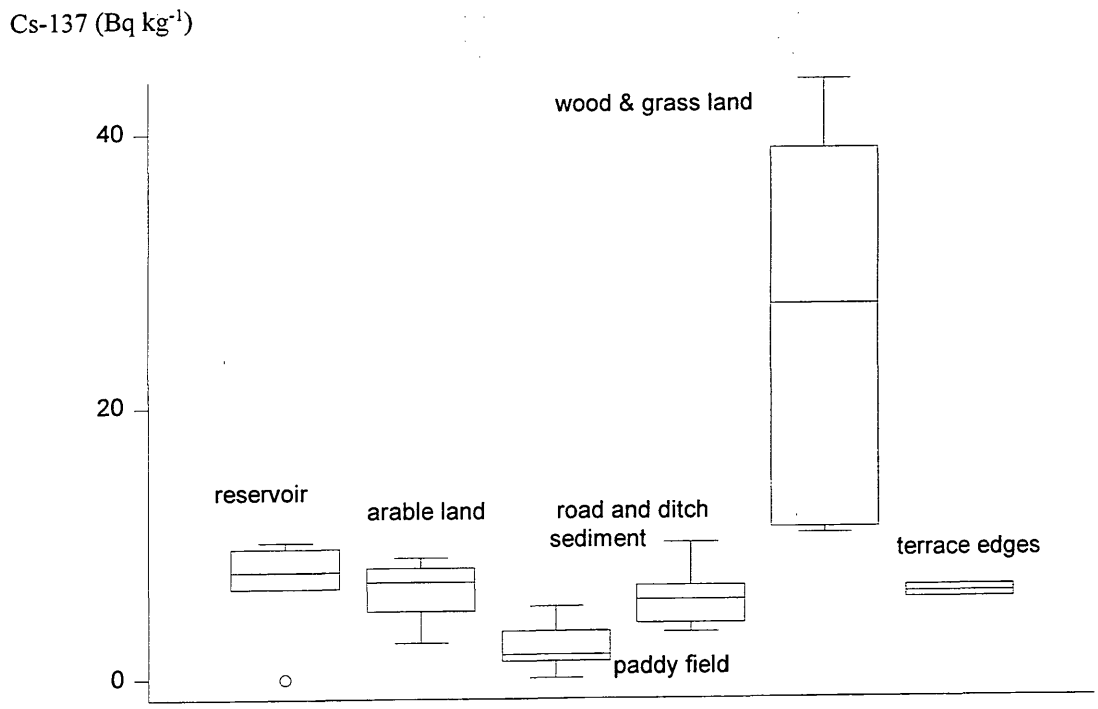

Figure 6–9, The variability of Cs-137 concentration (Bq kg^{-1}) for the potential sediment sources and sediment materials

Sedimentation rate is highly dependent on the catchment-reservoir area ratio. The sediment yield is quite high particularly for the latter, reflecting serious soil erosion within the catchment as discussed in Chapter 5.

Three dating layers, 1986, 1978 and 1963, can be identified by Cs-137 concentration profile, and two layers, 1982 and 1968 were distinguished based on downcore particle size distribution with the aid of rainfall data. The clear cut edges of the chronology are due to dominant process of autochthonous sedimentation. The changes of sedimentation rates and sediment yields over the 4 phases, Phase 1 (1958-67), Phase 2 (1968-77), Phase 3 (1978-85) and Phase 4 (1986-94) were reconstructed using those dating markers identified coupled with bathymetric measurements. The sedimentation rates and sediment yield were the highest for Phase 2 and the lowest for Phase 4. Through the analysis of rainfall data in terms of annual total rainfall and the frequency of daily rainfall of >25 and 50 mm, it is found that the sedimentation rates and sediment yield were consistent with rainfall data except for Phase 3, suggesting that annual rainfall as a whole plays an important role in generating sediment but the changes of sedimentation rates and sediment yield were mainly govern by land use changes. In other words, the major changes of sedimentation were mainly caused by human activity. The effect of human activity includes altering land use changes and exerting pressures on land use. The significant reduction of forest land in the area from the 1950s to the 1980s was mainly due to a massive deforestation campaign at the end of 1950s. It is believed that the incident was the main reason for higher sedimentation rates in the 1960s found in this study. The agricultural reform started from the beginning of the 1980s has also had a profound effect on land use such as deforestation at the beginning of the reform and in particular the reduction of land pressure in the 1990s due to farmer migration. This may significantly reduce soil erosion and hence sedimentation.

A tentative sediment budget is developed for the catchment. It is found that 16% of eroded soils are deposited in paddy fields, giving an average aggradation rate of 3300 $t\ km^{-2}\ yr^{-1}$, and 84% deposited in and beyond the reservoir. The high SDR may reflect the small size and steep slope of the catchment. By assuming the same

delivery ratio for the eroded soils from varied land use, sediment contribution from arable land, wood & grass, and gullies & terrace wall is tentatively estimated as 62%, 7% and 31%, respectively. Arable land as a main sediment source is confirmed by comparing Cs-137 activity among the main sediment sources and sinks.

Through this study it can be seen that a few dating years can be identified based on the Cs-137 profile with a combination of other information provided, such as rainfall and particle size. This is very useful for reconstructing the history of soil erosion induced by rainfall and land use changes. This highlights the potential application of the Cs-137 dating techniques for investigating the history of soil erosion and sedimentation combined with the information of historical land use and rainfall data. The numerous reservoirs built in the 1950s in China provide the opportunity for this application. Fuller understanding of the erosion mechanisms and chronology of reservoir sedimentation in the Three Gorges area will provide useful experience for local catchment management and, in particular, for consideration of the potential future impact of sedimentation in the ongoing Three Gorges Project.

7. SEDIMENT YIELD IN THE UPPER YANGTZE: SPATIAL VARIABILITY AND TEMPORAL CHANGES

7.1 INTRODUCTION

The previous two chapters examined soil erosion, sediment delivery and sedimentation using a small catchment as an example. These results can be very useful for appropriate management of newly exploited arable land due to population allocation. However, this small scale study can not provide a clear picture of soil erosion and sediment transport throughout the Upper Yangtze basin. This chapter and subsequent two will concentrate on investigating soil erosion and sediment transport throughout the Upper Yangtze using suspended sediment load data obtained from hydrographical stations throughout the basin.

The construction the world's largest hydro-power schemes on the Yangtze River, has aroused many debates on the assumptions of hydraulic models of reservoir sedimentation (Qian et al., 1993; Ryder and Barber, 1993) but relatively little attention has been paid to the controls on the source of sediment in the Upper Yangtze basin and the linkages between soil erosion and sediment delivery. Analysis of regional patterns of sediment yield is complicated by basin size and time-dependency of the data. Stations operating over different years cannot be compared directly because of the high variability of discharge from year to year. Similarly, as sediment yield is partly a function of the drainage basin area, correcting for the attenuation of sediment delivery is required.

Identifying the controls on recent changes in soil erosion, sediment delivery and sediment yield is an issue of concern to policy makers engaged in the management of rivers with high sediment loads. Although several examples of accelerated erosion

and increased sediment loads associated with anthropogenic activity, such as deforestation, vegetation clearance or land use change, some human activity may not lead to obvious trends, particularly in large catchments (Walling, 1997). For example, Alford (1992) reported that the Chao Phraya basin (14,028 km^2), draining the highlands of northern Thailand, showed no evidence of a significant increase in sediment yield during the period from the late 1950s to the mid 1980s, despite substantial deforestation and extensive expansion of agricultural activity within the basin. A similar situation has also been found in the Upper Yangtze river and several authors have noted that there is no systematic trend in sediment loads in the Upper Yangtze (Gu et al., 1987; Gu and Douglas, 1989; CVJV, 1988; Zhuo and Xiang, 1994; Dai and Tan, 1996). Most of the analysis has been based on large stations, particularly that at Yichang, and relatively little attention has been paid the entire gauging network within the catchment.

This chapter is designed to investigate spatial variability and temporal changes of sediment yield using sediment yield data obtained throughout the Upper Yangtze basin between 1956 and 1987. The main purposes of the chapter are:

1) to examine sediment yield - basin area relationships and its implication for sediment delivery;

2) to develop standardisation methods to evaluate spatial variability of basin area dependent sediment yield data;

3) to examine long-term sediment yield changes and possible reasons for the changes throughout the area;

4) to examine possible effects of recent socio-economic polices on hydrological sequences.

The controls of sediment yield variability will be further discussed in Chapter 6 using available environmental datasets. Sediment yield mapping methods will also be discussed in that chapter.

7.2 SPATIAL VARIABILITY

Spatial patterns of sediment yield in the Upper Yangtze can be complex, due to the combination of climatic, topographic, lithological and landuse controls. Some of these variables were introduced in Chapter 3, while more details will be further discussed in next chapter. This section is focused on the development of methods to examine spatial patterns, the controls of the spatial patterns will be discussed in next chapter.

7.2.1 Sediment yield - basin area relationships

Sediment yields from basins of widely varying size cannot be compared directly because of the likely relation between sediment yield and drainage basin area as discussed in Chapter 2. In order to examine yield area relations over consistent measurement periods and to investigate the changing nature of the relation over time, data have been divided into three time periods: 1956-65; 1966-76 and 1977-87. These represent near equal divisions of the record period but also coincide with profound changes in agricultural practice due to the three socio-economic incidents: the Great Leap Forward, the Cultural Revolution and the Land Responsibility Reform. Each of these incidents is considered to have had profound influences on land use and hence on erosion and sediment transport potential. During the Great Leap Forward from 1958 to 1961 national-wide deforestation occurred for small-scale iron smelting (Biot and Lu, 1993). During the decade of the Cultural Revolution from 1966-75, many water conservancy projects in fields (terraces and ditches) and in waterways (dams or reservoirs) were constructed. Inventories of

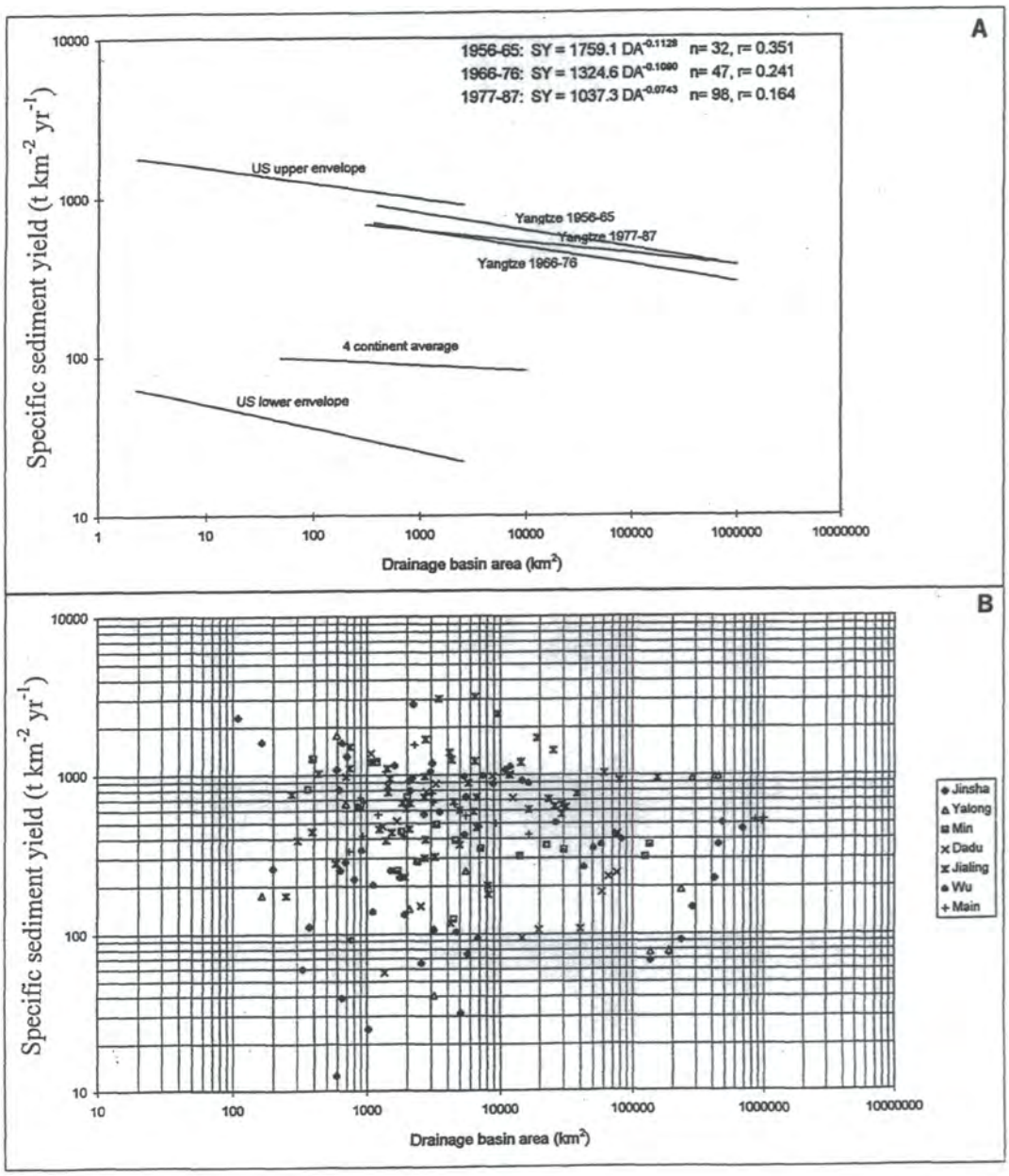

Figure 7-1, Relationships between specific sediment yield and drainage basin area. (A) Comparison of Yangtze data for different time periods with US and global cures (based on Glymph, 1951; Fleming, 1969; via Church et al., 1989). (B) Mean specific sediment yield for all stations with ≥ 5 years data.

agricultural land indicate an increasing extent of soil erosion during this period but the water conservancy schemes will have affected sediment delivery ratios. Land Responsibility Reform from the end of 1970s, resulted in a further phase of widespread deforestation, as the harvesting and selling of timber became lucrative. More detailed discussion about the environmental effects of model Chinese socio-economic polices is available elsewhere (Smil, 1987; 1993; Edmonds, 1994).

Regression relationships for the three time periods are indicated in Figure 7-1(A). In each case only stations with a complete record of sediment yield for the time were included, except for the 1956-65 period when fewer stations were operating. In this period, stations with at least 8 out of 10 years data are included. The regression relationships are compared with published relations for 51 basins in the Missouri, USA (Glymph, 1951) and an average relationship for 250 stations on four continents (Fleming, 1969). The Yangtze curves are considerably higher than the four continent average and lie just within the upper envelope of the US data. In each case an inverse relation is indicated, although the degree of explanation afforded by basin area is small. The equations for each relation are indicated in Figure 7-1(A) where it can be seen that the exponent decreases in each time period, suggesting an increasing sediment delivery ratio. Tests for the coincidence of each regression relationship, using the procedure of Kleinbaum et al. (1988), indicate no significant difference between intercepts, but a significant difference between the 1956-65 and 1977-87 exponents. It should however be noted that the mean and median basin area of the sample for 1956-65 were considerably larger than those in subsequent periods which may introduce bias into the analysis. Combining the data from each of the three periods, the following regression equation, which is significant at $\alpha = 0.01$, can be derived:

$$SY = 1126.2DA^{-0.0826}, (r = 0.197, \alpha = 0.01) \qquad \text{(Equation 7-1)}$$

Where SY = specific sediment yield ($t\ km^{-2}\ yr^{-1}$)

DA = drainage basin area (km^2)

Equation 1 is subsequently used to compare actual and predicted sediment yields in order to identify the relative contribution of different sized basins to the sediment load. Although noting considerable variation, Walling (1983) reported a typical world-wide exponent value of -0.125. The yield-area relations for the Yangtze suggest that the proportion of eroded materials transferred downstream is somewhat higher than the global average. The considerable scatter of the sediment yield-basin area relation is indicated in Figure 7-1(B), where all stations with at least five years of sediment yield measurements are plotted. The scatter is not unexpected given the climatic, topographic and landuse diversity of the basin. None of the individual tributaries provide statistically significant yield area relations.

7.2.2 Sediment yield variability

Management of sedimentation problem requires an effective understanding of source and transmission of material from diverse parts of the basin and of the trend in sediment supply and delivery. Evidence for a widespread increase in the area being affected by soil erosion since the mid 1950 as introduced in Chapter 3 is not clearly mirrored by the sediment yield data. Year to year variations have been compensated by using a five year running mean. As some stations have individual years where measurements have not been returned, qualification for the running mean required at least 3 of the 5 years of measurement. Using records of all stations larger than 25,000 km^2 with sufficient operational coverage, the mean sediment yields at the end of the measurement period (1983-87) were 17.7% up on the initial period (1956-60). However, compared to the period 1961-65, the most recent measurements were, on average, down 3.3%. Most stations record a slight increase in yields until the mid-late 1960s, followed by a decade of lower yields and a sharp increase in the late 1970s (Figure 7-2).

In order to illustrate general patterns, stations on the larger tributaries were selected and two methods of standardisation employed. None of these stations have overlapping catchment areas and a statistical summary of their sediment yield records is shown in Table 7-1. The first standardisation method employed the regression

relationship (Equation 1) to predict the expected sediment yield from the tributary basin area. Actual yield was then divided by predicted yield to derive a standardised proportional contribution which has been plotted against time (Figure 7-2(B)). It was found that the Jialin had a substantial relative contribution to the sediment load throughout the time period with a similar, though less exaggerated pattern for the Fu and Qu (which are tributaries of the greater Jialin). The latter has become an increasingly important source during the measurement period. These three rivers drain the agriculturally productive lands of the Sichuan Basin. In contrast, the tributaries originating in the mountainous terrain of the far west of the basin (the Jinsha and Yalong) have substantially smaller contributions relative to their drainage areas. The marked dip of most curves in the middle part of the time interval indicates the generally lower sediment yields recorded in the basin between the late-1960s to late-1970s. The second standardisation method Figure 7-2(C) adjusts for this effect and permits the relative contribution of each tributary for each 5-year running period to be assessed, using a weighted basin area, DA_{adj}. The ratio produces broadly similar patterns to Figure 7-2(B) but some features can be elaborated. Throughout the measurement period, the Jialin tributary contributes more than twice the sediment load than would be expected if sediment supply was spatially uniform, but its importance as a source area declined during the 1970s. The Fu and Dadu show similar trends, while the Wu reverses the pattern becoming a more important source in the 1970s. The Yalong and Jinsha have remained more or less constant and relatively unimportant, but the Qu has witnessed a dramatic rise in its importance as a sediment source throughout the period.

The above discussion concerns the trends at the outlets of the major tributaries but ignores the remainder of the dataset. In Figure 7-3, the standardised residuals (A) for the regression of the data plotted in Figure 7-3(A) and the coefficient of variation of the sediment yield (B) are mapped onto the station locations in Figure 7-3(B). The

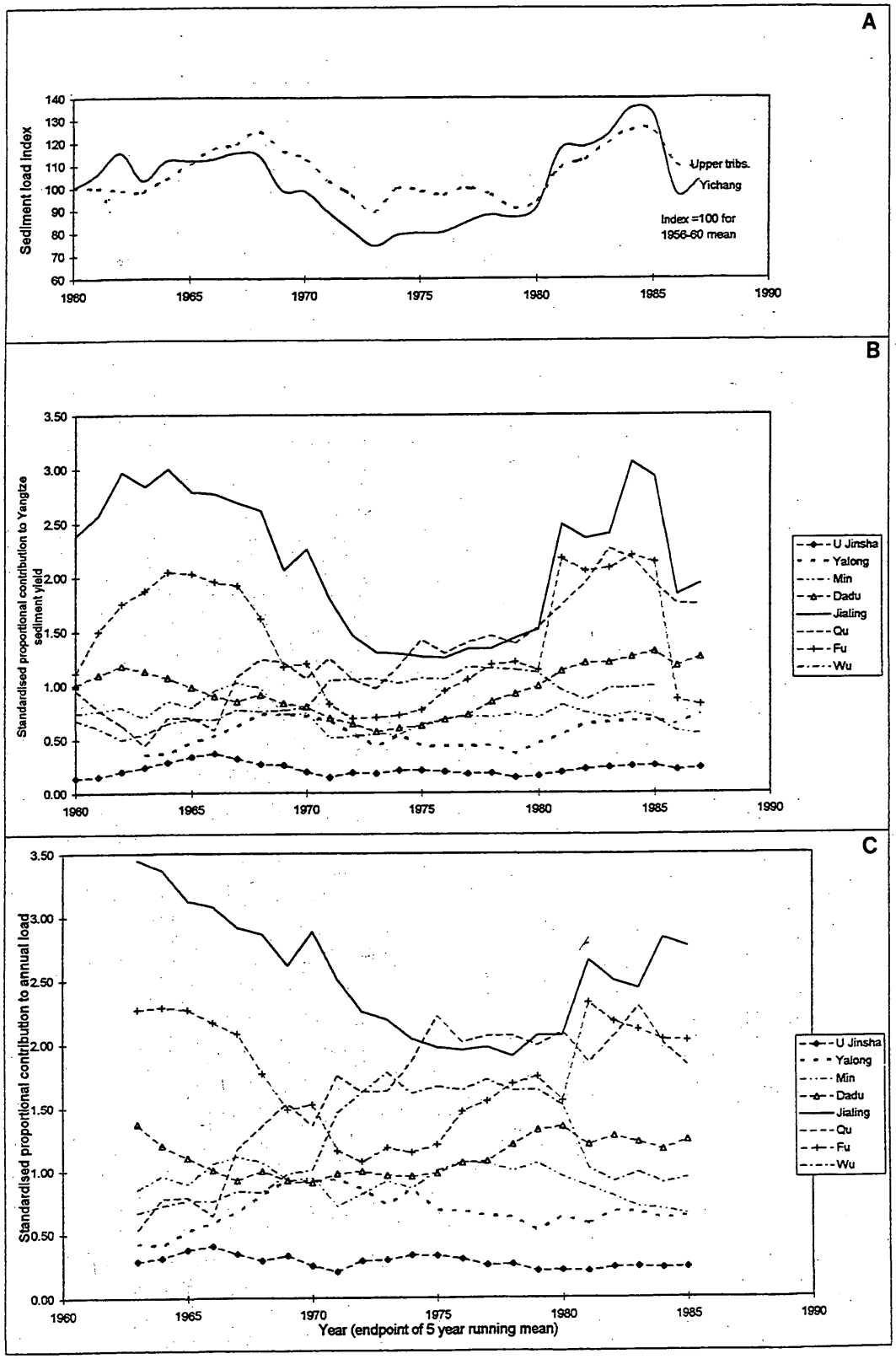

Figure 7-2, Contribution of upper Yangtze tributaries to sediment load expressed as (A) Five year running mean of sediment load index compared with Yichang; (B) standardised proportional contribution (actual yield / predicted yield from sediment yield-basin area regression and; (C) standardised proportional contribution to annual load, corrected for basin area. See text for further explanation of standardisation techniques.

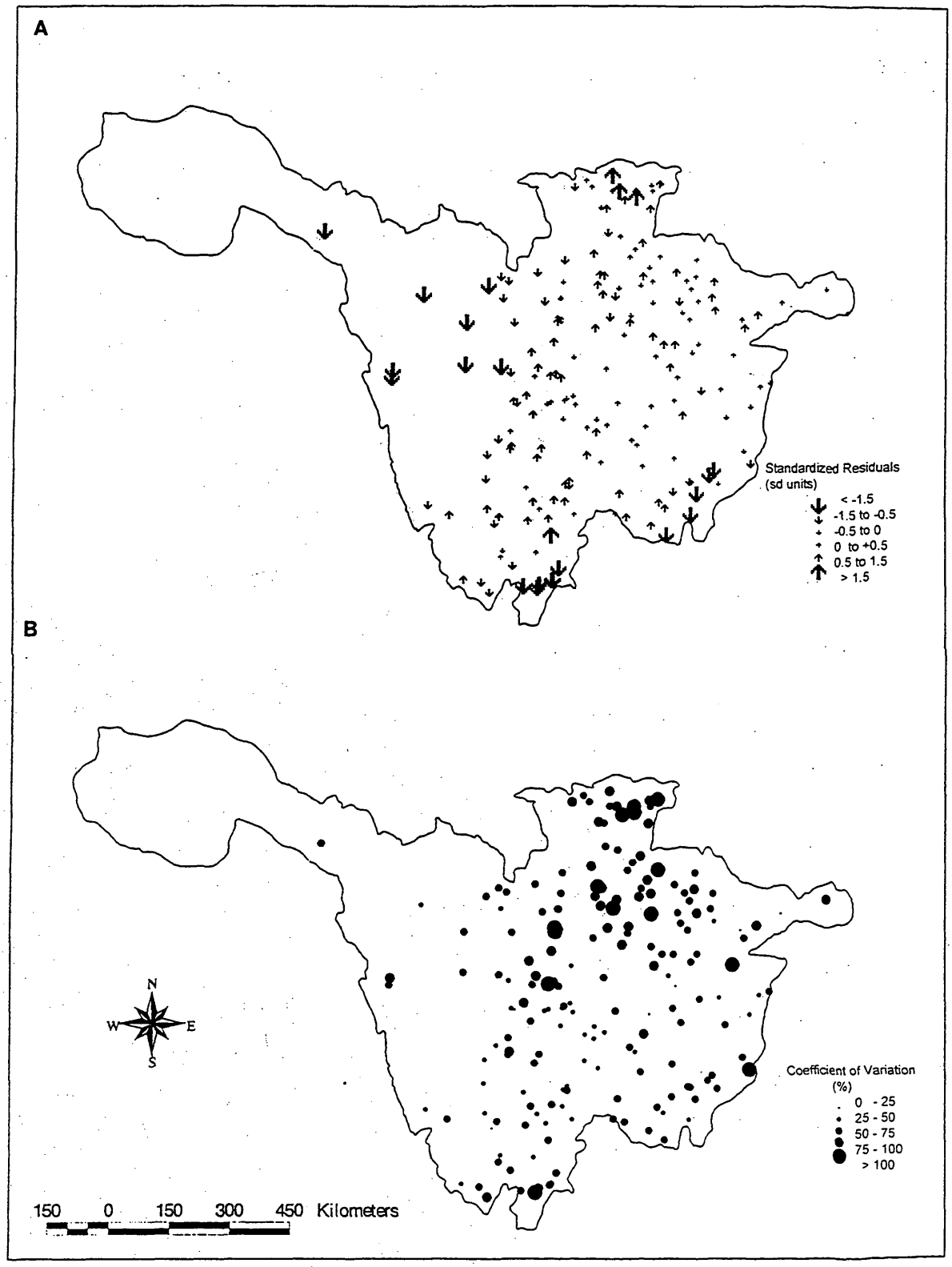

Figure 7-3, Maps of (A) standardised residual and (B) coefficient of variation of annual sediment yield.

distribution confirms the largest relative contribution from the Sichuan Basin while sediment yields from Guizhou, Yunnan and the mountainous west are lower. The largest degree of variability in annual sediment yields coincides with those areas which have experienced the greatest human influence, most notably in the Sichuan Basin.

Table 7-1, Sediment yields and relative contribution of Upper Yangtze tributaries.

Tributary	Station	DA (km^2)	Mean load ($Mt\ yr^{-1}$)	±sd ($Mt\ yr^{-1}$)	Max ($Mt\ yr^{-1}$)	Min ($Mt\ yr^{-1}$)	DA (%)	DA_{adj} (%)	Mean contribution (%)
Upper Jinsha	Shigu	232,651	21.22	9.80	42.29	6.97	34.2	32.04	8.89
Yalong	Xiaodeshi	118,294	29.42	13.47	64.38	12.69	17.4	17.23	12.11
Min	Pengshan	30,661	10.32	4.82	22.12	4.01	4.5	4.99	4.58
Dadu*	Shaping	75,016	32.22	10.49	54.91	14.17	11.0	11.34	13.62
Jialing	Wusheng	79,714	73.97	44.77	202.60	9.78	11.7	11.99	31.96
Fu	Guodukou	31,626	19.93	10.87	47.97	3.22	4.7	5.14	8.40
Qu	Xiaoheba	29,420	19.11	16.64	91.83	1.74	4.3	4.81	8.34
Wu	Wulong	83,035	32.42	12.31	60.59	11.14	12.2	12.45	14.42
Σtribs		680,417	238.61				100	100	100
Main	Yichang	1,005,501	527.22						

*Gauging station relocated from Tunjianzhi (DA=77,202 km2) in 1976. Mean Loads and contribution corrected for change in DA.

7.3 TEMPORAL CHANGES

The life span of the scheme could be threatened by extensive sedimentation although the dam engineers are confident that river regulation procedures can reduce the hazard. Widespread evidence that the extent and magnitude of soil erosion has increased dramatically over the last 40 years is not clearly matched by trends in the sediment load at Yichang, a long-term gauging station a short distance downstream

of the TGP dam site. Temporal variability of sediment transport is mainly due to climate and human activity such as deforestation, soil conservation and urbanisation (Walling and Webb, 1996). Long-term change in sediment yields has been investigated mainly through the reconstruction of the variable sediment input to the sea (Milliman et al., 1987; Degens et al., 1991) and lakes or reservoirs (Oldfield et al., 1980; Dearing et al., 1987), while direct measurement of sediment concentrations at gauging stations facilitates analysis of recent changes.

Rural China has experienced profound changes in land use in recent decades, including widespread deforestation and extension of agricultural land. For example, forest cover in Sichuan decreased from 19 to 12% between the 1950s and 1980s, while in neighbouring Guizhou it declined from 23 to 13% between the 1960s and 1980s (Yu et al., 1991). Consequently the reported extent of soil erosion in both provinces has dramatically increased. Inventories of erosion status undertaken in the 1950s and 1980s indicate a rise from 16 to 67% of land area affected in Sichuan and from 11 to 31% in Guizhou (Chen and Gao, 1988). Such a large increase in soil loss on slopes might be expected to lead to increasing sediment loads in the Upper Yangtze catchment. On the other hand, the initiation of water conservancy projects, including the construction of ponds, small check dams, ditches and headwater reservoirs, may trap a considerable proportion of eroded sediment and prevent its transfer to the river either temporarily or permanently (Luk and Whitney, 1993b). Together with larger HEP schemes, it is estimated that by the mid-1980s the total reservoir capacity in the Upper Yangtze exceeded 16 billion m^3 (Gu et al., 1987) with some 0.3 billion m^3 capacity lost to sedimentation each year (Chen and Gao, 1988). The interaction between factors controlling the input of sediment into the fluvial network and those controlling the efficiency of transmission, interposed with year to year hydrological variability, cause problems for the interpretation of trends of sediment yield based on data from Yichang gauging station alone. However, it is likely that trends in the relative importance of parts of the catchment will emerge from analysis based on all gauging station data.

7.3.1 Long-term trends in sediment yields

There are many methods to investigate time series data. The details were introduced in Chapter 2. Considering the larger dataset, the study employs a simple linear regression model in order to examine long term changes of sediment yield,

$$SY = a_1 + b_1 T \qquad \text{(Equation 7-2)}$$

was used to examine the relationship between sediment yield (SY) and the year of measurement (T). If the correlation coefficient was larger than the critical value at a 95% significance level, it is assumed that SY had experienced a significant change (increase or decrease) over the measurement period. The method, applied to the 187 stations with 5 years or longer of measurement series, provides information about the overall direction of trend. As year to year variations in sediment yield are likely to be affected by annual runoff, the stations which recorded significant trends in sediment yield were investigated for underlying trends in runoff (Q). Plots of cumulative runoff against cumulative sediment yield have been used elsewhere (e.g. Walling and Webb, 1996) to illustrate graphically the changing relationship between sediment yield and runoff. This can be supplemented by examining the temporal trend in the residuals from the SY-Q regression (Helsel and Hirsch, 1992).

The correlation coefficients of the linear regression equations indicate that the majority of stations did not experience a significant change in sediment yield across the time period. Among the 187 stations, however, there were 16 stations displaying significant change at the 95% confidence level. Of these, ten stations with a total incremental area of 78,963 km^2 (7.9% of catchment area) experienced increasing sediment yields and six with a total incremental area of 27,816 km^2 (2.8%) decreasing yields (Table 7-2). The stations are ranked in descending order of the slope coefficient of the regression (b_1). It can be noted that the rate of change in

upwardly trending sediment yields is considerably higher than the rate of change exhibited in downwardly trending sediment yields. The locations of the 16 stations exhibiting significant change were marked in Figure 7-4. The sharpest increases are recorded from diverse geographical locations but feature catchments smaller than 4000 km^2, which may suggest the impact of relatively localised land use changes. In order to establish whether the likelihood of identifying a trend is scale-dependent, correlation coefficients for the SY-T relationship have been plotted against catchment area (Figure 7-5). There is no apparent relationship between strength of trend and catchment size, although the majority of correlation coefficients are positive. Of the stations exhibiting significant change, it can be noted that six, Bikou (No 153), Sanleiba (No 154), Denyenyan (No 128), Shaping (No 116), Guodukou (No 180) and Wulong (No 207), were located on principal tributaries (Figure 7-4). Time series plots of these stations are shown in Figure 7-6. Bikou (No 153) and Sanleiba (No 154) on the Jialing and Denyenyan (No 128) on the Tuo experienced a decline in sediment yields. For the Jialing tributaries the experience can be explained by the construction of the Bikou Dam in 1975 with a 300 MW capacity. The impact of large reservoirs can be seen readily by comparing the time series of gauging stations upstream and downstream of the catchment's four largest dam; Bikou, Gongzui, Wujiadu and Gezhouba (Figure 7-7). Numerous smaller reservoir and other water conservancy projects have been developed within the catchment over the last 30 years with clear implications for the conveyance of fluvial sediment load. The distribution of water conservancy projects, in terms of reservoir capacity is also unevenly distributed (Table 7-3). The Tuo, Fu and Qu have high ratios of

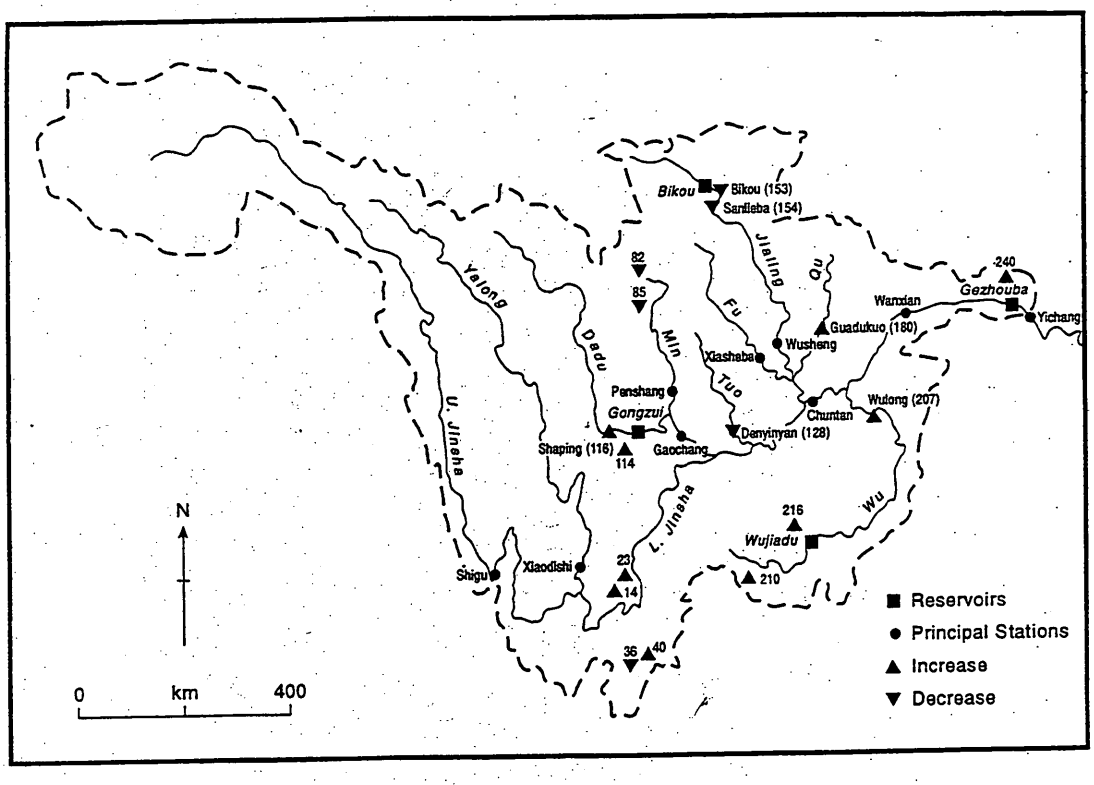

Figure 7-4, Distribution of gauging stations with significant sediment yield changes.

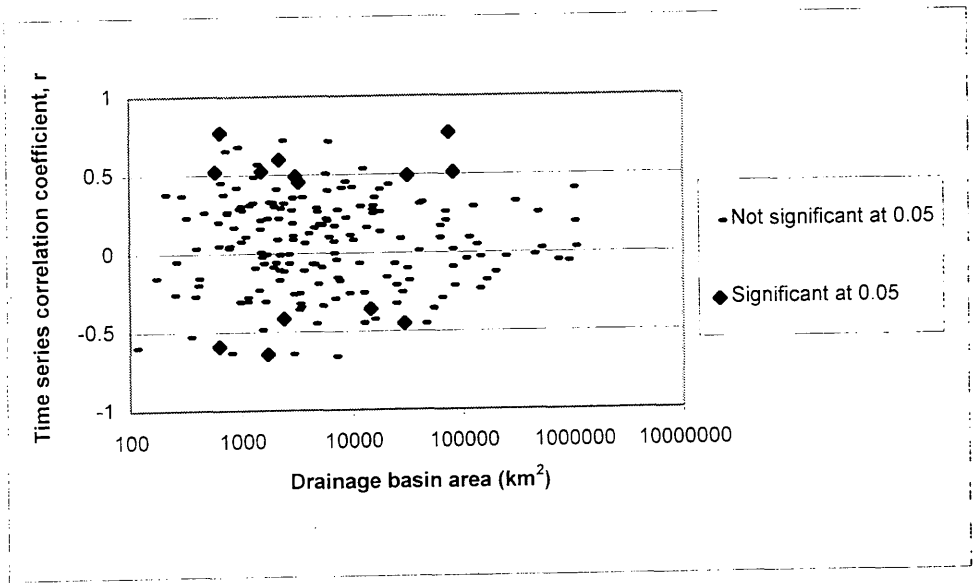

Figure 7-5, Plot of time series correlation coefficients against drainage area

Table 7-2, Stations with significant time series trends at significant level $\alpha = 0.05$

Station ID	Tributary	Station Name	Catchment area (km^2)	Length of record (years)	SY Correlation coefficient, r	b_1	Runoff Correlation coefficient, r	b_2	tau	p
14	Jinsha-Yalong	Huidongqiao	590	21	0.52	60.1	-0.13	-10.6	0.61	0.0001
210	Wu	Niuchishui	2210	20	0.60	58.9	0.12	1.9	0.54	0.001
23	Jinsha-Yalong	Ninnan	3074	25	0.49	45.3	-0.12	-1.8	0.43	0.003
249	Main Channel	Xingshan	1900	14	0.60	44.4	0.01	0.2	0.54	0.0086
114	Dadu-Min	Yanruen	3302	23	0.45	30.1	0.01	0.2	0.35	0.020
116	Dadu-Min	Shaping	75016	21	0.76	18.0	0.25	2.0	0.53	0.0008
180	Jialing	Guodukou	31626	30	0.49	17.9	0.33	8.3	0.24	0.087
216	Wu	Huoshiba	1527	19	0.52	13.3	0.05	1.1	0.36	0.036
207	Wu	Wulong	83035	27	0.51	9.0	0.27	4.0	0.28	0.052
40	Jinsha-Yalong	Xiaohekuo	649	7	0.77	7.2	0.70	70.5		
85	Dadu-Min	Zagunao	2404	26	-0.42	-8.3	-0.11	-1.6	-0.25	0.080
82	Dadu-Min	Heishui	1720	23	-0.64	-11.5	-0.35	-4.4	-0.52	0.0006
154	Jialing	Sanleiba	29247	29	-0.45	-12.2	-0.25	-2.3	-0.40	0.0004
128	Tou	Denyenyan	14484	31	-0.36	-14.4	-0.21	-3.0	-0.24	0.057
36	Jinsha-Yalong	Dianwei	630	29	-0.59	-16.2	-0.17	-0.8	-0.25	0.066
153	Jialing	Bikou	26086	27	-0.53	-19.3	-0.04	-0.3	-0.54	0.0001

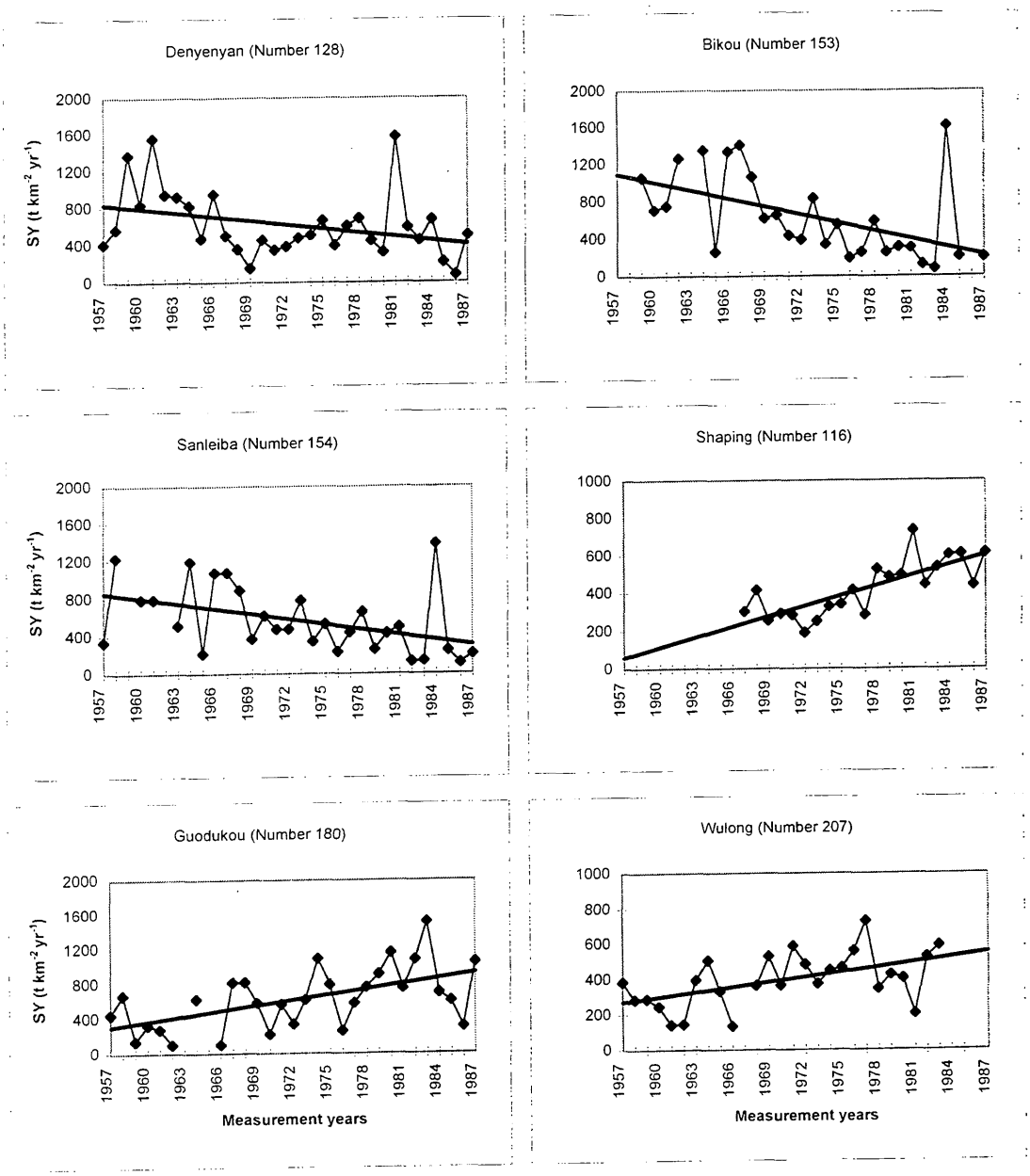

Figure 7-6, Sediment yield time series for six selected stations with large drainage area

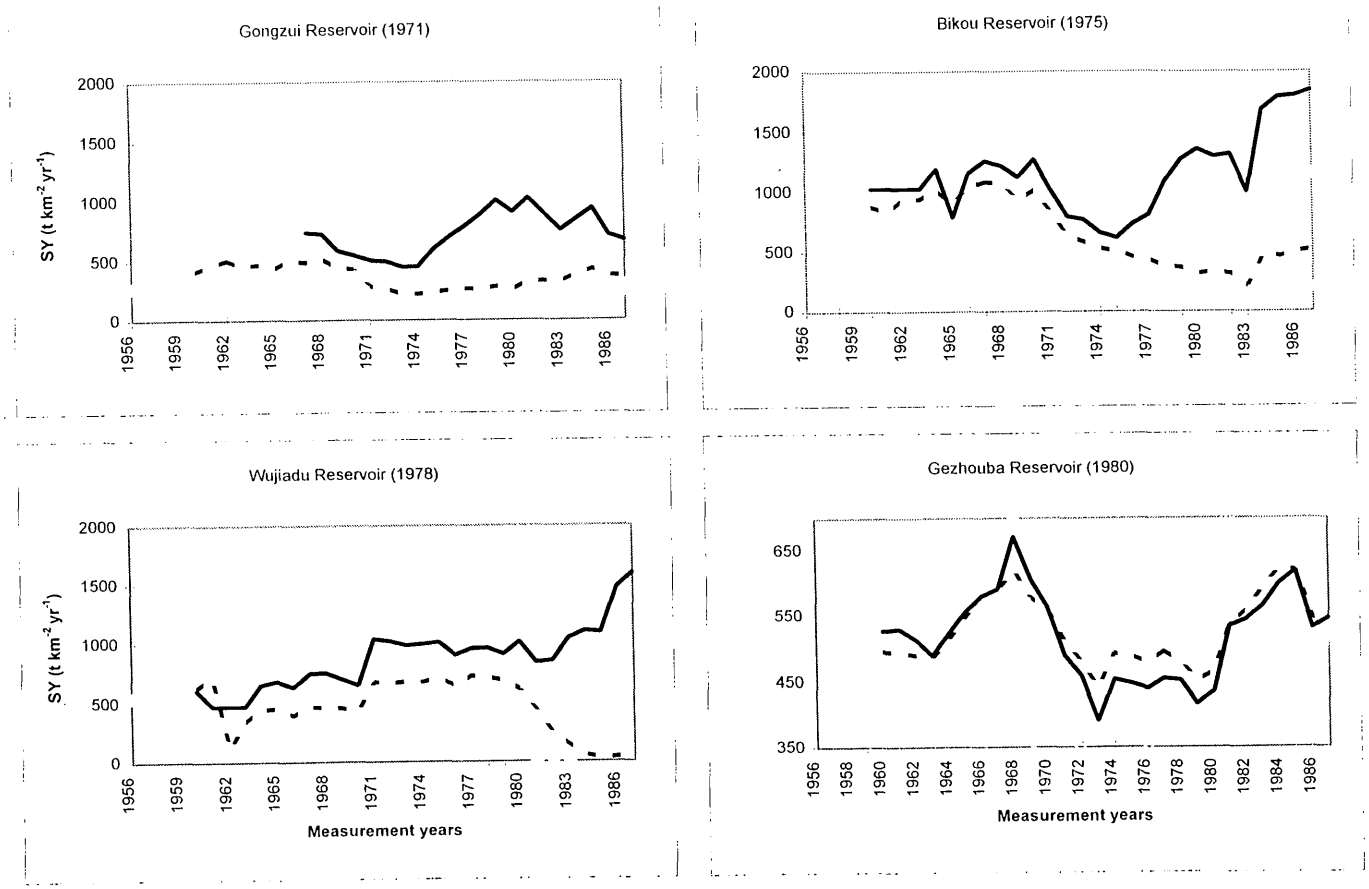

Figure 7-7, Impact of large reservoirs on sediment yield time series.
Solid lines indicate stations above the reservoir and dashed lines stations downstream of reservoir

reservoir capacity relative to catchment area, while the density of reservoir capacity is more limited in the Wu and Jinsha-Yalong tributaries. The significant decrease in sediment yield at Denyenyan station (No 128) on the Tuo might similarly be attributed to high aggregate reservoir capacity introduced to its catchment area during the period.

In contrast, the gauging stations at Shaping (No 116), Guodukou (No 180) and Wulong (No 207) experienced increasing sediment yields during the period. These

Table 7-3, Water conservancy capacities within the Upper Yangtze catchment (Reservoir capacity data derived from Gu and others, 1987).

Main Tributary	Total Reservoir Capacity (Mm^3)	Percentage of Upper Yangtze Reservoir Capacity	Ratio of reservoir capacity to catchment area ($10^3\ m^3\ km^{-2}$)
Jinsha-Yalong	1802	10.8	3.6
Dadu-Min	1737	10.4	13.1
Tuo	2549	15.2	91.1
Fu	1900	11.4	60.0
Jialing	2951	17.6	29.8
Qu	1548	9.3	52.6
Wu	578	3.5	8.0
Main Channel	3654	21.8	32.6
Total	16719	100.0	16.6

are the principal gauging stations for the Dadu, Qu and Wu, respectively (Figure 7-4). The Dadu catchment spans the transition between mountainous western Sichuan and the intensive agriculture of the Sichuan Basin, an area which has experienced

both deforestation and the extension of arable land. The Qu draining eastern Sichuan has witnessed a dramatic rise in its importance as a sediment source during the period. By the 1980s its specific sediment yields were roughly double the catchment average. The third tributary experiencing increasing sediment yield is the Wu, which mainly flows through Guizhou Province. This area, which is relatively poor, has experienced rapid deforestation and a marked increase in soil erosion during the period.

As noted elsewhere (Gu and Douglas, 1989; Zhuo and Xiang, 1994; Dai and Tan, 1996), the sediment yield measured at Yichang station has not exhibited any significant trend and the long term mean sediment load has formed the basis for most investigations of the prospective Three Gorges Dam sedimentation problem. The implication is that changes in upstream sediment transport dynamics are damped or lagged by the time they reach the main channel. In addition, the construction of the Gezhouba Dam on the main channel of the Yangtze upstream of Yichang in 1981 has had some impact on the sediment yields recorded at Yichang. Comparison between Yichang and Chuntan station (located upstream end of the Gezhouba Reservoir) show that from 1970-1980 specific sediment yield at Yichang was higher than that at Chuntan but the difference reduced after 1981 when the reservoir began to store water (Figure 7-7).

The discussion so far has considered evidence for the impact of land use changes and the construction of reservoirs. Year to year variability related to hydrological conditions is important since this may mask more subtle changes in sediment transfer. As in many studies elsewhere, sediment yield in the Upper Yangtze is highly dependent on annual streamflow (Zhu et al., 1993). In order to consider the effect of water discharge on sediment loads, a similar regression model, $Q = a_2 + b_2T$, is applied to the runoff for those stations experiencing significant trends in sediment yield determined above. The results were also summarised in Table 7-2. None of the correlation coefficients are significant at the 95% level for runoff. Two stations, Huidongqiao (No 14) and Niushishui (No 210), have negative correlation

coefficients for runoff but positive correlation coefficients for sediment yield, indicating stronger sediment yield increase trends. However, most stations have runoff and sediment yield trending in the same direction. The comparative increase in runoff and sediment yield can also be examined by plotting cumulative runoff against cumulative sediment yield as a double mass plot (Walling, 1997). Helsel and Hirsch (1992) suggest a more robust method to remove the effect of runoff variation, by examining trends in the residual of the SY-Q relationship. Runoff data were obtained for all of the stations and logarithmic least-squares linear regression equations between sediment yields and runoff were plotted (Figure 7-8 and Figure 7-9). All the regressions are significant, except for Zagunao (No 85). The residuals from the equations (the differences between the observed and predicted values of sediment yield in logarithmic units) can be used to measure the variations in the sediment yield caused by other factors rather than water discharge. The regression residuals were plotted against time (Figure 7-8 and Figure 7-9) . Significant trends were determined with the Mann-Kendall test (Helsel and Hirsch, 1992). It is found that the level of significance in the trend of residuals fall slightly below the 95% confidence level for five of the stations: Guodukou (No 180), Wulong (No 207) with increasing yields; and Zagunao (No 85), Deyenyan (No 128), Dianwei (No 36) with decreasing yields. The station at Xiaohekuo (No 40) has been omitted from residual analysis because of the limited length of record.

Upper Yangtze sediment yields viewed from the catchment outlet at Yichang alone, do not appear to have changed markedly in recent times. Further investigation from stations within the catchment, however, demonstrates some coincidence between evidence of increasing soil erosion and fluvial sediment transport but also that the Upper Yangtze has a huge capability to store sediment and buffer the effects of increasing sediment supply, particularly due to recent water conservancy projects.

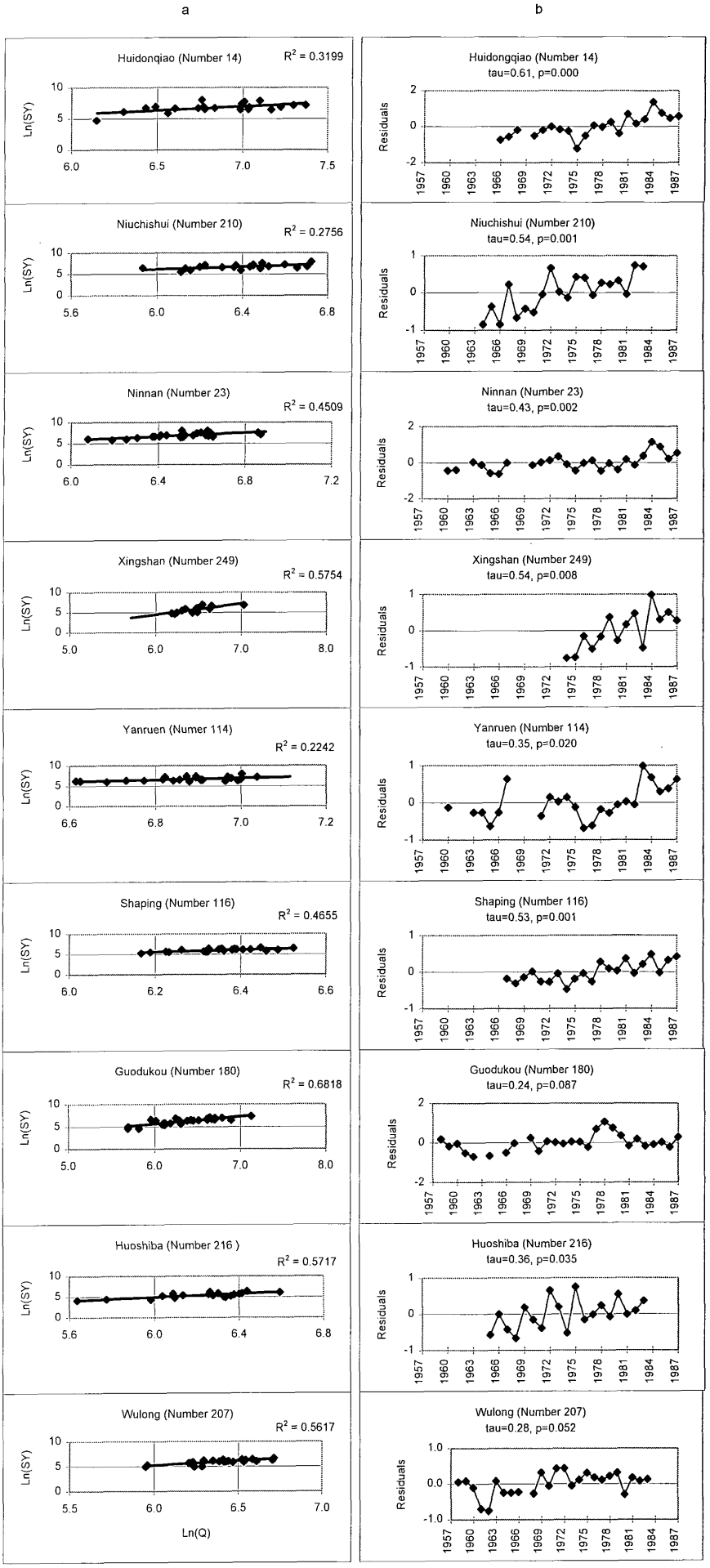

Figure 7-8, Sediment yield-runoff relationships (a), and time series plot of regression residuals for stations experiencing increasing sediment yields

Ln(SY): Log sediment yield (t km-2 yr-1), Ln(Q): Log runoff (mm), tau: Mann-Kendall rank correlation, p: significance level

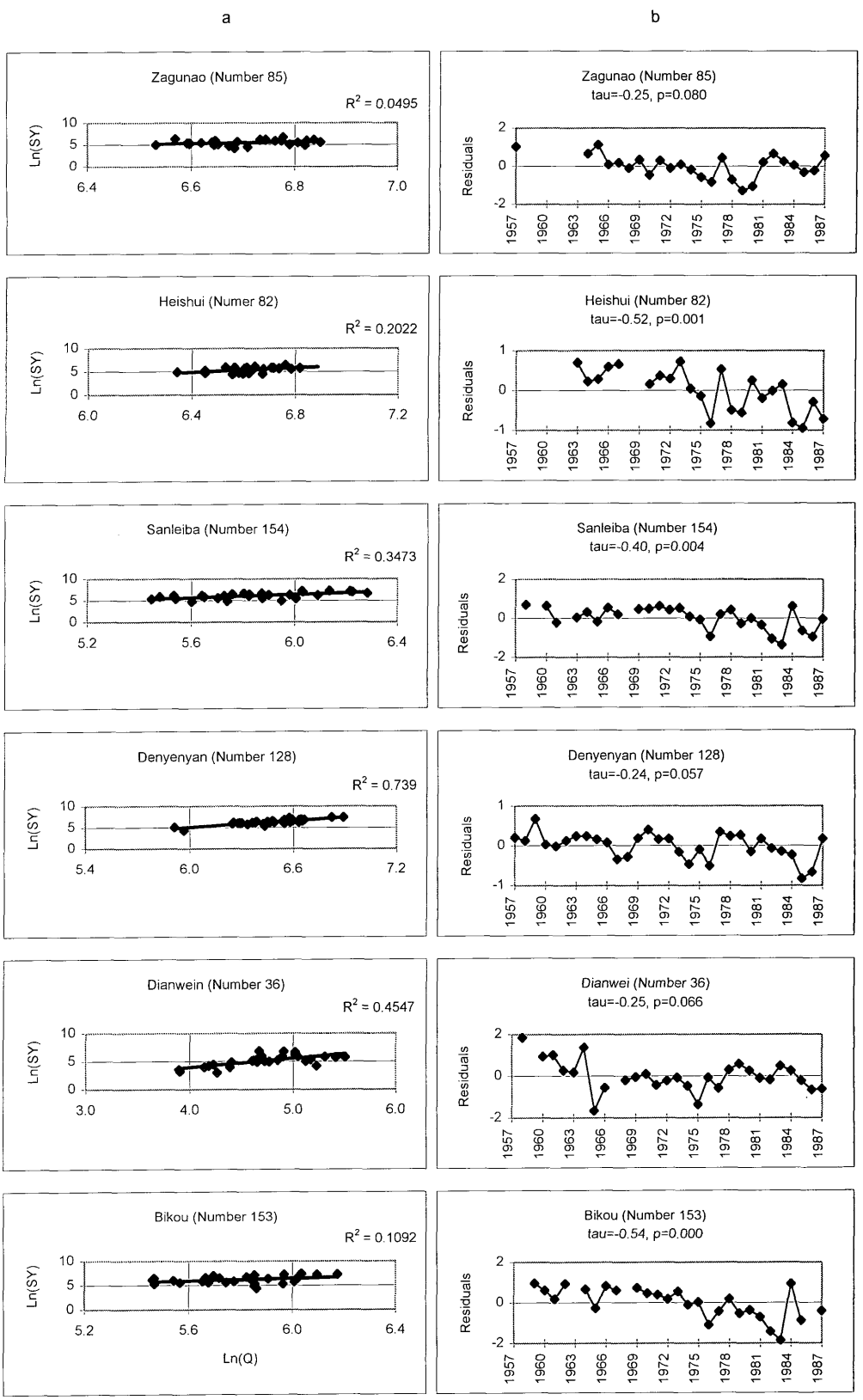

Figure 7-9, Sediment yield-runoff relationships (a), and time series plot of regression residuals for stations experiencing decreasing sediment yields

Ln(SY): Log sediment yield (t km-2 yr-1), Ln(Q): Log runoff (mm), tau: Mann-Kendall rank correlation, p: significa

7.3.2 Changes between the three periods

Having examined evidence for trends throughout the measurement period, the second method aimed to examine temporal variations within the time period. Analysis was confined to the 56 stations which have at least 25 years of data plus the addition of 6 stations from the Wu tributary which is not represented by long-term stations. The t-test for difference of means between two samples has been applied in studies of climatic changes (Sneyers, 1992; Loureiro and Coutinho, 1995) for evaluating the significance of change between defined periods. The sediment yield data were divided into three periods: 1956-67 (P1), 1968-77 (P2) and 1978-87 (P3), and a series of t-tests undertaken. The division gives approximately 10 years for each period, but also coincides with the three historical incidents: the Great Leap Forward, the Cultural Revolution and the Land Responsibility Reform. Again, the majority of stations, including Yichang show no significant changes between each of the periods which suggests that year to year hydrologic variability was more significant than the impact of land use changes (Zhou and Xiang, 1994). However, a number of stations do exhibit significant changes between each of the periods (listed in Figure 7-10). These feature both increases and decreases in different parts of the basin but, as reported elsewhere (Gu and Douglas, 1989) the main change in sediment yields was decreasing from P1 to P2 and increasing from P2 to P3 for most tributaries. The pattern for stations within the Wu tributary was generally reversed.

The areas experiencing significant difference of mean sediment yield are mapped in Figure 7-10. The mapping units are based on incremental catchment areas which deduct nested catchment boundaries unless they also exhibit significant change. From P1 to P2, mean sediment yield significantly increased at 2 stations, Wulong (No 207) and Gongtan (No 208) with a total incremental catchment area of 33,450 km^2 (3.3%) and decreased at 11 stations representing 132,684 km^2 (13.2%) mainly in the Jialing, Tuo and lower Dadu-Min tributaries. These decreases reflect a

Table 7-4, Stations exhibiting significant change between successive time periods.

Station ID	Tributary	Station Name	Catchment Area (km^2)		Time Periods			T-test	
					P1 1956-67	P2 1968-77	P3 1978-87	P2 v P1	P3 v P2
36	Jinsha-Yalong	Dianwei	120	SY ($t\ km^{-2}\ yr^{-1}$):	490	134	186	**	
				Runoff (mm):	134	112	113		
98	Dadu-Min	Gaochang	135378	SY ($t\ km^{-2}\ yr^{-1}$):	457	262	352	**	
				Runoff (mm):	676	603	631		
105	Dadu-Min	Dajin	40484	SY ($t\ km^{-2}\ yr^{-1}$):	100	77	140		*
				Runoff (mm):	415	384	415		
116	Dadu-Min	Shaping	75016	SY ($t\ km^{-2}\ yr^{-1}$):	302	305	546		**
				Runoff (mm):	581	555	595		
128	Tuo	Denyenyan	14484	SY ($t\ km^{-2}\ yr^{-1}$):	848	431	550	**	
				Runoff (mm):	720	600	638		
129	Tuo	Lijiawan	23283	SY ($t\ km^{-2}\ yr^{-1}$):	760	352	480	**	
				Runoff (mm):	603	477	531		
140	Jialing	Liuanyang	19206	SY ($t\ km^{-2}\ yr^{-1}$):	2186	990	1824	**	
				Runoff (mm):	244	136	219		
153	Jialing	Bikou	26086	SY ($t\ km^{-2}\ yr^{-1}$):	1012	531	407	*	
				Runoff (mm):	360	300	343		
156	Jialing	Tinzhikou	61089	SY ($t\ km^{-2}\ yr^{-1}$):	1426	622	1031	**	
				Runoff (mm):	402	274	321		
164	Jialing	Wusheng	79714	SY ($t\ km^{-2}\ yr^{-1}$):	1187	620	951	**	
				Runoff (mm):	398	287	336		
165	Jialing	Beipei	156142	SY ($t\ km^{-2}\ yr^{-1}$):	1130	742	937	*	
				Runoff (mm):	474	384	421		
180	Jialing	Guodukou	31626	SY ($t\ km^{-2}\ yr^{-1}$):	423	586	882		*
				Runoff (mm):	572	575	716		
195	Jialing	Shehong	23574	SY ($t\ km^{-2}\ yr^{-1}$):	931	507	658	*	
				Runoff (mm):	669	518	525		
197	Jialing	Xiaoheba	29420	SY ($t\ km^{-2}\ yr^{-1}$):	839	419	690	**	
				Runoff (mm):	585	459	479		
201	Wu	Wujiangdu	26496	SY ($t\ km^{-2}\ yr^{-1}$):	462	696	208		**
				Runoff (mm):	540	608	570		
206	Wu	Shinan	50791	SY ($t\ km^{-2}\ yr^{-1}$):	364	441	169		**
				Runoff (mm):	497	571	527		
207	Wu	Wulong	83035	SY ($t\ km^{-2}\ yr^{-1}$):	287	490	415	**	
				Runoff (mm):	574	638	600		
208	Wu	Gongtan	58346	SY ($t\ km^{-2}\ yr^{-1}$):	284	449	296	*	*
				Runoff (mm):	559	638	555		
243	Main Channel	Wanxian	974881	SY ($t\ km^{-2}\ yr^{-1}$):	450	445	559		*
				Runoff (mm):	434	416	427		

** = significant at $\alpha = 0.01$ * = significant at $\alpha = 0.05$

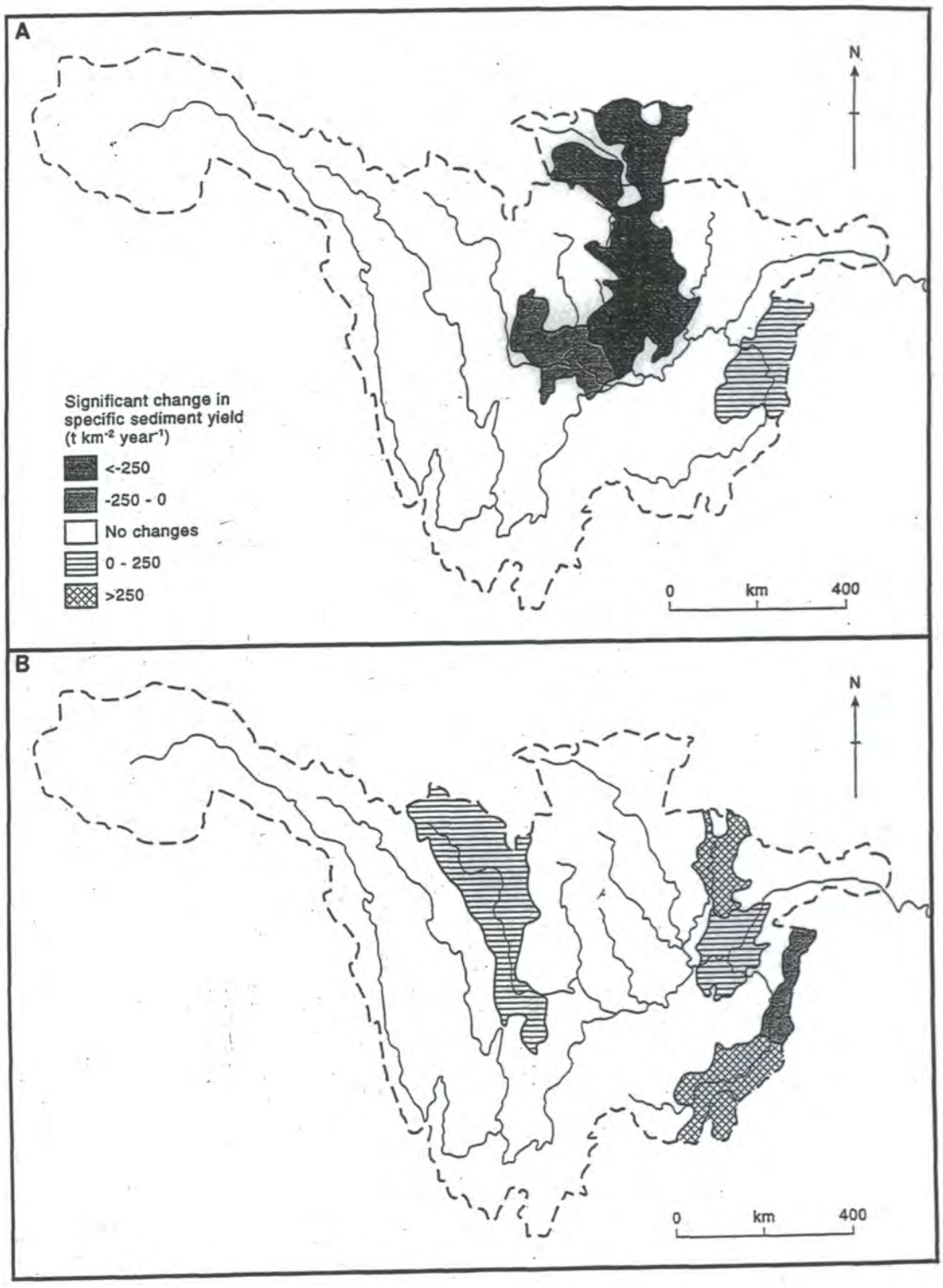

Figure 7-10, Incremental drainage areas undergoing significant change between (a) 1956-67 and 1968-77; (b) 1968-77 and 1978-87.

combination of massive deforestation in the first period and the establishment of water conservancy projects in second period. The decrease in yield in the Dadu-Min may be due to the trapping of sediment in the Gongzhui reservoir (see Figure 7-7). Runoff data for those stations were checked and indicated that the stations did not experience a significant change in runoff coincidental to the changes in sediment yield, except for Dianwei (No 36) from P2 to P3 (Figure 7-10).

From P2 to P3, mean sediment yield increased for 4 stations (116,363 km^2, 11.6%) and decreased for 3 stations (39,146 km^2, 3.9%). Sediment yields increased in the Dadu and upper Qu, neither of which recorded changes between the earlier periods. It is most likely that this reflects deforestation for timber supply and expansion of new arable lands triggered by Land Responsibility Reform. The affected areas are located at the transition between predominantly agricultural and forestry land uses.

7.4 SUMMARY AND CONCLUSION

The sediment yield dataset in the basin provide an opportunity to examine a few problems of most concern to geomorphologists and policy-makers. The chapter concerns two problems of spatial variability and temporal changes of sediment yields throughout the Upper Yangtze.

The main difficulty in analysing sediment yield is the basin size-dependency of the data. The study employs two standardisation methods to examine the sediment yield for the larger tributaries. None of these stations have overlapping catchment areas. The Jialing has a substantial relative contribution to the sediment load throughout the time period but its importance as a source area declined during the 1970s. Fu and Qu rivers (which are tributaries of the greater Jialing system) also have substantial contribution but the latter has become an increasingly important source during the measurement period. These three rivers drain the agriculturally productive lands of the Sichuan basin. By contrast the tributaries of the upper Jinsha and Yalong have substantially smaller contributions relative to their drainage area. Wu became a more important source after the 1970s. The spatial variations of sediment yield were also

examined using the data from the 187 stations with 5 years or longer of measurement series. Due to the diversity of influencing factors such as elevation, precipitation and population density, the spatial variability of sediment yields are quite obvious. The distribution indicates the largest relative contribution from the Sichuan basin and the lower Jinsha tributary, while sediment yields from the west plateau and Guizhou are lower.

Concerning temporal changes the study has demonstrated that sediment loads exported from large catchments mask a considerable amount of variability in the trajectories of soil erosion and sediment transport within different parts of the catchment. Oscillation around a non-trending mean value is usually attributed to hydrological variability but further investigation can demonstrate underlying changes in the sediment yield-runoff relationship. Examination of sediment yield data from stations within the Upper Yangtze collected between 1956 and 1987 reveal some patterns of temporal change. Sediment yield had mainly increased for the Dadu, Qu and Wu tributaries and decreased in the Tuo and upper Jialing. Most of the observed decreases in sediment yield can be related to the construction of large reservoir schemes interrupting the downstream conveyance of sediment.

Comparison of sediment yield and runoff data suggest that detectable changes in sediment delivery occurring in the Upper Yangtze reflect an increasing supply induced by human activities over the last 30 years. Comparison of three time periods framed by major shifts in the nature of resource exploitation (the Great Leap Forward, the Cultural Revolution and the Land Responsibility Reform) show changing patterns of sediment yield which are most likely related to the changing geographical expression of deforestation and of water conservancy project construction. Linking soil erosion on slopes to sediment transport in the fluvial system is hampered by the limited amount of quantitative data on soil erosion rates. Many geomorphologic systems are controlled by threshold conditions such that adjustment to controlling variables is likely to be non-linear. Although the patterns of changing sediment yield within the Upper Yangtze can be matched to known histories of human disturbance, the possibility that sediment yields are responding to

subtle changes in climate cannot be dismissed. However, suggestions that sediment yield patterns in China essentially reflect climatic controls (Xu, 1994) clearly do not hold within the upper Yangtze basin. Sediment yield variation modelling of the Upper Yangtze within a GIS framework indicates the importance of topographic variables, particularly slope and altitude in explaining sediment yield variability. The latter may be partly acting as a surrogate for human activity and precipitation which are both inversely related to altitude in the Upper Yangtze.

Detailed examination of spatial and temporal yield variation may have implications for policy makers concerned with the management of potential sedimentation. Discussion of the TGP reservoir sedimentation issue has largely focused around river regulation procedures and the design of sluices to maximise the discharge of sediment-laden waters (Qian et al, 1993). The lack of evidence for an increasing sediment yield at Yichang has justified the use of the long-term mean load and limited attention to long term changes in sediment supply to the Reservoir. The evidence for increasing sediment supply in the catchment buffered by increasing storage in intermediate reservoirs raises further concerns. As this reservoir storage begins to fill, the trap efficiency of individual reservoirs will decline and the conveyance of sediment downstream will increase. The long-term impact of the exhaustion of artificial reservoir capacity and the remobilisation of sediments from storage could be significant. Analysis of time series for individual stations suggests that 7.9% of the Upper Yangtze catchment had increasing sediment yields over the measurement period while 2.8% experienced decreasing yields. The variable response of large catchments to phases of human disturbance and river engineering provides many challenges to basin management, to which the detailed analysis of intra-catchment sediment yields may contribute.

8. SEDIMENT YIELD IN THE UPPER YANGTZE: SPATIAL VARIABILITY MODELLING AND MAPPING

8.1 INTRODUCTION

There have been a number of attempts to relate global or regional sediment yields to controlling factors. Langbein and Schumm (1958) produced a theoretical model of sediment yield in relation to effective precipitation, reaching a maximum in semi-arid environments (effective precipitation 300 mm) and declining as vegetation cover protects the land surface. As the availability of gauging station data has increased the complex relationship between sediment yield and precipitation (or runoff) has been noted (e.g. Wilson, 1972; Walling and Webb, 1983), not least because of the impact of human activity in disturbing natural vegetation cover and promoting soil erosion. The role of topography has also been highlighted (Milliman and Syvitski, 1992; Summerfield and Hulton, 1994) and the importance of small mountainous catchments identified as a major contributor to global continental sediment export. However, prediction of sediment yields is complicated by the interaction between controlling variables, the influence of human interference in the hydrological system and by scale effects of catchment size. In most areas the proportion of sediment mobilised on catchment slopes which is exported to the catchment outlet decreases as catchment size increases (Walling, 1983). This sediment delivery ratio makes direct comparison of specific sediment yields (load per unit time per unit area) difficult. Furthermore, human activity may serve to increase sediment mobilisation on slopes through soil erosion, but decrease sediment delivery ratios through the impoundment of sediments behind check dams and within reservoirs. The legacy of past sediment transport dynamics is also important. In the upper Mississippi sediment yields have remained high despite successful soil conservation, as material originally eroded in

the nineteenth century has been remobilised from valley floors (Trimble, 1981). A similar pattern has been identified in the Piedmont (Phillips, 1993).

A number of studies have investigated sediment yield data from the Upper Yangtze (Gu et al, 1987; Qian et al, 1993; Zhou and Xiang, 1994) and have concentrated on examining temporal and spatial patterns of sediment transfer. There has been little attempt to systematically examine the relationship between sediment yield and its controlling variables, presumably because of the difficulty of obtaining sufficiently detailed information over such a large catchment. However, the advent of global environmental datasets which offer detailed description of the hydroclimatic, biological, and geomorphologic characteristics of the earth (Ludwig and Probst, 1996) offer the potential for integration with sediment yield data. The resolution of global datasets has tended to restrict previous analyses to the global scale where individual catchments are represented by single sediment yield variables (Summerfield and Hulton, 1994; Ludwig and Probst, 1996). The application of such an approach to a large basin (>1 million km^2) containing a set of nested gauging stations appears to have had limited attention. This chapter is designed for sediment yield spatial variability analysis with emphasis on the variability modelling. The methods of sediment yield mapping will also be discussed. Therefore the chapter consists of the two main components, sediment yield variability modelling and mapping.

8.2 SEDIMENT YIELD VARIABILITY AND CATCHMENT VARIABLES

The marked spatial variability of sediment yield discussed in the previous chapter using standardisation procedures was argued to be due to a combination of climatic, topographic, lithological, soil and land use conditions. Some of those variables had been introduced in Chapter 2. This section is focused on elevation, slope, precipitation and population density. The data sources and extraction methods have been introduced in Chapter 4.

The topographical map (Figure 8-1) is produced from the Asian 30 arcsecond DEM based on five classes, 0-200, 200-500, 500-1000, 1000-3000 and >3000 m. It emphasises the large area of high elevation on the Qinghai-Tibet plateau and the very deep and narrow valleys draining it. A large number of the sub-catchments in the sediment yield dataset contain land above 3000 m in contrast to previous studies of global or regional controls on sediment yield which are skewed towards lower elevations (Milliman and Syvitski, 1992; Probst and Amiotte-Suchet, 1992; Summerfield and Hulton, 1994).

The slope map (Figure 8-2) indicates that the areas with steep slopes (>10 degrees) are mainly distributed on the western margins of the Sichuan Basin and along the incised valleys of the Jinsha, Yalong and Dadu tributaries. There are two relatively flat areas, the Chengdu Plain and the Qinghai-Tibet plateau, where the dominant mean slope angle is less than 1 degree. However, it should be noted that many flat areas (recorded as zero degrees) are generated by the GIS due to the inherent problems associated with the resolution of the DEM. This problem must be taken into account when the slope is applied in sediment yield modelling.

The precipitation map (Figure 8-3) also shows dramatic contrast between the arid / semi-arid northern Qinghai-Tibet Plateau and the eastern part of the basin where precipitation exceeds 1000 mm. The Qinghai-Tibet plateau has a significant influence on atmospheric circulation not only regionally but perhaps over the entire Northern Hemisphere (Ruddiman et al., 1989). The plateau constrains the penetration of the monsoon, resulting in a complex pattern of precipitation within the Upper Yangtze catchment.

Population densities (Figure 8-4) are generally inversely related to elevation with values less than 10 people km^{-2} in the Qinghai-Tibet Plateau to >500 people km^{-2} in Sichuan Basin, one of the highest population density areas in China. The total population of Sichuan province exceeds 0.1 billion. The Jialing, Tuo and Wu flow through the higher population density areas.

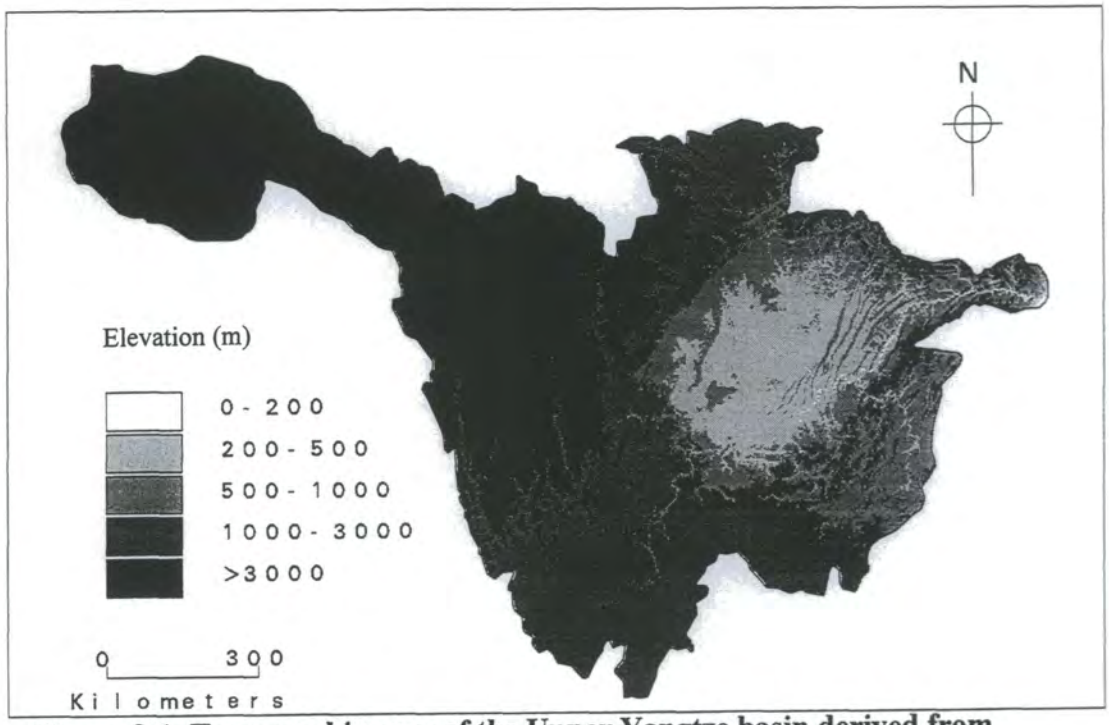

Figure 8-1, Topographic map of the Upper Yangtze basin derived from 30arcsecond

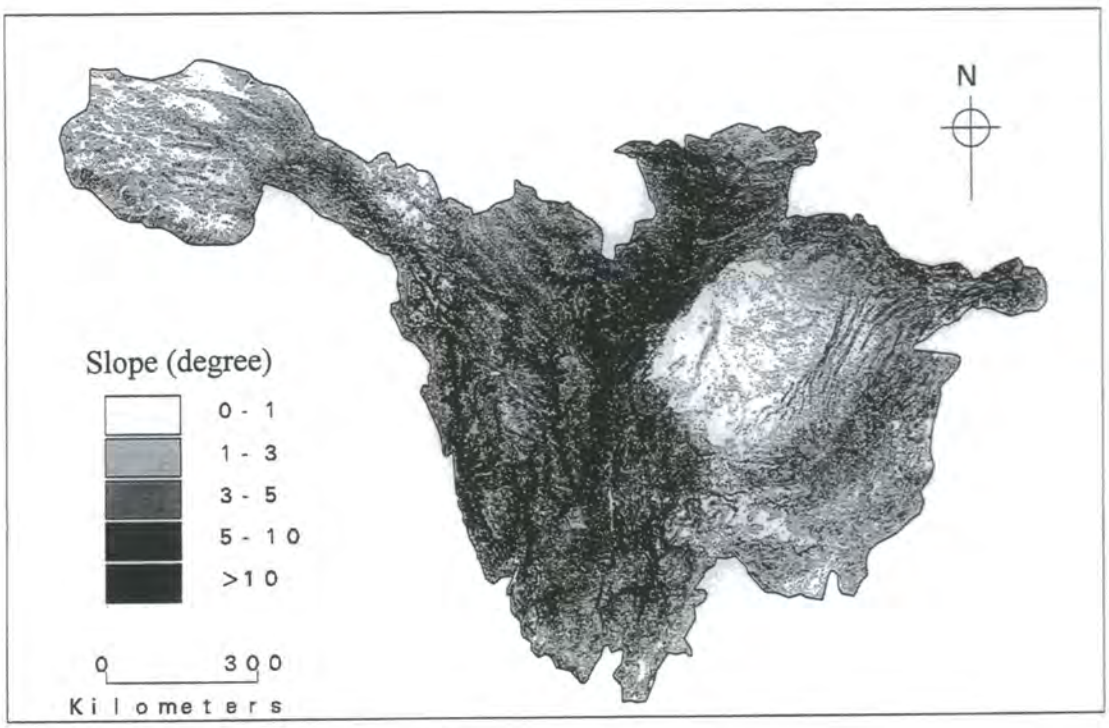

Figure 8-2, Slope (degrees) of the Upper Yangtze basin derived from 30arcsecond

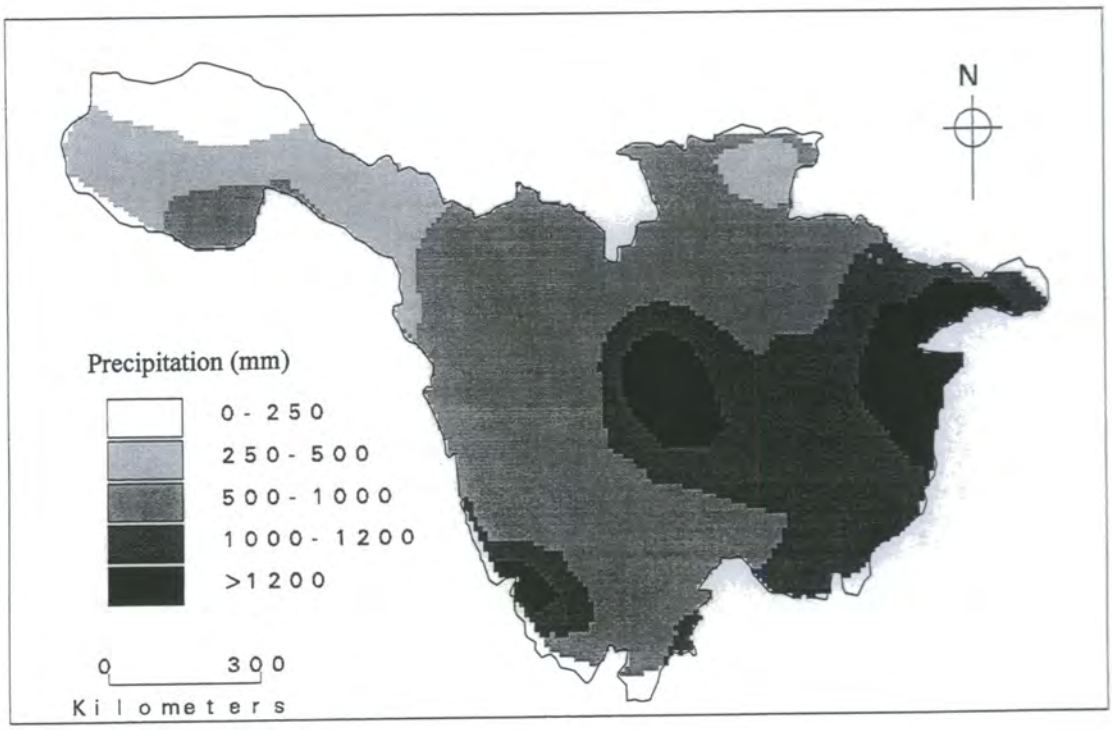

Figure 8-3, Precipitation map of the Upper Yangtze basin obtained from GED

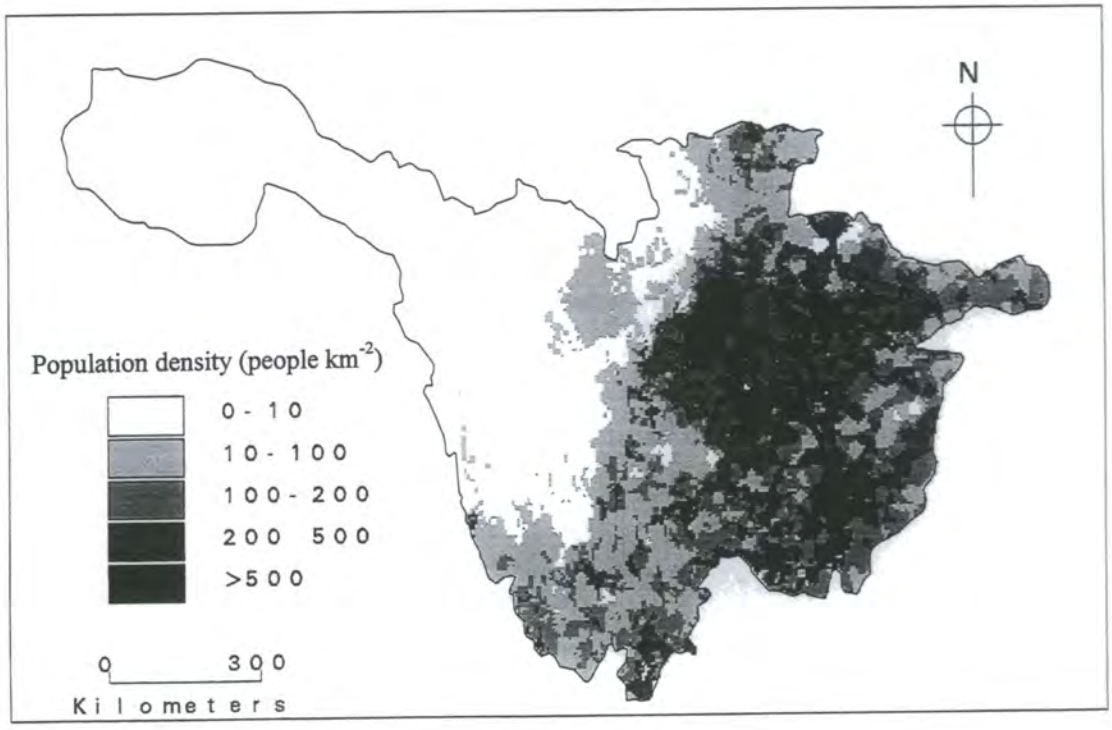

Figure 8-4, Population density of the Upper Yangtze basin

8.3 MODELLING SPATIAL VARIABILITY

8.3.1 Interrelationships between catchment variables

The GIS framework enables values for both individual cells (pixels) and defined sub-catchments to be calculated efficiently. Examination of the interrelationships between these catchment variables precedes analysis of their relationship with sediment yield. As many of the distributions of catchment variables do not closely approximate to normal distributions and because the interaction between variables may not be linear, parametric statistical techniques are not considered appropriate for examining relationships between variables. The spatial variability modelling uses the 62 stations with longer measurement series (Table 4-3 in Chapter 4). Results from the non-parametric Spearman's rank correlation matrix are presented in Table 8-1. As expected, mean elevation is significantly correlated with many variables. Mean slope increases with mean elevation, whereas mean population density and

Table 8-1, Spearman's correlation matrix of catchment variables (n=62)

* Significant at 95% level (critical value=0.255), ** Significant at 99% level (critical value=0.335)

	ME	BR	MS	PD	PP	RO	SY
ME	1						
BR	0.51**	1					
MS	0.63**	0.42**	1				
PD	-0.91**	-0.36**	-0.70**	1			
PP	-0.46**	-0.43**	-0.17	0.47**	1		
RO	-0.21	-0.14	-0.33**	0.14	0.67**	1	
SY	-0.31*	-0.05	0.21	0.23	0.11	0.39**	1

Note: ME: mean elevation (m), BR: basin relief (m), MS: mean slope (degree), PD: population density (number km^{-2}), PP: precipitation (mm yr^{-1}), RO: runoff (mm yr^{-1}), SY: sediment yield (t km^{-2} yr^{-1}).

precipitation decrease with mean elevation. However, the relationships are more complex at pixel level (Figure 8-5). The headwaters of Jinsha and Yalong on the Qinghai-Tibet plateau are areas of gentle relief such that mean slope generally increases with elevation up to 2500 m but then decreases. Population density sharply decreases with elevation above 1000 m elevation. Elevation and precipitation are inversely related but with a high degree of scatter in lower elevation areas.

8.3.2 Relationships between sediment yield and catchment variables

The high degree of spatial variability in both sediment yields and catchment characteristics causes difficulty for attempts to model controlling relationships using the whole data set. Spearman's rank correlation coefficients for the 62 catchment indicate that specific sediment yields are significantly correlated with only mean elevation and runoff (Table 8-1). Elevation itself has no physical control on soil erosion or sediment transport and is acting as a surrogate for aridity and human impact. Previous studies of sediment yields have attempted to reduce noise by grouping data on reasonable indices. In global scale studies, Milliman and Syvitski (1992) grouped sediment yield data by maximum elevation, while Ludwig and Probst (1996) and Jansson (1988) used climate type. The present study groups the 62 basins under the three scenarios, tributary, basin size and maximum elevation.

8.3.2.1 Basin grouping based on tributary

Noting the importance of intra-basin management, analysis is first based on tributary groupings: Jinsha-Yalong, Dadu-Min, Jialing (including Tuo) and Wu. As described above, a large proportion of the catchment areas within the Jinsha-Yalong and Dadu-Min tributaries are located in areas with elevation >3000 m and low population density, while the Jialing and Wu, particularly their lower branches, are located in areas of lower elevation and high population density. The group of stations for the Wu (which includes Shizhu) contains seven data points and the analysis must therefore be treated with caution.

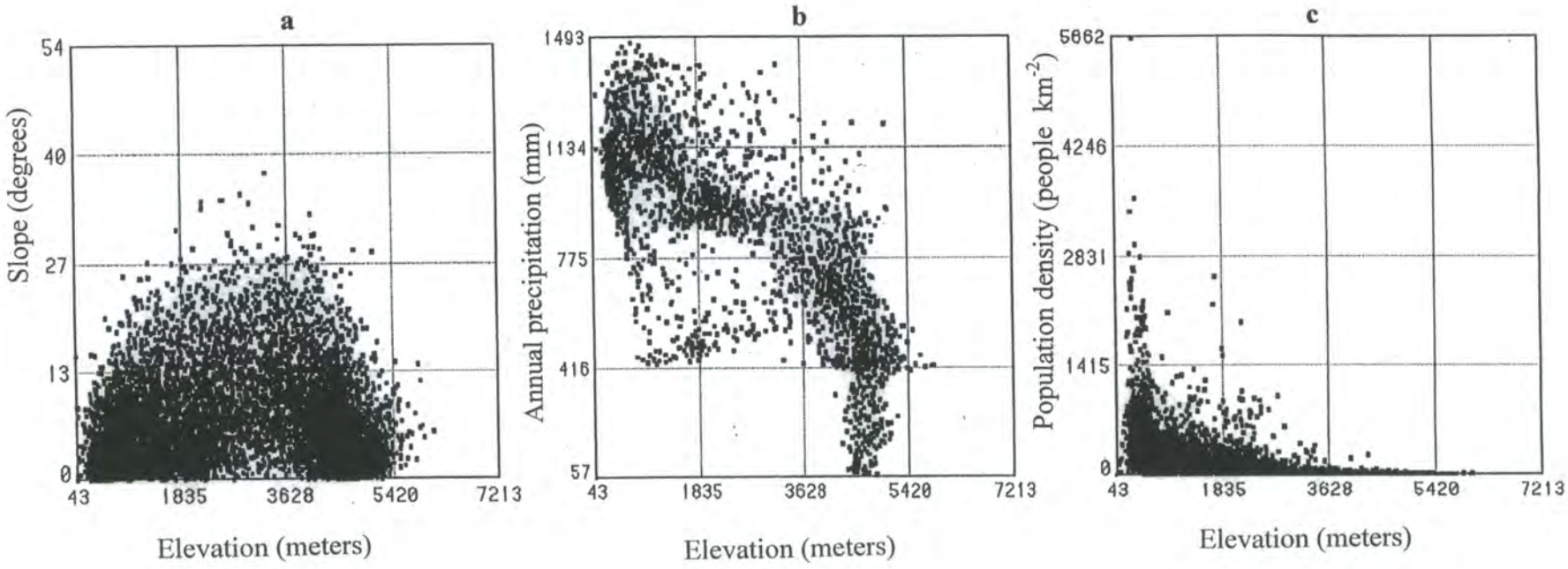

Figure 8-5, Plots of (a) slope, (b) annual precipitation, (c) population density against elevation at pixel level

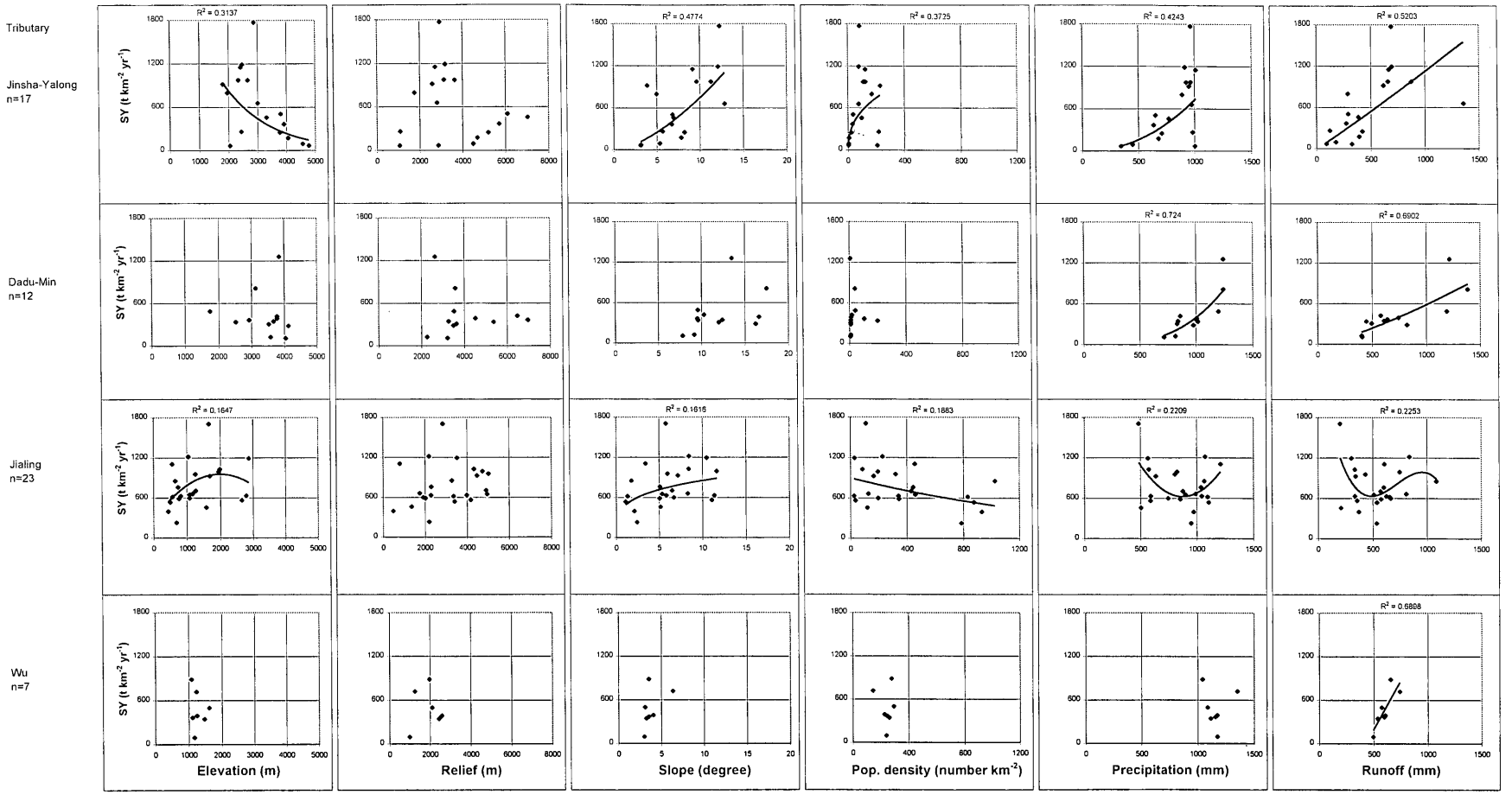

Figure 8-6, Sediment yield against catchment variables: tributary grouping

Specific sediment yield is plotted against all the variables (Figure 8-6). Generally, much scatter remains despite the tributary groupings. Previous studies have used various strategies to reduce the impact of scatter. Milliman and Syvitski (1992) removed outliers defined by degrees of standard deviation and recalculated regression equations. Summerfield and Hulton (1994) argued that this procedure masked the real degree of scatter and proposed logarithmic transformation before calculating Pearsonian correlation coefficients. Instead of transforming the variables, curve fitting techniques are applied to the data, with trendlines drawn on Figure 8-5 where relationships are significant at $\alpha = 0.05$ level. A number of the relationships between sediment yield and catchment variables are adequately described by a second or third order polynomial equation indicating the apparent presence of turning points or threshold conditions in the relationship.

There are marked contrasts in the range of significant correlation within each tributary grouping and in the nature of those relationships. The Jinsha-Yalong tributary, has significant correlation with all variables except for basin relief. The decline of sediment yield with elevation may at first appear surprising but represents the transition from the high altitude semi-arid Qinghai-Tibet Plateau to the deeply incised sub-humid valleys downstream. Sediment yields show a consistent increase with runoff and precipitation. The Dadu-Min and the Wu groups have fewer significant correlations - precipitation and runoff in the former and only runoff in the latter. The Jialing has the same range of significant correlation as the Jinsha-Yalong but there is some difference in the nature of the relationships. Sediment yield increase with elevation up to about 2000 m. Perhaps surprisingly, population density has an inverse relationship with sediment yields, although a greater impact on soil erosion might be expected. Possible explanations are that the highest levels of population density within the catchment area are within the flat Chengdu Plain and that the more densely populated areas tend to have a higher concentration of water conservancy structures which serve to trap sediment in storage. Polynomial relationships with precipitation and runoff are interesting. The apparent peak in sediment yield at an annual precipitation of 500 mm (or runoff around 250 mm) is similar to the classic Langbein and Schumm model while the increase beyond 1000

mm precipitation (or 700 mm runoff) has some resonance with the global relationship described by Wilson (1973) and Walling and Webb (1983). However, this pattern is not repeated in the other tributaries. It should also be noted that some particularly high levels of sediment yield in the upper Jialing are associated with neotectonics and loess soil. For example, Liuanyang catchment (No 140) recorded a 30-year average annual specific sediment yield of about 1700 t km^{-2} yr^{-1} with a maximum exceeding 6600 t km^{-2} yr^{-1} (see Table 4-3 in Chapter 4).

8.3.2.2 Basin grouping based on its size

Analysis grouped by tributary has some utility for recognising the variation in controlling factors between different geographical locations and providing guidance for the implementation of conservancy operations, but relationships are confused by scale effects. Sediment delivery characteristics can be summarised by the exponent of the specific sediment yield-catchment area relationship, although recent discussion has questioned the validity of regression between variables which have catchment area as a common term (De Boer and Crosby, 1996). A compromise is to group the catchments into four categorises based on catchment size: <1000 (6 catchments), 1000-10 000 (20 catchments), 10 000-100 000 (24 catchments) and >100 000 km^2 (12 catchments). It is found that the relationships between sediment yield and catchment variables improve as catchment size increases (Figure 8-7). There are no significant correlations in categories <10 000 km^2 groups. Better correlations are expected at larger catchment sizes as variations due to particular land use, soil or geology are minimised. The >100 000 km^2 group has strong positive relationships with relief, population density and precipitation with a decline in sediment yields with elevation. Once again there are curious contrasts in the relationships with precipitation and runoff within the different groupings. A distinct minimum turning point at around 500 mm runoff is depicted by the polynomial trendline for the 10 000-100 000 km^2 catchments. There is also a general decline in sediment yields with precipitation within this group in contrast to the relationship in larger catchments. With the small sample sizes involved the influence of outliers on the relationships may be significant.

8.3.2.3 Basin grouping based on maximum elevation

The importance of elevation as a control on other catchment characteristics has been noted earlier. Milliman and Syvitski (1992) used maximum elevation grouping to demonstrate the relative importance of small mountainous basins in supplying a large proportion of terrestrial sediment to the world's oceans. The four classes used are: <2500 (8 catchments), 2500-3500 (13 catchments), 3500-5000 (18 catchments) and >5000 m (23 catchments). The large number of catchments with maximum elevations greater than 5000m is in stark contrast to previous studies (Milliman and Syvitski, 1992; Probst and Amiotte-Suchet, 1992; Summerfield and Hulton, 1994), where the distribution is heavily skewed towards lower elevations. Relationships between sediment yields and catchment variables are highly scattered within lower elevation groupings (Figure 8-8). Sediment yields in lower elevation areas are likely to be influenced by agricultural activity which is not accounted for in the catchment variables selected. Stronger relationships are evident in the >5000 m grouping, with the familiar inverse relationship between sediment yield and mean elevation. Positive relationships are found with population density, precipitation and runoff.

8.3.3 Discriminating controls on regional sediment yields

Many attempts to explain sediment yields in terms of a number of controlling factors have encountered high degrees of scatter. The approach adopted in the present study to group catchments by tributary, size and maximum elevation has provided a means of identifying evidence of controlling factors on sediment yields and indicated that the nature of relationships can be quite varied. Reasons for the diversity in relationships between sediment yields and catchment variables within the Upper Yangtze are summarised below.

Grouping by tributary provided a number of significant relationships for two tributary groups. Multiple regression using the six catchment variables indicates that 87% and 95% of the variance in sediment yields can be explained in the Jinsha-Yalong and Dadu-Min, respectively. By contrast, only 33% of the variance is

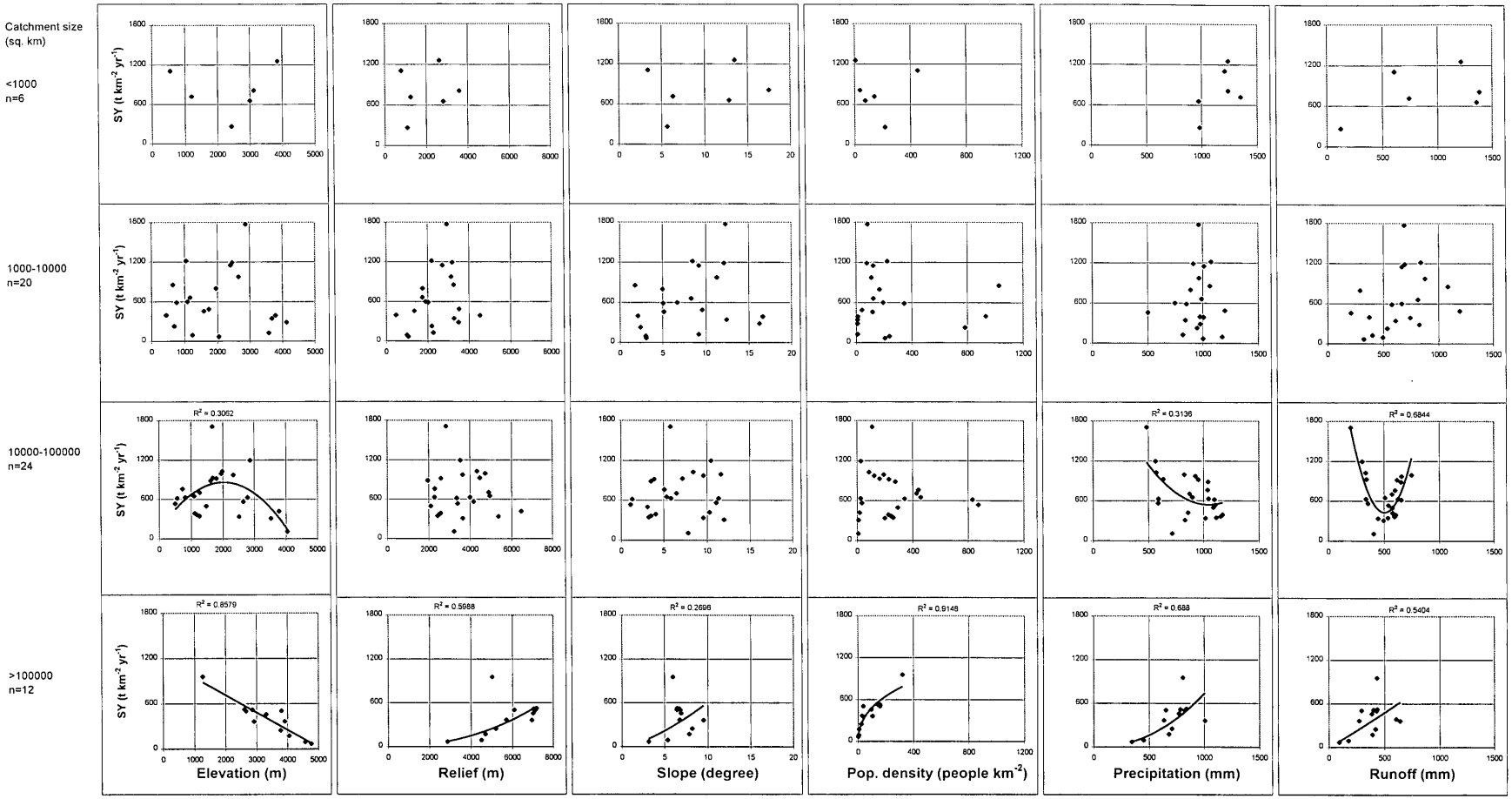

Figure 8-7, Sediment yield against catchment variables: catchment size grouping

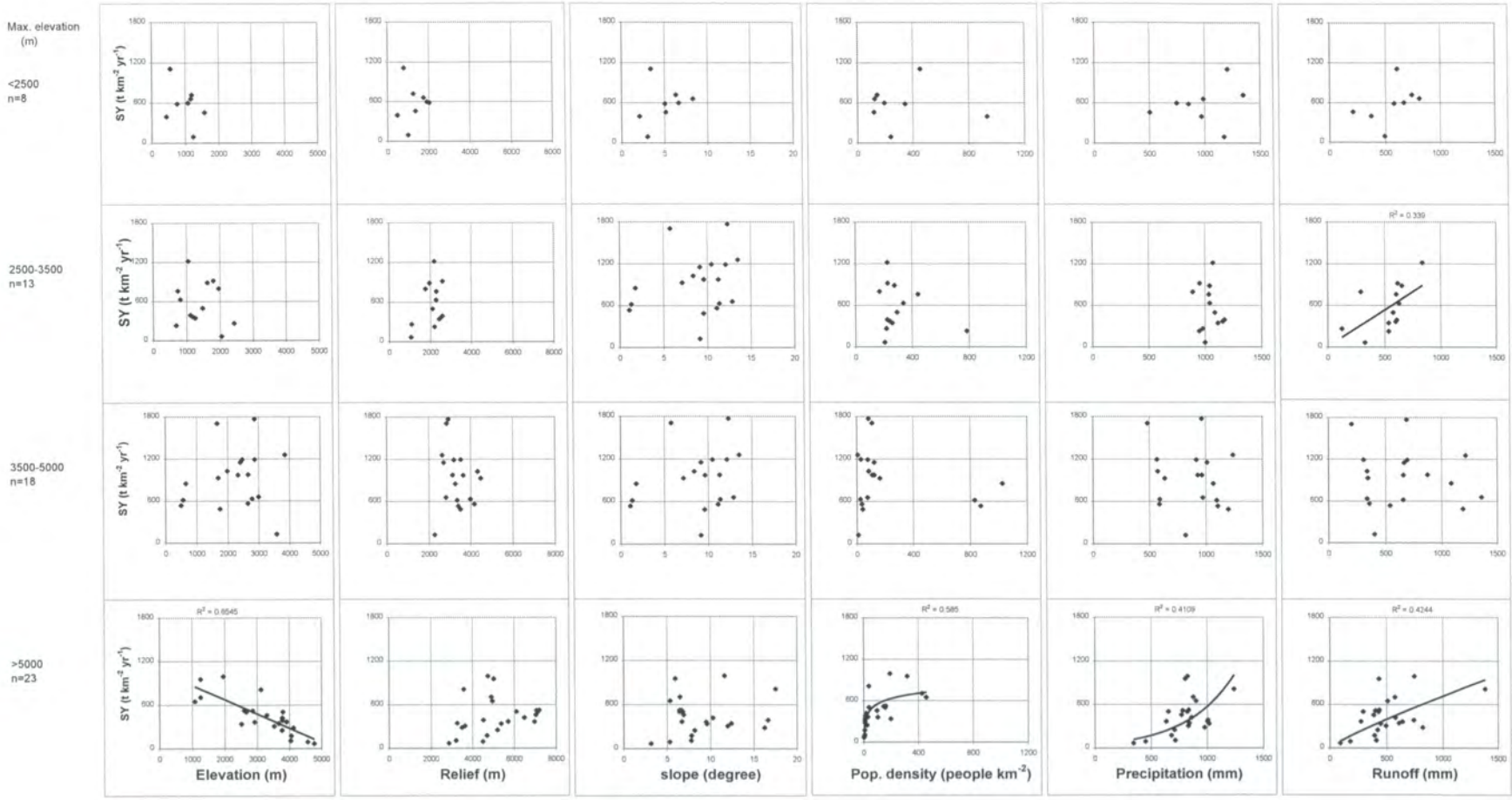

Figure 8-8, Sediment yield against catchment variables: maximum elevation grouping

explained in the Jialing. The contrast reflects the larger human impact in the Jialing. The six selected catchment variables reflect topographic and climatic variables which can be extracted from global datasets. Population density is the only variable which relates to human impact. Clearly the inclusion of land use, soils and geological information would greatly assist attempts to model regional sediment yield. Unfortunately, the resolution of digital information on these variable within the public domain is not yet sufficient for the extraction of catchment variables. Because the impact of land use, geology and soil is relatively localised, the analysis of larger scale catchments generates clearer results than smaller catchments. The strong inverse relationship between sediment yields and mean elevation in the >100 000 km^2 category reflects that elevation is acting as a surrogate for low precipitation, runoff and human impact. The nature of the relationship between elevation and sediment yields contravenes all previous studies of regional or global sediment yields (e.g. Milliman and Syvitski, 1992) but can be attributed to the particular geography of the Upper Yangtze. The high elevation portions of the catchment are areas of gentle relative relief, limited precipitation and low human activity. Consequently, fluvial erosion in most of Tibet is limited and does not export much material beyond the plateau (Fielding et al., 1994). In comparison, severe soil erosion on agricultural land, particularly around the margin of the Sichuan Basin means that sediment yields are relatively high at elevations below 5000 m.

Population density can be used as an indicator of the extent of human impact within the Upper Yangtze. Its relationship with sediment yield is positive in catchments with higher maximum elevation and in larger catchments, but is otherwise scattered. In the Jialing tributary there is a negative relationship between sediment yield and population density. The variation deserves further consideration. Firstly it should be noted that the population density data are derived from the 1992 census, while the sediment yield data are averages from the period 1956-1987. During the last four decades there have been significant changes in both population numbers and their distribution and impact within the Upper Yangtze, such that the statistical relations must be treated with caution. Secondly, population density is a crude measure of

human impact. The largest concentrations of population are in the relatively flat areas of the Sichuan Basin and Chengdu plain, whereas the most severe soil erosion occurs on the sloping land around the margins of these locations. Thirdly, much of the increase in soil erosion reported from central China during the measurement period is associated with deforestation and/or expansion of agricultural land. By its nature this tends to be in areas adjacent to high population densities. Further work is required to model the temporal impact of disturbance on sediment yields. Fourthly, the measurement period has witnessed a dramatic phase of water conservancy construction. Much of the sediment derived from soil erosion in the higher population areas of the Upper Yangtze may be trapped in temporary storage in ditches, ponds and reservoirs. Indeed, storage in small reservoirs may account for the discrepancy between estimates of increasing soil erosion in the Upper Yangtze and the lack of an upward trend in sediment yield at Yichang (see Chapter 7).

In general, sediment yield increases with precipitation and runoff in most groupings but displays polynomial relationships in the Jialing tributary and in catchments in the 10,000-100,000 km^2 size category. The variation reaffirms the contention that "no simple relationship exists" (Walling and Webb, 1983). A general increase with precipitation is consistent with other regional and global analysis (Probst and Amiotte-Suchet, 1992; Ludwig and Probst, 1996). Xu (1994), using data from 700 rivers in China, suggested sediment yield reaches a maximum around 400 mm runoff. The implication is that sediment yields in China fit the Langbein and Schumm (1958) model and are therefore primarily a natural phenomenon. There is little support for this in the Upper Yangtze data set. The multiple regression results suggest that much of the sediment yield variability in the west of the basin can be attributed to natural phenomena, but topographic and climatic variables afford relatively little explanation of sediment yields in the agricultural eastern portion of the basin.

The increasing availability and improving resolution of global environmental databases offers the prospect of examining the relationships between fluvial sediment yield and various catchment properties within the framework of GIS. To date, GIS-

based studies have tended to focus on global scale variation or comparison between different catchments in a regional context. The analysis of variation *within* large catchments offers considerable potential for the investigation and management of sediment-related problems. In the case of the Upper Yangtze catchment where the attention of environmentalists has been drawn to the Three Gorges Project, the integration of sediment yield records and environmental databases within GIS not only provides a basis for the empirical investigation of controls on the patterns of sediment yield but provides a platform for predictive modelling. The procedures for dealing with hierarchical data from a series of nested catchments raises many issues. Specific sediment yields are partly a function of catchment size and may require standardisation to a particular catchment size.

8.4 SEDIMENT YIELD MAPPING

The methods of standardisation employed in last chapter can clearly outline the general patterns of spatial variations and identify the relative importance of sediment sources. More importantly, compared with conventional methods, the standardisation methods employed can minimise the bias introduced by the size-dependant sediment yield data. However, it is difficult to answer the questions such as how many areas there are for a certain sediment yield class. Therefore, the emphasis in the section is addressed to the methods of sediment yield mapping, since the general pictures of spatial variations can be clearly drawn from a sediment yield map. A number of studies have attempted to map sediment yield at global (Walling and Webb, 1983; Lvovich et al., 1991) or regional scales (Neil and Mazari, 1993; Rooseboom and Lotriet, 1992; Gu and Douglas, 1989). However there are two issues concerning the use of sediment yield maps in the evaluation of an erosion problem. First, there is the difficulty of directly relating erosion on land surfaces to sediment loads in channels because of the intervening processes of sediment delivery. The 'sediment delivery problem' has been widely discussed (e.g. Walling, 1983). Second, the suitability of mapping methods has not been fully addressed by previous studies, particularly where the data set includes hierarchical relationships. In the case of the

Upper Yangtze there are several nested hydrographic stations. The aim of this section is to examine different methods of mapping sediment yield using GIS in the Upper Yangtze. On the basis of the maps produced, it is possible to discuss the whole picture of spatial patterns of soil erosion and sediment transport.

8.4.1 Specific sediment yield calibration

The river catchment is a lumped system. In other words, catchment properties, such as sediment yield are reported as spatially averaged values (Maidment, 1993). When greater detail is desired or required, a linked-lumped system is developed in which the catchment is divided into a series of sub-catchments which are each represented as lumped systems connected by stream links as indicated in Figure 8-9. The solid line represents the catchment area controlled by gauging station 1, which also contains three other stations. The shaded area represents the sub-catchment area controlled by gauging station 2 with the lighter shading indicating the incremental area added between stations. The linked-lumped system used in this schematic diagram is widely employed in surface water hydrology (Maidment, 1993). The 255 hydrological stations and their contributing sub-catchments are highly hierarchical in the Upper Yangtze.

An agreed procedure for mapping and interpreting sediment yield data from a series of overlapping catchments is not apparent in the current literature. In addition, analysis is complicated by the basin size- and time-dependency of the data. The effect of sediment delivery ratios means that it is difficult to make comparisons of specific sediment yields from sub-catchments of varying size without some allowance for calibration. Similarly, comparison of sediment yield data should be across coincidental time scales because of the year to year hydrological variability. Because of the patchy operation of some of the hydrographic stations, the analysis here again concentrates on 62 stations with longer measurements. This is not a problem for methodology discussion but it is better to use as many stations as possible for overall mapping.

As specific sediment yield tends to decline with catchment area, a calibration between yield and catchment area, the standardisation must be applied as discussed above. While the two standardisation methods outlined in above section (section 7.3) are suitable for a relative sediment yield comparison, a new correction method must be found for mapping purpose. The sediment yield and basin area relationship for the 62 stations is built as:

$$SY = 1141.4 - 53.4 \ln(DA), (r = 0.28, \alpha=0.05) \qquad \text{(Equation 8-1)}$$

Where, SY: sediment yield (t km^{-2} $year^{-1}$), DA: drainage area (t km^2). The equation reveals that a log-normal regression better describes the sediment yield -drainage area relationship for the 62 stations. Although the degree of scatter is high, the correlation is significant at 95% level and the equation can be used to compare sediment yields from sub-catchments of different sizes which provides an indication of variability in soil erosion rates. Equation 8-1 predicts a specific sediment yield of 895 t km^{-2} $year^{-1}$ for a standard 100 km^2 catchment. In turn, a sediment delivery ratio (SDR) expression can be derived where:

$$SDR (\%) = 127.5 - 6.0 \ln(DA) \qquad \text{(Equation 8-2)}$$

This indicates sediment delivery relative to a 100 km^2 catchment, which is somewhat different from previous studies which have examined much smaller sub-catchments. The gradient of the sediment delivery relationship is steeper than that reported for Northern Africa (Probst and Amiotte-Suchet, 1993) but gentler than that for agricultural land in humid temperate environments (Trimble, 1977; Walling, 1983). Using Equations 8-1 and 8-2, the sediment yield data for the 62 stations can be calibrated to a standard basin size of 100 km^2 for mapping purposes. Three alternative mapping methods are discussed below.

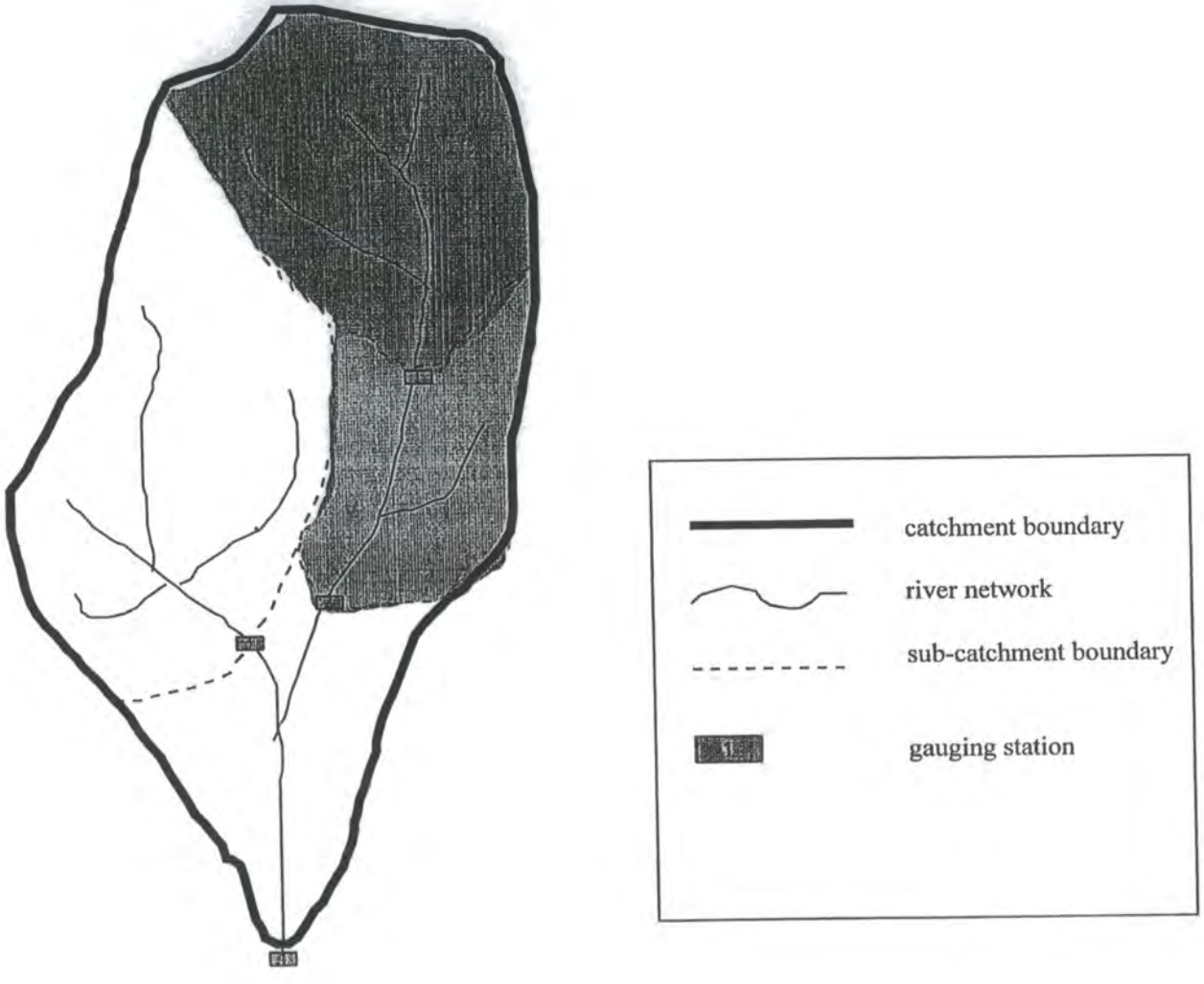

Figure 8-9, Schematic representation of the linked-lumped catchment system

8.4.2 Mapping methods

8.4.2.1 Polygon Attribution

The mapping unit for the first method is the individual catchment, so it is called polygon attribution. This method requires the identification and digitising of all sub-catchment boundaries. The 62 catchment boundaries delineated from the 30 arcsecond DEM or digitised from 1:1,500,000 scale maps (see Chapter 4 for details) are used here. Identification of the sub-catchment boundaries provides a total sub-catchment area, used in the calculation of specific sediment yield, but also allows the calculation of the incremental area which is not controlled by upstream stations and which is used for mapping. For example, Yichang station has a catchment area exceeding 1 million km^2, but only 34 666 km^2 is outside the catchment area of the next upstream station.

Having obtained a distribution of polygons representing sub-catchment mapping areas, the next stage is attribute sediment yield classes to those polygons. The sediment yield map was shaded based on the 5 classes, 0-250, 250-500, 500-1000, 1000-1500 and > 1500 t km^{-2} $year^{-1}$ (Figure 8-10). The map clearly outlines the geographical distribution of each class. The lower Jinsha, the Three Gorges and the Jialin had values >1000 t km^{-2} $year^{-1}$, while the areas in the mountainous west had the values of < 500 t km^{-2} $year^{-1}$. The high values associated with the Sichuan Basin (mainly Jialin and Tuo tributaries), reflect an area dominated by agricultural lands, with some of the highest population densities in China. Purple soil, one of the most erodible soils (Lu and Shi, 1992), is mainly located in this area. The highest sediment yields, located in the upper Jialin (Figure 8-10) are mainly related to landslides and debris flows (Yu et al., 1991). The geological structure and geomorphologic setting of the lower Jinsha is also conducive to landslide activity. In contrast, the lower sediment yields for upper Jinsha-Yalong and upper Min-Dadu are areas of lower population density and higher forest cover.

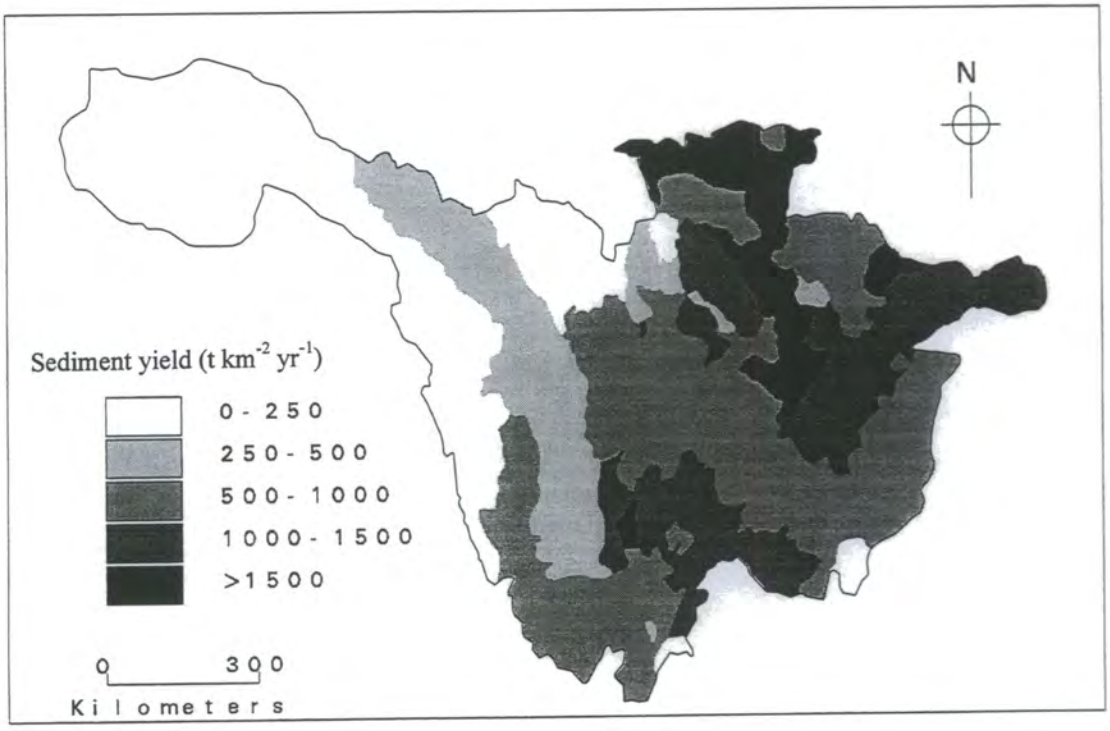

Figure 8-10, Sediment yield map generated by polygon attribution

8.4.2.2 Point Interpolation Procedures

As the specific sediment yield - catchment area is designed to remove the effect of size-dependency, an alternative mapping strategy is to treat the gauging station data as points and generate a sediment yield surface through interpolation. A similar approach has been employed in the Laurentian Great Lakes area of Canada (Stone and Saunderson, 1996), where average sediment yield was calculated for catchments with multiple stations such that 37 of the original 97 stations were used as a basis for interpolation. No account was taken of the size dependency of the sediment yield values, although a multiquadric interpolation method was used.

A large range of possible interpolation procedures are available with various advantages and limitations. Six alternatives are available in Arc/Info Version 7 (ESRI, 1994). The details on interpolation procedures were introduced in Chapter 4. These are CREATETIN (triangulated irregular network), IDW (inverse distance weighted), TREND (trend surface), SPLINE, KRIGING and TOPOGRID. CREATETIN and TOPOGRID were generally used for generating 3D terrain models and can handle both data types of point and contour line, while IDW, TREND, SPLINE and KRIGING can only use point data. The distribution of sample points and the type of surface to be simulated will determine which method is most appropriate. Based on the characteristics of the sediment yield data, IDW was used to generate a sediment yield surface in this study, after the specific sediment yield data from the 62 stations were first standardised to a 100 km^2 catchment size. IDW determines cell values using a linearly weighted combination of a set of sample points (ESRI, 1994). The weight is a function of inverse distance. The surface being interpolated should be that of a locationally dependent variable. Because the IDW is a weighted distance average, the average cannot be greater than the highest or less than the lowest input (ESRI, 1994). Using the same classes as the previous method, the sediment yield surface generated (Figure 8-11) is quite similar to the polygon based map (Figure 8-10).

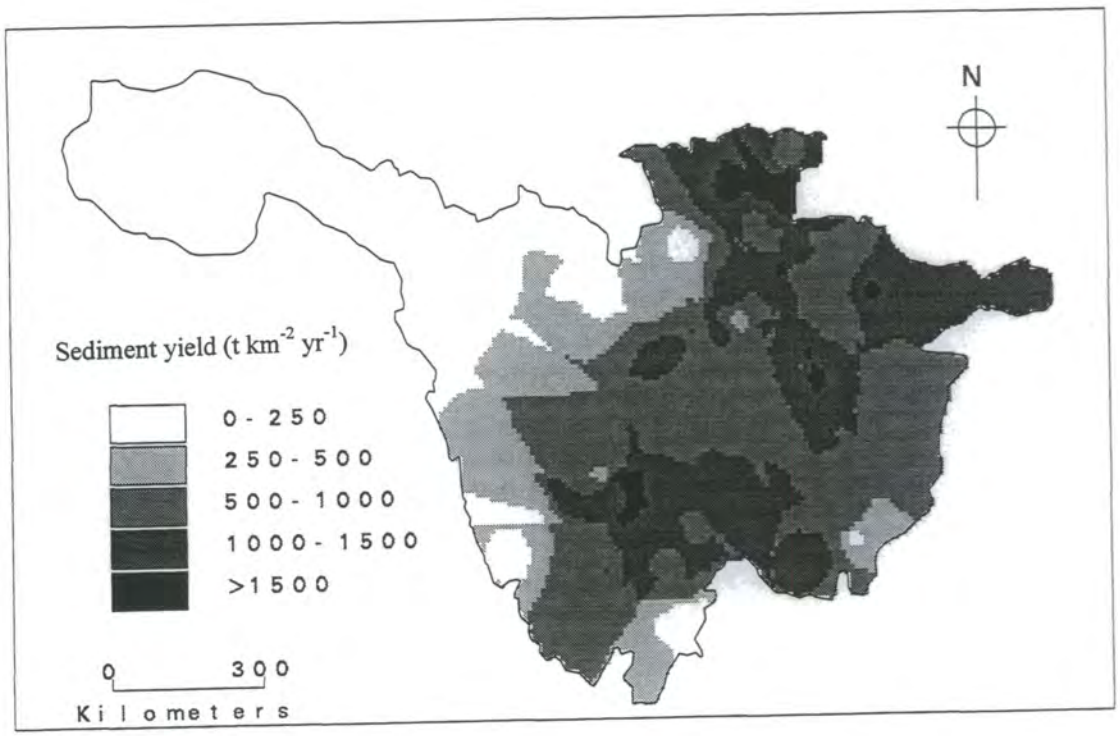

Figure 8-11, Sediment yield map generated by point interpolation procedures

The characteristics of the interpolated surface can be controlled by limiting the number of points used for calculating each interpolated value, or defining a radius within which all points are used in the interpolation. Similarly the interpolation can be constrained by varying the value of the exponent in the distance weighting. A large exponent of distance will result in less influence from surrounding points. A barriers option can also be introduced to confine the points used for interpolation to those on the same side of the barrier as the current processing cell. Such a procedure might be considered important in interpolations where values lie in different tributary catchments though it significantly increases the computer processing time. Without using barriers the sediment yield surface is generated from adjoining points regardless of whether they are in the same flow system. However, the distribution of land surfaces undergoing high rates of soil erosion does not necessarily coincide with catchment boundaries and there are arguments for not employing interpolation boundaries.

Sediment yield mapping through point interpolation procedures has two main problems. First, the interpolation assumes a gradual change in conditions between points, unless specific boundaries are incorporated into the interpolation procedure. It is known that the distribution of sediment sources may be highly concentrated in particular locations. Second, the procedure treats the data as a point value located at the sub-catchment outlet (the gauging station). This neither allows for a weighting of the value according to the size of the sub-catchment area nor includes any locational information about the sub-catchment position into the interpolation procedure. At present there appear to be no suitable methods for interpolating values that apply to irregular and different sized polygons as opposed to points.

8.4.2.3 Multiple regression modelling

Both of the previous methods employed a standardisation procedure for calibrating specific sediment yield with catchment size. Though designed to eliminate bias associated with the size dependency of sediment yield data, the calibration procedure

has several limitations. Sediment yield-basin area relations are very complicated and vary considerably within the Upper Yangtze catchment. The high degree of scatter indicates that it is unlikely that the calibration equation will be suitable across all parts of the catchment. Therefore a mapping procedure which does not require catchment size calibration may be attractive. One such possibility is modelling where sediment yield is predicted from a set of environmental variables (Neil and Mazari, 1993). The GIS offers considerable scope for generating maps based on a suitable model. Based on the modelling section (section 8.4) it can be seen that the main variables controlling the sediment yield are varied from tributary to tributary. This means that different models must be employed for different tributaries. Due to the shortage of the stations for Wu tributary and the shortage of the variables for Jialing tributary, it is impossible to build such models for those two tributaries. Here as an example the sediment yield data for all the 62 stations have been examined in relation to 13 potential influencing variables: catchment area, catchment perimeter, basin length, elevation, basin relief, local relief, slope, hypsometric integral, relief ratio, drainage density, precipitation, Fournier index and population density (see Appendix 8 for details). These have been derived from a variety of sources including freeware available from the Internet. Preliminary results indicate that much of the variability can be explained in terms of two variables:

$$SY = (24.72 + 1.247\,MS - 0.00454ME)^2,\ (r = 0.599,\ F=0.001) \qquad \text{(Equation 8-3)}$$

where SY = specific sediment yield (t km^{-2} yr^{-1})

MS = mean slope (degree)

ME = mean elevation (m)

With the aid of GIS it is possible to use this equation to map sediment yield at either catchment or pixel level. The necessity for catchment boundaries is eliminated and sediment yield can be plotted as a continuous variable rather than a polygon attribute. The sediment yield map produced (Figure 8-12) based on the same classes

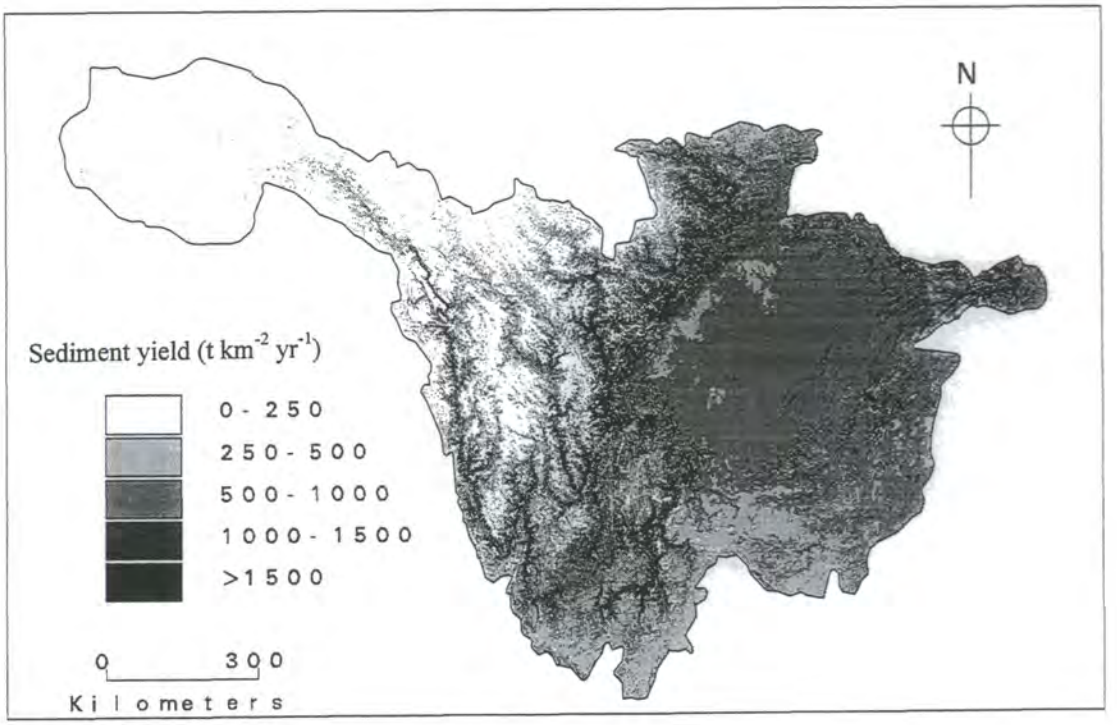

Figure 8-12, Sediment yield map generated by multiple regression modelling

as the previous maps consequently has a higher degree of coincidence with topography. The inverse relationship with elevation reflects the fact that the arid and sparsely populated west of the Upper Yangtze lies on the Tibet-Qinghai Plateau, whereas the densely populated humid east is at a lower altitude. In this way the elevation variable acts as a surrogate for climatic and human disturbance variables. Furthermore, potentially important variables such as geology, soils, forest cover and land use have been excluded from the analysis because the resolution of available databases is not yet sufficiently high. The two topographic variables (MS, ME) explain 36% of the variability of specific sediment yield across the Upper Yangtze and the incorporation of additional variables and high resolution databases come on line offers considerable scope for improving the degree of explanation.

Each method generates a reasonably consistent distribution of sediment yields which might form the basis for a large catchment management strategy to reduce soil erosion in key areas. The area of each sediment yield class generated by the three methods are summarised in Figure 8-13. The three different methods gave similar total areas for each sediment yield class, although the polygon attribution method generated a greater area in the highest and lowest classes. Interpolation procedures tend to generate a larger proportion of area in intermediate classes.

8.5 SUMMARY AND CONCLUSION

The chapter, first, examines the control of sediment yield spatial variability and then the methods of sediment yield mapping are discussed. Through the preliminary examination, the main summary and conclusion for the chapter are made below.

The utility of GIS to extract spatially distributed data for the analysis of intra-catchment sediment yields has been demonstrated. At the present time detailed information on land-use, geology and soils is not available in the public domain and the examination of sediment yield variability in the Upper Yangtze has been confined to six variables: mean elevation, basin relief, mean slope, mean annual runoff, mean

annual precipitation and population density. The high degree of scatter in the sediment yield data caused by the diverse characteristics of the catchment, is reduced by grouping the data into categories based on geographic location, catchment size and maximum elevation, prior to analysis.

The results generally indicate specific sediment yields increasing with precipitation, runoff , population density and mean slope, but decreasing with elevation. Elevation is highly correlated with other catchment variables and therefore an influential factor on sediment yields although it has no direct effect on erosion dynamics. The intrinsic geography of the Upper Yangtze catchment means that high elevation areas are mostly flat, semi-arid, sparsely populated with limited agricultural activity. Within the bivariate plots of sediment yield against catchment variables some interesting contrasts emerge, particularly in regard to runoff and precipitation. Of particular significance is the apparent scale dependency in the nature of the relationship of sediment yield with elevation, precipitation and runoff. Further attention is required towards removing scale effects from the analysis of controls on sediment yields.

The limited number of variables used in this study are capable of explaining the majority of variance within the Jinsha-Yalong and Dadu-Min tributaries but perform less well in the more heavily populated areas. The results indicate that topographic, climatic and crude human impact variables are reasonable at explaining sediment yield variations in comparatively natural environments but are inadequate in regions influenced by large scale agricultural activity. It is envisaged that the resolution of global datasets will continue to be improved, allowing the incorporation of variables representing geological, soil and human activity conditions into regional studies of sedimentation.

Mapping conventions for representing sediment yield within a series of nested catchments are also problematic and include shading polygons of incremental catchment area, point interpolation procedures, predictions from regression models or residuals from whole catchment yield-area relationships. First method uses sub-

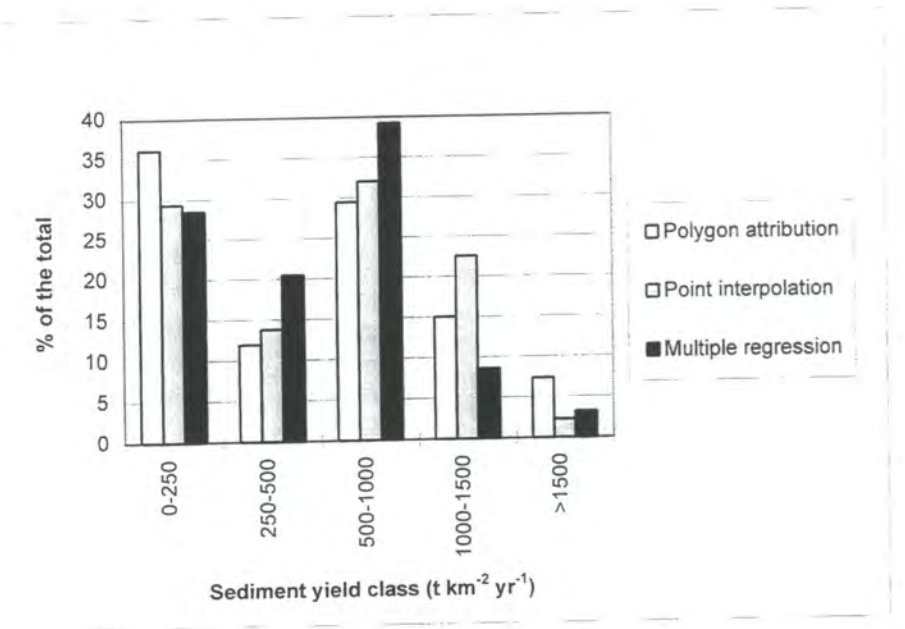

Figure 8-13, Comparision of sediment yield class distribution from alternative mapping procedures

catchments as basic mapping units, the second treats gauging station measurements as point data and the third predicts sediment yield from an empirically derived multiple regression model. Each method has its own advantages and limitations. Polygon attribution uses real values, but requires digitised boundaries and gives uniform values over the sub-catchment unit which may be misleading. Point interpolation procedures can be undertaken more efficiently as the amount of computing required is less time consuming. However, the choice of weights on the interpolation procedure and the question of whether sub-catchment barriers are necessary introduces some uncertainty. The final method, based on multiple regression modelling is attractive because it avoids the need for digitised boundaries or calibration of specific sediment yields to standard catchment sizes. However, the quality of the map output is dependent of the accuracy of the model. In this case the model is empirically-derived form analysis of the large Upper Yangtze data set. There are additional variables which would be useful to include and there is also scope to extend the approach to physically-based modelling.

It is hoped that this study has raised attention to the lack of a uniform approach to sediment yield mapping at present. The maps which have been generated have some utility for macro-scale management of problems imposed by high sediment transport, particularly in the identification of sediment sources attributable to soil erosion. The increasing availability of high resolution environmental databases and the potential for linking sediment yield data from relatively large sub-catchments (>100 km^2) with smaller sedimentation investigations (for example, local reservoir sedimentation surveys) suggests that integrated soil erosion and sediment transport management at a continuum of scales should become viable.

9. THE POTENTIAL TO MONITOR SEDIMENT YIELD USING REMOTELY SENSED NDVI DATA

9.1 INTRODUCTION

Having examined soil erosion and sedimentation in a small catchment and sediment yield in the whole Upper Yangtze basin, the final main chapter is designed to investigate the potential for monitoring catchment-scale sediment transport using remotely sensed Normalised Difference Vegetation Index (NDVI) data, derived from Advanced Very High Resolution Radiometer (AVHRR) satellite imagery. NDVI measures the reflectance values of plant canopy. Low values of NDVI represent surfaces with less vegetation or suffering from unfavourable growth. Therefore NDVI has been used for mapping and monitoring vegetation type and density (Townshend and Tucker, 1981; Tucker et al, 1984). NDVI has also been integrated to model global scale soil erosion (Drake et al., 1995; Zhang et al., 1997). Several investigations have reported that NDVI is significantly correlated with vegetation cover, and hence NDVI has been used to represent vegetation cover in the erosion model developed by Thornes (1985; 1989). However, there are many problems using NDVI value for an index of vegetation cover. First, there is much scatter in the NDVI-vegetation cover relationship due to the effect of other variables, notably soil backgrounds (Zhang et al., 1997). Second, though NDVI seems to be correlated with green vegetation cover and is a reasonable measure of vegetation cover in environments where green vegetation dominates, in semi-arid environments where erosion is most important, woody senescent and dead vegetation exert a large contribution to vegetation cover but not to NDVI (Drake et al., 1995). Third, in cold environments, such as in the areas with high latitude or high altitude, low NDVI may not necessarily indicate high soil erosion potential. Besides, the model itself was developed based on the data obtained at small scale (e.g. Zhang et al., 1997),

obviously it is problematic if applying the model to estimate soil erosion and sediment transfer at a global scale.

Extensive research has also shown that NDVI can be used for effective monitoring of rainfall and drought situations, which suggests the notion that NDVI might also have an indirect relationship with runoff and hence sediment transport. Factors such as precipitation, vegetation, soil type and soil moisture that influence spectral reflectance of the vegetation cover also affect soil erosion dynamics. This also suggests that it may be possible to directly predict or monitor soil erosion and sediment transport using the remotely sensed data. However, the mechanism of interaction among these factors need not imply a causative relationship. For example, an increase in rainfall and soil moisture may increase soil erosion, whereas an increases in vegetation cover may reduce soil erosion. Therefore the relationship between NDVI and runoff and sediment transport may be complicated. Little attempt has been made to develop a direct link between NDVI and soil erosion / sediment transport. If such a NDVI-runoff/sediment relationship can be developed, the temporal and spatial variations of the NDVI would provide a useful tool for monitoring climatic and human-induced hydrologic changes. The main aims of the chapter are to examine the relationships between NDVI, runoff and sediment transport, from which the possibility of monitoring runoff and sediment transport using NDVI data will be discussed. The main purposes of the chapter are:

1) to examine the possibility of monitoring runoff & sediment transport using the remotely sensed NDVI data;

2) to investigate the spatial variation of NDVI and its relationships with other variables;

3) to develop the relationships between NDVI and runoff & sediment transport.

9.2 NDVI AND THE CATCHMENTS

9.2.1 The Normalised Difference Vegetation Index (NDVI)

The remotely sensed NDVI data can characterise vegetation cover because they are related to plant canopy characteristics. The NDVI data are the Monthly Experimental Calibrated GVI with a resolution of 10 * 10 minutes from the Global Ecosystems Database (GED) CD-ROM developed from weekly visible and near-infrared AVHRR channel data from 1985-1990 (NOAA-EPA Global Ecosystems Database Project). The NDVI was computed as :

$$NDVI = (Ch2 - Ch1) / (Ch2 + Ch1) \qquad \text{(Equation 9-1)}$$

Where Ch1 and Ch2 are the reflectance in the visible (0.55-0.68 μm) and near-infrared (0.73-1.1 μm), respectively. The NDVI equation produces values in the range of -1.0 to 1.0, where increasing positive values indicate increasing green vegetation and negative values indicate non vegetated surface features such as water, barren ground, ice, and snow or clouds. The reflectance values of the visible and near-infrared data were computed from pre-launch calibration coefficients. The calibrated visible and near-infrared data, and solar zenith angle data included on the NOAA GVI product were used to screen the NDVI data for cloud contamination and low (less than 15 degrees) solar elevation at the time of data acquisition. Data were also screened for data drops. Two successive weeks of the screened NDVI data were then composited based on the maximum NDVI value of the two weeks. The biweekly NDVI data have been scaled to a byte format from the original NDVI value computed with the above equation, using the following conversion:

$$byteNDVI = (realNDVI * 100) + 100 \qquad \text{(Equation 9-2)}$$

Therefore the NDVI in original images was byteNDVI with values ranging from 0-200. The byteNDVI was extracted for each catchment (see Chapter 4 for methods) and then converted back to real value based on Equation 9-2. Monthly mean NDVI

values for individual catchment are averaged from all the cells over the whole catchment, whereas annual mean NDVI values are averaged from the monthly mean NDVI of 8 months for 1985, and 12 months for 1986 and 1987.

9.2.2 NDVI relations with ecoclimatic variables

The characteristics of NDVI have been summarised by Nicholson and Farrar (1994). NDVI is determined by chlorophyll absorption in the red wavelengths and by the reflectance of near infrared radiation. Absorption is proportional to leaf chlorophyll density, while reflectance is a function of green leaf density (Tucker et al., 1985). Therefore, NDVI correlates well with variables such as green leaf biomass, leaf area index (LAI), total dry matter accumulation, and annual net primary productivity (Curran, 1980; Tucker et al., 1981; 1983; 1985), although strictly it represents physiologically, a measure of the photosynthetic capacity of the canopy (Sellers, 1985; Tucker and Sellers, 1986). NDVI is also influenced by a number of measurement errors associated with satellite remote sensing. Factors contributing to the errors include atmospheric constituents, such as aerosols and water vapour (Holben et al., 1991; Justice et al., 1991), clouds (Gutman et al., 1987), viewing angle, solar illumination, and sensor calibration (Schultz and Halpert, 1995). More importantly NDVI is affected by soil background reflectance (Huete and Tucker, 1991). The index tends to decrease with increasing soil brightness for constant vegetation cover and appears to be independent of soil background influences only when plant areal coverage exceeds 70% (Nicholson and Farrar, 1994).

Because of close links between vegetation parameters and ecoclimatic variables, the relations between NDVI and such variables have been studied in numerous locations (Davenport and Nicholson, 1993; Malo and Nicholson, 1990; Nicholson and Farrar, 1994; Schultz and Halpert, 1995). All these studies have suggested that in general NDVI increases with increasing rainfall. However, the NDVI-rainfall relationship is more complex as demonstrated by Nicholson and his colleagues (Davenport and Nicholson, 1993; Malo and Nicholson, 1990; Nicholson and Farrar, 1994). In East Africa and the Sahel, NDVI and rainfall are linearly related only in a limited range of

rainfall conditions, generally between about 200-1200 mm annually and 25-200 mm for monthly rainfall (Davenport and Nicholson, 1993; Malo and Nicholson, 1990). Above the upper threshold, the index "saturates", and NDVI increases only very slowly with increasing rainfall or becomes constant. Also, the response of NDVI to rainfall is dependent on vegetation type and varies by geographical region. In semi-arid Botswana, Nicholson and Farrar (1994) demonstrated a similar situation where a linear NDVI-rainfall relationship exists up to a limit of approximately 500 mm/yr or 50-100 mm/month. Above these limits, a "saturation" response also occurs. The world-wide NDVI-precipitation relationships have been examined by Schultz and Halpert (1995), who have demonstrated that the largest NDVI-precipitation correlations occur in the regions where the annual cycles of both variables are quite pronounced and where the maxim occur in the summer such as eastern Asia, the interior of northern North America, the Sudan and western Sahel regions of Africa. They also demonstrated negative correlations in the regions where the precipitation maximum tends to occur in the winter, while the NDVI maximum occurs in the summer, in Mediterranean climates such as California, western Spain, and southern Chile. In such regions, the annual cycle of vegetation is driven primarily by temperature. Many regions have near-zero total correlations between NDVI and precipitation (Schultz and Halpert, 1995). The lack of pronounced NDVI and /or precipitation annual cycles in areas such as the south-eastern US or nothwestern South America tends to suppress the correlations. Tropical rainforests such as central Brazil and Indonesia and other regions with abundant rainfall have near-zero or slightly negative correlations.

The above brief review on NDVI-rainfall relations indicates that the relationships world-wide are very complicated depending on the characteristics of the region. In the Upper Yangtze, most of regions tend to have profound annual cycles of precipitation and hence runoff and the maximum occurs in the summer (see details in Chapter 3). In addition to NDVI-rainfall relations, NDVI has also been linked with temperature (Schultz and Halpert, 1995), soil moisture, soil temperature, potential evapotranspiration, soil physical properties and crop transpiration (see Yang et al., 1997). In mountainous catchments such as the Upper Yangtze, runoff response is

often closely linked with rainfall patterns and totals, which suggests a possible relationship between NDVI and runoff and hence a means of predicting variation in sediment transport.

9.2.3 The catchments

Thirteen catchments, comprising 12 sub-catchments within the basin, together with the whole Upper Yangtze (controlled by Yichang station) have been selected for the preliminary study of the relationship between NDVI and sediment transport. The selected sub-catchments represent varied elevation, precipitation and land use characteristics (Table 9-1). These catchments cover all the main tributaries except for the Wu tributary which has no runoff and sediment data available for the period overlapping with the satellite imagery available on the Global Ecosystems Database. General information on the study catchments is given in Table 9-1. The annual mean runoff and sediment yields are averaged from a longer period of measurement (>=25 years) for each catchment. There are 33 months from April 1985 to December 1987 during which runoff, sediment yield and NDVI data are available. Table 9-1 indicates that 1986 was a dry year, and 1985 and 1987 were normal years in the whole Upper Yangtze. For example, at Yichang station water discharge and sediment yields for 1985 and 1987 were close to average water discharge and sediment yields, and 1986 was below average. Due to the large scale of the basin, the representatives of hydrological conditions might be different for some sub-catchments within the basin. For example, Henjiang and Qinkoutang catchments from the Lower Jinsha were drier in 1987 than the other two years. It can also be noted that 1986 was a relatively wet year in the small experimental catchment of Yiwanshui in the Three Gorges area, but relatively dry for the Upper Yangtze as a whole. A detailed assessment of spatial and temporal variability of sediment yields in the basin were reported in Chapter 7 & 8. It must be stressed that runoff and sediment transport here were measured at the outlet

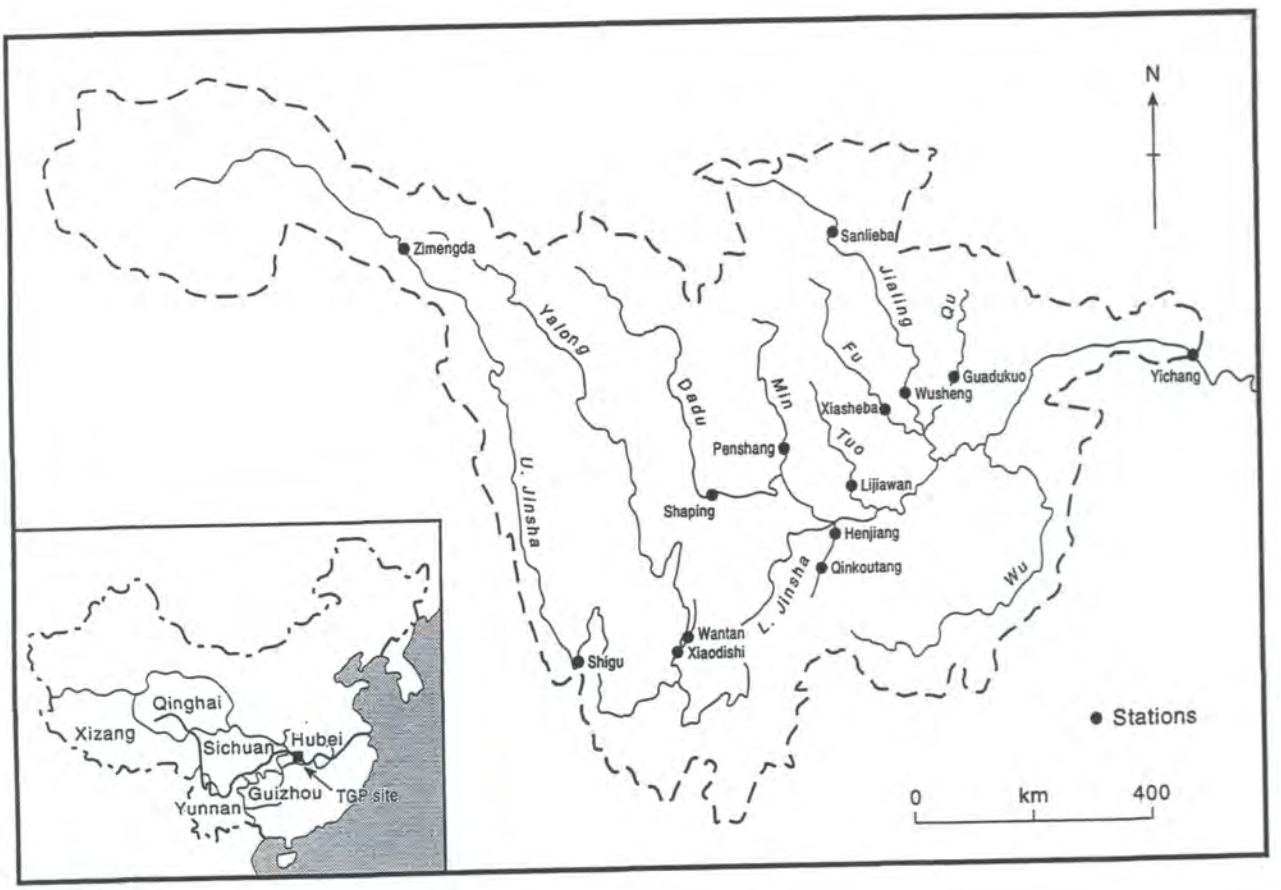

Figure 9-1, The catchments examined in the chapter

of each catchment, while NDVI was averaged throughout the catchment. This is somewhat different from previous studies on the relationships between NDVI and ecoclimatic variables, since most previous research was based on points (grid cell) value for NDVI and the examined variables (Nicholson and Farrar, 1994; Schultz and Halpert ,1995). Although Yang et al (1997) found that relations derived by using NDVI values over 3 by 3 pixel windows showed little difference from those using single pixel (1*1 km), it still can be argued that NDVI may be homogeneous but soil properties and its moisture regime can be very different. By contrast, the study uses averaged values for NDVI and runoff/sediment load throughout catchments.

Table 9-1, The catchments used in this chapter

Stations	Tributaries	Drainage area (km^2)	ST ($t\ km^{-2}\ yr^{-1}$) Mean	1985	1986	1987
Zimengda	Upper Jinsha	137704	68	58	40	58
Shigu	Upper Jinsha	232651	91	110	47	156
Henjiang	Lower Jinsha	14781	919	1055	1311	532
Qinkoutang	Lower Jinsha	2109	798	724	618	570
Xiaodeshi	Yalong	118294	249	355	236	544
Wantan	Yalong	11100	973	2707	1257	1373
Pengshan	Min	30661	337	202	261	253
Shaping	Dadu	75016	420	606	438	610
Lijiawan	Tuo	23283	537	194	94	389
Guoukou	Qu	31626	630	578	123	594
Wusheng	Jialing	79714	928	602	303	1048
Xiaoheba	Fu	29420	650	221	59	329
Yichang	Upper Yangtze	1005501	524	527	361	514

9.3 MONTHLY NDVI, RUNOFF AND SEDIMENT TRANSPORT

9.3.1 Patterns of monthly NDVI, runoff and sediment transport

The time series of monthly NDVI and monthly runoff (l km^{-2} sec^{-1}) and sediment transport (g km^{-2} sec^{-1}) for the 13 catchments were plotted in Figure 9-2 and Figure 9-3. These graphs show a strong temporal association between monthly NDVI and runoff and sediment transport across a wide range of different environmental and ecological conditions including elevation, precipitation, temperature, vegetation, land use and soil types. From November to April lower NDVI corresponds to lower runoff and sediment transport, whereas from July to September higher NDVI corresponds to higher runoff and sediment transport. While the monthly patterns are similar, two problems can be identified. First, peak sediment transport in general occurred in same month as peak runoff but peak NDVI frequently occurred one month later or earlier than peak runoff and sediment transport, depending on the catchment or the year (Figure 9-2 and Figure 9-3). For Lijiawan, Goudukou and Wusheng catchments, peak NDVI, runoff and sediment transport occurred all in same month (July) in 1987 but for most of the catchments peak NDVI occurred in August whereas peak runoff and sediment transport occurred in July. This indicates that NDVI may have a lagged response to precipitation and temperature while runoff and sediment responds more rapidly. For the 4 catchments with agricultural land use (Lijiawan, Guodukou, Wusheng and Xiaoheba) peak NDVI occurred in July, whereas peak runoff and sediment transport occurred in August in 1985. The earlier peak NDVI than runoff/sediment might be explained in terms of the agricultural calendar. After July, crops have matured or been harvested, resulting in lower NDVI. Second, in some catchments, the NDVI in summer (July to September) did not change dramatically even in the dry year of 1986 compared with runoff and sediment transport in particular (Figure 9-2 and Figure 9-3). In Zimenda and Shigu catchments during the winter of 1985, NDVI dropped to a very low levels. This may indicate the effects of other variables such as temperature on NDVI rather than precipitation but needs further study. These two problems of peak NDVI not corresponding to peak runoff and sediment transport depending on the catchment or the year, and of NDVI having limited sensitivity

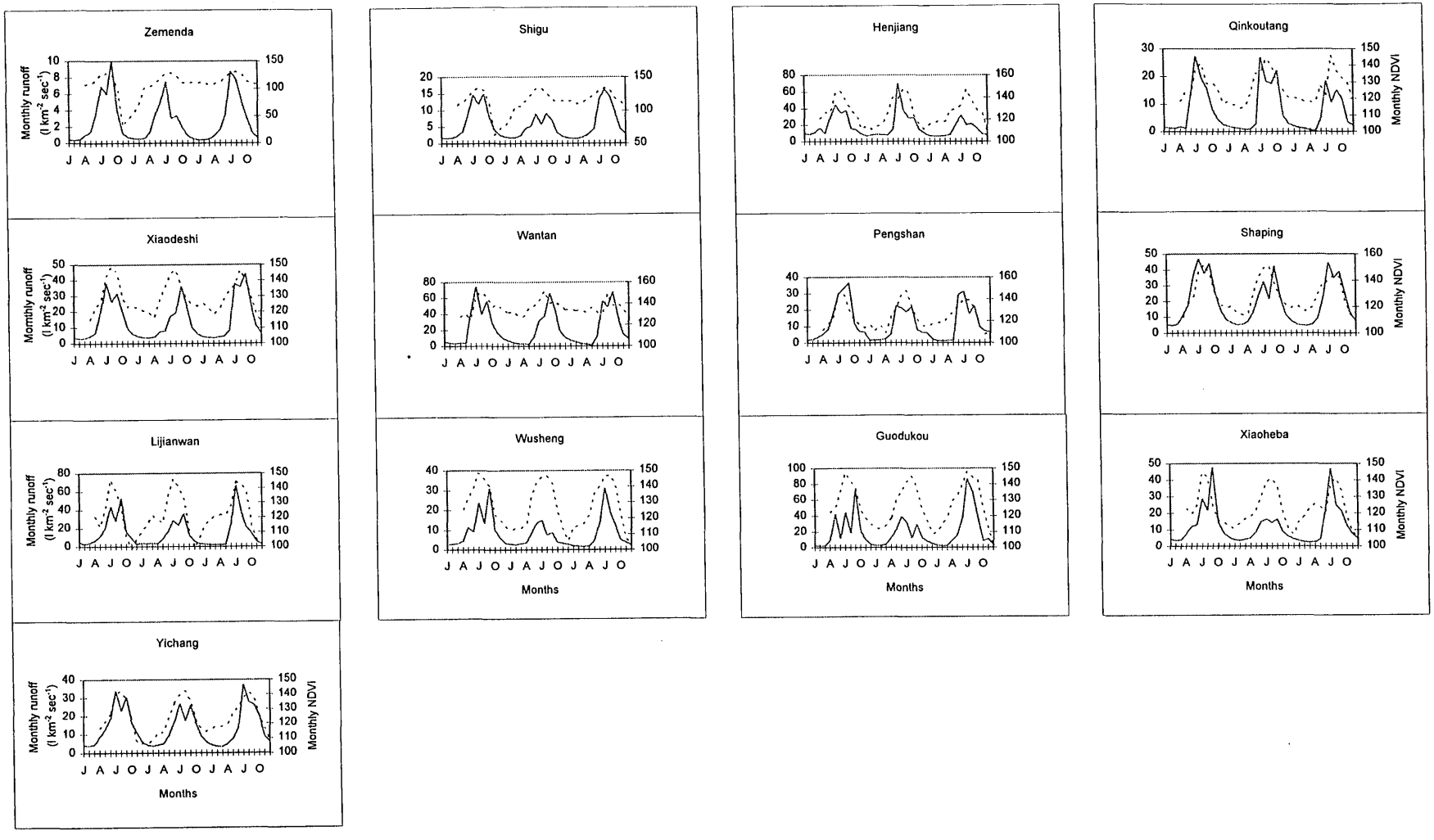

Figure 9-2, The patterns of monthly NDVI and runoff

Solid lines indicate runoff and dashed lines NDVI

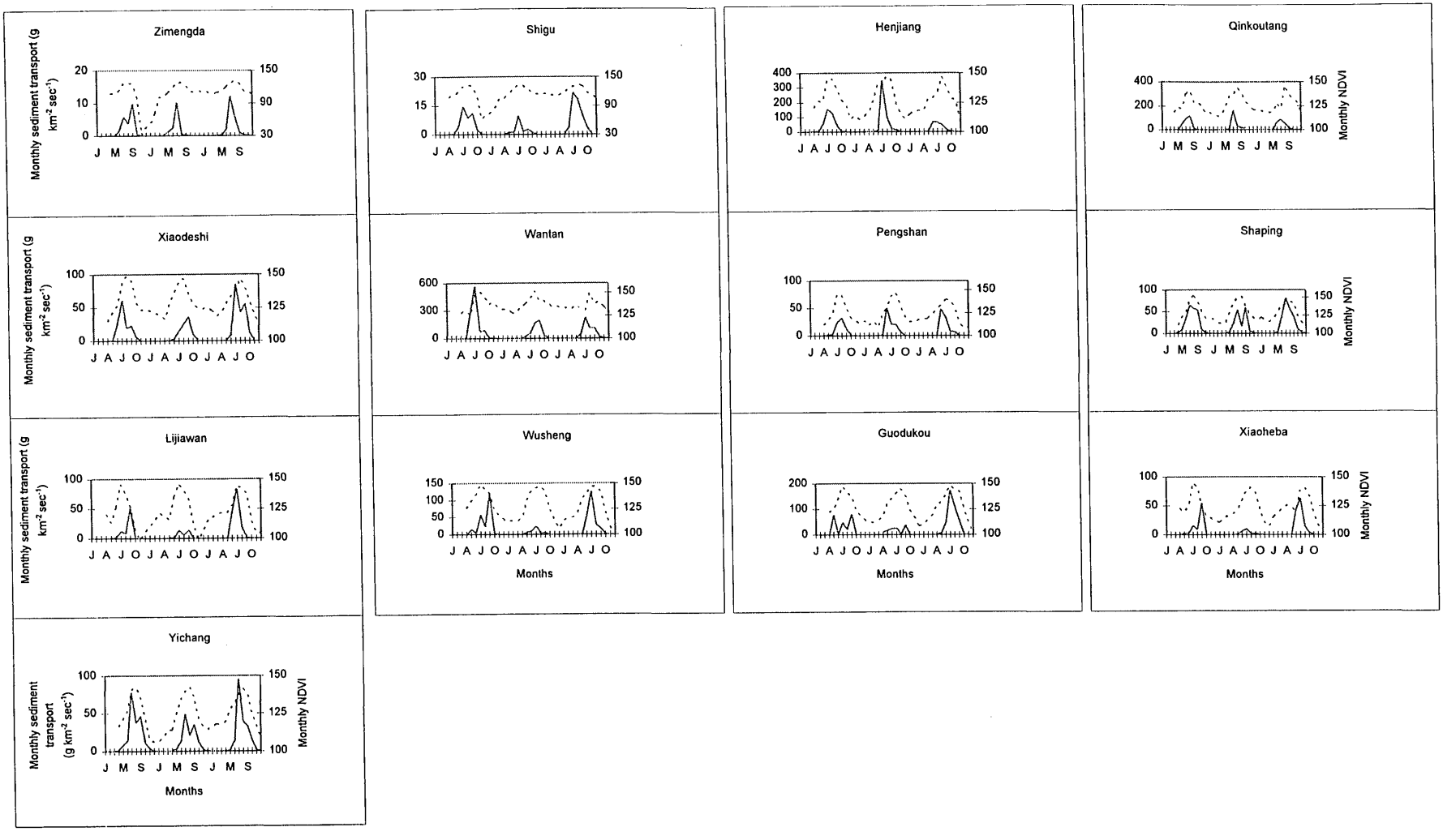

Figure 9-3, The patterns of monthly NDVI and sediment transport

Solid lines indicate sediment transport and dashed lines NDVI

compared with runoff and sediment transport during summer, may hamper the potential to predict or monitor runoff and sediment using only NDVI data.

9.3.2 Correlation between monthly NDVI, runoff and sediment transport

The detail of the relationship between monthly NDVI and runoff /sediment transport can be more easily seen in bivariate scatterplots. Figure 9-4 and Figure 9-5 show monthly runoff and sediment transport plotted against monthly NDVI (for total 33 months) and a trendline was fitted for each plot. As expected, monthly NDVI is strongly correlated with monthly runoff and sediment transport. Interestingly, it is noted for Zimenda and Shigu catchments that monthly runoff/sediment transport tends to decrease with increasing monthly NDVI when the NDVI value is below 0, whereas runoff and sediment transport tended to increase with increasing NDVI values when NDVI values were above 0. These two catchments flow through the Qinghai-Tibet plateau and west mountainous areas with very high mean elevation, 4800 and 4600 m (averaged from 30 arcsecond DEM throughout the catchments), respectively. The NDVI below 0 in general occurred in winter (Figure 9-4 and Figure 9-5), during which the precipitation mainly was in snow form and the ground was mainly covered by snow and /or ice and possibly just barren ground in the areas of such high altitude. In such cases it is reasonable to expect that NDVI values below 0 correspond higher winter runoff and sediment transport. For most of other catchments, monthly NDVI values were above 0 and monthly runoff and sediment transport increases with NDVI.

The strength of the relationships between monthly NDVI and runoff /sediment varied between sub-catchments. Wantan catchment had the worst relationships. The low correlation between monthly NDVI and sediment transport may be due to frequent mass movements (landslides) which generated anomalously high sediment yields (Table 9-1). One explanation for this is that the NDVI values were still quite high when runoff was low in the winter. The performance of the NDVI-sediment yield

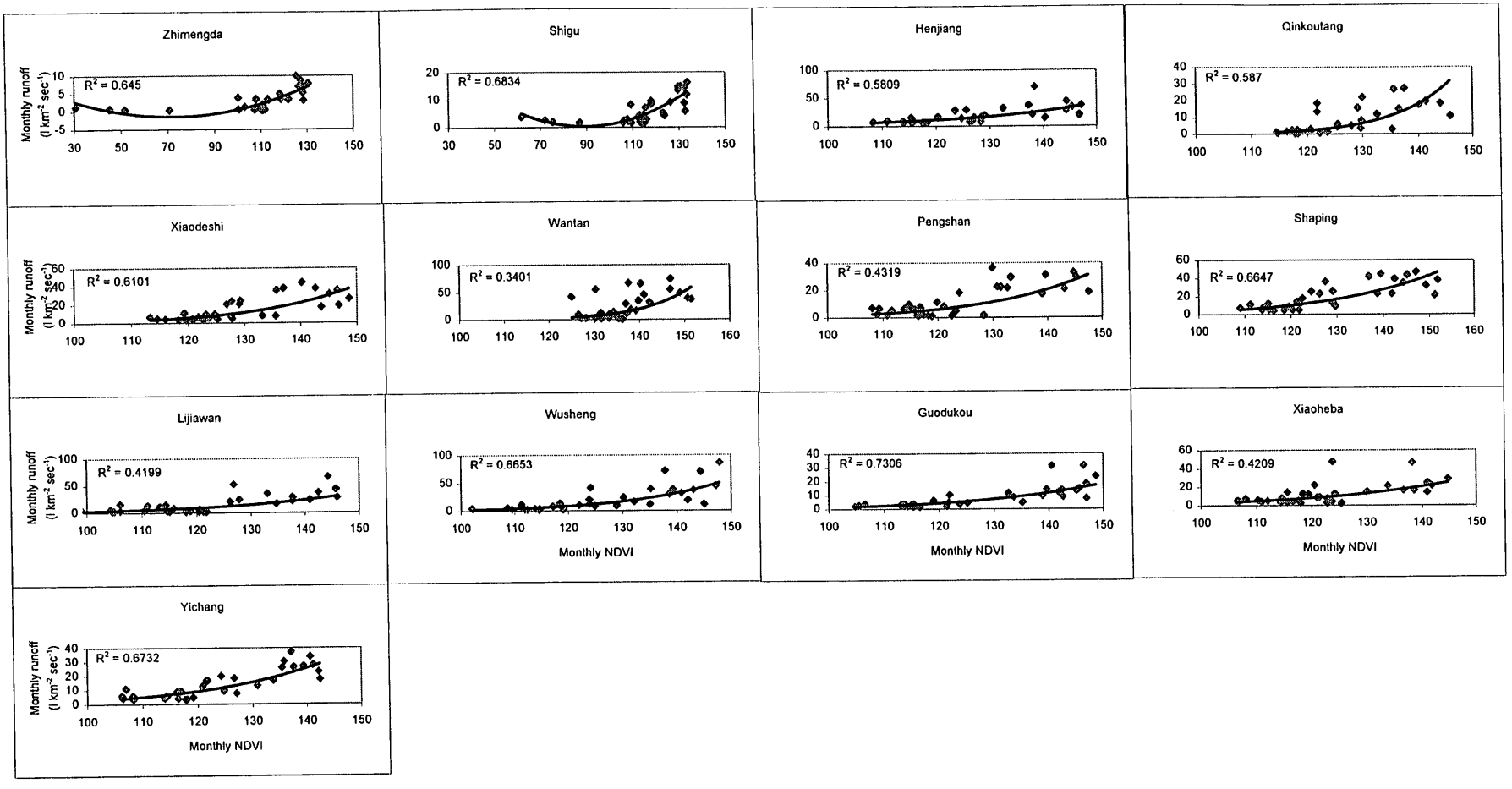

Figure 9-4, Monthly runoff against NDVI

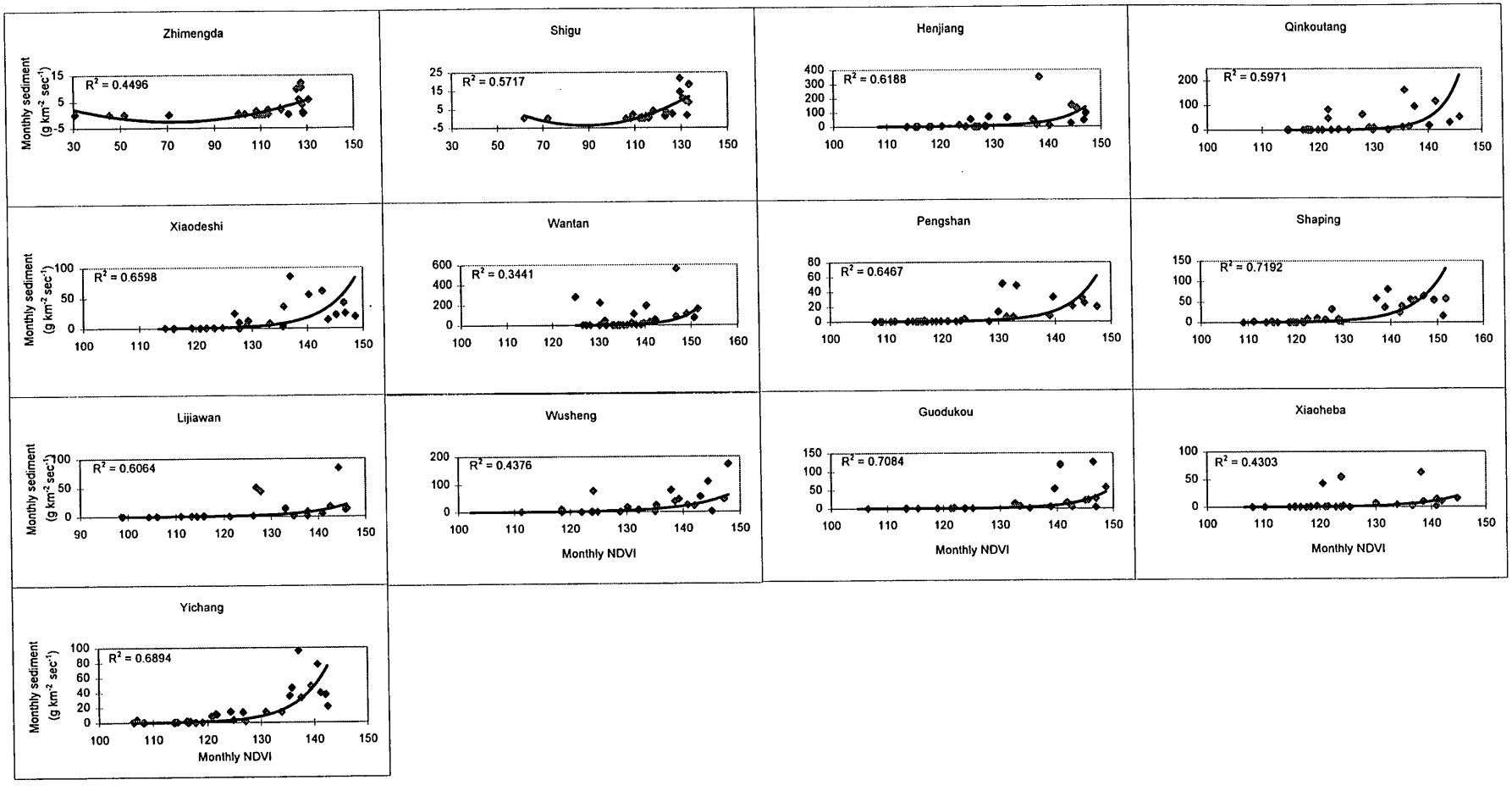

Figure 9-5, Monthly sediment transport against NDVI

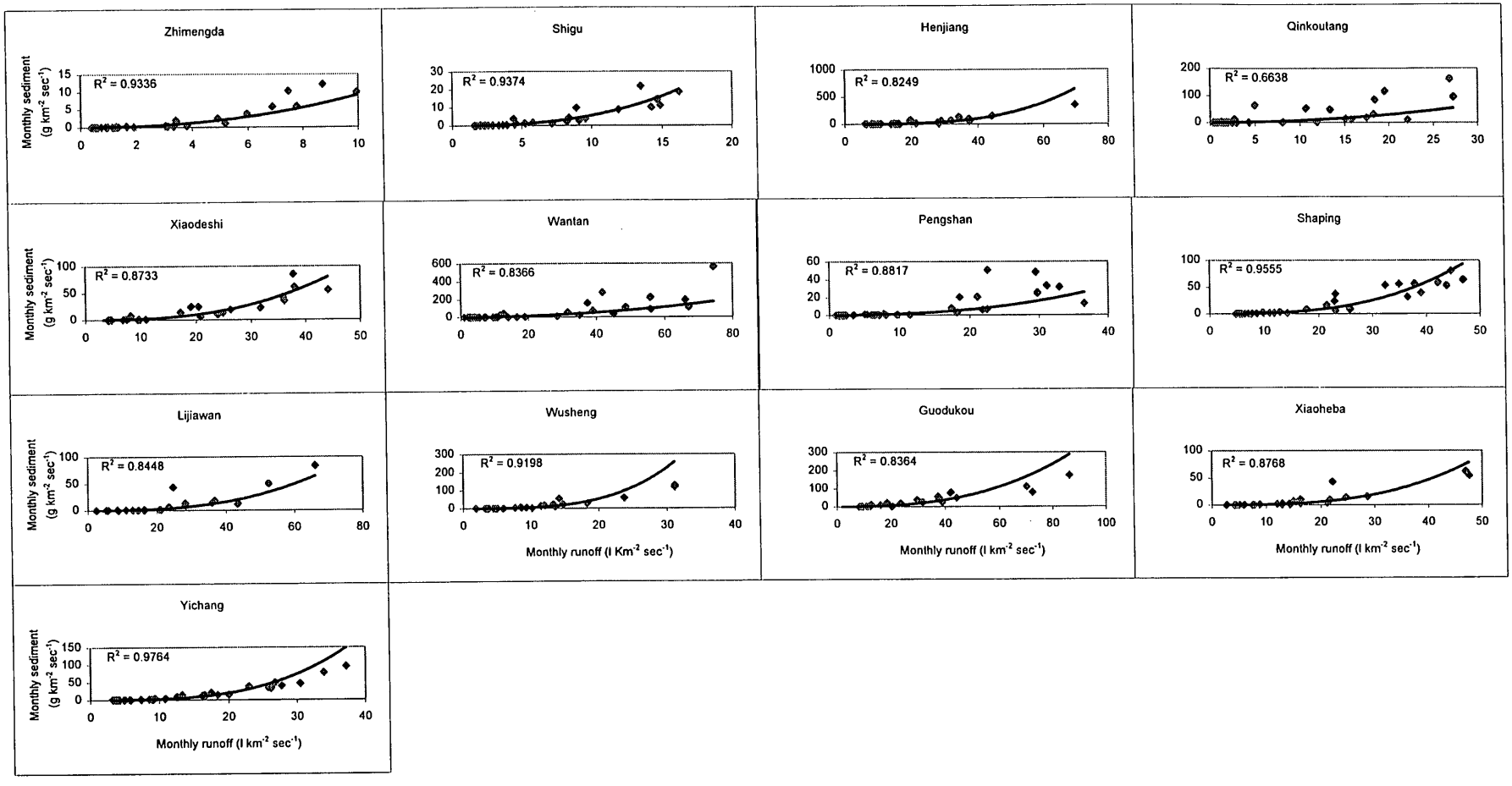

Figure 9-6, Monthly sediment transport against runoff

relationship is also not very good for the agricultural catchments such as Lijiawan and Xiaoheba. This may be due to the effects of human activities on vegetation. Crop scheduling, irrigation, fertilisation, deforestation, and reforestation are examples of human impacts on vegetation that may not be directly attributable climate anomalies (Schultz and Halpert, 1995). Irrigation in Sichuan basin is highly developed such as the well-known irrigation system of Dujiangyan located upstream of the Min-Dadu confluence. The correlation in Wusheng catchment is strong for NDVI-runoff but not for NDVI-sediment transport. The headwaters of the catchment are affected by mass movements and highly erodible loess soils are located in the area (see Chapter 7). The above results seem reasonable, since NDVI can only reflect ground surface conditions but sediment transport is affected by many factors such as sediment supply from channel and gully sources, which are not represented by NDVI measurement.

The correlation is surprisingly high for the whole basin (Yichang catchment) considering the complex factors influencing runoff and sediment transport within so large an area (Figure 9-4 and Figure 9-5). The scatter in the correlation between monthly NDVI, runoff and sediment transport were caused by limited change in NDVI during summer if monthly NDVI was plotted against monthly runoff and sediment transport for the whole time series of 33 months. The scatter in the correlation may also be due to the leads and lags shown in the time series plots. Due to the fact that peak NDVI did not correspond with peak sediment transport, different combinations of monthly NDVI and sediment transport over the 33 months were examined in order to achieve higher correlation coefficients. Using the Upper Yangtze as an example, the correlation of sediment yield with one month lead (R^2=0.68, n=32) was nearly same as the current month (R^2=0.69, n=33). The highest correlation (R^2=0.77, n=31) between monthly NDVI and sediment transport was achieved using the current month plus two previous months. This represents a running seasonal composite value that will tend to smooth out sudden changes in NDVI and it is not surprising that it should increase the level of correlation. The results highlight the possibility of predicting monthly runoff and sediment transport using the remotely sensed NDVI data. The time scale for the monitoring could be

one month early or at least in the current month. The main advantages of using NDVI to make such a prediction rather than using precipitation and runoff data are that the latter two variables are often difficult to obtain over a large catchment, but NDVI data are relatively inexpensive and available on a regular basis.

Although the monthly NDVI-sediment transport relationship is relatively close, it is still much worse than the monthly runoff-sediment transport relationship. Figure 9-6 shows that monthly sediment transport was highly correlated with monthly runoff for all the catchments, demonstrating that monthly sediment transport was directly controlled by monthly runoff. The processes of sediment generation are affected by many factors in addition to variation in precipitation, such as topography, land use and soils, such that monthly sediment yield data has a closer relationship with monthly runoff rather than precipitation.

9.4 ANNUAL NDVI, RUNOFF AND SEDIMENT TRANSPORT

The quantitative relationships between annual NDVI, runoff and sediment transport for a given catchment cannot be examined due to the short periods of overlapping data (less than 3 years). Annual relationships must be more complicated than monthly relationships, since the latter are mainly governed by seasonal precipitation, whereas the former may be controlled by multiple factors. The relationships will also be dependent on the characteristics of catchments in terms of ecoclimates, topography, vegetation, land use and soils. Conclusions can not be drawn until a detailed examination has been undertaken. For a given catchment, long-term evolution of low values indicate a major vegetation cover change either through deforestation or an extensive period of drought but NDVI measurement itself could cause errors for such temporal changes. NDVI is affected by various sources of errors including aerosol contamination, instrument degradation, and orbital drift. The global mean of NDVI, for example, varied by an average of 10 per cent per year from 1985 to 1992 (Schultz and Halpert, 1995). Some, but not all, of this interannual variability is due to systematic error, which in the year of the satellite changeover or following

the Mt. Pinatubo eruption, was probably at least 20 per cent (Schultz and Halpert, 1995). This error makes interannual monitoring difficult, since vegetation changes from one year to the next may be on the order of a few percent and can easily be dominated by the noise (Schultz and Halpert, 1995).

9.5 NDVI SPATIAL VARIATION AND ITS RELATION WITH RUNOFF AND SEDIMENT TRANSPORT

9.5.1 NDVI spatial variations

The averaged NDVIs for the 12 catchments are plotted in Figure 9-7. In general the catchments with lower NDVI values such as Zimenda and Shigu have higher interannual changes. Two groups might be identified based on the NDVI. Zimengda and Shigu have particularly low NDVI. Although the other catchments have less profound variations, two properties may be summarised. First, Wantan has a very high NDVI. This is consistent with its high index in winter as discussed above. Second, the catchments located in agricultural areas such as Lijiawan and Xiaoheba have lower NDVI values. Spatial variations of NDVI within the Upper Yangtze can be explained in terms of varied climates, land cover/land use, and soils. The vegetation in the basin can be broadly identified as meadow, forest and agricultural crops from west Qinghain-Tebit plateau and mountainous areas to Sichuan basin. Different vegetation assemblages have different NDVI values. For example, deciduous forests have higher index values than the vegetation in semi-arid conditions (Drake et al., 1995). The NDVI changes in the Upper Yangtze are consistent with vegetation changes from west to east. Soil properties such as permeability and available water capacity (Yang et al., 1997) and soil colour have effects on NDVI index. The soil in the Sichuan basin (also called Red basin) is dominated by brick-like purple soils. The lower NDVI values for the catchment of Lijiawan and Xiaoheba may also be caused by this soil colour or the crops themselves have lower NDVI compared with natural vegetation. In Chapter 8 it was found that in the Upper Yangtze basin, elevation can be used as a surrogate for a

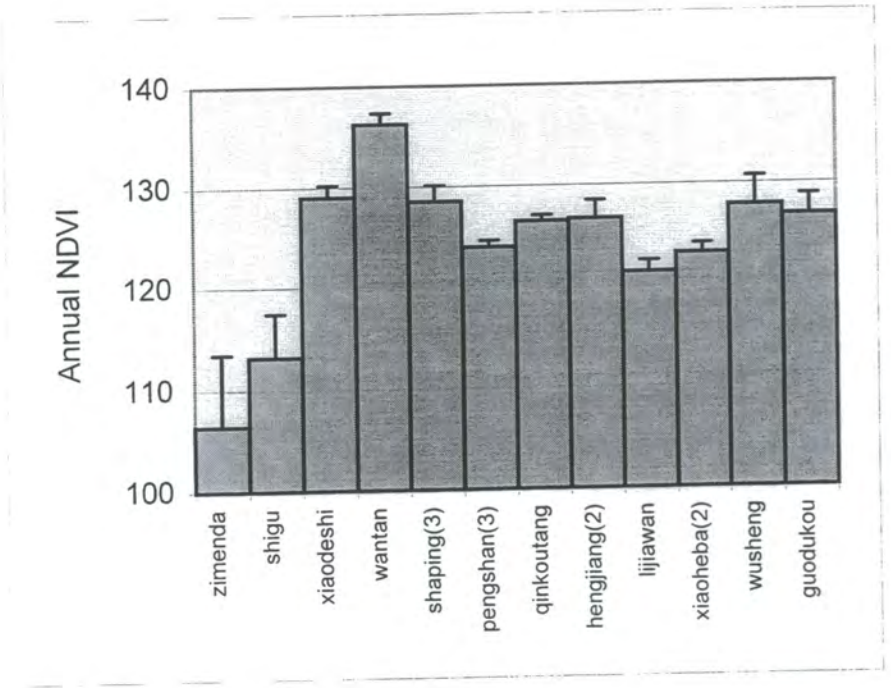

Figure 9-7, The averaged NDVI for the 12 catchments

series of variables including precipitation, temperature, vegetation, land use and soils, due to the effect of Qinghai-Tibet plateau on atmospheric circulation (Ruddiman et al., 1989). On the basis of the general analysis of NDVI spatial variation, the following two sections will be focused on the effects of elevation and precipitation on NDVI.

9.5.2 Effect of elevation on NDVI

The relationship between annual NDVI and mean elevation is plotted for the three years in Figure 9-8 (the whole upper basin is excluded for this analysis due to its lump with other 12 catchments and below is same). It can be seen that annual NDVI is highly correlated with elevation. However, the relations of elevation with NDVI is more complicated than that with long-term precipitation. There is a threshold value for the elevation-NDVI relationship. This critical elevation is around 2500 m, below which NDVI increased with elevation increase while above which NDVI decreased with elevation increase. The elevation threshold around 2500m is consistent with the results discussed in Chapter 8. The positive elevation-NDVI relationships below 2500 m is unexpected. One possible reason is that this may reflect different reflectance of vegetation, land use and soils at different elevations. The main agricultural areas in the basin are located in lower elevation areas with serious soil erosion (see details in Chapter 7), suggesting lower NDVI in these areas. As to the inverse elevation-NDVI relationships above 2500m, is due to the lower precipitation and temperature in higher elevation areas, which result in lower NDVI. More importantly, the areas with high elevations are frequently covered by seasonal ice and snow contributing to very low NDVI values.

9.5.3 Effect of precipitation on NDVI

The relationships between annual NDVI and precipitation for given catchments can not be examined directly due to a lack of corresponding precipitation data in the time period for which NDVI data are available. However, annual mean precipitation data available in the Global Ecosystems Database (GED) dataset which were used in

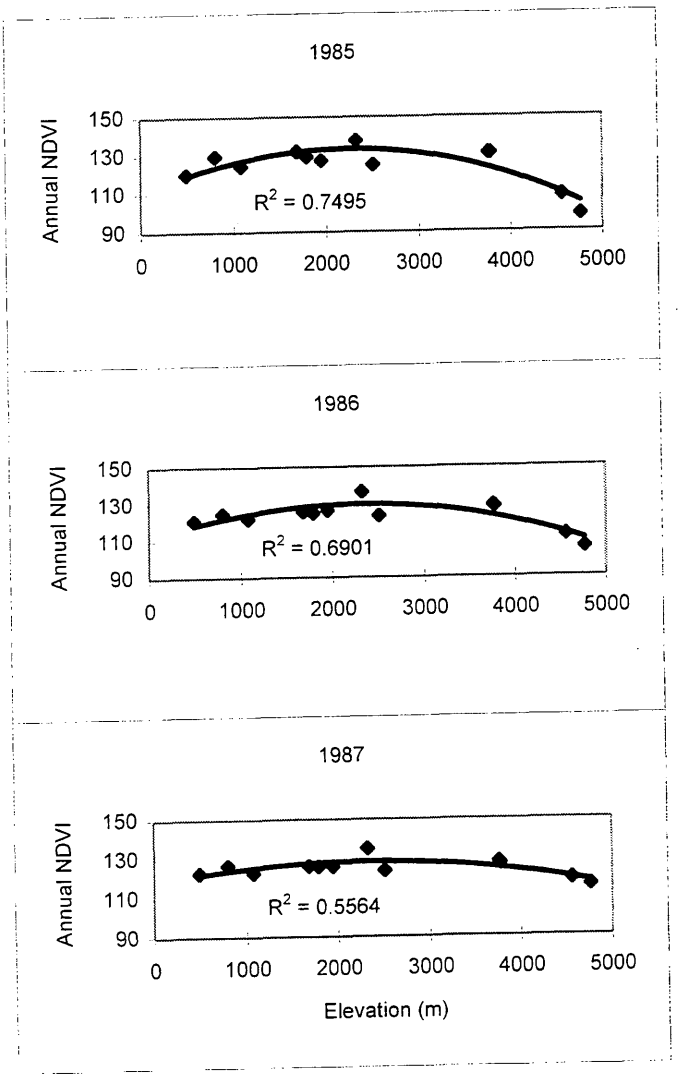

Figure 9-8, The relations between elevation and annual NDVI

Chapter 8, can also be used to investigate annual NDVI performance in relation to longer-term average precipitation. The annual NDVI variation with long-term precipitation is depicted in Figure 9-9. It can be seen that the NDVI-precipitation relationship is quite similar to the NDVI-elevation relationship. Annual NDVI performance with precipitation is also complex. Annual NDVI increases with precipitation below 800 mm but decreases with increasing precipitation above 800 mm. These results concur with the report by Nicholson and Farrar (1994), although they are not directly comparable. The areas with high precipitation are mainly located in Sichuan basin which is one of main agricultural areas in the Upper Yangtze. Crop cover is likely to yield lower NDVI values than natural vegetation in areas of higher precipitation. In addition, the vegetation cover may be poorer in the areas with higher precipitation in the basin as a result of soil erosion. Although it is conventional to consider vegetation cover as a controlling factor on erosion rates, there are parts of the red soil region in China, where severe soil erosion has truncated the A and B horizon of the soil and the land has subsequently been abandoned. In these situations it is difficult for plants to recolonise the indurated parent materials. In general, close NDVI-precipitation relationship is consistent with many reports (Schultz and Halpert, 1993; 1994; Malo and Nicholson, 1990; Davenport and Nicholson, 1993; Nicholson and Farrar, 1994). This close NDVI-precipitation relationship suggests that it is possible that NDVI will be closely related to runoff and hence sediment transport.

9.5.4 NDVI relations with runoff/sediment transport

While annual NDVI and runoff/sediment for a given catchment can not be examined, the implication of spatial NDVI variation to runoff and sediment transport can be examined using the data from the 12 catchments. Annual NDVI, runoff and sediment yield are plotted in Figure 9-10. Annual runoff and sediment yield have strong positive relationships with annual NDVI. The results are consistent with the relationships between monthly NDVI and monthly runoff and sediment transport discussed above. Among the three years examined, a poorer performance was observed in 1987 for runoff whereas a poorer performance occurred in 1986 for

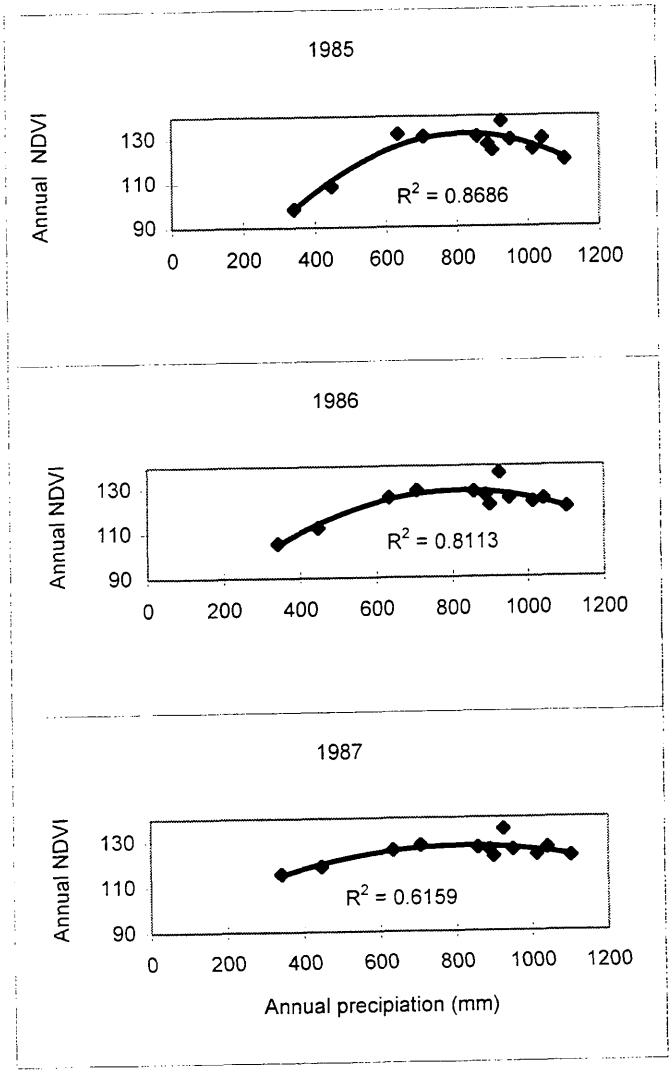

Figure 9-9, The relations between mean precipitation and annual NDVI

sediment yield. In a dry year, temperature plays an important role in the performance of NDVI. The scatter is attributed to the effects of vegetation, land use and soil types. Sediment yield data indicates both surface soil erosion and the sediment produced by mass movements and channel sources. It is obvious that the latter events can not be indicated by NDVI. Wantan catchment, in which mass movements (landslides) happened frequently as stated previously, plots as an outlier. In addition, specific sediment yield generally decreases with basin area due to sediment deposition (see Chapter 7). The basin areas for the 12 catchments vary over two orders of magnitude from the smallest to biggest (Table 9-1), which also contributes to the scatter. However, the overall performance is very good, considering varied conditions of vegetation, land use and soils within such large basins. For comparing the effect of NDVI and runoff on sediment yields, sediment yields are also plotted against runoff (Figure 9-11). Interestingly, this figure shows that spatial NDVI-sediment relationships are better than runoff-sediment relationships. This contrasts with the results in the situation, where monthly NDVI-sediment relationships are much worse than monthly runoff-sediment relationships. Sediment transport is determined by both sediment concentration and runoff. Due to its close relations with many soil properties, NDVI has relations with sediment generation, which may in part explain the close spatial NDVI-sediment transport relation. This close relation indicates that it may be possible to integrate NDVI into regional and global sediment yield studies, since little information on land cover has been investigated in previous sediment studies. While interannual NDVI change may be limited, its spatial variation is profound. This highlights the possibility to predict or monitor runoff and sediment yields in particular for the catchments without gauging stations using available runoff and sediment measurement from existing stations. This monitoring work is important for

an appropriate management of the Three Gorges reservoir in the near future. Furthermore, NDVI systematic errors, caused by aerosol contamination, instrument degradation, and orbital drift, as described above do not affect its spatial variation too much in any particular year.

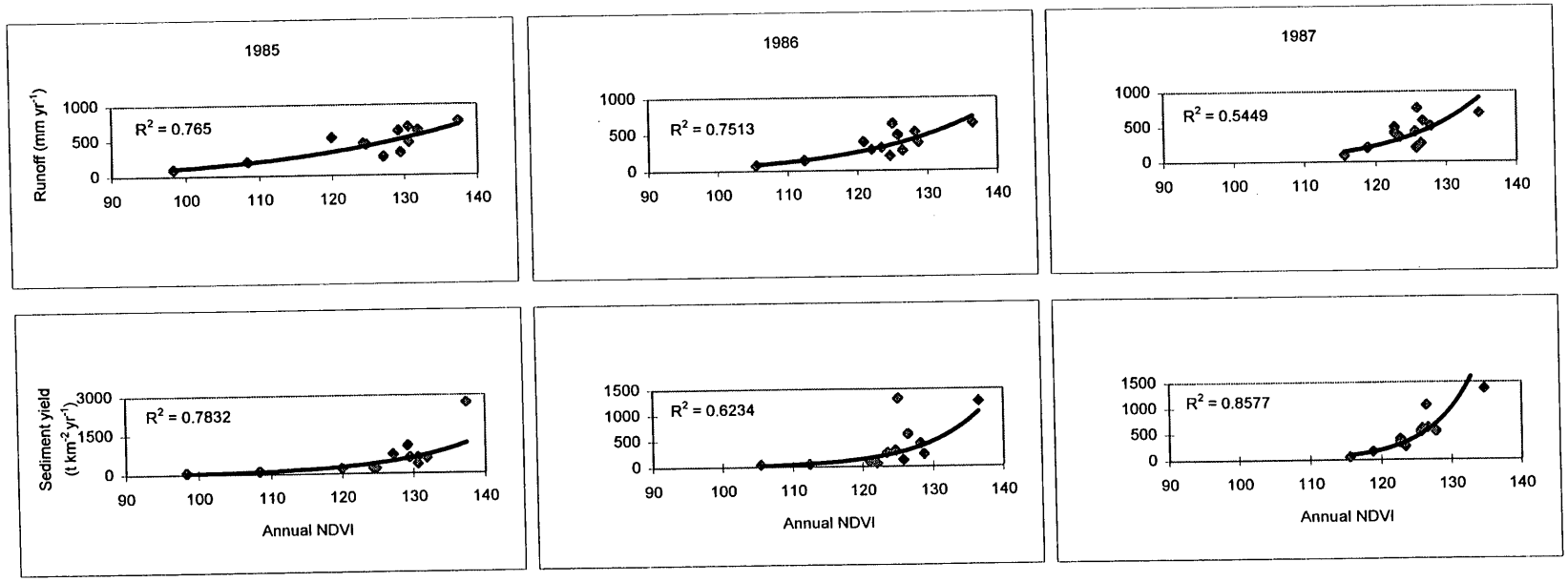

Figure 9-10, The relations between NDVI and runoff /sediment yields

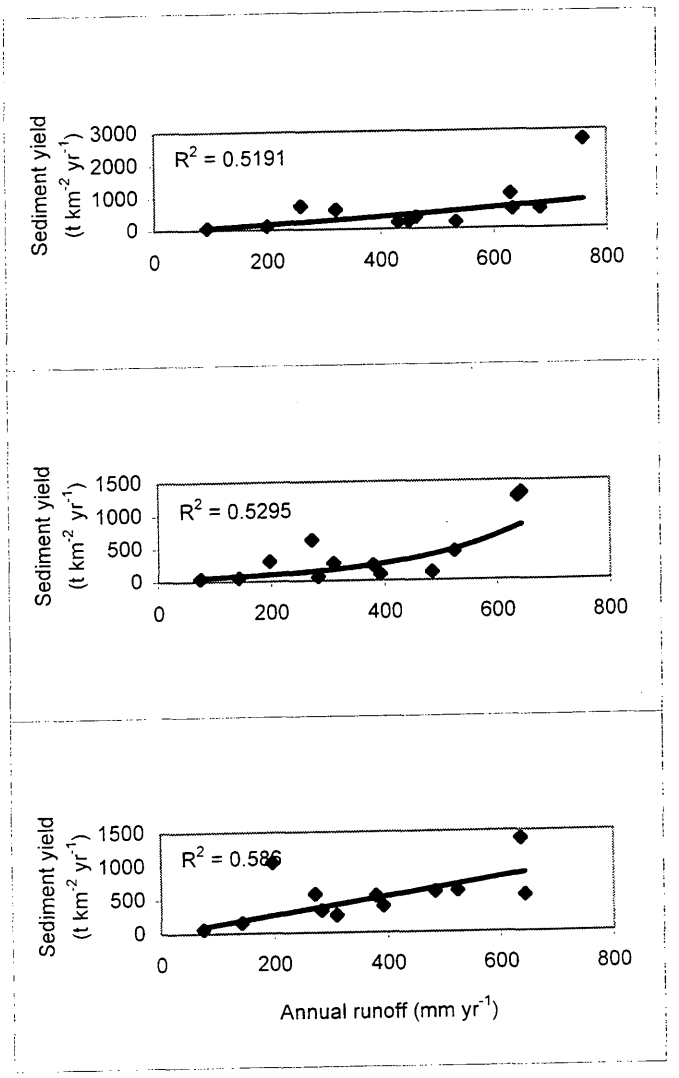

Figure 9-11, The relations between runoff and sediment yields

9.6 SUMMARY AND CONCLUSION

The relationships between NDVI, runoff and sediment yield using the 33 months data from April 1985 to December 1987 were examined in the Upper Yangtze. The patterns of monthly NDVI are similar to monthly runoff and sediment transport variation. The correlation between monthly NDVI and runoff and sediment transport are generally very good but depend upon catchment characteristic and the particular year. The relationships between annual NDVI, runoff and sediment yield for individual catchments cannot be examined due to the short period of overlapping data (less than 3 years). However, the relationships were examined spatially and the results indicate that annual NDVI is highly correlated with annual runoff and sediment yield. The variation in precipitation and NDVI is mainly controlled by elevation in the basin. The strong relationships between spatial NDVI and runoff and sediment yield in particular highlight the possibility to predict or monitor runoff and sediment transfer using remotely sensed NDVI data, particularly for those catchments without gauging stations. Using NDVI has many advantages over controversial methods based on rainfall-runoff models, since NDVI data are relative inexpensive, available on a regular basis and can be easily obtained throughout catchment. More importantly, monitoring of vegetation change can be integrated with this programme, since NDVI mainly indicates vegetation cover.

Although monthly NDVI is closely related to runoff and sediment yield, two problems were identified through the study which may hamper the predictive power of the technique by only using the NDVI data. First, monthly peak NDVI lagged one month behind or occurred one month earlier than peak runoff and sediment transport. Second, the NDVI exhibited little change compared with runoff and sediment transport during summer period, even in a drier year, between July and September. These problems might be due to temperature effects but can not be examined due to lack of corresponding data.

The main limitation of this study is time scale (only 33 months), because runoff and sediment data are not accessible after 1987 and no NDVI data before April 1985 is available from the GED CD-ROM. Therefore, the long-term relationship between NDVI, runoff and sediment transport requires further investigation. Precipitation, temperature and envapotranspiration data are available before 1987 in the Upper Yangtze, permitting a comprehensive study on the hydrological significance of NDVI in the area. If appropriate, relationships between NDVI and environmental variables can be developed, and the temporal and spatial variations of the NDVI would provide a useful tool for monitoring climatic and human-induced environmental changes.

10. CONCLUSION AND PROSPECT

10.1 A BRIEF OVERVIEW OF THE STUDY

The environmental effects of the mega TGP and its subsequent management have become a focal point, attracting extensive attention from all over the world. In the past 15 years some comprehensive feasibility studies on the environmental effects of the project have been carried out but those studies have been focused upon an integrated evaluation and macroscopic prediction as well as conceptual countermeasure strategies. The concern about the rapid increase of soil erosion over the last few decades and its consequence for downstream sedimentation still remains. The project has been undertaken with the aims of assembling information on soil erosion and sediment yields, which are important for an effective management of the potential sedimentation problem associated with the on-going TGP. It includes small-scale appraisal of soil erosion and sedimentation using the radionuclide tracer Cs-137 and a large-scale investigation of sediment transport using sediment load data within the Upper Yangtze basin, China. The main aims and objectives of the study are:

1) to examine the potential for using Cs-137 to investigate soil erosion and sedimentation in the particular area dominated with dissected terraces and coarse soil texture;

2) to investigate the long-term patterns and rates of soil erosion on slopes and sedimentation in the reservoir as well as their linkages;

3) to examine spatial variability and temporal changes and the reasons for the change throughout the Upper Yangtze basin;

4) to examine the spatial variability and its relationships with the potential influencing factors such as topographic, hydroclimatic and population density in the Upper Yangtze basin;

5) to investigate the potential to monitor sediment yields in catchment scale using remotely sensed NDVI data.

The purpose of the chapter is to give a brief summary of the findings of the thesis. This includes the main achievements, limitations and prospect for further study.

10.2 ACHIEVEMENTS FROM THE STUDY AND THEIR IMPLICATIONS

10.2.1 Long-term patterns and rates of net soil loss on slopes

Average net soil loss rates over past 40 years has been successfully estimated using the Cs-137 technique. More than 40% of sampling points have net soil loss of 2500-5000 t km^{-2} yr^{-1}. Mean net soil loss is 4400, ranging from 1,000 to 12,000 t km^{-2} yr^{-1} depending on the field situation such as the slope and the status of terrace maintenance. Mean soil loss falls in upper range of the "moderate" soil loss class (2,500-5,000 t km^{-2} yr^{-1}) according to the Chinese standard classification scheme. The high erosion rates are mainly due to steep slopes exacerbated by subtropical monsoon climates and highly erodible soils (purple soils). The slopes for those arable fields are still very steep, although farmers have attempted to reduce their angles through deliberate soil removal and terrace maintenance. Mean slope angles measured from around 47 fields is 25° with minimum of 15° and maximum of 36°. Water diversion from the top of each field can considerably reduce erosion but the diversion through the ditches must be managed well, otherwise considerable amounts of soil can be washed away through those ditches. Building terrace walls at the bottom of each field can also prevent soils transfer outside the field. These measures

should be recommended to local farmers but the overall solution to the problem is to build level terraces or to limit cultivation on those steep slopes.

The severe soil erosion is similar for sloping land in the whole Yangtze basin. One of the countermeasures to curb serious soil erosion is to establish soil and water conservation forests along the Upper and Middle reaches of the Yangtze river which were started in 1989. Emphasis on afforestation in the Three Gorges area began around 1992. Because of the effort, the area affected by soil erosion in the Three Gorges area decreased by more than 8,000 km^2 according to estimates by the Ministry of Forestry in early 1997. It is not reported yet how the newly planted forests are distributed in the area and to what extent they can keep growing. Even in the best case, the problem is still very severe, since the ecosystem in the area is very fragile due to steep slopes and the limited amount of forest land (the percentage of forest land accounts for less than 5% of the total land in most of the 20 counties around the Three Gorges and no more than 13% at best). According to the law of China's forestry to promote sustainable agriculture and favourable ecological environment in such a rugged region requires a forest coverage greater than 50%, and cultivation is not allowed if the slope of greater than 25 degree.

10.2.2 Sedimentation rate and sediment yield in Yiwanshui catchment

The average sedimentation rate based on the first core obtained from the small reservoir built in 1958 is 3.65 cm yr^{-1}. This is much lower than the 10 cm yr^{-1} average sedimentation rate estimated by the local government, but is very high compared with reports based on caesium-137 chronology elsewhere (Higgitt and Walling, 1993; Foster and Walling, 1994; He et al., 1996). The dating layers are successfully identified based on Cs-137 concentration profiles and the particle size distribution. A sediment yield of 3490 t km^{-2} yr^{-1}, has been estimated based on bathymetric measurement. The changes of sediment yield were reconstructed using Cs-137 dating layers. The highest sediment yield, around 6,000 t km^{-2} yr^{-1}, occurred during the period of 1968-77 and then decreased in the period of 1987-94. Sediment yield is highly influenced by precipitation but the main governing factor in the Three

Gorges area is land use change. Massive deforestation, starting in the late 1950s, was the main reason for the higher sediment yield towards the base of the core. The most serious soil erosion happened during a few years after the deforestation. The agricultural reforms started from the beginning of 1980s has reduced land pressures. This may significantly reduce soil erosion and hence the sedimentation problem.

10.2.3 Sediment delivery and budget for Yiwanshui catchment

With an estimate mean soil loss rate for the dominant sloping arable land and information about land use within the catchment, it is possible to estimate an average erosion rate for the whole catchment and the proportion of the eroded soil from varied sources. The estimated average erosion rate is 4170 t km^{-2} yr^{-1}, while the proportion of the soils eroded from sloping arable land, wood & grass and gully & terrace wall is 62%, 7% and 31%. This gives a sediment delivery ratio (SDR) of 0.84. The higher ratio is due to steep catchment slope and small catchment size since SDR in general decreases with increasing basin size. SDR also indicates that 16% of eroded soils were deposited before arriving in the reservoir. With little floodplain in the catchment, it is believed that most of this was deposited in paddy field. A sediment budget has also been estimated that the majority of sediment source comes from arable land is confirmed by comparing Cs-137 activity in the sediment of the reservoir with paddy fields and topsoils throughout the catchment.

10.2.4 Sediment yield in the Upper Yangtze: spatial variability and temporal changes

Spatial variability in sediment yields within the whole of the Upper Yangtze has been examined by employing various standardisation methods. It is found that the Jialing, followed by Fu and Qu tributaries, has a substantial relative contribution to the sediment load discharged to the Yangtze river. The Qu and Fu, the tributaries of the greater Jialing, have become increasingly important sources during the recent period. These three rivers drain the agricultural productive lands of the Sichuan basin. In addition, mass movement is very frequent in the upper Jialing which also contributes a considerable amount of sediment load directly to the river. In contrast, the

tributaries originating in the mountainous terrain of the far west of the basin (the Jinsha and Yalong) have substantially smaller contributions relative to their drainage area. The sediment yield is also very high in the lower Jinsha tributary due to frequent mass movement activity.

The study has also demonstrated that sediment loads exported from large catchments mask a considerable amount of variability in the trajectories of soil erosion and sediment transport within different parts of the catchment. Oscillation around a non-trending mean value is usually attributed to hydrological variability but further investigation can demonstrate underlying changes in the sediment yield-runoff relationship. Sediment yield has mainly increased for the Dadu, Qu and Wu tributaries and decreased in the Tuo and Upper Jialing. Most of the observed decreases in sediment yield can be related to the construction of large reservoir schemes interrupting the downstream conveyance of sediment. Comparison of sediment yield and runoff data suggest that detectable changes in sediment delivery occurring in the Upper Yangtze reflect an increasing supply induced by human activities over the last 30 years. The evidence for increasing sediment supply in the catchment buffered by increasing storage in intermediate reservoirs raises further concerns. As this reservoir storage begins to fill, the trap efficiency of individual reservoirs will decline and the conveyance of sediment downstream will increase. The long-term impact of the exhaustion of artificial reservoir capacity and the remobilisation of sediments from storage could be significant. The variable response of large catchments to phases of human disturbance and river engineering provides many challenges to basin management. The present study suggests that detailed analysis of intra-catchment sediment yield data, combined with spatially distributed information on both historical changes in land use and resource exploitation and on runoff variation could help to forecast future sedimentation potential.

10.2.5 Sediment yield in the Upper Yangtze: variability modelling

With the basic understanding of the temporal variability of Upper Yangtze sediment loads and its control (land use and mass movement), attempts have been made to

model the spatial variability using topographic, hydroclimatic and population variables. The dataset is quite 'noisy' due to the varied environmental conditions and human activities. The data have been grouped under the three scenarios, e.g. tributary, catchment size and maximum elevation. It is found that the relationships between sediment yields and those variables are complicated and in the form of a polynomial. Sediment yields tends to increase with mean elevation below 2000 m but decrease above 2000 m. The latter stands in contrast to investigations of global sediment yield which emphasise the importance of mountainous (high elevation catchments) as major suppliers of sediment to the world's oceans (Milliman and Syvitski, 1992). Originating from the Qinghai-Tibet plateau, most of the Upper Yangtze is located in areas with elevations above 3000 m. As a result, a large number of the sub-catchments in the sediment yield dataset contain land above 3000 m in contrast to previous studies of global or regional controls on sediment yield which are skewed towards lower elevations (Milliman and Syvitski, 1992; Probst and Amiotte-Suchet, 1992; Summerfield and Hulton, 1994). In general, sediment yields increase with population density but decrease if the population density was very high. The latter may indicate a lower contribution of sediment from plains since, in general, population density is very high in flat areas (of the Sichuam Basin) where soil erosion is minimal. In the Upper Yangtze basin this inverse relationship between sediment yield and population density may also indicate the effects of water conservancy projects on sediment yields, because most of those projects are located in the areas with high population. The relationships between sediment yields and hydroclimatic variables are also complicated. Sediment yields, in general, increase with precipitation and runoff but inverse relationships are also documented. These relationships are, at least in part, consistent with the report by Wilson (1973). The study suggests that the relationship between sediment yields and its variables may be completely different depending on the ranges of the variables. In terms of the tributaries, all the variables can explain 87% variance for Jinsha-Yalong, 95% for Dadu-Min and only 33% for the Jialing tributary. Multiple correlation was not undertaken for the Wu tributary since there are not many catchments in the tributary. For the heavily human-influenced Jialing tributary, land use and soils might be

important variables. None of these factors are presently available at sufficient resolution in the public domain for incorporation into the analysis.

10.2.6 Monitoring soil erosion and sediment yield using remote sensed NDVI data

Close environmental monitoring in the Upper Yangtze is necessary for an appropriate management of the Three Gorges Reservoir. The possibility of monitoring catchment scale water discharge and sediment yields using remotely sensed NDVI data is investigated using data from 13 catchments covering 33 months from April 1985 to December 1987. The patterns of monthly NDVI are similar to monthly runoff and sediment transport. The correlation between monthly NDVI and runoff and sediment transport are generally very good but depend upon catchment characteristic and the year. Annual NDVI is also highly correlated with annual runoff and sediment yields, because NDVI is closely related annual precipitation. The variations for precipitation and NDVI are mainly controlled by elevation in the basin. Although NDVI is closely related to runoff and sediment, two problems were identified through the study which may hamper the predictive power of the technique by only using the NDVI data. First, monthly peak NDVI lagged one month behind or lead one month early than peak runoff and sediment transport. Second, the NDVI exhibited little change, compared with runoff and sediment transport, during the summer period even in a drier year. These problems might be due to temperature effects but cannot be examined due to lack of corresponding data. Therefore, the long-term relationship between NDVI, runoff and sediment transport requires further investigation, but may offer a means of estimating sediment yields in ungauged catchments

10.3 ASSESSMENT OF CS-137 TECHNIQUE APPLICATION IN THE AREA

Among the methods of erosion quantification (see Chapter 1 for details), the Cs-137 technique seems one of most suitable methods for dissected arable land, due to the

flexibility of sampling. The technique has been successfully used for quantifying the patterns and rates of net soil loss on dissected terraces and for reconstructing sedimentation and sediment yield change over the past 40 years. The application of the technique is considered in two chapters (Chapter 5 and 6). The quantified net soil loss and reconstructed sediment yield changes are consistent with available information for the surrounding area. However, the problems discussed below are encountered through the study.

10.3.1 Suitability of Cs-137 reference sites

In order to use the fallout Cs-137 technique to investigate soil erosion, a baseline input of Cs-137 (or Cs-137 reference) must be determined. Ideally, the samples should be collected from flat grassed land or forest land without any evidence of erosion or deposition. It is difficult to find such sites in the small catchment. It is likely that such sites are difficult to find throughout China, due to extensive human activity. The inaccuracy in estimation of the reference value will have a direct effect on soil erosion estimation. Cs-137 reference value was estimated using soil samples from a small field located in the watershed boundary. The averaged Cs-137 value is 2163 Bq m^{-2}. Although the samples have a low variability of 13.6% of coefficient variation (CV) and the reference value is comparable to the value of 2600 Bq m^{-2} used by Quine et al. (1992) in their study near Chengdu, Shichuan, uncertainty about the reliability of the baseline activity still exists due to frequent irrigation and drainage activity operated on paddy field. Although the topographic setting of the field suggests limited connectivity in sediment transport pathways, it is not clear whether agricultural activities can bring in or export considerable amounts of sediment.

10.3.2 Coarser texture of soils

The susceptibility of the sandstone to weathering combined with the high rate of soil erosion, means that the texture of purple soil is very coarse, with a sizeable percentage of particles size over 2 mm. It is assumed that Cs-137 fallout is absorbed by fine soil particles and its subsequent transport is associated with sediment. This is one of the principles underpinning the Cs-137 technique. The coarse materials of

purple soil indicate that preferential transport of fine soils must happen, suggesting that Cs-137 enrichment ratio must be integrated into erosion quantification. Without detailed collection of sediment samples, it is difficult to estimate the ratio. The study estimates the ratio using reservoir deposits and the topsoil samples taken throughout the catchment. The estimation also takes into consideration the erosion contribution from different land use types. The estimated enrichment ratio is as high as 1.5. As the enrichment ratio is likely to vary with rainfall and land use change, there is a problem associated with its estimation.

10.3.3 Deliberate soil removal

The differential distribution of Cs-137 activity can be partly caused by deliberate soil removal (or retrieval), a frequent activity in the area in order to maintain land productivity. The removal process includes adding the newly-weathered materials from terrace walls and retrieving the sediment deposited in ditch or channel. The removal also includes deliberate soil redistribution from the top to bottom of the terrace. There are no doubts that the deliberate soil removal and retrieval will result in Cs-137 redistribution vertically within the soil profile and spatially across the field as well. The dimension and magnitude of the removal cannot be assessed without further information, although its impact of Cs-137 flux may be small compared to the action of erosion processes. Nevertheless, the estimated net soil loss will include an unknown proportion caused by deliberate removal.

10.3.4 Uncertainty associated with radionuclide fallout

The Cs-137 technique is also hampered by uncertainty about ambient levels of Cs-137 fallout from Chinese weapons tests and the Chernobyl accident. Unlike western countries, there is no public domain report on the records of radionuclide fallout in China. While the global patterns of fallout may be similar, local fallout generated from Chinese nuclear weapons tests and the Chernobyl nuclear power accident in 1986 may be different. Chinese tests started in 1964 and reached the highest in 1977-78. Based on the data recorded in the Meteorological Research Institute of Japan (Hirose et al., 1987) the majority of global fallout after 1976, if not all, was contributed from Chinese tests. There was, however, far more activity in the most recently deposited sediments than can be explained by the direct atmospheric fallout

of the Cs-137 record. Possible local Cs-137 fallout generated from Chinese tests cannot be fully ruled out. Some deposition from Chernobyl fallout must also have happened in China but cannot be evaluated due to the lack of information in China. Any evidence of Chernobyl fallout derived from the presence of Cs-134 can no longer be identified due to its relatively short half-life (2.2 years). Uncertainty regarding the temporal variation of incoming fallout deposition imposes some constraints on the quantification of soil erosion from Cs-137 measurements using existing calibration techniques, particularly mass balance models.

10.3.5 Calibration from Cs-137 to soil erosion rates

The two methods, full mass balance and simplified mass balance model, were employed to quantify soil erosion rates using Cs-137 measurements. It is found that the simplified model overestimates soil loss due to the simplification that all atmospheric Cs-137 fallout happened in 1963 and to the model's sensitivity to an estimate of the plough layer thickness. This demonstrates that annual fallout is necessary information for erosion quantification, if the mass balance model procedure is accepted. However, as stated above, there is no fallout record information in China. This requires an estimate of annual fallout in addition to reference value development. The study uses the Sarmiento and Gwinn (1986) model to estimate Cs-137 fallout from 1954-1974. The amount of Cs-137 fallout during the period accounts to 80% of the total fallout estimated by soil reference samples. Together with the fallout from 1975-94, it is very close to the estimate constructed from soil samples. This highlights the possibility of integrating annual fallout into the quantification of soil erosion.

10.4 THE LIMITATIONS OF THE STUDY

10.4.1 Soil sampling in the small catchment

The study has concentrated on sloping arable land using the Cs-137 technique to quantify the patterns and rates of soil erosion. Little attention has been drawn to

forest land and paddy fields in the small catchments. No systematic soil sampling was undertaken on those lands which means that overall evaluation of soil erosion rates on non-arable land and sediment deposition before the reservoir cannot be confirmed. The distribution of paddy fields located in the valley and lower land is very typical in south China but a systematic assessment of the role of paddy fields as an influence on the conveyance of sediment has not been fully addressed yet. The paddy field is developed on depositional materials by farmers and the magnitude of trapping of sediment from upslope locations is still not very clear. The systematic evaluation of soil erosion and sediment redistribution in such system is needed. The role of paddy fields in the sediment delivery systems may be important for maintaining sustainable agricultural development throughout south China.

10.4.2 Data availability and access

The study obtained abundant data from many different sources. However, the analysis can be further improved if additional related data could be obtained. The shortage of the data are due to a few reasons. First, some data are not accessible after 1987 due to recent strict control of data in China. Rainfall data after 1987 in Changshou county and runoff and sediment load data for the whole Upper Yangtze basin after this date is restricted, partly due to the controversy arising from the Three Gorges Project. The difficulty in obtaining necessary data results in an incomplete integrated analysis. For example, the complete analysis of the reservoir core needs rainfall data after 1987 to examine any coarse layers near the sediment water interface. The temporal analysis of sediment transport within the whole Upper Yangtze would be much better if the data after 1987 were available. In addition, the examination on the relationships between NDVI and runoff & sediment transport is very preliminary due the short overlap in the two datasets. More importantly, land use data of high resolution across China are available in digital format. The data are maintained by the China Research Centre at Griffith University but cannot be obtained due to a confidentiality agreement made by Australian and Chinese partners. Otherwise the land use data could have been integrated in the sediment yield variability modelling. The land use types may be very important factors in

controlling sediment yield variability particularly in Jialing tributary (see Chapter 5 for details). Second, some data are available but very expensive to buy for a PhD programme. Precipitation data, for example, were recorded together with runoff and sediment load. Temperature, precipitation and evapotranspiration data are all available from 1950s to 1980s in the Upper Yangtze, making it possible to conduct a comprehensive study on NDVI's hydrological significance in the area. For some data, the shortage will be improved by the development of global and regional databases. This is quite promising for an integrated environmental study.

10.5 PROSPECTS AND FURTHER RESEARCH

10.5.1 Cs-137 technique application in the area

The quantification of soil erosion is very difficult in dissected steep arable land using conventional methods such as runoff plots and model estimation. The flexibility of soil sampling for Cs-137 measurement made the technique promising for this area. Some of the problems arising from the study can be overcome or integrated in future studies. More importantly, the Cs-137 technique can be integrated with traditional methods such as bathymetric investigation of sediment yield. This makes the technique very competitive compared with other methods. The uncertainties on Cs-137 fallout cause difficulties for quantifying soil erosion and sediment redistribution but, on the other hand, provide opportunity to dating years. The peak from Chinese test in 1977-78 and Chernobyl accident in 1986 may provide new dating layers in depositional chronologies. Both peaks were documented in the study and are useful for reconstructing the history of sediment yield change. The understanding of the mechanisms of reservoir sedimentation in small catchments in the Three Gorges area should provide useful information for the management of the larger Three Gorges reservoir. For example, comparatively little is known about the implications of reservoir sedimentation on trap efficiency and the extent to which larger amounts of sediment will be conveyed downstream as tributary reservoirs begin to fill up.

10.5.2 GIS application for large scale catchment modelling

The modelling of sediment yield with multi-variables, requires data capture, management and manipulation. The increasing availability and improving resolution of global environmental databases offer the prospect of examining the relationships between fluvial sediment yield and various catchment properties within the framework of powerful GIS. To date, GIS-based studies have tended to focus on global scale variation or comparison between different catchments in a regional context. The analysis of variation within large catchments offers considerable potential for the investigation and management of sediment-related problems. In the case of the Upper Yangtze basin where the attention of environmentalists has been drawn to the Three Gorges Project, the integration of sediment yield records and environmental databases within GIS not only provides a basis for the investigation of controls on the patterns of sediment yield but provides a platform for predictive modelling. GIS can be used in many ways in catchment modelling, including DEM construction, catchment boundary delineation, derivation of topographic features and extraction of the variables in digital format.

10.5.3 NDVI application for monitoring soil erosion and sediment yield

The preliminary results from the study indicate that the relationships between NDVI and runoff and sediment are strong. This suggests that it is possible to predict or monitor runoff & sediment using remotely sensed NDVI data, particularly for the catchments without gauging stations. Using NDVI has many advantages over controversial methods which rely on precipitation to estimate runoff and sediment transport, since NDVI data are relative inexpensive, available on a regular basis and can be easily obtained throughout catchment. More importantly, this runoff and sediment yield monitoring programme using NDVI can be integrated with vegetation changes monitoring in a large scale catchment as the Upper Yangtze, where environmental change monitoring is important for the management of the Three Gorges Project. It was reported in 1996 that China is to establish a network to monitor the environmental changes. The Chinese government has approved the allocation of 90 million Yuan for the setting up of the network. But the network would consist of only 9 hydrological stations enhanced by a few more instruments

for water and air quality, and three ecological monitoring stations. This is far from enough for adequate monitoring in a region larger than Taiwan. More importantly, the majority of the sediment load in the Upper Yangtze is from areas outside the Three Gorges area, so an environmental monitoring across the whole Upper Yangtze basin is necessary for sedimentation management of the reservoir. Such monitoring will be a long-term research issue, as noted by Burt (1994), to go along with the dam construction, population relocation and the reservoir management.

10.6 SCALE AND HIERARCHICAL PROBLEMS

At the outset of the thesis the apparent contradiction between the long term trends of soil erosion in the Upper Yangtze catchment and those of sediment yield at the catchment outlet at Yichang were noted. Despite the evidence for an increasing extent and magnitude of soil erosion there is no clear increase in sediment delivery to the Three Gorges Reservoir site. In the second half of the thesis the detailed pattern of temporal trends from gauging stations within the catchment has been examined and spatial variability in the time series has been highlighted. Nevertheless, the issue of comparing trends in sediment production (i.e. erosion) and sediment output (i.e. sediment loads) draws attention to problems of scale. It is important to consider the degree to which detailed measurements of soil transfer in small catchments are relevant to the management of sedimentation in a mega-project such as the Three Gorges. In particular, the issue of extrapolating results from small catchments to larger ones is commonly encountered in geomorphologic research. Many of the issues are encapsulated in the "sediment delivery problem" (Walling, 1983) which identifies the consequences of aggregating data at different scales. Here, issues of temporal aggregation, spatial scales and hierarchical data sets are discussed.

10.6.1 Temporal scale problems

The caesium-137 technique, appraised in section 10.3, provides a temporally averaged erosion rate for the period since the commencement of bomb-test fallout. This has certain advantages over alternative erosion estimation techniques because

short term measurements are often prone to unusual conditions (for example particularly wet or dry years). However, the application of Cs-137 may cause some difficulties in environments where land use changes have been frequent and marked. It is also not possible to compare the Cs-137 derived estimates directly with historical measurements of sediment yield, such as the gauging station record used in the thesis.

In comparison, sediment load data measured from hydrological stations record large fluctuations in sediment flux due to human activity or possible climatic changes. The dataset obtained throughout the Upper Yangtze comprises average monthly values of water discharge and sediment transport, but this study only concentrated on aggregated annual values. The hydrological responses to land use and climatic changes might be more obvious at seasonal scales, because of the marked variation between dry and wet seasons, throughout the Upper Yangtze. Clearly further examination of seasonal water discharge and sediment transport could be undertaken based on the available datasets. As to spatial variability, the study was focused on the 62 catchments with around 30 years of measurements and ignored the majority of the catchments. This is mainly for achieving a reliable value representing a relatively long-term period for each catchment considering marked year to year rainfall variation as discussed in Chapter 4. However, this process integrated the variance of runoff and sediment caused by the changes due to human activity. The obvious examples are the catchments where a large reservoir was built, and hence the annual average sediment yield should only include the measurements before the reservoir closure. Human impact on sediment delivery might be one of the reasons explaining the marked scatters of data. The rapid development of reservoir and river regulation schemes world-wide has major consequences for the interpretation of historical sediment load data.

10.6.2 Spatial scale problems

In addition to problems caused by the aggregation of temporally variable data and the handling of time series analysis where sediment yields vary considerably from year to year, the analysis of sediment yield data in a large catchment is profoundly

affected by spatial scale issues. These problems were principally encountered when obtaining explanatory variables from global environmental datasets and when examining sediment yield spatial variability.

Runoff and sediment transport are generated by complex processes on extremely heterogeneous materials and surfaces. The explanatory variables include catchment characteristics such as precipitation, land use, topography, soil and geology. The topographical features including elevation and elevation dependent variables such as flow direction, flow routes, drainage density and slopes/relief, can now be evaluated using DEM within GIS. All these features are scale-related. For example, the averaged value over all the cells from a 10×10 m^2 grid is not represented by same average from a 1000×1000 m^2 grid. The resolution of the data employed will be dependent on many factors such as the purpose of study, data availability and computer space demand. Care is needed when extracting catchment-averaged values of environmental variables for the sediment yield regression analysis, especially if catchments are of varying size.

Issues of scale and representativeness also affect the research methodology employed in small catchment. Soil samples for erosion quantification using the Cs-137 radionuclide as a tracer within the small catchment were taken from individual fields. The development of relationships between erosion and topographical features requires a higher resolution DEM representing the features of dissected sloping land. However, the DEM built upon the available contour map of 1:10,000 cannot indicate the dissected feature, and hence has a limited usage, since the Cs-137 inventory is extremely sensitive to micro-topographical features. Due to the prominence of man-made features in the Chinese landscape, application of a DEM derived from available contour maps to small scale hydrological studies will face similar difficulties. The development of GPS techniques might be useful for mapping man-made features.

When changing from a small to a large scale in space, the resolution requirement for the topographical information is less demanding. The environmental data used for the large scale sediment yield study are from different sources with varied resolutions as

discussed in the Section 4.4 of Chapter 4. The elevation is from global DEM (30×30 seconds) from USGS, precipitation (30×30 minutes) and NDVI (10×10 minutes) from Global Ecosystems Database (GED) and population density (2.5×2.5 minutes) from Asian Population Database (APD). These data have the highest resolution available in the public domain. By comparison with most previous studies at the global scale, the data have a relatively high resolution and can describe a reasonably good heterogeneity within subcatchments. The global DEM can be used to extract a varieties of morphometric variables. The study, for example, has successfully delineated the boundaries for around 40 subcatchments and developed most of major drainage from the 30arcsecond DEM using Arc/Info surface hydrological analysis functions. However, the resolution for some data is still not high enough for certain purposes. Again, taking the DEM as an example, the resolution is not high enough to undertake catchment delineation in relatively flat areas notably in the Sichuan Plain. The drainage network, a highly scale-dependent variable, was extracted from the 30arcsecond DEM and can be used as a flow route for registration of hydrological stations but might not be appropriate to be used as an independent variable for a sediment yield study, because many small streams cannot be obtained from routine GIS analysis. Another example is precipitation data. Each cell for the 30×30 minute resolution grid is equivalent to approximately 1,600 km^2 in the study area. Obviously this cannot indicate any rainfall heterogeneity for those subcatchments with drainage area of less than 1,600 km^2 (which includes 10 basins from the set of 62 subcatchments used for the variability modelling in Chapter 8). The variables from different resolution datasets may be valid for a multivariate analysis as employed by the study but problematic for further hydrological model applications. The use of fractal dimensions for extrapolating between different scale resolutions may help overcome some of the problems.

The study examines sediment delivery within catchments of widely varying sizes. The implementation of the Cs-137 technique (Chapter 5 and Chapter 6) requires a manageable small catchment due to a large number of soil samples involved. The small catchment of Yiwanshui in which the Cs-137 techniques were used to quantify soil erosion rates and to date sediment yield changes, is very typical of the Sichuan

Basin in terms of soil, land use and topography, but obviously cannot cover the variety of environmental characteristics and soil erosion forms, notably mass movement (landslide and debris flow) and bank erosion, throughout the vast Upper Yangtze basin. This is complemented by the large scale sediment yield study using the sediment load data obtained across the whole basin. As discussed in Chapter 1 the sediment load measured at an outlet of catchment is a lumped and an averaged sediment yield and provides no information about the heterogeneity of soil erosion within the catchment. This, in return, requires a disaggregated study to understand detailed controls on sediment production and the spatial patterns of soil loss and accumulation within the catchment. The large-scale study itself employed the data from drainage areas varying from around 100 to 1 million km^2 for all the 255 stations and from 300 to over 1 million km^2 for the sub-dataset with longer measurements (see details in Chapter 4). As discussed in Chapter 7, sediment yields from basins of widely varying size cannot be compared directly because of the likely relation between sediment yield and drainage basin area. Brune (1948) developed a relationship to correct the sediment yield from varying basin area. After correction, the values represented mean annual sediment yield from drainage basins with an area of 259 km^2 (= 100 sq miles) (Wilson, 1973). However, in subsequent global and regional studies, this technique has not been employed. Instead, sediment yield-basin area relationships have often been examined through plotting sediment yield against drainage area. Because sediment yields are strongly dependent upon the size of the drainage basin, Milliman and Syvitski (1992) stated that sediment yields cannot be portrayed accurately on a map. The study employed two methods in order to remove the effect. A standardisation method developed based on a sediment yield-drainage area relationship was employed for comparison of spatial variability in Chapter 7. The bivariate relations between sediment yield and environmental variables were analysed for different catchment sizes, and a calibration method which again was developed based on sediment yield-drainage area was used for mapping purposes in Chapter 8. Consideration of the spatial scale problem is also crucial for undertaking temporal analysis for detection of sediment yield changes. The Upper Yangtze sediment yields, viewed from the catchment outlet at Yichang alone, do not appear to have changed markedly in recent years, but the changing trend of sediment yield is

detectable for smaller catchments. This is the basis for carrying out the time series analysis as introduced in Chapter 1 and Chapter 7. The Upper Yangtze as a whole has a huge capability to store sediment and buffer the effects of increasing sediment supply due to recent water conservancy projects. The study demonstrates that the detection of sediment yield changes due to human activities and possible climatic change requires detailed study from small catchments and that the analysis of larger catchments' data could be misleading. Little research has been conducted on the longer-term implications of sediment interception, storage and subsequent reduction in trap efficiencies of reservoirs of varying sizes. The large volume of existing reservoir capacity in the Upper Yangtze, combined with its rapid loss through sedimentation suggests that modelling of trap efficiency and sediment delivery would be a logical extension of the current study. Attempts to map sediment yield at the scale of the whole basin, as attempted with multiple regression techniques in Chapter 8, can provide generalised information on the spatial variability of sediment fluxes, but will have shortcomings as a management tool, because of the combined effects of catchment scale variability, residual variation from the regression routine and the impact of water conservation structures on the downstream conveyance of sediment. In summary, scale-related problems represent a very complex issue in hydrological study and require further attention.

10.6.3 Hierarchical problems

The hierarchical (nested) problem has not been fully addressed by previous global and regional studies of sediment yields. There is no clear method on how to calculate sediment yield for nested catchments. An agreed procedure for mapping and interpreting sediment yield data from a series of overlapping catchment is not apparent in the current literature (see section 1.3.4 of Chapter 1 for details). In addition, the overlapping problem is further complicated by the scale problems as discussed above. The basic concept in the raster-based hydrological modelling (ESRI, 1994) may be adapted to the network flow system (vector system), so that such functions as flow direction, flow accumulation and flow length can be used. However, the modelling units of the watersheds are not regular shapes as the cells in

the raster GIS. It is clear that further studies on the hierarchical problem and the problems associated with it are needed.

10.7 CONCLUDING REMARKS

The period of three years for a PhD programme is not short, but clearly is not adequate for developing a full understanding of the complicated issue of soil erosion and sediment yield in such a large basin. By undertaking a dual approach to the investigation of sediment dynamics, the study has been divided between sediment delivery systems of vastly differing scales. It has been argued within the thesis that studies at the scale of small experimental catchments are necessary to highlight the detailed controls on sediment production transfer and deposition, the spatial patterns of soil loss and accumulation and the pathways and dynamics of sediment transfer. Equally, when considering the impact of sedimentation on a mega-project like the Three Gorges Reservoir, it is necessary to consider the broader picture and compile information on controls over sediment yields at the regional scale. The transition between an experimental catchment of 1 km^2 and a network of gauging stations in a basin over 1 million km^2 is not straightforward, but it is hoped that the combination of scales draws attention to the necessity of combating erosion and sedimentation at the local and regional scale. Attempts to manage sediment transfer in a large catchment such as the Upper Yangtze requires the operation of sound soil and water conservation strategies applied at local scales.

The absence of a clear trend in the sediment load transported to Yichang station indicates the difficulty of establishing controls on soil erosion and sediment yields from the integration of many sub-catchments. Even when the hydrographic station record is examined in detail, patterns of sediment transport reflect spatial aggregation across catchment areas of at least 300 km^2 and more typically in the order of 1000-10000 km^2. Further attention is needed to examine sediment delivery processes over intermediate scales, in the order of 1000 km^2. At these scales the competing effects of accelerating soil erosion and the trapping of sediment by water conservancy projects could be analysed in more detail. Regional reservoir sedimentation surveys

might provide useful data in this respect and provide information towards the development of models of catchment sediment delivery.

The recommendations arising from this attempt to characterise sediment dynamics in the Upper Yangtze has relevance for many other planned huge hydropower projects in and beyond the basin. It was reported in 1997 that China is preparing to build another gigantic hydropower plant, the Xiluodu project, costing an estimated 40 billion Yuan (about 5 billion US dollars), with construction scheduled to begin in 1998. The new project, located in the upper reaches of the Jinsha River (including Yalong tributary) in Sichuan province, is designed to have an installed capacity of 11 GW, capable of generating 52.6 billion kWh of electricity a year, which will be slightly less than two-thirds the size of the TGP. It is obvious that the monitoring and comprehensive evaluation of soil erosion and sediment transport using different techniques in the basin is necessary for effective management of these gigantic projects.

APPENDIX 1, GENERAL INFORMATION OF SOIL SAMPLES FROM SLOPES

No	Filed position	Bed rocks	Landuse	Filed degree (°)	Field length (m)
1	M	Yellow	Arable	20	7.0
2	M	Yellow	Arable	19	4.5
3	M	Purple	Arable	20	4.5
4	M	Purple	Arable	24	5.0
5	M	Purple	Arable	28	6.0
6*	M	Yellow	Paddy	--	--
7	M	Purple	Arable	31	9
8*	M	Purple	Wood	23	5.0
9	U, M, L	Purple	Arable	32	12.0
10	M	Purple	Arable	21	13.6
11	M	Purple	Arable	26	10.0
12	U, M, L	Purple	Arable	16	15.0
13	M	Purple	Arable	22	7.0
14	M	Purple	Arable	21.5	7.0
15	M	Purple	Arable	34	3.0
16	M	Purple	Arable	29	18.0
17	M	Purple	Arable	24	5.5
18	M	Purple	Arable	25	10.0
19	U, M, L	Purple	Arable	22	9.0
20	M	Purple	Arable	21.5	7.5
21	U, M, L	Purple	Arable	19	8.5
22	U, L	Purple	Arable	24.5	3.0
23	U, M, L	Purple	Arable	22	6.4
24	M	Purple	Arable	25.5	5.5
25	M	Purple	Arable	23.5	5.5
26	M	Purple	Arable	20.5	6.5
27	M	Purple	Arable	28	6.5
28	M	Purple	Arable	23	7.6
29	M	Purple	Arable	25	6.5
30	M	Purple	Arable	23.5	7.5
31	M	Purple	Arable	29	3.5
32	U, M, L	Purple	Arable	26	7.0
33*	M	Purple	Paddy	--	--
34*	M	Purple	Paddy	--	--
35	M	Yellow	Arable	19	12.0
36	U, M, L	Purple	Arable	18.5	7.5
37*	M	Yellow	Wood	--	--
38	M	Purple	Arable	26	4.0
39	M	Purple	Arable	19	10.0
40	M	Purple	Arable	16	6.5
41	M	Purple	Arable	21.5	6.5
42	M	Purple	Arable	28	9.0
43	U, M, L	Purple	Arable	33	13.0
44	M	Purple	Arable	23	9.0
45	M	Purple	Arable	30	2.5
46	M	Purple	Arable	24	6.0
47	M, U, L	Purple	Arable	29	9.0
48	M	Purple	Arable	22	6.5
49	M	Purple	Arable	28	11.0
50	M	Purple	Arable	22	8.0
51	M, U, L	Yellow	Arable	19	9.5
52*	M	Yellow	Wood	25	---
53*	M	Yellow	Wood	20	--

Note: U: upper field; M: middle field; and L: lower field.

APPENDIX 2, THE SUMMARY OF COLLECTED SOIL SAMPLES FOR SEDIMENT SOURCES IDENTIFICATION

Sample Number	Field description
LXJR1	Yellow sandstone derived soils, soil depth >15 cm, flat suface, sample taken from area of tree-throw
LXJR2	Yellow sandstone 30 m from previous site. Uneven bedrock surface, soil of variable depth sample taken from localised pocket of deeper soil. Diameter of fir trees (12, 9, 9, 10, 9, 12, 18, 12, 16 cm, 20-30 year old plantation?). No evidence of cultivation, though probably cleared.
LXJR3	Some evidence of former terracing though three diameters consistent with other site. Slope angle 15°, soils >5 cm deep.
LXJR4	Slope angle 25 °, fir trees with oak understorey. Hummocky topography with isolated bedrock knolls (10-20 cm high) and pockets of deeper soil. relatively long slope facet (50 m), intercepted by cross-drain. Some evidence of small degraded terraces. Tree diameters 6-13 cm, possibly related to replanting following the Great Leap Forward? Yellow uniform texture evidencing no profile differentiation)site of former cultivation?).
LXJR5	25 °, 2 m from cross-ditch, relatively deep soil >10 cm.
LXJR6/7	Yellow sand soils on 7 m wide terrace, slope angle 8 °. Sweet potatoes growing, corn stlks also present. Terrace directly below forested knoll. Considerable evidence of erosion on field surface with distictive corn stalk pedastals [differntiate 4 month or 1 year erosion?, see photographs]. Also considerable evidence of in-filed deposition i.e. mud-cake with dissication polygons.
LXJR8/10	Yellow soils on plateau top, slope 2 °. Deep soil with sweet potatoes, corn, chilli pepers and lots of scrub birch and Rowan (?). Also some grass cover present. Sandstone outcrops displaying horizontal bedding structures (i.e., probably near anticline axis).
LXJR11	20 ° slope, again yellow soils upon the yellow sandstone. Mr Xiang described as "very hard and shallow soils". Lots of scrubby birch/oak. Large fir trees maximum diameter 20 cm.
LXJR12	Sample obtained from the base of 10 cm 'gully' incised into 20 ° slope.
LXJR13	Sample from materials collected in cross-ditch with 5 ° running left to right)looking upslope) and defining 5 m wide terrace. Note: Break between the yellow soils developed on the sandstone lithology and the purple soils developed on the shales/mudstones occurs about 1/3 of the way from the top. 20.5 ° slope and very badly eroding fields supporting only tussock grass and small scrubby trees. tomb in this area (see topographic map?), fir tree in the area 13-18 cm diameter. Bedrock 60% of the ground cover. Below the tomb area, come into an area with mulberry trees (silk production?), some peas growing on steep fields (21 °).
LXJR14	From head scarp developed at the top of a field, evidencing soil shifting by local farmer.
LXJR15	2 m from the top of the field, sample of purple soil on arable field. Mulberry trees

	appears to also be grown in the field along with the corn and peas. Large dessication cracks evident and considerable local soil movement. Slope of field 27°!
LXJR16	26° slope angle further down the concave field. High degree of surface disturbance giving considerable effective 'roughness'.
LXJR17	Next field following break of slope (16°). Coarse red/purple sandstone/shale clitter coming from small 3 m high rock slide. Highly deformed bedding (dip angle 65-80°).
LXJR18	Approximately now in the mid-slope area. Small poorly maintained terraces, lots of grass and scrub on purple soils. Abundant outcrops of purple sandstone.
LXJR19	Sample taken from the base of a narrow terrace 22° slope, soil surface badly crusted. Base of the field represented by 25 cm drop (i.e. small scarp where material appears to be excavated). No retention structures, i.e. a wall or berm used to buffer the base of the field.
LXJR20	Base of the 25 cm high scarp representing the boundary of the next field.
LXJR21	28° slope in the middle of the terrace. Soil appears deeper and bedrock only occassionally visible.
LXJR22/23	Base of third field from reservoir. Many stones exhumed by surface wash, corn stalks exposed to a maximum depth of 7 cm.
LXJR24/25	From 1.5 m to terrace section, coarse blocky sandstone found at base of profile.
LXJR26	Side ditch of field system. Well developed armour layer in the base of the ditch indicating significant flows during rains.
LXJR27	True left bank (i.e. left looking downslope) of gully 13° slope angle.
LXJR28/32	Samples randomly collected from the bottom field. Crops predominately sweet potatoes and corn. Soils relatively fine-grained purpule soils.
LXJR33/34	Samples from buffer strip between lowest fields and the reservoir. Slope angles vary 11-15° and evidence signs of localised deposition.
LXJR35	Sample taken from the delta formed by eroded material from sub-catchment.
LXJR36	Interfluve between two field gullies.
LXJR37	Sample taken from water-line of the reservoir (will be inundated during high water period.
UP1-UP4	Upper paddy field with yellow sandstone derived soils (taken from the same field as reference samples), crops rice or wheat in spring.
UP5-UP6	Upper paddy field with yellow sandstone derived soils, the location is close to the samples up1-up4 but a bit down slope (i.e. valley head).
UP7-UP8	Upper paddy field with purple sandstone derived soils.
VP1-VP5	Valley paddy fields
YA1-YA8	Yellow sandstone derived arable land close the reference site.

PAU1-PAU2	Purple arable soils in upper hills,
PAU3-PAU6	Purple arable soils in upper hills, slope 22° with a convex form.
PAU7-PAU8	Purple arable soils in upper hills, soil is hard and shallow.
PAM1-PAM5	Purple arable soils in middle hills, terrace slope 10o but whole slope 32°.
PAL1-PAL5	Purple arable soils in lower hills
WL1-WL2	Woodlands
TW1-TW4	Terrace walls
CB1-CB2	Channel banks
CDS1-CDS4	Channel depositions (i.e. the sediment deposited in channels).
TES1-TES2	Terrace sediments (i.e. the sediment deposited in terrace field).
PS1-PS2	Path sediments (i.e. the sediment deposited on path).
DS1(pa)-DS(pa)2	Deposition in paddy fields

APPENDIX 3, CS-137 MEASUREMENTS

Table 1, Cs-137 concentration for soil samples at reference site

Sample Number	Depth (cm)	Gross	Net	+/-	LT(Sec.)	Weight(g)	Cs-137 in < 2mm (Bq kg^{-1})
I1	0-10	661	421	44	30022	526.07	7.20
	10-20	666	456	42	28981.2	560.78	7.58
	20-30	1461	861	69	66291.4	568.3	6.17
	30-40	1524	677	78	87014.3	537.87	3.91
I2	i0-10	539	292	43	28820.1	476.48	5.74
	10-20	1199	764	59	57202	526.89	6.84
	20-30	753	401	51	55918	566.46	3.42
	30-40	727	-120	73	89231.1	493.25	0.00
I3	0-10	575	238	49	27516.1	540.57	4.32
	10-20	1229	644	66	57751.5	563.76	5.34
	20-30	1953	866	89	116757.2	553.36	3.62
	30-40	682	-30	67	71197.4	616.55	0.00
B1	0-20	1409	844	70	79504.4	482.76	5.93
	20-40	947	212	70	77984.2	551.16	1.33
B2	0-20	1718	938	77	83372	473.83	6.41
	20-37	2053	703	97	171264	481.66	2.30
B3	0-20	1508	901	69	84009.9	492.27	5.88
	20-40	834	309	61	65723.5	544.3	2.33
B4	0-20	1463	796	71	82506.5	491.16	5.30
	20-40	368	166	38	28891.7	532.61	2.91
B5	0-20	1271	739	64	68129.2	473.79	6.18
	20-40	891	299	64	68555.5	500.81	2.35

Table 2, Cs-137 concentration for soil samples from the detailed sampling site

Sample Number	Depth (cm)	Gross	Net	+/-	LT(Sec.)	Weight(g)	Cs-137 in < 2mm ($Bq\ kg^{-1}$)
I	0-5	335	-2	46	27644.5	572.34	0.00
	5-10	730	198	60	56361.9	578.17	1.64
	10-15	736	256	58	56692.7	600.33	2.03
	15-20	779	112	66	72728.4	561.62	0.74
	20-25	270	-60	45	27422.9	592.08	0.00
	25-30						
II	0-5	353	121	40	28804	583.16	1.94
	5-10	987	110	76	77772	576.61	0.66
	10-15	923	308	65	71092.9	588.3	1.99
	15-20	586	84	57	50890.1	600.15	0.74
	20-25	117	-18	29	25163.1	262.92	0.00
	25-30	382	-8	50	58596.9	560.52	0.00
III	0-5	342	42	44	28768.4	563.95	0.70
	5-10	399	2	50	29415	550.62	0.03
	10-15	365	118	41	30303.7	588.73	1.79
	15-20	275	65	37	28805.4	612.53	0.99
	20-25	710	-32	69	90417.2	564.28	0.00
IV	0-5	340	78	42	28197.2	583.54	1.28
	5-10	309	174	32	28539.7	543.89	3.03
	10-15	285	60	39	28844.3	572.43	0.98
	15-20	332	107	39	28505.4	605.66	1.67
	20-25	767	2	70	81421.4	601.13	0.01
V	0-5	377	55	46	28791.1	580.13	0.89
	5-10	689	209	57	58837.3	535.6	1.79
	10-15	923	308	65	71092.9	570.44	2.05
	15-20	471	-9	55	56803.1	551.13	0.00
	20-25	395	50	47	51277.4	547.39	0.48
VI	0-5	430	153	44	28914.3	554.97	2.57
	5-10	433	216	40	28948.2	549.02	3.67
	10-15	928	388	62	57245.5	582.41	3.14
	15-20	939	384	63	57901.8	559.82	3.20
	20-25	846	404	57	56959.3	581.91	3.29

Table 3, Cs-137 concentration for soil samples from slopes

Sample Numbers	% of >2 mm	Gross	Net	+/-	LT(Sec.)	Weight(g)	Cs-137 in < 2mm ($Bq\ kg^{-1}$)
1	8.7	461	221	42	29315.9	612.75	3.32
2	0.0	352	135	39	29217.8	585.3	2.13
3	39.9	865	213	66	54052.5	623.84	1.71
4	36.2	1023	453	64	54943.6	561.1	3.97
5	22.4	543	273	45	29430	600.02	4.17
7	7.7	879	272	64	58768.4	553.42	2.26
9u	9.8	785	365	55	56976.8	486.36	3.56
9m	13.5	773	241	60	57483.3	461.48	2.45
9l	11.2	727	277	56	57528.5	447.17	2.91
10	3.8	575	275	47	29333.1	544.7	4.65
11	14.7	1211	484	72	64076.1	597.38	3.41
12u	0.0	761	281	58	55702.2	518.08	2.63
12m	4.2	497	302	39	29284.3	504.34	5.52
12l	0.0	1122	515	66	63420.9	527.39	4.16
13	7.6	845	358	59	56863.8	553.38	3.07
14	15.3	791	439	52	30386.7	583.53	6.68
15	21.5	1614	1119	65	56786.6	561.68	9.47
16	21.5	990	390	65	57237	575.56	3.20
17	10.6	1390	685	72	76022.2	588.05	4.14
18	19.5	575	328	44	30024.2	556.02	5.30
19u	22.7	482	220	43	29047.6	535.73	3.82
19m	8.5	1043	458	65	56484.4	541.55	4.04
19l	12.8	530	313	41	29876.8	547.11	5.17
20	11.9	774	347	55	47591.3	579.99	3.39
21u	29.6	350	13	46	29575.3	545.59	0.22
21m	7.3	856	331	61	54910.8	552.47	2.95
21l	0.9	474	182	45	28329.2	546.36	3.17
22u	8.3	916	429	59	67061.5	394.07	4.38
22l	0.0	1085	643	59	56449.3	545.91	5.63
23u	0.0	480	210	44	29659	534.79	3.57
23m	4.2	418	186	41	29648	512.14	3.31
23l	0.0	944	284	67	79874.6	528.95	1.81
24	3.1	654	317	50	35187.8	539.45	4.51
25	13.5	1039	507	62	62941.6	573.35	3.79
26	8.9	531	179	49	28806.6	584.27	2.87
27	10.7	1226	409	75	91850.6	557.86	2.16
28	19.1	537	147	51	28805.4	635.16	2.17
29	6.6	658	373	47	29079.7	575.62	6.02
30	10.5	536	229	47	29068.7	546.77	3.89
31	45.7	1456	654	76	56814.3	637.98	4.87
32u	36.7	468	161	46	29159.7	554.03	2.69
32m	15.1	1006	376	66	56801.2	600.75	2.98
32l	16.3	470	208	43	29302.7	606.24	3.16
35	7.1	458	256	39	29013.7	573.21	4.16
36u	9.7	506	154	49	29153.6	550.79	2.59
36m	3.4	1052	265	73	61562.9	543.42	2.14
36l	8.7	1038	468	64	55928.7	502.5	4.50

38	1.1	420	225	38	29707.8	521.95	3.92
39	31.9	1003	381	66	55526	558.06	3.32
40	11.3	780	233	61	56140.1	546.43	2.05
41	26.0	1024	259	72	56272.5	586.83	2.12
42	0.7	460	205	43	32870.4	571.87	2.94
43u	63.3	549	69	56	50436	489.45	0.75
43m	53.1	314	44	42	28591.2	534.43	0.78
43l	24.2	700	243	56	51185.4	552.91	2.32
44	1.8	1001	491	61	53765.7	586.56	4.20
45a	25.2	608	331	46	28800	531	5.84
45b	47.1	490	258	42	28800	541	4.47
46	41.5	444	129	46	30900.4	587.02	1.92
47u	28.7	364	87	43	28432.6	532.66	1.55
47m	19.8	366	104	42	29248	564.82	1.70
47l	27.5	439	109	47	31127.7	557.74	1.70
48	32.6	734	157	62	50195.9	590.75	1.43
49	22.7	942	350	64	55515.7	618.19	2.75
50	20.7	743	338	54	32441.9	584.94	4.81
51u	3.1	1763	1103	73	87244.6	515.63	6.62
51m	3.5	577	337	43	30232.2	531.77	5.66
51l	2.2	911	454	58	52841.4	511.7	4.53

Table 4, Cs-137 concentration for sediment from reservoir cores

Core 1

Depth (cm)	% of >2 mm	DBD (g/cm^3)	Gross	Net	+/-	LT (Sec.)	Weight (g)	Cs-137 in < 2mm ($Bq\ kg^{-1}$)
0-5	0.00	0.34	238	88.0	32.0	83468.1	16.48	8.08
5-10	0.00	0.45	297	117	35	86400.0	21.88	7.81
10-15	0.00	0.46	285	90	36	86400.0	22.48	5.85
15-20	0.00	0.52	344	149	37	86400.0	25.65	8.49
20-25	0.00	0.53	334	117	39	86400.0	25.79	6.63
25-30	0.00	0.66	322	97	39	86400.0	25.38	5.59
30-35	0.00	0.59	272	-35	44	78627.0	25.43	0.00
35-40	11.24	0.68	266	49	38	86400.0	25.62	2.79
40-45	7.61	0.73	325	123	37	86400.0	25.49	7.05
45-50	0.00	0.73	394	132	42	86400.0	25.67	7.51
50-55	0.00	0.59	373	201	36	85595.4	25.61	11.58
55-60	0.00	0.67	360	143	39	86400.0	25.53	8.19
60-65	0.00	0.81	357	140	39	86400.0	25.55	8.01
65-70	3.32	0.91	296	79	38	87789.0	25.55	4.45
70-75	0.00	0.94	293	106	36	86848.6	25.65	6.01
75-80	0.00	0.99	279	39	39	84842.6	25.68	2.26
80-86	13.63	1.17	263	76	35	86400.0	25.60	4.34
86-90	0.00	1.15	287	25	41	86400.0	25.52	1.43
90-95	9.49	1.12	270	-15	42	86400.0	25.68	0.00
95-100	23.01	1.25	276	36	39	86400.0	25.59	2.06
100-105	32.31	1.13	265	153	29	86400.0	25.75	8.68
105-110	30.99	1.14	267	42	38	86400.0	25.62	2.40
110-114	0.00	1.06	238	36	36	78815.2	25.57	2.26
114-119	1.09	0.88	561	284	45	86400.0	25.62	16.20
119-124	0.00	0.96	470	245	41	86400.0	25.68	13.94
124-129	0.00	0.87	380	193	37	86014.4	25.55	11.09
129-134	0.00	0.86	267	65	37	86400.0	25.55	3.72
134-160	0.00	1.15	273	18	40	86193.8	25.61	1.03
45-50(R)	0.00	0.63	344	172	35	84979.9	25.64	0.08
90-95(R)	2.22	0.92	253	73	35	85606.6	25.63	0.03

Core 2

Depth (cm)	% of >2 mm	DBD (g/cm^3)	Gross	Net	+/-	LT (Sec.)	Weight (g)	Cs-137 in < 2mm ($Bq\ kg^{-1}$)
0-5	0.00	0.24	244	117	30	86400.0	11.50	14.87
5-10	0.00	0.34	296	86	38	86400.0	16.00	7.85
10-15	0.00	0.44	336	164	35	86400.0	20.61	11.63
15-20	0.00	0.46	452	250	39	86115.1	22.61	16.21
20-25	0.00	0.51	385	85	45	86400.0	23.74	5.23
25-30	0.00	0.52	372	87	44	85501.4	25.00	5.14
30-35	0.00	0.56	379	154	40	86400.0	25.52	8.82
35-40	0.00	0.62	346	106	40	82967.9	25.52	6.32
40-45	0.00	0.71	425	163	43	86400.0	25.50	9.34
45-50	0.00	0.68	426	164	43	86248.1	25.53	9.40
50-55	0.00	0.80	312	87	39	86400.0	25.56	4.97
55-60	0.00	0.77	343	163	36	85947.8	25.51	9.39
60-65	0.00	0.68	368	76	44	86400.0	25.57	4.34
65-70	0.00	0.61	429	279	35	86400.0	25.60	15.93
70-75	0.00	0.71	356	169	37	82162.7	25.51	10.18
75-80	0.00	0.66	451	211	42	86400.0	25.54	12.07
80-86	0.00	0.64	462	237	41	86400.0	25.50	13.58
86-90	0.00	0.66	432	207	40	86053.7	25.53	11.90
90-95	0.00	0.62	641	416	43	86400.0	25.54	23.80
95-100	0.00	0.64	616	294	48	85920.0	25.56	16.90
100-105	0.00	0.70	798	588	44	86400.0	25.53	33.66
0-6(R)	0.00	0.28	286	106	35	86400.0	14.91	10.39
6-11(R)	0.00	0.33	265	70	36	81723.3	16.17	6.69
11-16(R)	0.00	0.45	362	130	40	83505.1	20.30	9.68
16-21(R)	0.00	0.45	433	216	40	86400.0	22.41	14.09
40-45(R)	0.00	0.57	405	180	40	85097.2	25.56	10.45
90-95(R)	0.00	0.72	403	238	36	86244.3	25.52	13.65

Table 5, Cs-137 concentration for the topsoils and deposited materials

Samples	% of >2mm	Gross	Net	+/-	LT (Sec.)	Weight (g)	Cs-137 in < 2mm (Bq kg^{-1})
pal1	12.79	412	157	42	86454.8	54.46	5.16
pal2	23.16	350	65	43	72966.3	48.04	2.87
pal3	2.32	286	129	33	83626.9	30.86	7.73
pal4	11.73	262	15	40	89400.8	20.1	1.29
pal5	20.53	398	158	41	85809.6	55.55	5.13
pam1	36.82	432	110	46	95780.6	50.54	3.51
pam2	15.10	433	133	45	84806.8	50.04	4.85
pam3	23.12	422	160	43	81336.7	50.46	6.03
pam4	29.78	402	95	45	86621.9	50.05	3.39
pam5	17.37	379	102	43	83781.9	50.87	3.70
pau1	24.42	388	133	42	85772.6	50.12	4.78
pau2	29.41	325	78	41	83810.7	50.66	2.84
pau3	43.98	378	168	39	89072.8	50.69	5.75
pau4	22.86	416	131	44	82510.4	50.27	4.88
pau5	22.22	449	89	49	88852.9	50.09	3.09
pau6	21.54	492	237	43	85401.3	50.79	8.45
pau7	25.07	442	195	42	87937.6	50.63	6.77
pau8	20.58	367	150	39	86429.4	50.09	5.36
ya1	0.00	317	145	35	86875.8	50.82	5.08
ya2	0.00	361	91	42	92895.5	50.06	3.03
ya3	0.00	414	227	38	79370.2	50.41	8.77
ya4	0.00	460	258	39	86586.1	50.15	9.19
ya5	0.00	427	165	43	91018.3	50.88	5.51
ya6	0.00	283	81	37	82463.1	50.05	3.04
ya7	0.00	401	139	42	84956	50.51	5.01
ya8	0.00	376	99	43	84691.4	50.54	3.58
tes1	4.09	236	56	35	60000	50	2.89
tes2	3.46	237	80	33	60000	50.14	4.11
wl1	19.59	644	382	45	86468.4	50.85	13.44
wl2	1.97	447	237	40	77112	50.8	9.36
cds1	0.00	802	360	56	57464.4	605.66	1.60
cds2	0.00	405	180	40	29333.3	589.25	1.61
cds3	0.00	252	87	34	60000	50.62	4.43
cds4	0.00	244	19	38	60000	50.75	0.97
ds1(pa)	0.00	348	101	41	29090.8	487.18	1.10
ds2(pa)	0.00	749	232	59	57594	479.34	1.30
ds1	0.00	167	25	30	60000	50.02	1.29
ds2	0.00	156	6	31	60000	50.48	0.31
ds3	35.19	201	21	34	60000	50.49	1.07
ds4	8.39	202	82	29	60000	50.19	4.21
up1	0.00	325	145	36	60000	50.25	7.44
up2	0.00	275	133	32	60000	50.89	6.74
up3	0.00	329	134	37	60000	50.22	6.88
up4	0.00	226	121	28	60000	50.01	6.24
up5	0.00	216	81	30	60000	50.04	4.17
up6	0.00	282	42	40	60000	50.17	2.16
up7	0.00	312	147	34	60000	50.31	7.53
up8	0.00	302	70	39	60000	50.31	3.59

vp1	0.00	270	143	31	60000	50.73	7.27
vp2	0.00	296	116	35	60000	50.12	5.97
vp3	0.00	318	86	39	60000	50.76	4.37
vp4	0.00	278	46	39	60000	50.53	2.35
vp5	0.00	266	109	33	60000	50.2	5.60
tw1	49.39	306	96	38	60000	50.3	4.92
tw2	25.69	282	110	35	60000	50.11	5.66
tw3	57.35	223	103	29	60000	50.18	5.29
tw4	64.36	174	-13	34	60000	50.21	Non-detective
ps1	0.00	175	-12	34	60000	50.48	Non-detective
ps2	0.00	141	44	26	60000	50.25	2.26
cb1	23.08	245	88	33	60000	50.66	4.48
cb2	9.40	196	46	31	60000	50.23	2.36
ifs1	22.15	256	121	31	60000	50.19	6.21
ifs2	17.77	279	24	41	60000	50.07	1.24
lxjr1	0.00	317	175	33	60000	50.32	8.96
lxjr2	0.00	793	643	40	60000	50.09	33.09
lxjr3	0.00	955	730	46	60000	50.24	37.45
lxjr4	0.00	715	513	42	60000	50.2	26.34
lxjr5	0.00	626	454	39	60000	50.1	23.36
lxjr6	0.00	275	50	38	60000	50.34	2.56
lxjr7	0.00	350	193	34	60000	50.46	9.86
lxjr8	3.11	349	229	31	60000	50.12	11.78
lxjr9	0.00	381	246	33	60000	50.15	12.64
lxjr10	0.00	384	249	33	60000	50.02	12.83
lxjr11	0.00	528	363	37	60000	50.62	18.48
lxjr12	0.00	733	531	42	60000	50.22	27.25
lxjr13	0.00	536	364	38	60000	50.2	18.69
lxjr14	0.00	203	-7	36	60000	50.58	Non-detective
lxjr15	0.00	215	73	31	60000	50.8	3.70
lxjr16	0.00	296	94	37	60000	50.25	4.82
lxjr17	0.00	206	34	33	60000	50.57	1.73
lxjr18	0.00	247	82	33	60000	50.46	4.19
lxjr19	0.00	280	85	36	60000	50.66	4.32
lxjr20	0.00	240	75	33	60000	50.46	3.83
lxjr21	0.00	295	138	34	60000	50	7.11
lxjr22	0.00	281	71	37	60000	50.55	3.62
lxjr23	0.00	263	31	39	60000	50.24	1.59
lxjr24	0.00	256	99	33	60000	50.55	5.05
lxjr25	0.00	292	30	41	60000	50.72	1.52
lxjr26	0.00	263	113	32	60000	50.23	5.80
lxjr27	0.00	265	55	37	60000	50.34	2.82
lxjr28	0.00	227	25	36	60000	50.31	1.28
lxjr29	0.00	286	99	36	60000	50.48	5.06
lxjr30	0.00	240	105	31	60000	50.05	5.41
lxjr31	0.00	229	72	33	60000	50.31	3.69
lxjr32	0.00	248	68	35	60000	50.91	3.44
lxjr33	0.00	200	13	35	60000	50.57	0.66
lxjr34	0.00	206	4	36	60000	50.2	0.21
lxjr35	0.00	217	75	31	60000	50.47	3.83
lxjr36	0.00	203	113	26	60000	50.44	5.77
lxjr37	0.00	266	161	29	60000	50.83	8.16

APPENDIX 4, THE PARTICLE SIZE DISTRIBUTION FOR SELECTED SOIL SAMPLES FROM ARABLE LAND

Sample No	2-1 mm	1- 0.5 mm	0.5-0.25 mm	0.25-0.1 mm	0.1-0.05 mm	0.05-0.002 mm	<0.002 mm
12 u	0	0.8	8.0	24.3	10.2	36.5	20.2
m	0	1.0	9.0	21.5	10.3	38.5	19.7
l	0	0.4	7.7	29.6	14.0	32.9	15.4
19 u	0	0.3	0.7	21.9	15.0	45.2	16.9
m	0	0.7	1.2	2.5	31.3	47.9	16.4
l	0	0.4	1.4	20.3	13.8	46.3	17.8
21 u	0	0.2	0.5	19.1	16.2	39.5	24.5
m	0	0	0.2	5.2	11.4	58.3	24.9
l	0	0.1	0.2	9.3	16.4	51.4	22.6
23 u	0	0	0.2	8.0	6.9	63.4	21.5
m	0	0	0.3	8.4	5.3	61.1	24.9
l	0	0	0.2	7.2	11.3	56.2	25.1
32 u	0	0	0.5	7.3	14.4	57.0	20.8
m	0	0	0.3	7.5	15.1	56.1	21.0
l	0	0.1	0.7	0.9	21.2	55.5	21.6
36 u	0	0.2	0.3	0.9	17.7	56.4	24.5
m	0	0	0.2	1.0	12.2	56.0	30.6
l	0.2	0.2	0.4	0.6	18.3	52.9	27.4
43 u	0	0	1.3	0.7	19.9	55.3	22.8
m	0	0	0.8	11.4	18.6	50.0	19.2
l	0	0	0.4	10.2	17.6	51.9	19.9
47 u	0	0	0.4	8.0	14.5	57.8	19.3
m	0	0.1	0.4	6.9	11.8	59.7	21.1
l	0	0.1	0.4	9.1	13.0	55.9	21.5
51 u	0.2	0.9	6.8	22.6	14.6	38.5	16.4
m	0.1	1.3	7.5	20.9	17.2	37.0	16.0
l	0.1	1.3	7.5	24.2	14.9	35.6	16.4

APPENDIX 5, PARTICLE SIZE ANALYSIS FOR RESERVOIR CORE 1

Depth (cm)	>2 mm	2-0.002	<0.002 mm
0-5	0.0	83.3	16.7
5-10	0.0	82.6	17.4
10-15	0.0	83.0	17.0
15-20	0.0	81.2	18.8
20-25	0.0	81.1	18.9
25-30	0.0	82.1	17.9
30-35	0.0	88.3	11.7
35-40	11.2	81.2	7.5
40-45	7.6	80.9	11.5
45-50	0.0	85.4	14.6
50-55	0.0	76.1	24.0
55-60	0.0	76.5	23.5
60-65	0.0	85.2	14.8
65-70	3.3	86.0	10.7
70-75	0.0	88.4	11.6
75-80	0.0	90.5	9.5
80-86	13.6	79.0	7.3
86-90	0.0	89.7	10.3
90-95	9.5	80.7	9.8
95-100	23.0	64.5	12.5
100-105	32.3	61.2	6.5
105-110	31.0	60.5	8.5
110-114	0.0	88.5	11.5
114-119	1.1	82.3	16.6
119-124	0.0	81.4	18.6
124-129	0.0	81.4	18.6
129-134	0.0	81.5	18.5
134-160	0.0	81.5	18.5

Appendix 6, An example showing the calculation of erosion rates using the mass balance model. The model was performed in Excel 5.0.

Cs-137 enrichment ratio K2=1.5,	Soil mass M=130 kg sq. m (assumes builk density of 1.3 g per qubic cm),																		Radioactive decay constant for Cs-137 k1=0.023								
Dt: atmospheric deposition rate of Cs-137 (Bq m-2 yr-1),										At: total Cs-137 in plough layer (Bq m-2).																	
Year	1953	1954	1955	1956	1957	1958	1959	1960	1961	1962	1963	1964	1965	1966	1967	1968	1969	1970	1971	~~~	1989	1990	1991	1992	1993	1994
Ei=0 t km-2 yr-1 (average erosion rate)																										
Dt	0	59	172	194	191	139	278	71	90	430	868	675	230	91	50	60	51	69	74	~~~	0	0	0	0	0	0
At	0	58	227	413	593	717	976	1024	1089	1489	2313	2928	3088	3108	3087	3076	3057	3055	3059	~~~	2426	2371	2317	2265	2213	**2163**
Ei=1000 t km-2 yr-1																										
Dt	0	59	172	194	191	139	278	71	90	430	868	675	230	91	50	60	51	69	74	~~~	0	0	0	0	0	0
At	0	58	225	408	582	699	949	986	1041	1428	2232	2820	2950	2939	2888	2850	2803	2776	2755	~~~	1837	1775	1715	1656	1600	1546
Ei=2000 t km-2 yr-1																										
Dt	0	59	172	194	191	139	278	71	90	430	868	675	230	91	50	60	51	69	74	~~~	0	0	0	0	0	0
At	0	57	223	403	571	682	923	950	995	1371	2157	2720	2821	2783	2706	2643	2575	2526	2485	~~~	1402	1338	1278	1221	1166	1113
Ei=4000 t km-2 yr-1																										
Dt	0	59	172	194	191	139	278	71	90	430	868	675	230	91	50	60	51	69	74	~~~	0	0	0	0	0	0
At	0	57	219	392	550	648	874	884	911	1266	2020	2537	2589	2504	2385	2284	2181	2101	2033	~~~	836	780	728	679	634	592
Ei=6000 t km-2 yr-1																										
Dt	0	59	172	194	191	139	278	71	90	430	868	675	230	91	50	60	51	69	74	~~~	0	0	0	0	0	0
At	0	56	216	382	531	617	829	823	836	1173	1899	2376	2386	2263	2111	1983	1857	1759	1675	~~~	517	472	430	392	358	326
Ei=8000 t km-2 yr-1																										
Dt	0	59	172	194	191	139	278	71	90	430	868	675	230	91	50	60	51	69	74	~~~	0	0	0	0	0	0
At	0	55	212	372	512	588	787	768	769	1091	1792	2234	2208	2053	1877	1729	1589	1481	1390	~~~	333	297	265	236	210	187
Ei=10000 t km-2 yr-1																										
Dt	0	59	172	194	191	139	278	71	90	430	868	675	230	91	50	60	51	69	74	~~~	0	0	0	0	0	0
At	0	55	209	363	494	561	748	717	708	1018	1697	2108	2050	1870	1675	1515	1367	1254	1162	~~~	224	195	170	148	129	112
Ei=30000 t km-2 yr-1																										
Dt	0	59	172	194	191	139	278	71	90	430	868	675	230	91	50	60	51	69	74	~~~	0	0	0	0	0	0
At	0	49	178	285	357	363	484	393	347	599	1140	1353	1127	855	633	488	380	320	284	~~~	19	13	9	6	4	3

Notes:

1, Equation 5-7 can be integrated over specific time periods in which the erosion and deposition rate are considered constant and and successive values of total Cs-137 (At) calculated in a step-wise manner (Kachanoski and De Jong, 1984),

2, Annual Cs-137 fallout, based on Sarmiento and Gwinn (1986) model from 1954-74 and the records in Japan (Hirose et al., 1987), is corrected by the reference value (2163 Bq per sq. m) estimated from soil samples.

3, A regression model is developed based on the assumed erosion rates and residual Cs-137 inventory.

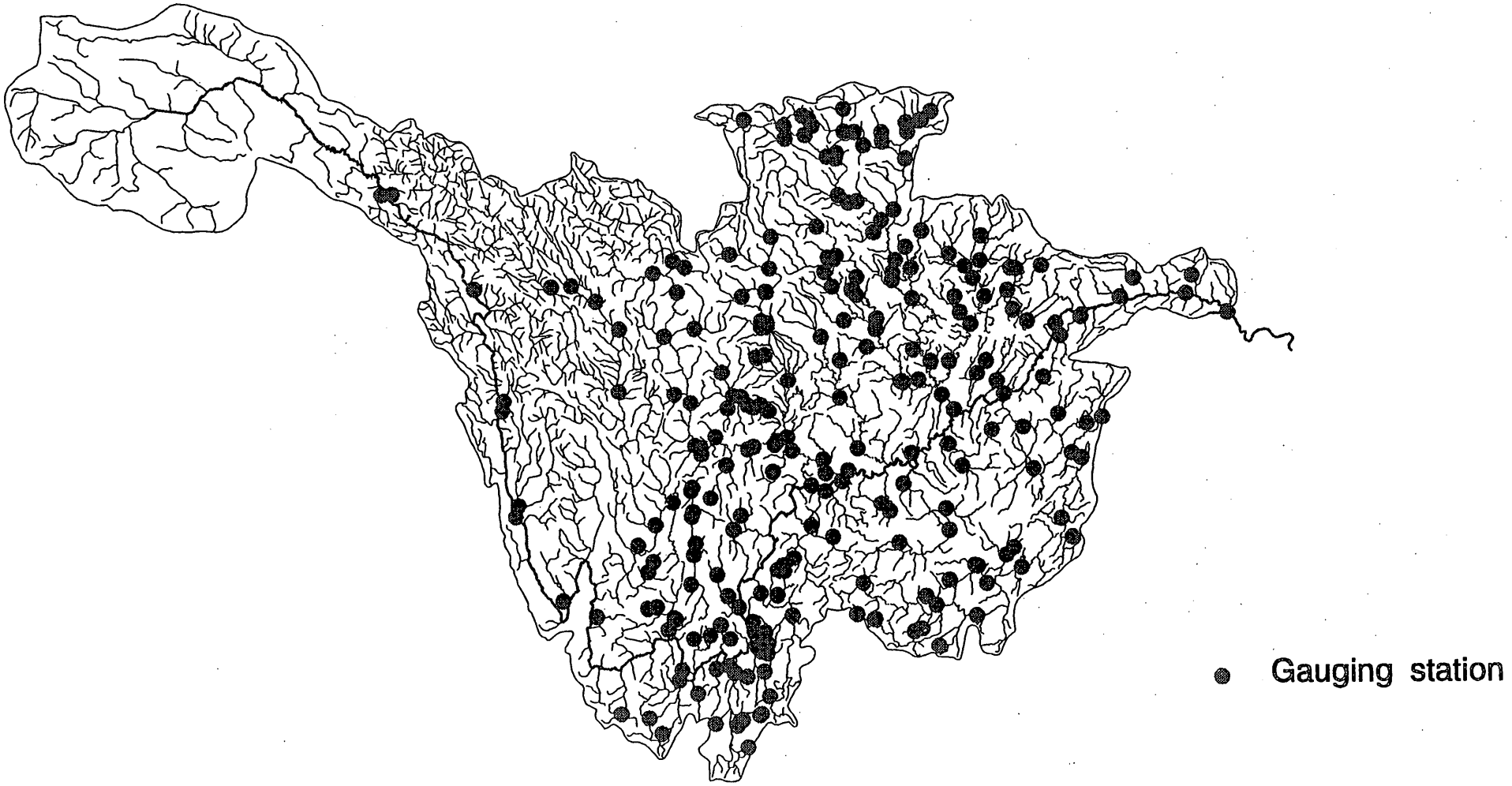

APPENDIX 7, THE DRAINAGE NETWORK DIGITISED FROM MAPS

APPENDIX 8, ALL THE AMLS USED TO EXTRACT VARIABLES FROM THE VARIED DATABASE

1. Master.txt (catchment numbers in text format edited by VI on UNIX, each catchment must have a polygon coverage) used in all the AMLs below

1 6 16 23 25 29 30 31 32 36 42 64 67 69 70 71 73 81 83 84 85 86 91 92 94 97 98 105
116 125 128 129 133 140 149 153 154 156 160 164 165 168 171 178 179 180 182
183 189 190 195 197 200 201
206 207 208 220 236 242 243 250

2. An AML used to extract summary statistic (mean, max., min. and SD from any grid such as elevation, slope, precipitation, population density and NDVI)

```
/* aml file to extract catchment data 12/08/96
/* will only work on ARC-INFO v.7

&type WARNING: DIRECTORIES DISSOLVE,CLIP,GRID,DBASE
&type WILL BE DELETED IN /TMP !!!

&setvar continue := [response 'Do you wish to continue? (Y/N)']
 &if %continue% = Y or %continue% = y &then
  &do

&setvar coverage := [response 'Enter map to clip (incl. path)']
&setvar catchno := [response 'How many catchments do you wish to process?']

&type Removing directories in /tmp ...
rm -r /tmp/dissolve
rm -r /tmp/clip
rm -r /tmp/grid
rm -r /tmp/dbase
&type Finished ...

&type Creating directories in /tmp ...
mkdir /tmp/dissolve
mkdir /tmp/clip
mkdir /tmp/grid
mkdir /tmp/dbase
&type Finished ...

&setvar fileunit := [open master.txt openstat -r]
&do i := 1 &to %catchno% &by 1  /* beginning of &do &to &by loop
&setvar nodeid := [read %fileunit% readstat]
/* &type DISSOLVING CATCHMENT C%nodeid% (Cat no. %i%)
/* dissolve ../catch/c%nodeid% /tmp/dissolve/c%nodeid% dissolve poly
```

```
&type CLIPPING LANDUSE FOR CATCHMENT C%nodeid% (Cat no. %i%)
latticeclip %coverage% c%nodeid% /tmp/clip/c%nodeid% minimum
&end /* end of &do &to &by loop
&setvar closestat := [close %fileunit%]

grid
&setvar fileunit := [open master.txt openstat -r]
&do i := 1 &to %catchno% &by 1  /* beginning of &do &to &by loop
&setvar nodeid := [read %fileunit% readstat]
&type CREATING INTEGER GRID FOR CATCHMENT C%nodeid% (Cat no.
%i%)
/tmp/grid/c%nodeid% = int(/tmp/clip/c%nodeid% + 0.5)
buildvat /tmp/grid/c%nodeid%
&end /* end of &do &to &by loop
&setvar closestat := [close %fileunit%]
quit


&workspace /tmp/grid
tables
&setvar fileunit = [open /home/alfred/dgg/dgg3xl/sediment/master.txt openstat -r]
&do i := 1 &to %catchno% &by 1  /* beginning of &do &to &by loop
&setvar nodeid := [read %fileunit% readstat]
&type EXPORTING STA -> DBF FOR CATCHMENT C%nodeid% (Cat no. %i%)
sel c%nodeid%.sta
unload ele.sta

&end /* end of &do &to &by loop
&setvar closestat := [close %fileunit%]
quit

&end
 &else
  &return

&return
&workspace ~/sediment
```

3. An AML used to calculate the maximum distance from outlet point to the farest point on catchment boundary (e.g. basin length)

```
/*aml to calculate pointdistance, 10/10/96

&setvar catchno = [response 'how many catchment do you wish to process?']
&type removing a directory from /tmp....
rm -r /tmp/pointcov1
rm -r distance
```

```
&type creating a directroy from /tmp....
mkdir /tmp/pointcov1
mkdir distance
&setvar fileunit = [open master1.txt openstat -r]
&do i = 1 &to %catchno% &by 1
&setvar nodeid = [read %fileunit% readstat]
build c%nodeid% line
arcpoint c%nodeid% /tmp/pointcov1/p1%nodeid% line c%nodeid%-id 1000
build /tmp/pointcov1/p1%nodeid% point
pointdistance /tmp/pointcov1/p1%nodeid% /tmp/pointcov/p%nodeid%
distance/d%nodeid%

&workspace distance
statistics d%nodeid% d%nodeid%ma

maximum distance
end

tables
sel d%nodeid%ma
unload max_dis
quit
&end
&setvar closestat = [close %fileunit%]
```

4, An AML used to extract total stream length from a drainage network coverage

```
/* aml file to extract stream length 12/10/96
/* will only work on ARC-INFO v.7


&type WARNING: DIRECTORIES DISSOLVE,CLIP,GRID,DBASE
&type WILL BE DELETED IN /TMP !!!

&setvar continue := [response 'Do you wish to continue? (Y/N)']
  &if %continue% = Y or %continue% = y &then
    &do


&setvar coverage := [response 'Enter map to clip (incl. path)']
&setvar catchno := [response 'How many catchments do you wish to process?']


&type Removing directories in /tmp ...
rm -r /tmp/dissolve
rm -r /tmp/clip
rm -r /tmp/grid
rm -r /tmp/dbase
```

```
&type Finished ...

&type Creating directories in /tmp ...
mkdir /tmp/dissolve
mkdir /tmp/clip
mkdir /tmp/grid
mkdir /tmp/dbase
&type Finished ...


&setvar fileunit := [open master.txt openstat -r]
&do i := 1 &to %catchno% &by 1  /* beginning of &do &to &by loop
&setvar nodeid := [read %fileunit% readstat]
/* &type DISSOLVING CATCHMENT C%nodeid% (Cat no. %i%)
/* dissolve ../catch/c%nodeid% /tmp/dissolve/c%nodeid% dissolve poly
&type CLIPPING LANDUSE FOR CATCHMENT C%nodeid% (Cat no. %i%)
clip %coverage% c%nodeid% /tmp/clip/c%nodeid% line
&end /* end of &do &to &by loop
&setvar closestat = [close %fileunit%]


&workspace /tmp/clip
&setvar fileunit = [open /home/alfred/dgg/dgg3xl/sediment/master.txt ~
openstat -r]
&do i = 1 &to %catchno% &by 1
&setvar nodeid = [read %fileunit% readstat]
/* &typing Statistics catchment c%nodeid% (cat no %i%)
statistics c%nodeid%.aat c%nodeid%l
sum length
end
tables
sel c%nodeid%l
unload rlength
quit
```

5, An AML used to reselect point from a point coverage

```
/*aml to reselect point from pointme
&setvar coverage = [response 'enter coverage to reselect ']
&setvar catchno = [response 'how many catchment do you want to process?']
&type removing the directory of /tmp/pointcov
rm -r /tmp/pointcov
&type creating the directory of /tmp/pointcov
mkdir /tmp/pointcov
arcedit
&setvar fileunit = [open master.txt openstat -r]
&do i = 1 &to %catchno% &by 1
```

```
&setvar nodeid = [read %fileunit% readstat]
edit %coverage%
editfea point
sel %coverage%-id <> %nodeid%
delete
save %coverage% /tmp/pointcov/p%nodeid%


&end
&setvar closestat = [close %fileunit%]
quit
```

APPENDIX 9, THE CATCHMENT VARIABLES FOR THE 62 BASINS IN THE UPPER YANGTZE

NO	RIVER	STATION	CA(sq. km)	PE(km)	BL(km)	ME(m)	BR(m)	RR(m/km)	LR(m)	HI(%)	MS(deg)	Dd(m/sq.k	P(mm/yr.)	Fournier (m	POPD (n km-2
1	Jinsha-Ya	zimenda	137704	1764	636	4768	2858	4.5	217.8	43.5	3.1	193.1	341.4	62.1	1.0
6		shigu	232651	3609	1260	4562	4489	3.6	364.3	59.0	5.3	145.6	446.8	76.8	3.6
16		huatan(qiaojia)	450696	4807	1469	3907	5693	3.9	457.8	56.0	6.7	124.7	632.2	100.7	29.3
23		ninnan	3074	244	95	2456	3193	33.5	819.7	47.5	12.1	44.6	913.0	140.6	76.5
25		qianxinqiao	2549	265	90	2031	1047	11.7	212.4	41.5	3.1	110.7	999.0	143.6	205.5
29		meigu	1607	160	35	2402	2713	77.2	614.8	48.5	9.2	66.6	1009.0	147.5	123.0
30		pingshang	485099	5328	1447	3793	6089	4.2	462.2	57.0	6.8	120.9	650.7	103.1	36.4
31		hengjiang(2)	14781	773	218	1785	2589	11.9	253.1	53.0	3.9	86.8	950.3	127.1	227.3
32		zhutuo(3)	694725	5212	1565	3298	7009	4.5	470.3	43.5	6.9	115.0	768.0	114.2	95.7
36		dianwei	630	107	48	2416	1068	22.4	374.2	54.5	5.6	74.3	979.0	141.8	216.6
42		qinkoutang	2109	237	67	1945	1746	26.1	332.1	53.5	5.0	111.7	888.0	127.8	167.5
64		lounin	108083	2340	796	4050	4689	5.9	532.7	54.0	7.8	123.2	677.9	104.8	5.3
67		xiaodeshi	118294	2684	952	3764	5188	5.4	556.0	52.5	8.2	124.9	706.9	112.0	21.8
69		anninqiao	937	142	36	2993	2815	78.5	871.6	39.5	12.8	65.8	971.0	145.3	75.3
70		sunshuiguan(2	1596	189	66	2872	2935	44.3	825.0	38.5	12.3	65.1	964.0	145.8	83.0
71		manshuiwan	3817	281	75	2647	3137	42.1	749.2	35.5	11.2	46.9	964.0	148.5	108.5
73		wantan	11100	638	244	2326	3630	14.9	639.8	35.5	9.6	62.0	924.7	146.5	122.8
81	Dadu-Min	zengjianguan	4486	299	77	3571	2267	29.4	631.1	53.5	9.1	73.4	816.5	103.8	7.5
83		shaba	7231	397	129	3663	3262	25.3	829.6	56.5	12.4	87.7	839.0	114.0	8.3
84		jiangsheba(sh	14279	507	163	3520	3630	22.2	813.4	58.5	12.0	79.6	830.0	112.9	8.5
85		zagunao	2404	234	59	4121	3489	58.9	1126.1	53.0	16.2	80.2	975.0	135.5	7.6
86		shuangping	4629	287	93	3777	4511	48.5	1143.0	56.0	16.6	67.8	1005.0	139.1	9.2
91		yanliuping(3)	363	80	15	3116	3582	238.8	1162.7	43.0	17.5	31.8	1237.0	174.0	37.1
92		xinxinchang(2)	396	95	22	3843	2636	119.8	914.7	56.0	13.5	57.1	1237.0	164.0	5.9
94		pengshan(3)	30661	952	308	2508	5353	17.4	652.7	40.0	9.6	100.3	1014.1	148.0	197.9
97		qinshuixi(2)	3330	283	115	1729	3507	30.4	656.7	36.5	9.5	69.5	1196.0	159.7	39.8
98		gaochang(5)	135378	2230	661	2914	6946	10.5	647.2	38.0	9.5	103.6	1003.6	135.5	102.3
105		dajin	40484	1124	283	4041	3211	11.3	538.7	59.0	7.8	136.5	713.9	94.1	6.4
116		shaping(3)	75016	1831	560	3778	6462	11.5	701.9	47.0	10.3	107.3	857.0	111.2	16.1
125	Tuo	shanhuangmia	6590	432	90	642	3259	36.1	126.6	8.0	1.7	145.8	1063.3	158.3	1025.9
128		denyenyan	14484	627	190	557	3345	17.6	91.8	7.5	1.3	121.8	1094.5	159.2	830.3
129		lijiawan	23283	810	278	493	3390	12.2	77.7	7.0	1.1	116.8	1103.1	156.9	872.7
133	Jialin	yunninzeng	2071	180	66	1570	1338	20.3	374.7	51.5	5.1	52.5	502.0	67.2	117.2
140		liuanyang	19206	689	183	1655	2852	15.6	405.9	36.0	5.8	70.9	482.7	68.1	109.5
149		wudu(2)	14288	798	236	2863	3521	14.9	725.2	55.5	10.5	76.0	564.2	77.8	27.0

APPENDIX 9, THE CATCHMENT VARIABLES FOR THE 62 BASINS IN THE UPPER YANGTZE

153		bikou	26086	884	294	2777	3981	13.5	779.7	52.0	11.3	80.2	589.0	81.8	23.4
154		sanleiba(qianf	29247	957	343	2645	4166	12.2	762.0	59.5	11.1	78.5	586.1	84.1	33.2
156		tinzhikou	61089	1352	397	1975	4323	10.9	581.9	36.5	8.4	81.6	571.3	85.1	84.0
160		qinquanxian	5011	374	142	1080	1897	13.3	462.6	35.5	6.7	66.1	746.0	110.3	194.1
164		wusheng	79714	1809	548	1680	4467	8.2	496.7	21.0	7.2	89.2	634.4	92.6	161.9
165		beipei(2)	156142	2346	600	1248	5014	8.4	413.5	21.0	5.9	102.0	804.6	109.4	318.8
168		bixi(3)	2124	219	70	1157	1737	24.6	577.4	42.5	8.3	79.7	987.0	122.8	124.0
171		qilitou	6382	356	117	753	2017	17.3	347.6	22.0	5.0	103.6	851.0	113.1	343.4
178		dunlin(chihua)	6462	378	136	1041	2195	16.2	582.2	31.5	8.4	93.8	1071.5	138.3	225.2
179		minyuantan	736	112	30	551	777	26.3	221.2	35.5	3.4	133.7	1207.0	143.5	453.1
180		guodukou	31626	858	215	802	2279	10.6	401.7	23.5	5.8	114.9	1041.8	127.8	338.4
182		jinbian(fendou)	2740	237	91	435	463	5.1	155.5	28.0	2.1	103.4	971.0	113.3	931.6
183		luoduxi(2)	38071	972	284	726	2297	8.1	351.7	22.5	5.1	121.7	1034.2	125.7	441.4
189		fujiangqiao	11903	474	162	1942	4734	29.3	807.0	31.5	11.6	71.8	824.3	117.5	192.5
190		guanyinchang(	1933	280	103	679	2190	21.3	176.7	11.5	2.4	94.5	947.0	143.3	782.2
195		shehong(taihe	23574	673	257	1250	4891	19.0	451.7	19.0	6.5	90.1	872.9	126.1	426.9
197		xiaoheba(2)	29420	847	358	1078	4948	13.8	374.6	16.5	5.3	93.4	898.8	127.2	457.3
200	Wu	yachihe	16541	612	175	1607	1959	11.2	246.6	40.5	3.5	79.1	1040.2	132.2	275.2
201		wujiangdu	26496	798	248	1466	2101	8.5	218.0	38.0	3.1	78.0	1085.5	133.2	291.9
206		shinan	50791	1312	402	1242	2428	6.0	228.4	36.5	3.2	73.2	1112.9	132.1	258.4
207		wulong	83035	1816	434	1104	2578	5.9	280.9	34.5	4.0	74.4	1169.7	134.8	223.7
208		gongtan	58346	1832	469	1166	2494	5.3	244.5	35.0	3.5	81.4	1154.3	134.4	244.1
220		duntou	6917	332	118	1225	975	8.2	214.5	54.5	3.0	60.9	1172.0	136.3	238.4
236	Mai chan	chuntang	866559	6834	1605	2859	7034	4.4	456.8	37.5	6.7	112.4	781.6	113.4	145.5
242		shizhu(2)	898	119	36	1188	1230	34.2	431.1	52.0	6.3	107.2	1349.0	152.6	141.8
243		wanxian	974881	7131	1727	2656	7112	4.1	438.6	35.5	6.4	109.1	821.7	115.8	156.8
250		yichuang	1005501	7372	1995	2596	7170	3.6	439.8	35.0	6.4	108.7	833.8	116.6	159.5

BIBILOGRAPHY

Abrahart, R.J., Kirkby, M.J. and McMahon, M.L., 1994, MEDRUSH-a combined Geographical Information System and large scale distributed process model, pp.67-76, in *Proceedings 2nd National Conference on GIS Research*, Leicester, UK.

Ahnert, F., 1970, Functional relationships between denudation, relief, and uplift in large mid-latitude drainage basins, *Am. J. Sci.*, 268: 243-263.

Alford, D., 1992, Streamflow and sediment transport from mountain watersheds of the Chao Phraya basin, northern Thailand: a reconnaissance study, *Mountain Research and Development*, 12: 257-268.

Aoyama, M., Hirose, K., Suzuki, Y., Inoue, H. and Sugimura, Y., 1986, High level radioactive nuclides in Japan in May, *Nature*, 321: 819-820.

Bachhuber, H., Bunzl, K., Schimmack, W., 1987, Spatial variability of fallout Cs-137 in the soil of a cultivated field, *Environmental Monitoring and Assessment*, 8: 93-101.

Basher, L.R. and Matthews, K.M., 1993, Relationship between ^{137}Cs in some undisturbed New Zealand soils and rainfall, *Aust. J. Soil Res.*, 31:655-663.

Beasley, D.B., Huggins, L.F. and Manke, E.J., 1982, Modelling sediment yields from agricultural watersheds, *J. Soil and Water Cons.*, 37: 113-116.

Begg, C.B.M., 1982, *Assessment of soil erosion in Saskatchewan*, M.S. Thesis, University of Saskatchewan, Saskatoon.

Biot, Y. and Lu, X.X., 1993, Assessing the severity of the problem and the urgency for action, pp.165-191 in Baum, E., Wolff, P. and M.A. Zöbisch (eds.) *Acceptance of soil and water conservation strategies and technologies*. The German Institute for Tropical and Subtropical Agriculture (DITSL), Witzenhausen.

Bollinne, A., 1978, Study of the importance of splash and wash on cultivated loamy soils in Hesbaye (Belgium), *Earth Surface Processes*, 3(1): 71-84.

Brown, R.B., Cutshall, N.H. and King, G.F., 1981, Agricultural erosion indicated by caesium redistribution: I. Level and distribution of caesium-137 activity in soils, *Soil Sci. Soc. Am. J.*, 45:1184-1190.

Brown, R.B., King, G.F. and Cutshall, N.H., 1981, Agricultural erosion indicated by caesium redistribution: II. Estimates of erosion rates, *Soil Sci. Soc. Am. J.*, 45:1191-1197.

Bruijneel, L.A. and Critichley, W.R.S., 1996, A new approach towards the quantification of runoff and eroded sediment from bench terraces in humid tropical steeplands and its application in South-Central Java, Indonesia, pp.921-937, in Anderson, M.G. and Brooks, S.M. (eds.) *Advances in Hillslope Processes*, Vol. 2, John Wiley & Sons, Chichester.

Brune, G.M., 1953, Trap efficiency of reservoirs, *Trans. Amer. Geophys. Union*, 34: 407-418.

Bunzel, K. and Kracke, W., 1988, Cumulative deposition of Cs-137, Pu-238, Pu-239+240 and Am-242 from global fallout in soils from forest, grassland and arable land in Bavaria (FRG), *J. Environ. Radioact.*, 8: 1-12.

Burt, T.P., 1994, Long-term study of the natural environment-perceptive science or mindless monitoring? *Progress in Physical Geography*, 18(4): 475-496.

Busacca, A.J., Cook, C.A. and Mulla, D.J., 1993, Comparing land-scape-scale estimation of soil erosion in the Palouse using Cs-137 and RUSLE, *J. Soil and Water Conservation*, 48: 361-367.

Callender, E. and Robbins, J.A., 1993, Transport and accumulation of radionuclides and stable elements in a Missouri River reservoir, *Water Resources Research*, 29(6): 1787-1804.

Cambray, R.S., Playford, K. and Lewis, N.J., 1983, Radioactive fallout in air and rain: Results to the end of 1982, *U.K. Atomic Energy Authority Rep. AERE-R-10859. U.K. AERE,* Harwell, U.K.

Cambray, R.S., Playford, K., Lewis, G.N.J. and Carpenter, R.G., 1989, Radioactive fallout in air and rain: results to the end of 1987, *AERE R13226*, UK Atomic Energe Authority, Harwell.

Campbell, B.L., Elliott, G.L. and Loughran, R.J., 1985, Nuclear fallout as an aid to measuring soil erosion, *J. Soil Conserv.*, 41: 86-89.

Campbell, B.L., Loughran, R.J. and Elliott, G.L., 1988, A method for determining sediment budgets using caesium-137, *IAHS Publ.*, 174: 171-179.

Campbell, B.L., Loughran, R.J. and Elliott, G.L., 1982, Caesium-137 as an indicator of geomorphic processes in a drainage basin, *Australian Geographical Studies*, 20: 49-64.

CAS (Chinese Academy of Sciences), Leading Group of the Three Gorges Project Ecology and Environment Research Project, 1987, *Collected Papers on*

Ecological and Environmental Impact of the Three Gorges Project and Countermeasures, Science Press, Beijing (in Chinese).

Chemelil, M. C., 1995, *The effects of human-induced watershed changes on streamflows,* Unpublished PhD thesis, Loughborough University, pp.250.

Chen, G.J. and Gao, F.H., 1988, The ecology and environment of the Yangtze and the Three Gorges project, pp.1-15, in Chinese Academy of Sciences, Leading Group of the Three Gorges Project Ecology and Environment Research Project (ed.)*The Effect of the Yangtze Three Gorges project on Ecology and Environment and Countermeasures*, Science Press, Beijing (in Chinese).

Chu, W.H., 1988, PSL model under support of GIS in Loess Plateau, pp. 290-299, in *Loess Plateau Investigation using Remote Sensing,* Science Press, Beijing (in Chinese).

Church, M., Kellerhals, R. and Day, T.J., 1989, Regional clastic sediment yield in British Columbia, *Canadian Journal of Earth Science*, 26: 31-45.

CYJV (Canadian International Project Managers Ltd._Yangtze Joint Venture), 1988, *Three Gorges Water Control Project Feasibility Study*, 1-11.

Collins, A.L., D.E. Walling and Leeks, G.J.L., 1997, Source type ascription for fluvial suspended sediment based on a quantitative composite fingerprinting technique, *CATENA*, 29: 1-27.

Comans, R.N.J., Haller, M. and Depreter, P.,1991, Sorption of cesium on illite: nonequilibrium behaviour and reversibility, *Geochim. Cosmochim. Acta*, 55: 433-440.

Curran, P.J., 1980, Multispectral remote sensing of vegetation amount, *Progress in Physical Geography,* 4: 175-184.

Dai, D. Z. and Y. Tan, 1996, Soil erosion and sediment yield in the Upper Yangtze River basin, pp.191-203 in D.E. Walling and B.W. Webb. (eds.) *Erosion and Sediment Yield: Global and Regional Perspectives* (Proceedings of the Exeter Symposium, July 1996), IAHS Publ. no 236.

Dalgleish, H.Y. and I.D.L., Foster, 1996, Cs-137 losses from a loamy surface water gleyed soil (Inceptisol); a laboratory simulation experiment, *CATENA*, 26: 227-245.

Davenport, M.L. and Nicholson, S.E., 1992, Erosion and sediment yield in mountain region of the World, pp.29-36, in Walling, D.E., Davies, T.R. and Hasholt, B. (eds.) *Erosion, Debris Flows and Environment in Mountain Regions* (Proc. Chengdu Symp., July 1992), IAHS Publ. no.209.

Davenport, M.L. and Nicholson, S.E., 1993, On the relationship between rainfall and the Normalized Difference Vegetation Index for diverse vegetation types of East Africa, *Int. J. Remote Sens.*, 14: 2369-2389.

Davis, J.J.,1963, Cesium and its relationship to potassium in ecology, pp.539-556, in Schultz, V. and Klement, A.E. (eds.) *Radioecology*, Reinhold, New York.

De Boer, D.H. and Crosby, G., 1996, Specific sediment yield and drainage basin scale, pp.333-338, in D.E. Walling and B.W. Webb. (eds.) *Erosion and Sediment Yield: Global and Regional Perspectives* (Proceedings of the Exeter Symposium, July 1996). IAHS Publ. no. 236.

De Jong, E., Begg, C.B.M. and Kachanoski, R.G., 1983, Estimates of soil erosion and deposition for some Saskatchewan soils, *Can. J. Soil Sci.* 63: 607-617.

De Jong, E. and Kachanoski, R.G., 1988, The importance of erosion in the carbon balance of prairie soils, *Can. J. Soil Sci.* 68: 111-119.

De Jong, E., Villar, H. and Bettany, J.R.,1982, Preliminary investigations on the use of Cs-137 to estimate erosion in Saskatchewan, *Can. J. Soil Sci.*, 62: 673-683.

De Jong, E., Wang, C. and Rees, H.W., 1986, Soil redistribution on three cultivated New Brunswick hillslopes calculated from Cs-137 measurements, solum data and USLE, *Can. J. Soil Sci.*, 66: 721-730.

De Roo, A.P.J., 1991, The use of ^{137}Cs as a tracer in an erosion study in South Limburg (The Netherlands) and the influence of Chernobyl fallout, *Hydrological Processes,* 5: 215-227.

Dearing, J.A., H., Hakansson, B., Liedberg-Johnsson, A., Persson, S., Skansjo, D., Widholm and F., El Daoushy, 1987, Lake sediments used to quantify the erosional response to land use change in southern Sweden, *Oikos,* 50: 60-78.

Dedkov, A.P. and Moszherin, V.I., 1992, Erosion and sediment yield in mountain regions of the world, pp.29-36, in Walling, D.E., Davies, T.R. and Hasholt, B. (eds.) *Erosion, debris flows and environment in mountain regions* (Proceedings of the Chengdu Symposium, July 1992), IAHS Publ. no. 209.

Degens, E.T., Kempe, S. and Richey, J.E., 1991, Summary: biogeochemistry of major world rivers, pp.323-347, in E.T. Degens, S. Kempe and J.E. Richey (eds.) *Biogeochemistry of Major World Rivers*. Wiley, Chichester, UK.

Demmak, A., 1984, Recherche d'une relation empirique entre apports solides specifiques et parametres physico-climatiques des bassins: application au cas algerien, pp.403-414, in *Challenges in African Hydrology and Water Resources* (Proceedings of the Harare Symposium, July 1984) IAHS Publ. no. 144.

Department of Water and Soil Conservancy, 1988, *Technological standard SD238-87 of soil and water conservation,* Water and Electricity Press, Beijing (in Chinese).

Dominik, J., Burrus, D. and Vernet, J.P., 1987, Transport of the environmental radionuclides in an alpine watershed, *Earth and Planetary Science Letters*, 84: 165-180.

Douglas, I., 1967, Man, vegetation and the sediment yield of rivers, *Nature*, 215: 925-928.

Drake, N.A., Vafeidis, A., Wainwright, J. and Zhang, X.Y., 1995, Modelling soil erosion using remote sensing and GIS techniques, pp.217-224, in *Proceedings of RSS 95 Remote Sensing in Action, 11-14 September 1995, Southampton, UK.*

Edgington, D.N. and Robbins, J.A., 1990, Focusing time scales in Lake Michigan as revealed by fallout Cs-137, pp.210-223, in M. Tilzer and C. Serruya (eds) *Large Lakes: Ecological Structrure and Function, Brock/Springer Ser. Contemp. Biosci.* Springer-Verlag, New York.

Edgington, D.N., Klump, J.V., Robbins, J.A., Kusner, Y.S., Pampura, V.D. and Sandimirov, I.V., 1991, Sedimentation rates, residence times and radionuclid inventories in Lake Baikal from Cs-137 and Pb-210 in sediment cores, *Nature*, 350: 601-604.

Edmonds, R.L., 1994, *Patterns of China's lost harmony: a survey of the country's environmental degradation and protection*, Routledge, London

Edmond, R., 1996, Three Gorges dam: recent developments and prospects, *China Review*, 4: 4-9.

Eklundh, L. and Martensson, U.L., 1995, Rapid generation of digital elevation models from topographic maps, *Int. J. Geographical Information Systems*, 9(3): 329-340.

Elwell, H.A., 1981, A soil loss estimation technique for southern Africa, pp.281-292, in R.P.C. Morgan (ed) *Soil Conservation-Problems and Prospects*, Wiley, Chichester, UK.

ESRI, 1993, The digital chart of the world for use with Arc/Info.

ESRI, 1994, Cell-based modelling with GRID, *ArcDoc version 7.0.2* on-line help.

Eyman, L.D. and Kevern, N.R., 1975, Cesium-137 and stable cesium in a hypereutrophic lake, *Health Physics,* 28: 549-555.

Fairbridge, R.W., 1968, Terrace, fluvial-environmental controls, in 1124-1138, in Fairbridge, R.W. (ed.) *Encyclopedia of Geomorphology*, New York, Reinhold Book Corp.

FAO-UNESCO, 1977, *Soil map of the world (Scale: 1:5,000,000),* Paris: UNESCO (in English, French, Spanish, and Russian).

Farrar, T.J., Nicholson, S.E. and Lare, A.R., 1994, The influence of soil type on the relations between NDVI, rainfall, and soil-moisture in the semiarid Botswana: 2. NDVI response to soil-moisture, *Remote Sensing of Environment*, 50(2): 121-133.

Favis-Mortlock, D.T., Quinton, J.N. and Dickinson, W.T., 1996, The GCTE validation of soil erosion models for global change studies, *J. of Soil and Water Conservation*, 397-398.

Ferro, V. and Minacapilli, M., 1995, Sediment delivery processes at basin scale, *Hydrological Sciences*, 40(6): 703-717.

Fielding, E., Isacks, B., Barazangi, C. and Duncan, C., 1994, How flat is Tibet? *Geology*, 22: 163-167.

Fleming, G., 1969, Design curves for suspended load estimation, *Proceedings of the Institute of Civil Engineers,* 43: 1-9.

Forsyth, T.J., 1994, The use of caesium-137 measurement of soil erosion and farmers' perceptions to indicate land degradation amongst shifting cultivation in Northern Thailand, *Mountain Research and Development,* 14: 229-244.

Foster, I.D.L., 1995, Lake and reservoir bottom sediments as a source of soil erosion and sediment transport data in the UK, pp.265-283, in I.D.L. Foster, A.M. Gurnell and B.W.Webb (eds.)*Sediment and Water Quality in River Catchment,* John Wiley & Sons Ltd.

Foster, I.D.L. and Walling, D.E., 1994, Using reservoir deposits to reconstruct changing sediment yields and sources in the catchment of the Old Mill Reservoir, South Devon, UK, over the past 50 years, *Hydrological Sciences*, 39(4): 347-368.

Fournier, M.F., 1949, Les facteurs climatiques de l'erosion du sol, *Assoc. Geog.* Francais Bull., 203.

Fournier, F., 1960, *Climate et Erosion.* Presses Universitaires de France, Paris, 201pp.

Fredericks, C.W. and Perrens., S.J., 1988, Estimating erosion using caesium-137: II. Estimating rates of soil loss, pp. 233-240, in *Sediment Budgets* (Proc. Port Alegre Symp.), IAHS Publ. no.174.

Fredericks, C.W., Norris, V. and Perrens., S.J., 1988, Estimating erosion using caesium-137: I. Measuring caesium-137 activity in a soil, pp. 225-231, in *Sediment Budgets* (Proc. Port Alegre Symp.), IAHS Publ. no.174.

Frissel, M.J., Stoutjesdijk, J.F., Koolwijk, A.C. and Koster, H.W., 1987, The Cs-137 contamination of soils in Netherlands and its consequences for the contamination of crop products, *Netherlands Journal of Agricultural Science*, 35: 339-346.

Froehlich, W. and Walling D.E., 1992, The use of fallout radionuclides in investigations of erosion and sediment delivery in the Polish Flysch, pp. 61-76. in Walling, D.E., Davies, T.R. and Hasholt, B.(eds.) *Erosion, Debris Flows and Environment in Mountain Regions* (Proceedings of Chengdu Symposium, July, 1992), IAHS Publ. no. 209.

Giakoumakis, S.G. and Baloutsos, G., 1997, Investigation of trend in hydrological time series of the Evinos River basin, *Hydrological Sciences*, 42(1): 81-88.

Glymph, L.M. 1951, Relation of sedimentation to accelerated erosion in the Missouri River basin, USDA, *Soil Conservation Service Technical Paper 102.*

Govers, G., Quine, T.A. and Walling, D.E., 1993, The effect of water erosion and tillage movement on hillslope profile development: a comparison of field observations and model results: pp.285-300, in Wicherek, S. (ed.)*Farmland Erosion in Temperate Plains Environment and Hills*, Elserier, Amsterdam.

Govers, G., Vandaele, K., Desmet, P.J.J., Poesen, J. and Bunte, K., 1994, The role of tillage in soil redistribution on hillslopes, *Eur. J. Soil Sci.*, 45: 469-478.

Graham, E.R, 1963, Factors affecting Sr-85 and I-131 removed by runoff water, *Water Sewage Works*, 11: 407-410.

Grimshaw, D.L. and Lewin, J., 1980, Source identification for suspended sediments, *J. Hydrol.*, 43: 151-161.

Grist, J., Nicholson, S.E. and Mpolokang, A., 1997, On the use of NDVI for estimating rainfall fields in Kalahari of Botswana, *J. of Arid Environments*, 35: 195-214.

Gu, H.Y., Ai, N.S. and Ma, H.L., 1987, Sediment sources and trend of sedimentation in the Three Gorges reservoir area, pp. 522-541. in Chinese Academy of Sciences, Leading Group of the Three Gorges Project Ecology and Environment Research Project (ed.) *Collected Papers on Ecological and Environmental Impact of the Three Gorges Project and Countermeasures*, Science Press, Beijing (in Chinese).

Gu H.Y. and Douglas, I., 1989, Spatial and temporal dynamics of land degradation and fluvial erosion in the middle and upper Yangtze River basin, China, *Land Degradation & Rehabilitation*, 1: 217-235.

Gutman, G.G., Tarpley, D. and Ohring, G., 1987, Cloud screening for determination of land surface characteristics in a reduced resolution satellite data set, *Inte. J. of Remote Sensing,* 8: 859-870.

Haigh, M.J., 1977, Use of erosion pins in the study of slope evolution, *British Geomorphological Research Group Technical Bulletin*, 18: 20-47.

He, D.M., 1989, Soil erosion and sediment mathematical model development on GIS basis, pp.129-133, in *National Labratory of Resource and Environment Information System Annual Report*, Survey Press, Beijing (in Chinese).

He, N.W., 1989, Downstream effects of soil and water conservation and protection forestry in the upper reaches of the Yangtze river, pp.317-325, in Tian, F. and Lin, F.T. (eds.) *Zailun Sanxia Gongcheng De Honguan Juance* (In Chinese).

He, Q.P. and Walling, D.E., 1995, Rates of overbank sedimentation on the floodplains of British lowland rivers documented using fallout Cs-137, *Geogra. Ann.*, 78A (4): 223-234.

He, Q.P., Walling, D.E. and Owens, P.N., 1996, Interpreting the Cs-137 profiles observed in several small lakes and reservoirs in southern England, *Chemical Geology*, 129: 115-131.

Helsel, D.R. and Hirsch, R.M., 1992, *Statistical methods in water resources*: Studies in environmental science 49, Elsevier, Amsterdam.

Higgitt, D.L., 1995, The development and application of caesium-137 measurements in erosion investigations, pp.287-305, in Foster, I.D.L., Gurnell, A.M. and Webb, B.W.(eds.) *Sediment and Water Quality in River Catchments*, Johan Wiley & Sons Ltd.

Higgitt, D.L., Froehlich, W. and Walling, D.E., 1992, Applications and limitations of Chernobyl radiocaesium measurements in a Carpathian erosion investigation, Poland, *Land Degradation and Rehabilitation*, 3: 15-26.

Higgitt, D.L. and Rowan, J.S., 1995, Erosion assessment and administration in subtropical China: a case study from Fujian Province, *Land Degred. Rehab.*, 6.

Higgitt, D.L., Rowan, J.S. and Walling, D.E., 1993, Catchment-scale deposition and redistribution of Chernobyl radiocaesium in upland Britain. *Environment International*, 19:155-166.

Higgitt, D.L. and Walling, D.E., 1993, The value of caesium-137 measurements for estimating soil erosion and sediment delivery in an agricultural catchment, Avon, UK, pp.301-315, in S.Wicherek (ed.) *Farm Land Erosion in Temperate Plains Environment and Hills*, Amsterdam, Elsevier.

Higgitt, D.L., Walling, D.E. and Haigh, M.J., 1994, Estimating rates of ground retreat on spoils using caesium-137, *Applied Geography*, 14: 294-307.

Hirose, K., Aoyama, M., Katsuragi, Y. and Sugimura, Y., 1987, Annual deposition of Sr-90, Cs-137 and Pu-239, 240 from the 1961-1980 nuclear explositions: a simple model, *Journal of the Meterological Society of Japan*, 65(2): 259-277.

Hohenemser, C., Deicher, M., Hofsass, H. and Lindner, G., 1986, Agricultural impact of Chernobyl: a warning, *Nature,* 321, 817.

Holben, B.N., Eck, T.F., and Fraser, R.S., 1991, Temporal and spatial variability of aerosol optical depth in the Sahel region in relation to vegetation remote sensing, *Inte. J. of Remote Sensing*, 12: 1147-1163.

Hu, C.H., 1995, Controlling reservoir sedimentation in China, pp.50-52, in *Hydropower and Dams*, March issue,.

Huang, X.Q., 1982, *Chinese rivers*, Shao Wu Yin Shu Guan, Beijing (in Chinese).

Hudson, N.W., 1995, *Soil Conservation*, 3rd edn. Iowa State University Press, Ankeny, Iowa.

Huete, A.R. and Tucker, C.J., 1991, Investigation of soil influences in AVHRR red and near-IR vegetation index imagery, *Int. J. Remote Sens.,* 12: 1223-1242.

Hutchinson, M.F., 1988, Calculation of hydrological sound digital elevation models, *Third International Symposium on Spatial Data Handling,* Sydney, Columbus, Ohio: International Geographical Union.

Hutchinson, M.F., 1989, A new procedure for gridding elevation and stream line data automatic removal of spurious pits, *Journal of Hydrology*, 106: 211-232.

Jansen, J.M.L. and Painter, R.B., 1974, Predicting sediment yield from climate and topography, *Journal of Hydrology.*, 21: 371-380.

Jansson, M.B., 1988, A global survey of sediment yield, *Geogra. Ann.*, 70A: 81-98.

Justice, C.O., Townshend, J.R.G. and KALB, V.T., 1991, Representation of vegetation by continental data sets derived from NOAA-AVHRR data, *Int. J. Remote Sensing,* 12: 999-1021.

Justice, C.O., Townshend, J.R.G., Holben, B.N. and Tucker, C.J., 1985, Analysis of the phenology of global vegetation using meteorological satellite data, *Int. J. Remote Sensing*, 6: 1271-1381.

Kachanoski, R.G., 1987, Comparision of measured soil Cs-137 losses and erosion rates, *Can J. Soil Sci.*, 67: 199-203.

Kachanoski, R.G., 1993, Estimating soil loss from changes in soil caesium-137, *Can J. Soil Sci.*, 73: 629-632.

Kachanoski, R.G. and De Jong, E., 1984, Predicting the temporal relationship between soil caesium-137 and erosion rate, *J. Environ. Qual.*, 13: 301-304.

Kirkby, M.J., Baird, A.J., Lockwood, J.G., McMahon, M.D., Mitchell, P.J., Shao, J., Sheehy, J.E., Thornes, J.B. and Woodward, F.I., 1993, MEDALUS Project A1: Physical based process models: final report, in J.B. Thornes (ed.) *MEDALUS I final report.*

Kiss, J.J., De Jong, E. and Bettany, J.R., 1988, The distribution of natural radionuclides in native soils of Southern Saskatchewan, Canada, *J. Environ. Qual.*, 17: 437-445.

Kiss, J.J., De Jong, E. and Rostad, H.P.W., 1986, An assessment of soil erosion in West-central Saskatchewan using caesium-137, *Can. J. Soil Sci.*, 66: 591-600.

Kleinbaum, D.G., Kupper, L.L. and Muller, K.E., 1988, *Appllied Regression Analysis and Other Multivariate Methods* (2nd edn), PWS-Kent, Boston.

Knisel, W.G., 1980, CREAMS: a field scale model for chemicals, runoff and erosion from agricultural management systems, *USDA Conservation Research Report* No. 26.

Kottegoda, N.T., 1980, *Stochastic Water Resources Technology*, McMillan Press, Hong Kong.

Lajczak, A. and Jansson, M.B., 1993, Suspended sediment yield in the Baltic drainage basin, *Nordic Hydrology*, 24: 31-52.

Lance, J.C., McIntyre, S.C., Naney, J.W. and Rousseva, S.S., 1986, Measuring sediment movement at low erosion rates using caesium-137, *J. Soil Sci. Soc. Am.*, 50: 1303-1309.

Lane, E.W. and Borland, W.M., 1951, Estimateing bed load, *Trans. Am. Geophys. Union,* 32(1).

Langbein, W.B., and Schumm, S.A., 1958, Yield of sediment in relation to mean annual precipitation: *Transactions of the American Geophysical Union*, 39: 1076-1084.

Legates, D.R. and Willmost, C.J., 1992 Monthly average surface air temperature and precipitation. Digital Raster Data on a 30 minutes Geographic (lat/long) 360*720 grid. In: *Global Ecosystems Database Version 1.0*: Disc A. Boulder, CO: NOAA National Geophysical Data Centre.

Leonard, R.A., W.G. Knisel, and D.A. Still, 1987, GLEAMS: Groud water lading effects of agricultrual management systems. Transactions of the American Society of Agricultral Engineers, 30(5): 1403-1418.

Leopold, L.B., 1996, Sediment problems at Three Gorges Dam, *(http://www.irn/irn/programs/3g/leopold.html).*

Li, Q.Y., 1993, The determination and prediction of catchment scale erosion rates in purple soil areas of central Shichuan basin (Unpublished)(in Chinese).

Lindstrom, M.J., Nelson, W.W., and Schumacher, T.E., 1992, Quantifying tillage erosion rates due to moldboard plowing, *Soil Tillage Res.,* 24: 243-255.

Ling, B.N., Dou, G.R., Xian, J.H., Dai, D.Z., Cheng, J.S., Tang, R.C. and Zhang, R., 1990, Some latest research results on the sediment problems of the Three Gorges project, pp. 205-223. in Chinese Water Conservancy Society (ed.) *The Feasibility Studies of the Three Gorges Project,* Chinese Social Science Press, Beijing (in Chinese).

Liu, J.G., Qian, Z.X., Yang, Y.S. and Liang L., 1991, Studies on soil loss on slope cultivated lands with purple soil in the Yangtze Three Gorges region, *Acta Conservationis Soli Et Aquae Sinica*, 5: 36-44 (in Chinese).

Lomenick, T.F. and Tamura, T. 1965. Naturally occurring fixation of caesium-137 on sediment of lacustrine origin, *Soil Sci. Soc. Am. Proc.*, 29: 383-386.

Loughran, R.J., Campbell, B.L., Elliot, G.L. and Shelley, D.J. 1990. Determination of rates of sheet erosion on grazing land using caesium-137, *Applied Geography,* 10: 125-133.

Loughran, R.J., Campbell, B.L., Shelley, D.J and Elliot, G.L., 1992, Developing a sediment budget for a small drainage basin in Australia, *Hydrological Processes,* 6: 145-158.

Loughran, R.J., Campbell, B.L. and Walling, D.E., 1987, Soil erosion and sedimentation indicated by caesium-137: Jackmoor Brook catchment, Devon, England, *Catena,* 14: 201-212.

Loughran, R.J., Elliot, G.L., Campbell, B.L. and Shelley, D.J., 1988, Estimation of soil erosion from caesium-137 measurements in a small cultivated catchment in Australia. *Radiat. Isot.*, 39: 1153-1157.

Longmore, M.E., O'Leary, B.M., Rose, C.W. and Chandia, A.L., 1983, Mapping soil erosion and accumulation with the fallout isotope caesium-137, *Aust. J. Soil Res.*, 21: 373-386.

Loureiro, N. S., and M. A. Coutinho, 1995, Rainfall changes and rainfall erosivity increase in the Algarve (Portugal), *Catena,* 24: 55-67.

Lu X.X. and Shi D.M., 1992, Soil erosion and revegetation in the hilly areas of South China, pp.31-34, in *Proceedings of an international symposium on forage development of the red soils of South Central China*, Australian Centre for International Agricultural Research, Canberra.

Lu, X.X. and Shi, D.M., 1992, Study on characteristics of sediment eroded from red soil, pp.152-154, in Gong, Z.T. (ed.) *Proceedings of International symposium on Management and Development of Red Soils in Asia and Pacific Region.* Science Press, Beijing, New York.

Lu, X.X. and Shi, D.M., 1994, Advances in soil erosion model, *Progresses in Soil Science*, 22(2): 9-14.

Ludwig, W. and Probst, J.L., 1996, A global modelling of the climatic, morphological, and lithological control of river sediment discharges to the oceans, pp21-28, in Walling, D.E. and Webb, B.W. (eds.)*Erosion and Sediment Yield: Global and Regional Perspectives* (Proceedings of the Exeter Symposium, July 1996). IAHS Publ. no.236.

Luk, S.H. and Whitney, J., 1993a, *Megaproject: A Case Study of China's Three Gorges Project*, Armonk, New York and London, England.

Luk, S.H. and Whitney, J., 1993b, Unresolved issues: perspectives from China, pp.89- 99. in Barber, M. and Ryder, G. (eds.) *Damming the Three Gorges, What Dam Builders Don't Want to Know, A Critique of the Three Gorges Water Control Project Feasibility Study,* Second Edition. Probe International. Earthscan. London-Toronto.

Lvovich, M.I., Karasik, G.Y., Bratseva, N.L., Medvedeva, G.P. and Maleshko, A.V., 1991, *Contemporary intensity of the world land intracontinental erosion. USSR*, Academy of Sciences, Moscow.

Maidment, D.R., 1993, GIS and hydrologic modelling, pp.147-167, in Goodchild, M.F., Parks, B.O. and Steyaert, L.T. (eds.) *Environmental modelling with GIS*, Oxford University Press, Oxford.

Malo, A.R. and Nicholson, S.E., 1990, A study of rainfall and vegetation dynamics in the AFRICAN Sahel using Normalized Difference Vegetation Index, *J. Arid Environ.*, 19: 1-24.

Martz, L.W., 1992, The variation of soil erodibility with slope position in a cultivated Canadian prairie landscape, *Earth Surface Processes and Landforms,* 17: 543- 556.

Martz, L.W. and De Jong, E., 1987, Using caesium-137 to assess the variability of net soil erosion and its association with topography in a Canadian Prairie landscape, *Catena,* 14: 439-451.

Mathews, K.M., 1989, *Radioactive fallout in the South Pacific: a history, Part 1. Deposition in New Zealand. Report NRL 1989/2,* National Radiation Laboratory, Christchurch.

McCall, P.L., Robbins, J.A. and Matisoff, G., 1984, Cs-137 and Pb-210 transport and geochronologies in urbanized reservoirs with rapidly increasing sedimentation rates, *Chem. Geol.*, 44: 33-65.

McCallan, M.E., O'Leary, B.M. and Rose, C.W., 1980, Redistribution of caesium-137 by erosion and deposition in an Australian soil, *Australian Journal of Soil Research,* 18: 119-128.

McFarlane, D.J., Loughran, R.J. and Campbell, B.L., 1992, Soil erosion of agricultural land in western Australia estimated by caesium-137, *Aust. J. Soil Res.,* 30: 533-546.

McHenry, J.R., 1968, Use of tracer techniques in soil erosion research, *Transactions of the American Society of Agricultural Engineers,* 11(5): 619-625.

McHenry, J.R., Ritchie, J.C. and Gill, A.C., 1973, Accumulation of fallout caesium-137 in soils and sediments in selected watersheds, *Water Resour. Res.*, 9:676-686.

McIntyre, S.C., Lance, J.C., Campbell, B.L. and Miller, R.L., 1987, Using caesium-137 to estimate soil erosion on a clearcut hillside, *J. Soil and Water Conservation*, 42: 117-120.

Meade, R.H. and Parker, R.S., 1985, Sediment in rivers of the United States, pp.49-60, *U.S. Geol. Survey Water-Supply Pap.* 2275.

Megumi, K. and Mamuro, T., 1977, Concentration of uranium series nuclides in soil particles in relation to their size, *J. of Geophysical Research*, 82(2): 353-356.

Menzel, R.G., 1974, Land surface erosion and rainfall as sources of strontium-90 in streams, *J. Environ. Qual.,* 3: 219-223.

Menzel, R.G., Jung, P, Ryu, K. and Um, K., 1987, Estimating soil erosion losses in Korea with fallout caesium-137, *J. Appl. Radiat. Isot.,* 38: 451-454.

Milliman, J.D. and Meade, R.H., 1983, World-wide delivery of river sediment to the oceans, *J. Geology*, 91: 1-21.

Milliman, J.D. and Syvitski, J.P.M., 1992, Geomorphic/tectonic control of sediment discharge to the ocean: the importance of small mountainous rivers, *Journal of Geology*, 100, 525-544.

Milliman, J.D., Y.S. Qin, M.E. Ren and Y. Saito, 1987, Man's influence on the erosion and transport of sediment by Asian rivers: the Yellow River (Huanghe) example, *Journal of Geology,* 95: 751-762.

Morgan, R.P.C., J.N., Quinton, and R.J. Rickson, 1992, *EUROSEM documentation manual*, Silsoe College, Silsoe, Bedford, UK.

Murray, A.S., Marten, R., Johnston, A. and Martin, P. 1987 Analysis for naturally occurring radionuclides at environmental concentrations by gamma spectrometry. *Journal of Radioanalytical and Nuclear Chemistry, Articles*, 115, 263-288.

Musgrave, G.W., 1947, The quantitative evaluation of factors in water erosion-a first approximation, *J. Soil and Water Conservation, 2(3):* 133-138, 170.

NISS-CAS (Nanjing Institute of Soil Science-Chinese Academy of Sciences), 1988, Soils of China, Beijing , Science Press (in Chinese and English).

Navas, A. and Walling, D.E., 1992, Using caesium-137 to assess sediment movement on slopes in a semiarid upland environment in Spain, pp.129-138, in Walling, D.E., Davies, T.R. and Hasholt, B. (eds.) *Erosion, Debris Flows and Environment in Mountain Regions* (Proc. Chengdu Symp., July 1992), IAHS Publ. no.209.

Nearing, M.A., G.R. Foster, L.J., Lane, and S.C. Finckner, 1989, A process-based soil erosion model for USDA-water erosion prediction project technology, *Transations of the American Society of Agricultrual Engineers*, 32: 1587-1593.

Neil D.T. and Mazari, R.K. 1993, Sediment yield mapping using small dam sedimentation surveys, Southern Tablelands, New South Wales, *Catena*, 20: 13-25.

Nicholson, S.E. and Farrar, T.J., 1994, The influence of soil type on the relations between NDVI, rainfall, and soil-moisture in the semiarid Botswana: 1, NDVI response to rainfall, *Remote Sensing of Environment*, 50(2): 107-120.

NOAA-EPA Global Ecosystem Project, 1992, *Global Ecosystems Database Version 1.0* . User's Guide, Documention, Reprints, and Digital Data on CD-ROM. USDOC/NOAA National Geophysical Data Center, Boulder, CO.

Nolin, M.C., Cao, Y.Z., Coote, D.R. and Wang, C., 1993, Short-range variability of fallout Cs-137 in an uneroded forest soil, *Can. J. Soil Sci.*, 73: 381-385.

Oldfield, F., P.G. and Clark, R.L., 1990, Lake sediment-based studies of soil erosion, pp.201-228, in Boardman, J., Foster, I.D.L. and Dearing, J.A.(eds.) *Soil erosion on agricultural land,* John Wiley & Sons Ltd.

Oldfield, F., P.G. Appleby, and R. Thompson 1980 Palaeoecological studies of lakes in the Highlands of Papua New Guinea. I. The chronology of sedimentation, *Journal of Ecology,* 68: 457-477.

Oldfield, F., P.G. Rummery, T.A., Thompson, R. and Walling, D.E., 1979, Identification of suspended sediment sources by means of magnetic measurements: some preliminary results, *Water Resour. Res.*, 15: 211-219.

Olley, J.M., Murray, A.S., Mackenzie, D.H. and Edwards, K., 1993, Identifying sediment sources in a gullied catchment using natural and anthropogenic radioactivity, *Water Resource Research,* 29(4), 1037-1043.

Owens, P.N. and Walling, D.E., 1996, The variability of caesium-137 inventories at reference sites: an example from two constrasting sites in England and Zimbabwe, *Appl. Radiat. Isot.* 47(7): 699-707.

Owens, P.N., Walling, D.E., He, Q.P., Shanahan, J. and Foster. I.D.L., 1997, The use of caesium-137 measurements to establish a sediment budget for the Start catchment, Devon, UK, *Hydrological Sciences*, 42(3): 405-423.

Ozturk, F., 1996, Suspended sediment yields of rivers in Turkey, pp.65-71, in Walling, D.E. and Webb, B.W. (eds)*Erosion and Sediment Yield: Global and Regional Perspectives* (Proceedings of the Exeter Symposium, July 1996), IAHS Publ. no.236.

Pan, J.Z. 1990. The beginning and end of the Three Gorges Project Feasibility Studies, pp.1-12, in Chinese Water Conservancy Society (ed.) *The Feasibility Studies of the Three Gorges Project*, Chinese Social Science Press, Beijing (in Chinese).

Peart, M.R. and Walling, D.E., 1986, Fingerprinting sediment sources: the example of a small drainage basin in Devon, UK, pp.41-55, in R.F. Hadley (ed.) *Drainage Basin Sediment Delivery* (Proceedings of the Albuquerque Symp., July 1986), IAHS Publ. no. 159.

Peart, M.R. and Walling, D.E., 1988, Techniques for establishing suspended sediment sources in two drainage basins in Devon, UK: a comparative assessment, pp.269-279, in M.P. Bordas and Walling, D.E. (eds.) *Sediment Budgets* (Proceedings of the Porto Alegre Symp., Dec. 1988), IAHS Publ. no.174.

Peart, M.R., 1990, Methodologies currently available for the determination of suspended sediment sources: a critical review, pp. 150-157, in *Proceedings 4th Int. Symp. on River Sediment (Beijing, June 1989),* IRTCES, Beijing.

Phillips, J.D., 1993, Pre- and post-colonial sediment sources and storage in the Lower Neuse Basin, North Carolina, *Physical Geography,* 14: 272-284.

Pinet, P. and Souriau, M., 1988, Continental erosion and large-scale relief: *Tectonics,* 7: 563-582.

Probst, J.L. and Amiotte-Suchet, P., 1992, Fluvial suspended sediment transport and mechanical erosion in the Maghreb (North Africa), *Hydrological Sciences Journal*, 37, 621-637.

Pu, L.J., 1997, *Land degradation and soil erosion quantification*, Unpublished PhD thesis. pp.93 (in Chinese).

Qian N., Zhang R. and Chen Z.C., 1993, Some aspects of sedimentation at the Three Gorges Project, pp121-160, in Luk, S-H. and Whitney, J.B. (eds.) *Megaproject A case Study of China's Three Gorges Project*, M.E. Sharpe, Armonk. NY.

Qian, N., Zhang, R. and Chen, Z.C., 1988, Answering a few questions on the sediment problems of the Three Gorges project, pp. 362-389, in Chong, E. et al. (eds.) *The Feasibility and Decision of the Three Gorges Project*, Shanghai Scientific & Technological Bibliographical Press, Shanghai (in Chinese).

Quine, T.A., 1995, Estimation of erosion rates from Caesium-137 data: the calibration question, pp.307-329, in I.D.L.Foster, A.M.Gurnell and B.W.Webb (eds.) *Sediment and Water Quality in River Catchments*.

Quine, T.A., Walling, D.E. and Govers, G., 1996, Simulation of radiocaesium redistribution on cultivated hillslopes using a mass-balance model: an aid to process interpretation and erosion rates estimation, pp.561-588, in M.G.Anderson and S.M. Brooks (eds.) *Advances in Hillslope Processes, Volume 1.*

Quine, T.A., Walling, D.E., Zhang, X. and Wang, Y., 1992, Investigation of soil erosion on terraced fields near Yanting, Sichuan Province, China, using caesium-137, pp. 155-168, in Walling, D.E., Davies, T.R. and Hasholt, B. (eds.) *Erosion, Debris Flows and Environment in Mountain Regions* (Proc. Chengdu Symp., July 1992), IAHS Publ. no.209.

Rango, A., 1970, Possible effects of precipitation modification on stream channel geometry and sediment yield, *Water Resources Research*, 6: 1765-1770.

Renard, R.G., 1995, Overview of RUSLE and its factors, pp.161-177, in *Proceedings of Sino-Amwrican Workshop on Steepland Soil Erosion Estimation Technology*, National Pingtung Polytechnic Institute, Pingtung, Taiwan.

Renard, R.G., G.R. Foster, G.A. Weesies, and J.P. Porter, 1991, RUSLE-revised universal soil loss equation, Journal of Soil and Water Conservation, 46(1): 30-33.

Ritchie, J.C. and McHenry, J.R., 1990, Application of radioactive caesium-137 for measuring soil erosion and sediment accumulation rates and patterns: a review, *J. Environ. Qual.*, 19: 215-233.

Ritchie, J.C., Hawks, P.H. and McHenry, J.R., 1975, Deposition rates in valleys determined using fallout cesium-137, *Geol. Soc. Am. Bull*, 86: 1128-1130.

Ritchie, J.C., McHenry, J.R. and Gill, A.C., 1972, The distribution of caesium-137 in the upper 10 cm of soil under different cover types in northern Mississippi, *Health Phys.*, 22:197-198.

Ritchie, J.C., McHenry, J.R. Gill, A.C. and Hawks, P.H., 1970, Distribution of fallout caesium-137 in sediment profile, *Health Phys.*, 19: 334.

Ritchie, J.C., Spraberry, J.A. and McHenry, J.R., 1974, Estimating soil erosion from the redistribution of fallout caesium-137, *Soil Sci. Soc. Am. Proc.* 38:137-139.

Rogowski, A.S. and Tamura, T, 1965. Movement of caesium-137 by runoff, erosion and infiltration on the alluvial Captina silt loam, *Health Phys.*, 11: 1333-1340.

Rogowski, A.S. and Tamura, T., 1970, Erosional behavior of cesium-137, *Health Phys.*, 18: 467-477.

Romkens, M.J.M., Wang, J.Y. and Darden, R.W., 1988, A laser microrelief meter, *Transactions of the American Society of Agricultural Engineers,* 31(2): 408-413.

Rooseboom A. and Lotriet, H.H., 1992, The new sediment yield map for Southern Africa, in Bogen, J., Walling, D.E. and Day, T.J. (eds.) *Erosion and Sediment Transport Monitoring Programmes in River Basins* (Proceedings of the Oslo Symposium, August 1992), IAHS Publ. no. 210.

Rose, C.W., Williams, J.R., Sander, G.C. and Barry, D.A., 1983, A mathematical model of soil erosion and deposition processes: I: Theory for a plane land element, *Soil Sci.Soc. Am. J.*, 47: 991-995.

Rowan, J.S., Higgitt, D.L. and Walling, D.E., 1993, Incorporation of Chernobyl-derived radiocaesium into reservoir sedimentary sequences, pp.55-71, in McManus and R.W. Duck (eds.) *Geomorphology and Sedimentology of Lakes and Reservoirs,* John Wiley & Sons Ltd.

Ruddiman, W.F., Prell, W.L., and Raymo, M.E., 1989, Late Cenozoic uplift in southern Asia and the American West: Rationale for general circulation modeling experiments, *Journal of Geophysical Research*, 94: 18,379-18,391.

Ryder, G. and Barber, M., 1993, Chapter one, Damming the Three Gorges: 1920-1993, pp.1-22. in Barber, M. and Ryder, G. (eds.) *Damming the Three Gorges, What Dam Builders Don't Want to Know, A Critique of the Three Gorges Water Control Project Feasibility Study*, Second Edition. Probe International. Earthscan. London-Toronto.

Santschi, P.H., Bollhalder, S., Farrenkothen, K., Lueck, A., Zingg, S. and Sturm, M., 1988, Chernobyl radionuclides in the environment: Tracers for the tight coupling of atmospheric, terrestrial, and aquatic geochemical processes.

Santschi, P.H., Bollhalder, S., Zingg, S., Lueck, A. and Farrenkothen, K., 1990, The self-cleaning capacity of surface waters after radioactive fallout: Evidence from European waters after Chernobyl, 1986-1988, *Environ. Sci. Technol.*, 24: 519-527.

Sarmiento, J.L. and Gwinn, E., 1986, Strontium 90 fallout prediction, *J. Geophys. Res.*, 91: 7631-7646.

Sauders, I. and Young, A., 1983, Rates of surface processes on slopes, slope retreat, and denudation, *Earth Surface Process and Landforms*, 8: 473-501.

Schultz, P.A. and Halpert, M.S., 1993, Global correlation of temerature, NDVI and preciptation, *Advances in Space Research*, 13(5): 277-280.

Schultz, P.A. and Halpert, M.S., 1995, Global analysis of the relationship among a vegetation index, preciptation and land surface temperature, *Int. J. Remote Sensing*, 16(7): 1289-1302.

Schultz, R.K., Overstreet, R. and Barshad, I., 1960, On the soil chemistry of caesium-137, *Soil Sci.*, 89: 19-27.

Sellers, P.J., 1985, Canopy reflectance, photosynthesis, and transpiration, *Int. J. Remote Sens.*, 6: 1335-1372.

Shi, D.M., Shi, X.R., Li, D.M. and Liang Y., 1996, Study on dynamic monitoring of soil erosion using remote sensing technique, *Acata Pedologica Sinica,* 33(1): 48-58 (in Chinese).

Shi, D.M., Yang, Y.S. and Lu, X.X., 1987, The impact of soil erosion on sediment sources in the Three Gorges project reservoir area and countermeasures, pp. 498-521. in Chinese Academy of Sciences, Leading Group of the Three Gorges Project Ecology and Environment Research Project (ed.) *Collected papers on ecological and environmental impact of the Three Gorges project and countermeasures*, Science Press, Beijing (in Chinese).

Shi, D.M., Yang, Y.S., Lu, X.X. and Liang, Y., 1992, The analysis of soil erosion pattern and sediment sources in the Three Gorges area of the Yangtze River, *Acta Conservationis Soli Et Aquae Sinica,* 5: 9-21(in Chinese).

Slaymaker, O., 1987, Sediment and solute yields in British Columbia and Yukon: their geomorphic significance re-examined, pp.925-945,in Gardiner, V. (ed.) *International Geomorphology 1986 (Part 1)*, John Wiley, Chichester.

Smil, V., 1987, Land degradation in China: an ancient problem getting worse, pp. 214-222, in P. Blaikie and H. Brookfield (eds.) *Land Degradation and Society*, Methuen, London.

Smil, V., 1993, *China's Environmental Crisis: an inquiry into the limits of national development*, M.E. Sharpe, New York.

Smith, D.D., 1941, Interpretation of soil conservation data for field use, *Agricultural Engineering,* 22(5): 173-175.

Smith, J.N., and Ellis, K.M., 1982, Transport mechanism for Pb-210, Cs-137 and Pu fallout radionuclides through fluvial marine systems, *Geochim. Cosmochim. Acta,* 46: 941-945.

Smith, J.N., Ellis, K.M. and Nelson, D.M., 1987, Time-dependent modelling of fallout radionuclide transport in a drainage basin: significance of "slow" erosional and "fast" hydrological components, *Chem. Geol.,* 63: 157-180.

Sneyers, R., 1992, Use and misuse of statistical methods for the detection of climatic change. Report on the informal planning meeting on statistical procedures for climate change detection, *World Climate Data Programme* Series 20, Annex 3, WMO, Geneva.

Soil and Water Conservation Office of Sichuan Changshou County, 1988, A report of soil and water conservation plan (unpublished) (in Chinese).

Soil and Water Conservation Office of Sichuan Nanchong County, 1988, A control plan of soil and water conservation plan (unpublished) (in Chinese).

Soil and Water Conservation Office of Sichuan Pengxi County, 1988, A plan report of soil and water conservation (unpublished) (in Chinese).

Soil and Water Conservation Office of Sichuan Province, 1983, An investigation report of soil and water loss (unpublished) (in Chinese).

Soileau, J.M., Hajek, B.F. and Touchton, J.T. 1990. Soil erosion and deposition evidence in a small watershed using fallout caesium-137, *Soil Sci. Soc. Am. J.,* 54: 1712-1719.

Stanners, A.A. and Aston, S.R., 1984, The use of reprocessing effluent radionuclides in the geochronology of recent sediment, In: J.A. Robbins (Guest-Editor), *Geochronology of Recent Deposits. Chem. Geol.,* 44: 19-32.

Stone, M. and Saunderson, H.C., 1996, Regional patterns of sediment yield in the Laurentian Great Lakes basin, pp.125-131, in Walling, D.E. and Webb, B.W. (eds.) *Erosion and Sediment Yield: Global and Regional Perspectives* (Proceedings of the Exeter Symposium, July 1996), IAHS Publ. no. 236.

Summerfield, M. A., 1991, *Global geomorphology*. Wiley, Chichester.

Summerfield, M.A. and Hulton, N.J., 1994, Natural controls of fluvial denudation rates in major world drainage basins, *Journal of Geophysical Research*, 99(B7): 13,871-13,883.

Sutherland, R.A., 1989, Quantification of accelerated soil erosion using environmental tracer caesium-137, *Land Degradation and Rehabilitation*, 1: 199-208.

Sutherland, R.A.,1991, Examination of caesium-137 areal activities in control (uneroded) locations, *Soil Technology*, 4: 33-50.

Tamura, T., 1964, Reaction of caesium-137 and strontium-90 with soil minerals and sesquioxides, pp.465-478. in *8th Int. Congr. of Soil Sci., Bucharest, Romania. 31 August--9 September. Int. Soc. of Soil Sci.*, Wageningen, Netherlands.

Thornes, J.B., 1985, The ecology of erosion, *Geography,* 70: 222-234.

Thornes, J.B., 1989, Erosional equilibria under grazing, pp.193-210 in Bintliff, J., Davidson, D. and Grant, E. (eds.) *Conceptual Issues in environmental Archaeology*, Edingburgh University Press.

Townshend, J.R.G. and Justice, C.O., 1990, The spatial variation of vegetation changes at very coarse scales, *Int. J. Remote Sensing,* 11: 149-157.

Townshend, J.R.G. and Tucker, C.J., 1981, Utility of AVHRR of NOAA-6 and NOAA-7 for vegetation mapping, pp.97-107, in *Proceedings Matching Remote Sensing Technologies and Application* (London: Remote Sensing Society).

Townshend, J.R.G., Justice, C.O. and Kalb, V.T., 1987, Characterization and classification of South American land cover types using satellite data, *Int. J. Remote Sensing*, 8: 1189-1207.

Trimble, S.W., 1981, Changes in sediment storage in the Coon Creek basin, Driftless Area, Wisconsin, 1853-1975, *Science*, 214: 181-183.

Trimble, S.W., 1977, The fallacy of stream equilibrium in contemporary denudation studies, *American Journal of Science*, 277: 876-887.

Tucker, C.J. Vanpraet, C.L., Boerwinkle, E. and Easton, A., 1983, Satellite remote sensing of total dry matter accumulation in the Senegaless Sahel, *Remote Sensing of Environment,* 13: 461-469.

Tucker, C.J., Gatlin, J.A. and Schneider, S.R., 1984, Monitoring vegetation in the Nile Delta with NOAA-6 and NOAA-7 AVHRR imagery, *Photogrammetric Engineering and Remote Sensing,* 50: 53-61.

Tucker, C.J. and Sellers, P.J., 1986, Satellite remote sensing of primary production, *Int. J. Remote Sens.*, 7: 1395-1416.

Tucker, C.J., Townshend, J.R.G. and Goff, T.E., 1985, African land-cover classification using satellite data, *Science*, 227: 369-375.

Van Slyke, L.P., 1988, *Yangtze: nature, history, and the river*, Addison-Wesley Publishing Company, Inc. pp.211.

Vorosmarty, C.J., Meybeck, M., Fekete and Sharma, K., 1997, The potential impact of neo-Castorization on sediment transport by the global network of rivers, pp.261-273, in D.E. Walling and J-B Probst (eds.) *Human Impact on Erosion and Sedimentation* (Proceedings of the Rabat Symposium S6, April 1997), IAHS Publ. no. 245.

Wall, G.J. and Wilding, L.P., 1976, Mineralogy and related parameters of fluvial suspended sediments in Northwestern Ohio, *J. Environ. Qual.*, 5: 168-173.

Wallbrink, P.J. and Murray, A.S., 1993, Use of fallout radionuclides as indicators of erosion processes, *Hydrological Processes*, 7: 297-304.

Wallbrink, P.J. and Murray, A.S., 1996, Distribution and variability of Be-7 in soils under different surface cover conditions and its potential for describing soil redistribution processes, *Water Resources Research*, 32(2): 467-476.

Walling, D.E. and Quine, T.A., 1990a, Use of caesium-137 to investigate patterns and rates of soil erosion on arable fields, pp.33-53, in J. Boardman, I.D.L. Foster and J.A. Dearing (eds.) *Soil erosion on agricultural land*, John Wiley & Sons, Chichester.

Walling, D.E. and Quine, T.A., 1990b, Calibration of caesium-137 measurements to provide quantitative erosion rate data, *Land Degradation & Rehabilitation*, 2: 161-175.

Walling, D.E. and Quine, T.A., 1991, The use of caesium-137 measurements to investigate soil erosion on arable fields in the UK: potential applications and limitations, *J. Soil Sci.*, 42:147-165.

Walling, D.E. and Woodward, J.C., 1992, Use of radiometric fingerprints to derive information on sediment sources, pp.153-163, in Bogen, J., Walling, D.E. and T., Day (eds.) *Erosion and Sediment Transport Monitoring Programmes in River Basins,* IAHS Publ. no.210.

Walling, D.E., 1983, The sediment delivery problem, *Journal of Hydrology*, 65: 209-237.

Walling, D.E., 1997, The response of sediment yields to environmental change, pp. 77-89, in D.E. Walling and J-B Probst (eds.) *Human Impact on Erosion and*

Sedimentation (Proceedings of the Rabat Symposium S6, April 1997), IAHS Publ. no. 245.

Walling, D.E., and Webb, B.W., 1983, Patterns of sediment yield, pp.61-100, in K.J. Gregory (ed.) *Background to Palaeohydrology*, Wiley, Chichester.

Walling, D.E., and Webb, B.W., 1996, Erosion and sediment yield, a global overview, pp.3-19, in D.E. Walling and B.W. Webb (eds.) *Erosion and Sediment Yield: Global and Regional Perspectives* (Proceedings of the Exeter Symposium, July 1996), IAHS Publ. no. 236.

Wan, G.J., Lin, W.Z., Huang, G.R. and Cheng, Z.L., 1990, Caesium-137 dating and erosion tracing in Hongfeng Lake, *Science Bulletin*, 19, 1487-1490 (in Chinese).

Wang, Y.C, Zhang, X.B., Li, S.L., Zhao, Q.C., Jiao, J.J., Zhang, Y.Y., Yan, M.Q. and Bai, L.X., 1991, The quantification of siltation depth of arable land in the Gaoqiao of the Three Gorges area using Cs-137, *Geography*, 4 (1): 63-64 (in Chinese).

Ward, P.R.B., 1980, Sediment transport and a reservoir siltation for Zimbabwe-Rhodesia, *Die Siviele Ingenier in Suid-Afrika* (January 1980).

Waythomas, C.F. and Williams, G.P. 1988 Sediment yield and spurious correlation - Toward a better portrayal of the annual suspended sediment load of rivers, *Geomorphology*, 1: 309-316.

Whitmore, T.J., Brenner, M., Engstrom, D.R. and Song, X.L., 1994, Accelerated soil erosion in watersheds of Yunnan Province, China, *J. Soil and Water Cons.*, 49(1): 67-72.

Williams, J.R., 1985, The physical components of the EPIC model. pp.272-284, in S.A.EL-Swaify, W.C. Moldenhauer, and A. Lo (eds.) *Soil Erosion and Conservation,* Soil Conservation Society of America, Ankeny, Iowa.

Williams, J.R., Nicks, A.R., Nearing, M.A., Skidmore, E. and Valentin, C., 1996, Using soil erosion models for global change studies, *J. of Soil and Water Conservation*, 51(5).

Wilson, L., 1973, Variation in mean annual sediment yield as a function of mean annual precipitation, *American Journal of Science*, 273: 335-349.

Wischmeier, W.H., and D.D. Smith, 1958, Rainfall energy and its relationship to soil loss, *Trans Am. Geophys. Un.*, 39: 285-291.

Wischmeier, W.H., and D.D. Smith, 1978, Predicting rainfall erosion losses. *U.S. Department of Agricultrure, Agricultural Research Service, Handbook No. 537*, 58pp.

Wise, S.M., 1980, Caesium-137 and lead-210: A review of techniques and some application in geomorphology, pp.109-127, in R.A. Cullingford et al. (eds.) *Timescales in geomorphology*, John Wiley & Sons, Chichester.

Xiang, L., Wang, S.M. and Xuang, B., 1993, Chernobyl Cs-137 deposition and dating in Jiangsu and Anhui (unpublished, in Chinese).

Xu, B.B., 1987, Relationships between soil reflectance and soil chemical and physical properties, *Soil Bulletin*, 41 (in Chinese).

Xu, B.B., 1991, Soil reflectance studies, *Environmental Remote Sensing*, 6(1): 62-70 (in Chinese).

Xu, J.X., 1994, Zonal distribution of river basin erosion and sediment yield in China, *China Science Bulletin*, 39, 1356-1361.

Yang, W., Yang, L. and Merchant, J.W., 1997, An assessment of AVHRR/NDVI-ecoclimatological relations in Nebraska, U.S.A., *Int. J. Remote Sensing*, 18(10): 2161-2180.

Yang, Y.S., 1985, Slope soil erosion prediction, *Soil and Water Conservation Bulletin*, 3: 51-55 (in Chinese).

Yang, Y.S. and Shi, D.M., 1994, *Soil Eerosion in the Three Gorges Area*, Southeastern University Press, Nanjing, pp.300 (in Chinese).

Yang, Y.S., Shi, D.M. and Lu, X.X., 1991, Research of the amount of soil loss on slope surfaces and the sediment into the Yangtze River in the Three Gorges area, *Acta Conservationis Soil Et Aquae Sinica*, 5:22-28 (in Chinese).

Young, R.A. and Onstad, C.A., 1987, Soil erosion: measurement and prediction, pp.91-111, in J.M. Harlin and G.M. Berardi (eds.) *Agricultural Soil Loss: Processes, Policies and Prospects*, Westview Press, Boulder, Colorado.

Young, R.A., Onstad, C.A., Bosch, D.D. and Anderson, W.P., 1989, AGNPS: a nonpoint-source pollution model for evaluating agricultral watersheds, *Journal of Soil and Water Conservation*, 44(2): 168-173.

Yu, J.R., Shi, L.R., Feng, M.H. and Li, R.H., 1991, The surface erosion and fluvial silt in the upper reaches of Changjiang River, *Bulletin of Soil and Water Conservation*, 11(1): 9-17 (in Chinese).

Zhang, X.B., Higgitt, D.L. and Walling, D.E., 1990, A preliminary assessment of the potential for using caesium-137 to estimate rates of soil erosion in the Loess Plateau of China, *Hydrological Sciences Journal*, 35: 267-276.

Zhang, X.B., Li, C.L., Quine, T.A. and Walling, D.E., 1993, Tillage effect on soil erosion quantification of arable land using Cs-137, *Chinese Science Bulletin*, 38 (22): 2072-2076 (in Chinese).

Zhang, X.B., Quine, T.A., Walling, D.E. and Li, Z., 1994, Application of the caesium-137 technique in a study of soil erosion on gully slopes in a Yuan area of the Loess Plateau near Xifeng, Gansu province, China, *Geografiska Annaler, Series A, Physical Geography*, 76: 103-120.

Zhang, X.Y., Drake, N.A., Wainwright, J. and Mulligan, M., 1997, Global scale overland flow and soil erosion modelling using remote sensing and GIS techniques: model implementation and scaling, pp.379-384, in G. Griffiths and D. Pearson (eds.) *Observations & Interactions (The Proceedings of 23rd Annual Conference and Exhibition of the Remote Sensing Society, 2-4 September, Reading, UK).*

Zhao, S.Q., 1994, *Geography of China: environment, resource, population, and development,* New York: Wiley, pp.332.

Zhou, G.Y. and Xiang, Z., 1994, Sediment transport in the Yangtze basin. pp.291-296, in L.J. Oliver, R.J. Loughran and J.A. Kesby (eds.) *Variability in Stream Erosion and Sediment Transport* (Proceedings of the Canberra Symposium, December 1994), IAHS Publ. no. 224.

Zhou, G.Y. and Xiang, Z., 1994, Sediment transport in the Yangtze basin, in *Variability in Stream Erosion and Sediment Transport* (Proceedings of the Canberra Symposium, December 1994), IAHS Publ. no. 224.

Zhu, A.G., Lin, C.H. and Zhu, H.S., 1993, Research on the laws of sediment yield in the middle and upper reaches of the Wujiang River. *Journal of Soil and Water Conservation*, 7(3): 53-57 (in Chinese).

Zingg, A.W., 1940, Degree and length of landslope as it affects soil loss in runoff, *Agricultural Engineering*, 21: 59-64.